LANDSCAPE CONTROLS ON AND PHYSIOLOGICAL BENEFITS OF DEEP ROOTING BY TREES IN QUINTANA ROO, MEXICO

A Dissertation

by

RACHEL ESTEE ADAMS

Submitted to the Office of Graduate and Professional Studies of
Texas A&M University
in partial fulfillment of the requirements for the degree of

DOCTOR OF PHILOSOPHY

Chair of Committee,	Jason B. West
Co-Chair of Committee,	Thomas M. Iliffe
Committee Members,	F. Andrew Jones
	Bradford P. Wilcox
Head of Department,	Kirk Winemiller

May 2020

Major Subject: Ecosystem Science and Management

ABSTRACT

Deep rooting is an advantageous plant strategy because it expands a tree's available water sources to reliable deep pools and is predicted to be more common in ecosystems with seasonal precipitation regimes, allowing trees to maintain positive water status throughout dry periods. Studying deep roots without disturbance is difficult, yet, caves existing close to the surface present such an opportunity. In the Yucatán Peninsula, Mexico, caves have formed in the limestone bedrock. Overlying thin soils appear unable to retain enough water to support dense subtropical forests. In the state of Quintana Roo, deep roots emerge from ceilings and walls of shallow caves, some directly contacting water. Despite their prevalence, it is unknown which species provide these roots and how they impact surface processes. Therefore, above and below ground diversity and biomass was evaluated at caves to investigate deep rooting specialization as well as patterns in water use and water use efficiency among co-occurring species.

Through DNA barcoding, 38 species were identified with roots in the caves, though root diversity was dominated by *Ficus* spp. While deep rooting specialization was apparent, root abundance was not predicted by tree size or functional groups. Overlapping root systems, seemingly the result of local bedrock characteristics, suggest competition for space and resources. Tree and root abundance decreased with site distance inland, showing increased depth to groundwater alters water access and community composition in Quintana Roo. Stable isotope data from stem water and leaves revealed significant variation in water use and water use efficiency among species. However, this was not explained by root abundance or functional groups. Tree size was informative, with larger trees utilizing more deep water while small trees were successfully supported by shallow water sources. Further, natural history, morphological, and physiological differences provided insight into water use strategies, suggesting inter- and intraspecific variation may explain plant responses to water limitation and help predict impacts of disturbance and climate change. This novel research describes a holistic view of deep rooting by trees in a seasonally dry karst landscape, unraveling the complexity of these biological structures and their importance in water-limited ecosystems around the world.

ACKNOWLEDGEMENTS

I would first like to thank my committee co-chairs, Drs Jason West and Tom Iliffe, for their mentorship and encouragement during my time at Texas A&M University. It was a pleasure and a joy to work in their respective labs as well as work alongside each other in the field. Many thanks go to my committee members, Drs Andy Jones and Brad Wilcox, for guidance and support throughout their time on my committee and throughout my research.

This work had notable field and laboratory components, none of which could have been accomplished without numerous people. First, Peter Sprouse and his band of cavers, who have spent countless hours underground to survey caves, provided necessary cave maps and site access to conduct the data collection. Each trip to Mexico was a new, exciting adventure and I am grateful to all the people I met along the way. Second, the genetics campaign was aided by Drs Nithya Subramanian, Claudio Casola, and Daniel Spalink, from training, to troubleshooting (and more troubleshooting), to data analysis. Third, Dr. Ayumi Hyodo and the assistants in the Stable Isotope for Biosphere Sciences laboratory were integral in conducting the sampling processing and subsequent stable isotope analysis. Ayumi's joy in the form of a smile or chocolate was always appreciated.

Many thanks and hugs go to my fellow graduate students, all of whom were integral in my experience at Texas A&M. I specifically want to thank Ryan Muskinski and Yong Zhou, my original officemates, for welcoming and embracing me when I first arrived in College Station,

and to Harrison Raub and Nicole Havrilchak, my current labmates, for the moral support, jokes, and comradery.

I would not be the person I am today without the love and encouragement from my friends and family. I am forever grateful to my parents, who taught me to work hard and persevere in order to chase my dreams. My brothers and sister were always there, cheering me on every step of the way. And most importantly, thank you to my wonderful husband, Vincent, for your unyielding love, patience, and support. I am blessed to dance through life with you.

CONTRIBUTORS AND FUNDING SOURCES

Contributors

This work was supervised by a dissertation committee consisting of Drs Jason West (chair), Thomas Iliffe (co-chair), F. Andrew Jones (committee member), and Bradford Wilcox (committee member).

As noted in chapters 2, 4, and 5, survey data and site access was provided by Peter Sprouse from Zara Environmental, LLC. Training, laboratory space, and data interpretation assistance for the genetics campaign associated with chapters 2 and 4 was provided by Drs Nithya Subramanian (AgriGenomics Laboratory), Claudio Casola (Department of Ecology and Conservation Biology), and Daniel Spalink (Department of Ecology and Conservation Biology) at Texas A&M University. Sanger sequencing was conducted by the Laboratory for Genome Technology at the Institute for Plant Genomics and Biotechnology at Texas A&M. Stable isotope analysis for chapters 3 and 5 was conducted by Dr. Ayumi Hyodo at the Stable Isotope for Biosphere Sciences laboratory at Texas A&M. For chapter 3, Xiangmin Sun provided the soils from Oklahoma as well as performed initial experiments, which provided a foundation for the study. Dr. Youjun Deng and Bidemi T. Fashina from the Soil Mineralogy laboratory in the Department of Soil and Crop Sciences at Texas A&M University performed the XRD analysis and offered assistance to interpret the results.

All other work conducted for the dissertation was completed by the student independently.

Funding Sources

Graduate study was supported by the Sid Kyle Graduate Merit Assistantship and the Franklin F. Wasko Graduate Merit Fellowship from the Department of Ecosystem Science and Management at Texas A&M University.

This work was also made possible in part by the National Geographic Society under Grant Number CP-090ER-17. Further support was received from the MSC L.T. Jordan Institute for International Awareness at Texas A&M University and USDA/NIFA Hatch Projects 1002535 and 1003961. The contents of this dissertation are solely the responsibility of the authors and do not necessarily represent the official views of the funding offices.

TABLE OF CONTENTS

LIST OF FIGURES

LIST OF TABLES

Page

1. INTRODUCTION

Drylands collectively comprise about 41% of the globe's terrestrial surface and include arid, semi-arid, and sub-humid regions where annual precipitation is less than potential evapotranspiration (Newman et al. 2006). These water-limited ecosystems function as agricultural and urban centers, support high levels of biodiversity, and provide numerous needed ecosystem services (Reynolds et al. 2007, Maestre et al. 2012). In addition, they are increasingly recognized as drivers of inter-annual variability in atmospheric CO_2 and are particularly sensitive to variation in precipitation (Poulter et al. 2014). A key plant trait commonly associated with water limitation is deep rooting (Casper et al. 2003, Santiago et al. 2016). While there is not a central definition for deep roots, they are generally described as reaching soil beyond two meters in depth (Schenk and Jackson 2005). Trees with deep roots often have more consistent sap flow, increased hydraulic conductance, more positive water potential and overall lower water stress during dry seasons (McElrone et al. 2004, Bleby et al. 2010, Doody and Benyon 2011, Johnson et al. 2014a). These deep roots have also been shown in some cases to perform hydraulic lift, moving water from deep, wetter layers directly to shallow, drier layers of soil (Peñuelas et al. 2003, Bleby et al. 2010). Deep roots that have access to groundwater can offer particular stability during droughts (Meinzer et al. 1999, Mitchell et al. 2008, Johnson et al. 2014b). Some species have been shown to shift water sources from shallower to deeper soil layers in the dry season, maintain good performance and then shifting back to shallower sources in the wet season when soil is rewetted (Meinzer et al. 1999, Bleby et al. 2010, Nardini et al. 2016). This avoids expending unnecessary resources to bring water from depth when it is available for use closer to the surface.

While there are examples of grasses and shrubs with deep rooting capabilities (Canadell et al. 1996, Maeght et al. 2013), the main focus on the research has been on woody plants and trees (Silvertown et al. 2015). The repeated observation that species with significant above ground biomass support large root systems has led to global-scale modeling of deep rooting probabilities. Modelled using climate and soil characteristics, the highest probabilities are often predicted for dryland regions, particularly in tropical to subtropical regions (Schenk and Jackson 2005). However, in spite of its clear importance and decades of significant research focus, available data to support models of deep rooting are based on a spatially biased sampling, largely missing regions where highest probability deep rooting is predicted. A recent paper on groundwater uptake by trees still shows limited sampling outside of temperate ecosystems, with 87 out of 145 studies in temperate and Mediterranean climates and only 31 in tropical and subtropical regions (Evaristo and McDonnell 2017). Only three studies were in tropical and subtropical dry forests (Figure 1.1).

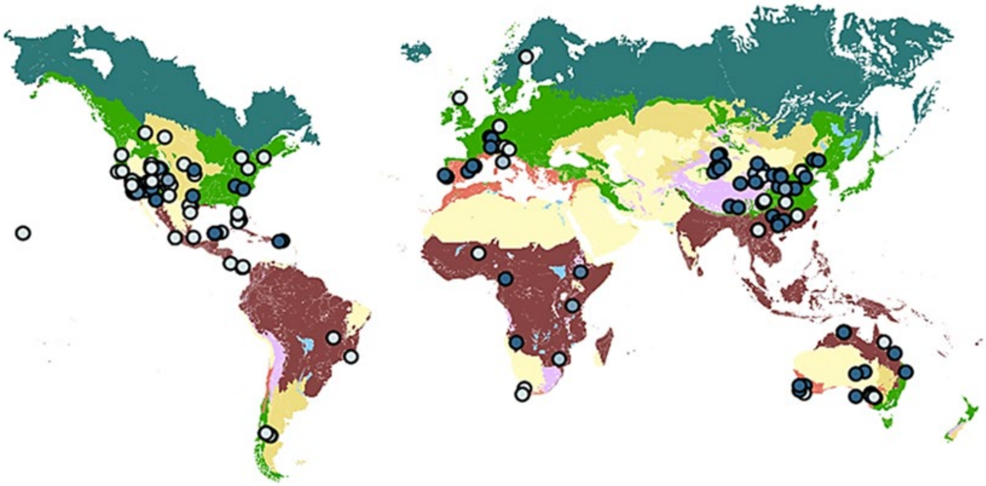

Figure 1.1 Groundwater use based on estimates from 162 sites in the global meta-analysis database. Color variation in circles represents percent prevalence of groundwater uptake, with lighter shades corresponding to less uptake and darker shades corresponding to more uptake. Reprinted from Evaristo and McDonnell (2017).

Since Schenk and Jackson 2005, there is evidence that deep rooting may be less common than expected. Several studies that hypothesized large trees would have access to groundwater concluded that they in fact did not (Meinzer et al. 1999, Querejeta et al. 2006, 2007, Estrada-Medina et al. 2013a, Schwartz et al. 2013). In addition, the existence of deep roots does not necessarily result in significant access to deep water (Santiago et al. 2016). Finally, there are species differences, environmental influences, and mechanistic trade-offs, which make the phenomenon of deep rooting rather complicated and unclear (Fan 2015, Silvertown et al. 2015, Weemstra et al. 2016). Thus, deep rooting may exhibit much more complex occurrences, potentially contradicting our current understanding of the distribution and ecological impact of these roots. The objective of research outlined in this dissertation is to expand studies on rooting depth and groundwater access to an underrepresented seasonally dry tropical region: the Yucatán Peninsula in Mexico.

Studying deep roots has obvious limitations because of the inability to access them directly without disturbance. Major excavations are costly and preclude physiological measurements. Other methods like ground penetrating radar and electrical resistivity tomography show promise, but have limits on range and accuracy. However, cave systems that exist close to the surface offer a unique opportunity to study deep roots directly. In addition, when caves are associated with groundwater, this is also where tree access to deep water may be expected (Peñuelas et al. 2003, McElrone et al. 2004, Nardini et al. 2016). Karst landscapes are ideal in this context and have been the subject of numerous investigations of deep rooting (Peñuelas et al. 2003, McElrone et al. 2004, Gregory et al. 2009, Bleby et al. 2010, Doody and Benyon 2011, Kukowski et al. 2013, Schwartz et al. 2013, Johnson et al. 2014a, Nardini et al. 2016). Because of the fractures and natural porosity of limestone, surface water rapidly percolates downwards. This often supplies caves with water all year, varying from small pools to underground streams, and even completely submerged passages below the water table. Although rooting depth in some karst environments may be restricted by overlying bedrock, it is not uncommon for trees to grow through the bedrock using pre-existing fissures to reach reliable water at depth (Schwinning 2010, Gao et al. 2016). In these situations, roots may hang from the ceiling or protrude from the walls of caves and can result in substantial root masses in the cave water. The subterranean world thus provides the perfect setting to observe and study deep roots that would otherwise be unachievable without significant ecosystem alterations.

Because of the Edwards Plateau's karst topography, central Texas has been the site of direct studies on deep roots, many of these limited to a single, now iconic location: Powell’s Cave (Jackson et al. 1999, McElrone et al. 2004, Bleby et al. 2010, Johnson et al. 2014a). The results from these studies have been frequently cited in subsequent articles, dramatically advancing what we know about deep rooting. Although we have learned much from it, this is an ecosystem with low plant biodiversity and a specific climate. It remains an open question how representative observations in this system are of other landscapes. Of course, work on other karst systems exists (Peñuelas et al. 2003, Mitchell et al. 2008, Doody and Benyon 2011, Kukowski et al. 2013, Schwartz et al. 2013, Swaffer et al. 2014, del Castillo et al. 2016, Nardini et al. 2016), but these are also often in temperate zones and, paradoxically, often not in zones where models predict the highest probability of deep rooting. Therefore, it is crucial to expand the knowledge about deep roots in other water-limited ecosystems, particularly those with greater biodiversity and higher deep rooting probabilities. The Yucatán Peninsula in Mexico is one of these regions. The Yucatán offers an opportunity to assess the role of biodiversity and a much broader range of water use strategies in the context of this study.

The Yucatán Peninsula is a compelling region due to the combination of the existence of groundwater potentially accessible to deeply rooted trees and the shallow soils covering the vast karst topography (Durán-García et al. 2016). The thin soils appear unable to retain enough water to support the often dense subtropical forests growing on them. Trees therefore extend roots into the limestone bedrock and access deeper water (Estrada-Medina et al. 2013b). Numerous observations of roots in both dry and flooded cave passages confirm this expectation (Figure 1.2A and 1.2B). However, a few studies have surprisingly shown large trees with maximum rooting depths of less than five meters, apparently unable to reach stable groundwater resources in a number of cases (Querejeta et al. 2006, 2007, Hasselquist et al. 2010, Estrada-Medina et al. 2013a, 2013b). These contradictions beg the question: why are deep roots present in some areas and not others and what controls this variation? My research sought to understand the relationships between surface biodiversity, the spatial distribution, and physiological importance of deep rooting.

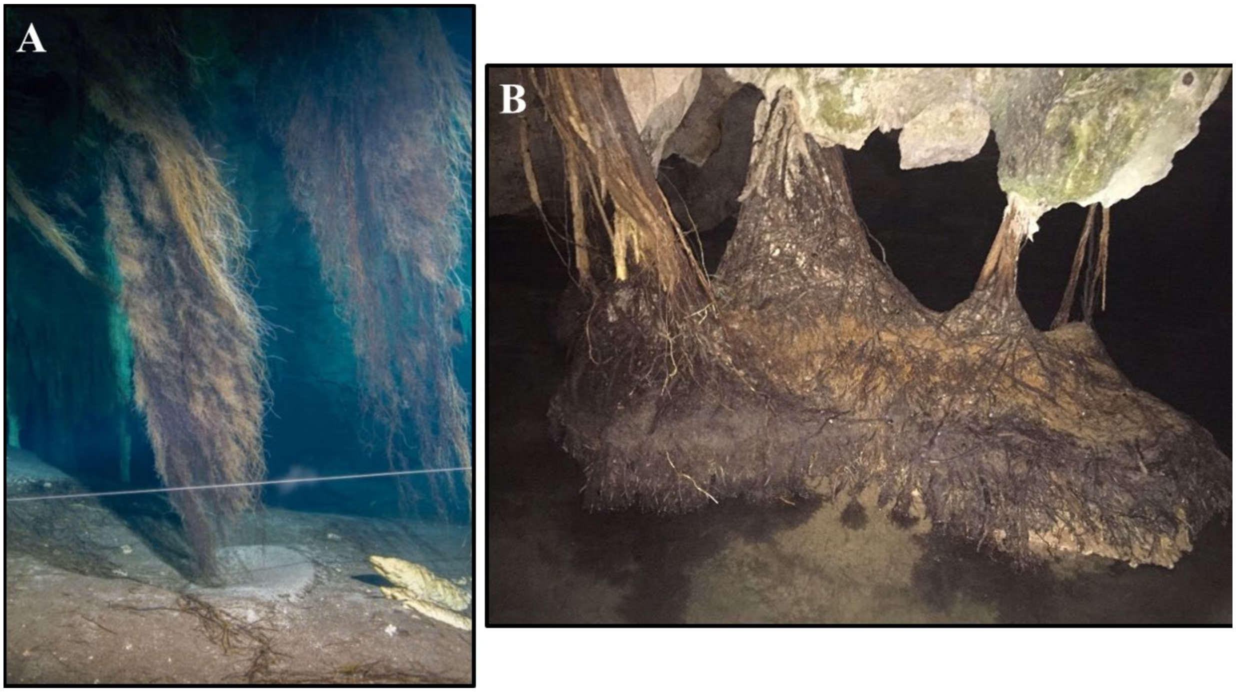

Figure 1.2 Submerged roots (A) and roots at the water's surface (B) in caves in the Yucatán Peninsula. Photograph: Petra Kovač-Konrad (A) and Rachel E. Adams (B).

1.1. General Description of the Yucatán Peninsula and the State of Quintana Roo

The Yucatán Peninsula in Mexico is a highly diverse, seasonally dry subtropical forest ecosystem. The annual mean temperature is 26°C with little variability between the summer and winter months. Despite receiving on average 1000 millimeters of annual rainfall, there is a distinct dry season between November and May, in which only 20% of the total rainfall is deposited (Durán-García et al. 2016). A precipitation gradient increasing from west to east results in different community compositions, with more deciduous species in the west and more evergreen species in the east. Common trees throughout the peninsula include *Ficus continifolia* Kunth, *Bursera simaruba* (L.) Sarg., *Brosimum alicastrum* Sw., *Piscidia piscipula* (L.) Sarg., *Lysiloma latisliquum* (L.) Benth., *Cedrela odorata* L., *Metopium brownei* (Jacq.) Urban, and *Ceiba* spp. (Pennington and Sarukhán 1998).

As mentioned previously, the soils in the Yucatán Peninsula are thin, generally no more than ten centimeters thick. They are classified as leptisols (lithic subgroups of other soils) overlying limestone bedrock (Bautista and Zinck 2010). The distribution of the soil is very heterogeneous. It is common to see areas without soil and exposed rock relatively close to soil-filled conduits. These conduits are small-scale fractures and pores in the bedrock formed from weathering of the limestone. The Cenozoic limestone is relatively young and is, therefore, rather porous, with an average porosity of 17% near the coast (Ramos 1975, Worthington et al. 2000). The bedrock also supports one of the largest karst aquifers on the planet, which acts at the sole water source as surface water bodies here are scarce (Gondwe et al. 2010). The aquifer underneath the Yucatán Peninsula is very stable. Hydraulic gradients along the coastal plains range from 1 to 10 centimeters per kilometer (Bauer-Gottwein et al. 2011). The water level is in equilibrium with the ocean, which reduces water table level fluctuations (Figure 1.3). Despite this stability, subtle changes in elevation or bedrock thickness increase the distance between the surface and the groundwater. Along the Caribbean coast in Quintana Roo, shallow caves allow for easy access to the groundwater. Further inland, the elevation increases (Smart et al. 2006), causing the distance to the water table to increase.

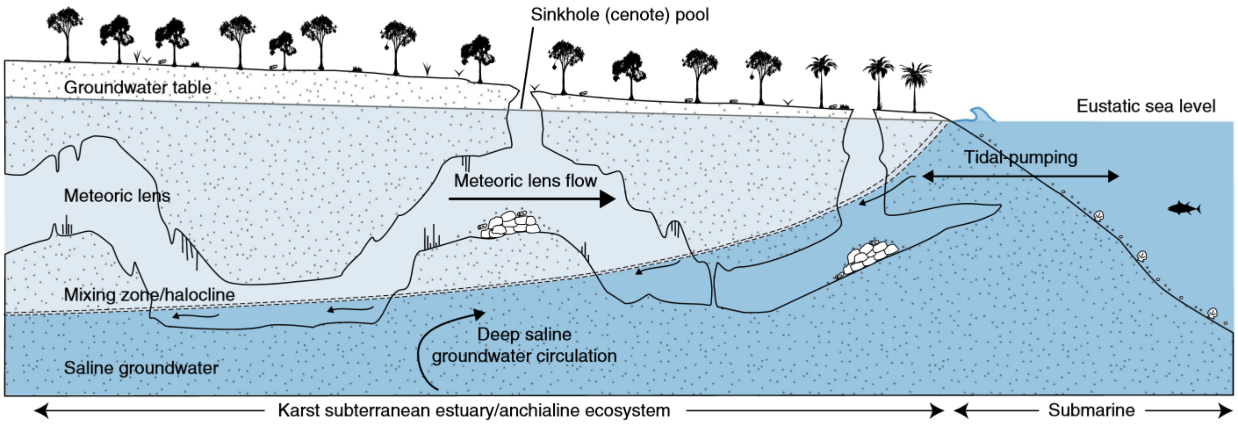

Figure 1.3 A conceptual model of the karst aquifer of the Yucatán Peninsula. Reprinted from Brankovits et al. (2017).

In the state of Quintana Roo, the shallow, cave systems were rapidly expand through the mixing of fresh and salt water as well as from precipitation (Smart et al. 2006). They are generally characterized by maze passages that run perpendicularly to the Caribbean coast. These caves can stretch up to eight to twelve kilometers inland from the coast. These caves are dry, semi-dry or completely submerged. If filled with water, openings to these systems, called cenotes, formed from the collapse of the bedrock after sea level dropped, draining the water that supported the ceiling of the cave. In the state of the Yucatán, cenotes are organized in a semi-circle around the site of the Chicxulub impact crater (Figure 1.4), which was the result of the large asteroid that struck the earth 65 million years ago and lead to the extinction of the dinosaurs (Perry et al. 1995). These cenotes and caves increase permeability and hydraulic conductivity in the bedrock, forming natural pathways that promote large-scale groundwater flow underneath the entire peninsula (Bauer-Gottwein et al. 2011).

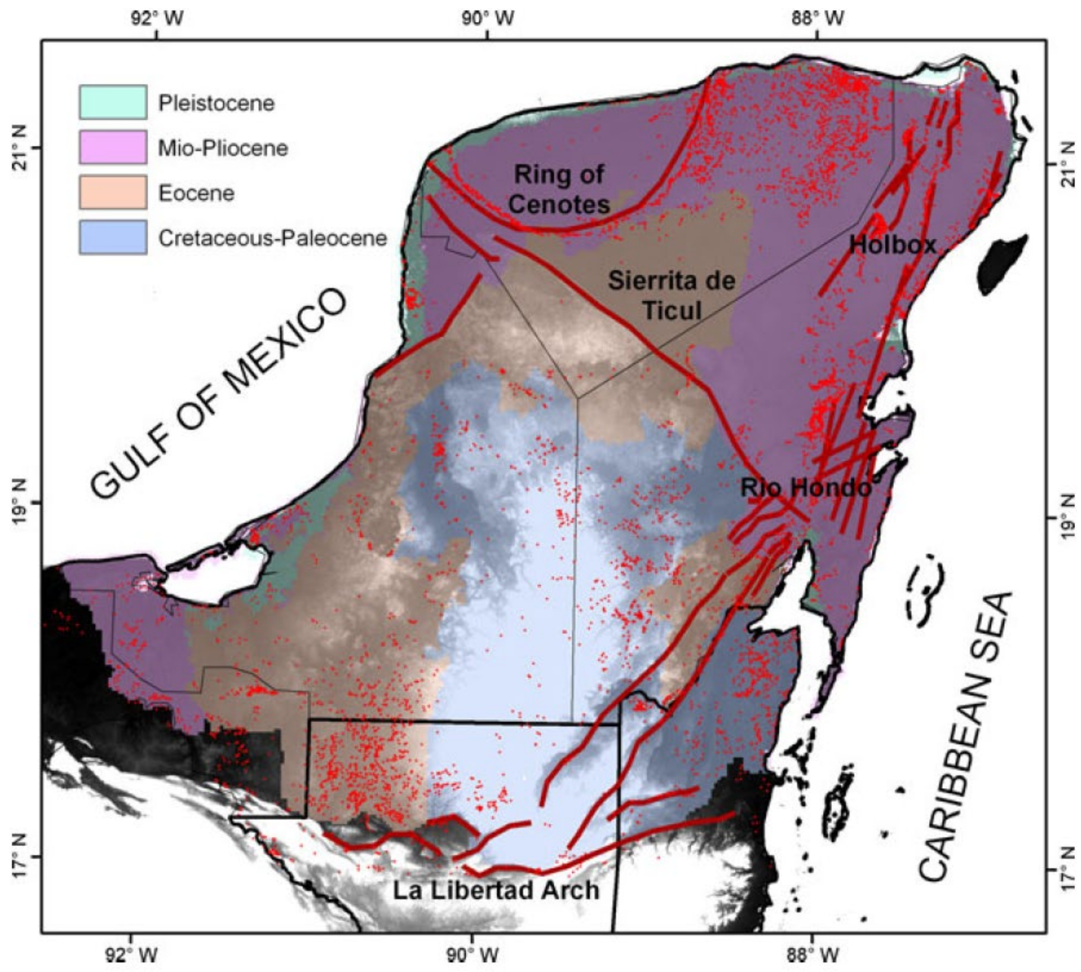

Figure 1.4 Location of large-scale fractures and cenotes across the Yucatán Peninsula. Reprinted from Bauer-Gottwein et al. (2011).

1.2. Overall Objectives

The overall goal of this research was to determine the controls, prevalence, and benefits of deep rooting in an understudied seasonally dry tropical region. The first chapter of this dissertation outlined general observations of the roots in caves along with species-species root morphology. Compared to the extensive knowledge on the above ground community composition (Hernández-Stefanoni et al. 2014, Durán-García et al. 2016), little is known about the presence and dominance of tree species that have the ability to root deeply and potentially reach groundwater. This chapter is one of the first formal description of the roots in caves, providing foundational knowledge about the below ground environment and biodiversity in the Yucatán Peninsula. As investigation of water use using stable isotopes were employed in this research, we conducted a laboratory-based experiment, comparing soil water extraction methods on soils with varying properties. This study, outlined in the second chapter, provided insight on our processing, evaluating, and interpretation of data collected for other portions of this work. The third chapter of this dissertation focuses on the relationships between above and below ground biodiversity and the landscape controls on root abundance in cave in Quintana Roo. This comparison of surface and subterranean community composition allowed us to identify patterns in rooting habit along species. Dominance below ground of select species below ground implied species-specific water access and use strategies. Furthermore, evaluating root abundance in relation to site characteristics such as elevation and distance from the coast provided explanations for root presence and prevalence across caves. Lastly, the fourth chapter employed stable isotopes to identity water source and water use efficiency among co-occurring tropical trees, exposing different processes and strategies to survive in a dynamic seasonally dry ecosystem. Together, these endeavors explored the underlying controls on deep rooting, their role in landscape composition, and their physiological importance for individuals. This research significant contributes to our understanding of deep rooting as a general phenomenon, but also as an important characteristic of many water-limited ecosystems globally.

1.3. References

Bauer-Gottwein, P., B. R. N. N. Gondwe, G. Charvet, L. E. Marín, M. Rebolledo-Vieyra, and G. Merediz-Alonso. 2011. Review: The Yucatán Peninsula karst aquifer, Mexico. *Hydrogeology Journal* 19:507–524.

Bautista, F., and J. A. Zinck. 2010. Construction of an Yucatec Maya soil classification and comparison with the WRB framework. *Journal of Ethnobiology and Ethnomedicine* 6:1-11.

Bleby, T. M., A. J. McElrone, and R. B. Jackson. 2010. Water uptake and hydraulic redistribution across large woody root systems to 20 m depth. *Plant, Cell & Environment* 33:2132–2148.

Brankovits, D., J. W. Pohlman, H. Niemann, M. B. Leigh, M. C. Leewis, K. W. Becker, T. M. Iliffe, F. Alvarez, M. F. Lehmann, and B. Phillips. 2017. Methane- and dissolved organic carbon-fueled microbial loop supports a tropical subterranean estuary ecosystem. *Nature Communications* 8:1835.

Canadell, J., R. B. Jackson, J. R. Ehleringer, H. A. Mooney, O. E. Sala, and E. D. Schulze. 1996. Maximum Rooting Depth of Vegetation Types at the Global Scale. *Oecologia* 108:583–595.

Casper, B. B., H. J. Schenk, and R. B. Jackson. 2003. Defining a plant's belowground zone of influence. *Ecology* 84:2313–2321.

del Castillo, J., C. Comas, J. Voltas, and J. P. Ferrio. 2016. Dynamics of competition over water in a mixed oak-pine Mediterranean forest: Spatio-temporal and physiological components. *Forest Ecology and Management* 382:214–224.

Doody, T. M., and R. G. Benyon. 2011. Direct measurement of groundwater uptake through tree roots in a cave. *Ecohydrology* 4:644–649.

Durán-García, R., M. Méndez-Gonzalez, and A. Larqué-Saavedra. 2016. The biodiversity of the Yucatán Peninsula: a natural laboratory. *Progress in Botany* 78:237–258.

Estrada-Medina, H., R. C. Graham, M. F. Allen, J. J. Jiménez-Osornio, and S. Robles-Casolco. 2013a. The importance of limestone bedrock and dissolution karst features on tree root distribution in northern Yucatán, México. *Plant and Soil* 362:37–50.

Estrada-Medina, H., L. S. Santiago, R. C. Graham, M. F. Allen, and J. J. Jiménez-Osornio. 2013b. Source water, phenology and growth of two tropical dry forest tree species growing on shallow karst soils. *Trees* 27:1297–1307.

Evaristo, J., and J. J. McDonnell. 2017. Prevalence and magnitude of groundwater use by vegetation: a global stable isotope meta-analysis. *Scientific Reports* 7:1-12.

Fan, Y. 2015. Groundwater in the Earth's critical zones: Relevance to large-scale patterns and processes. *Water Resources Research* 51:3052–3069.

Gao, W., L. Hodgkinson, K. Jin, C. W. Watts, R. W. Ashton, J. Shen, T. Ren, I. C. Dodd, A. Binley, A. L. Phillips, P. Hedden, M. J. Hawkesford, and W. R. Whalley. 2016. Deep roots and soil structure. *Plant, Cell & Environment* 39:1662–1668.

Gondwe, B. R. N., S. Lerer, S. Stisen, L. Marín, M. Rebolledo-Vieyra, G. Merediz-Alonso, and P. Bauer-Gottwein. 2010. Hydrogeology of the south-eastern Yucatán Peninsula: New insights from water level measurements, geochemistry, geophysics and remote sensing. *Journal of Hydrology* 389:1–17.

Gregory, L., B. P. Wilcox, B. Shade, C. Munster, K. Owens, and G. Veni. 2009. Large-scale rainfall simulation over shallow caves on karst shrublands. *Ecohydrology* 2:72–80.

Hasselquist, N. J., M. F. Allen, and L. S. Santiago. 2010. Water relations of evergreen and drought-deciduous trees along a seasonally dry tropical forest chronosequence. *Oecologia* 164:881–890.

Hernández-Stefanoni, J. L., J. M. Dupuy, K. D. Johnson, R. Birdsey, F. Tun-Dzul, A. Peduzzi, J. P. Caamal-Sosa, G. Sánchez-Santos, and D. López-Merlín. 2014. Improving species diversity and biomass estimates of tropical dry forests using airborne LiDAR. *Remote Sensing* 6:4741–4763.

Jackson, R. B., L. A. Moore, W. A. Hoffmann, W. T. Pockman, and C. R. Linder. 1999. Ecosystem rooting depth determined with caves and DNA. *Proceedings of the National Academy of Sciences of the United States of America* 96:11387–92.

Johnson, D. M., C. R. Brodersen, M. Reed, J. C. Domec, and R. B. Jackson. 2014a. Contrasting hydraulic architecture and function in deep and shallow roots of tree species from a semi-arid habitat. *Annals of Botany* 113:617–627.

Johnson, D. M., M. E. Sherrard, J. C. Domec, and R. B. Jackson. 2014b. Role of aquaporin activity in regulating deep and shallow root hydraulic conductance during extreme drought. *Trees* 28:1323–1331.

Kukowski, K. R., S. Schwinning, and B. F. Schwartz. 2013. Hydraulic responses to extreme drought conditions in three co-dominant tree species in shallow soil over bedrock. *Oecologia* 171:819–830.

Maeght, J.-L., B. Rewald, and A. Pierret. 2013. How to study deep roots-and why it matters. *Frontiers in Plant Science* 4:1–14.

Maestre, F. T., J. L. Quero, N. J. Gotelli, A. Escudero, V. Ochoa, M. Delgado-Baquerizo, M. García-Gómez, M. A. Bowker, S. Soliveres, C. Escolar, P. García-Palacios, M. Berdugo, E. Valencia, B. Gozalo, A. Gallardo, L. Aguilera, T. Arredondo, J. Blones, B. Boeken, D. Bran, A. Conceicao, and O. Cabrera. 2012. Plant species richness and ecosystem multifunctionality in global drylands. *Science* 335:214–218.

McElrone, A. J., W. T. Pockman, J. Martínez-Vilalta, and R. B. Jackson. 2004. Variation in xylem structure and function in stems and roots of trees to 20 m depth. *New Phytologist* 163:507–517.

Meinzer, C. F., L. J. Andrade, G. Goldstein, M. N. Holbrook, J. Cavelier, and J. S. Wright. 1999. Partitioning of soil water among canopy trees in a seasonally dry tropical forest. *Oecologia* 121:293–301.

Mitchell, P. J., E. J. Veneklaas, H. Lambers, and S. S. O. Burgess. 2008. Leaf water relations during summer water deficit: Differential responses in turgor maintenance and variation in leaf structure among different plant communities in south-western Australia. *Plant, Cell & Environment* 31:1791–1802.

Nardini, A., V. Casolo, A. Dal Borgo, T. Savi, B. Stenni, P. Bertoncin, L. Zini, and N. G. Mcdowell. 2016. Rooting depth, water relations and non-structural carbohydrate dynamics in three woody angiosperms differentially affected by an extreme summer drought. *Plant, Cell & Environment* 39:618–627.

Newman, B. D., B. P. Wilcox, S. R. Archer, D. D. Breshears, C. N. Dahm, C. J. Duffy, N. G. McDowell, F. M. Phillips, B. R. Scanlon, and E. R. Vivoni. 2006. Ecohydrology of water-limited environments: A scientific vision. *Water Resources Research* 42:1–15.

Pennington, T. D., and J. Sarukhán. 1998. *Árboles tropicales de México: Manual para la identificación de las principales especies*. México: Universidad Nacional Autónoma de México Fondo de Cultura Económica.

Peñuelas, J., I. Filella, J. Peñuelas, and I. Filella. 2003. Deuterium labelling of roots provides evidence of deep water access and hydraulic lift by *Pinus nigra* in a Mediterranean forest of NE Spain. *Environmental and Experimental Botany* 49:201–208.

Perry, E., L. Marin, J. McClain, and G. Velazquez. 1995. Ring of Cenotes (sinkholes), northwest Yucatán, Mexico: its hydrogeologic characteristics and possible association with the Chicxulub impact crater. *Geology* 23:17–20.

Poulter, B., D. Frank, P. Ciais, R. B. Myneni, N. Andela, J. Bi, G. Broquet, J. G. Canadell, F. Chevallier, Y. Y. Liu, S. W. Running, S. Sitch, and G. R. Van Der Werf. 2014. Contribution of semi-arid ecosystems to interannual variability of the global carbon cycle. *Nature* 509:600–603.

Querejeta, J. I., H. Estrada-Medina, M. F. Allen, and J. J. Jiménez-Osornio. 2007. Water source partitioning among trees growing on shallow karst soils in a seasonally dry tropical climate. *Oecologia* 152:26–36.

Querejeta, J. I., H. Estrada-Medina, M. F. Allen, J. J. Jiménez-Osornio, and R. Ruenes. 2006. Utilization of bedrock water by *Brosimum alicastrum* trees growing on shallow soil atop limestone in a dry tropical climate. *Plant and Soil* 287:187–197.

Ramos, E. L. 1975. Geological Summary of the Yucatán Peninsula. Pages 257–282 *in* A.E.M. Nairn and F.G. Stehli, editors. *The Gulf of Mexico and the Caribbean*. Boston, Massachusetts, USA: Springer.

Reynolds, J. F., D. M. S. Smith, E. F. Lambin, B. L. Turner, M. Mortimore, S. P. J. Batterbury, T. E. Downing, H. Dowlatabadi, R. J. Fernández, J. E. Herrick, E. Huber-Sannwald, H. Jiang, R. Leemans, T. Lynam, F. T. Maestre, M. Ayarza, and B. Walker. 2007. Global desertification: building a science for dryland development. *Science* 316:847–851.

Santiago, S. L., D. Bonal, M. E. De Guzman, and E. Ávila-Lovera. 2016. Drought Survival Strategies of Tropical Trees. *Tropical Tree Physiology* 6:243–258.

Schenk, H. J., and R. B. Jackson. 2005. Mapping the global distribution of deep roots in relation to climate and soil characteristics. *Geoderma* 126:129–140.

Schwartz, B. F., S. Schwinning, B. Gerard, K. R. Kukowski, C. L. Stinson, H. C. Dammeyer, H. C. Dam, C. L. Stinson, and H. C. Dammeyer. 2013. Using hydrogeochemical and ecohydrologic responses to understand epikarst process in semi-arid systems, Edwards Plateau, Texas, USA. *Acta Carsologica* 42:315–325.

Schwinning, S. 2010. The ecohydrology of roots in rocks. *Ecohydrology* 3:238–245.

Silvertown, J., Y. Araya, and D. Gowing. 2015. Hydrological niches in terrestrial plant communities: A review. *Journal of Ecology* 103:93–108.

Smart, P. L., P. A. Beddows, J. Coke, S. Doerr, S. Smith, and F. F. Whitaker. 2006. Cave Development on the Caribbean coast of the Yucatan Peninsula, Quintana Roo, Mexico. *Geological Society of America* 2404:105–128.

Swaffer, B. A., K. L. Holland, T. M. Doody, C. Li, and J. Hutson. 2014. Water use strategies of two co-occurring tree species in a semi-arid karst environment. *Hydrological Processes* 28:2003–2017.

Weemstra, M., L. Mommer, E. J. W. Visser, J. van Ruijven, T. W. Kuyper, G. M. J. Mohren, and F. J. Sterck. 2016. Towards a multidimensional root trait framework: a tree root review. *New Phytologist* 211:1159–1169.

Worthington, S. R. H., D. C. Ford, and P. A. Beddows. 2000. Porosity and permeability enhancement in unconfined carbonate aquifers as a result of solution. Pages 463–471 *in* A. Klimchouk, D. Ford, A. Palmer, and W. Dreybrodt, editors. *Speleogenesis: Evolution of Karst Aquifers*. Huntsville, AL, USA: The National Speleological Society.

2. IDENTIFYING TREE ROOTS IN THE CAVES OF QUINTANA ROO, MEXICO AS A STEP TOWARDS ECOLOGICAL INSIGHTS AND IMPROVED CONSERVATION[*]

2.1. Societal impact statement

Caves in Quintana Roo, Mexico are known for spectacular calcite formations, blue water, and their significance in Mayan culture. A fascinating feature of these caves is the tree roots that emerge from ceilings, walls, and floors. Little is known about these incredible natural structures which form a key part of the ecosystem, linking to the forests above. This work documents and identifies the species that use this deep rooting strategy as well as expands our understanding of the relationships between the surface and subterranean and the implications for the management and conservation of these natural structures and their resources.

2.2. Introduction

In Mayan culture, the world tree is depicted as a large Kapok or Ceiba tree (*Ceiba pentandra*), with branches that reach into the sky and touch the heavens (McDonald, 2016). The trunk intersects the earthly forest, while the roots extend deep below ground. Roots reach into the underworld, Xibalba, connecting the physical world to celestial and subterranean spiritual realms. Inside caves of Quintana Roo, Mexico, a physical representation of the world tree can be seen alongside ceremonial altars, sculptures, pots, and tools: tree roots commonly emerge from the ceilings and walls of caves, linking the above and below ground environments. In contrast to the focus on archaeological studies within these caves, the roots have remained understudied,

---

[*] Reprinted with permission from "Identifying tree roots in the caves of Quintana Roo, Mexico as a step toward ecological insights and improved conservation" by Adams, R.E., Iliffe, T.M. and West J.B., 2020. *Plants, People, Planet*, Vol. 2, pp 133-139, Copyright 2020 John Wiley & Sons, Ltd.

despite being photographed and noted in journal articles, new stories, and blog posts. Because of this, the importance of the roots is sometimes disregarded, particularly when a cave is commercialized for tourism, during which roots are often cut, potentially harming the associated tree on the surface. This can be particularly problematic for trees that rely on deep water sources within a seasonally dry ecosystem.

Seasonally dry and subhumid tropical forests are among the most threatened of the global tropical forests. Quite understudied compared to their wet counterparts, these tropical forests are critical centers of biodiversity and play an important role in global carbon cycling (Sánchez-Azofeifa et al., 2005; Poulter et al., 2014). In order to be successful in ecosystems with seasonal dry periods and high potential evapotranspiration, plants must have physiological adaptations to acquire water or reduce water loss. Deep rooting is an advantageous trait because it can expand a plant's search for water and enable it to reach reliable water at depth (Casper et al., 2003). The occurrence of deep roots is predicted to be more common in dry or subhumid regions, yet, they remain understudied in these types of locations (Schenk & Jackson, 2005).

Studying deep roots has obvious limitations because of the inability to access them directly without disturbance (Maeght et al., 2013). Major excavations are costly and generally preclude physiological measurements. However, cave systems that exist close to the surface offer a unique opportunity to study deep roots directly. In addition, when caves are associated with water, this is where tree access to deep water may be expected (Bleby et al., 2010). Although rooting depth in karst environments may be restricted by overlying bedrock, it is not uncommon for trees to grow through pre-existing fissures in the bedrock to reach reliable water at depth (Schwinning, 2010).

In these situations, roots may hang from the ceiling or protrude from the walls of caves and can result in substantial root masses in the cave water. The subterranean world thus provides an ideal setting to observe and study deep roots that would otherwise be inaccessible without significant ecosystem alterations and disturbances.

The state of Quintana Roo on the Caribbean coast of the Yucatán Peninsula in Mexico is an interesting region due to the combination of groundwater potentially accessible to deeply rooted trees and the shallow soils covering the vast karst topography (Durán-García et al., 2016). While the region receives approximately 1200 millimeters of rainfall annually, there is a dry period from November to April in which less than 60 millimeters of rain falls each month (Ellis et al., 2015). Thin soils appear unable to retain enough water to support the often-dense tropical forests growing on them. Trees therefore extend roots into the limestone bedrock to access water, either from cave pools or directly from the aquifer (Estrada-Medina et al., 2013). Numerous observations of roots by cavers and cave divers in dry and flooded cave passages confirm this. In dry caves, it is common to see roots growing out of a ceiling conduit or sticking out of stalactites. Large masses of intertwined roots can also be substantial features within these caves and can be mistaken for speleothems at first glance (Figure 2.1). In submerged cave systems, bundles of fine roots are suspended in the water column and flow with the current. Where there are roots, there is also heterotrophic life. Cave environments are considered to be nutrient deficient, subject to organic matter that falls or washes in. Therefore, tree roots provide an excellent source of food and shelter for subterranean animals, trogloxenes (cave visitors) and troglobites (cave dwellers) alike (Jasinska et al., 1996, Howarth et al., 2007). Roots can also become covered in calcite, earning them the name “rootsicles” (Taboroši, 2006). Eventually, they can be completely incorporated into cave formations, suggesting that the locations of these roots become important spots for the origin and growth of speleothems. Despite the prevalence of roots in caves of Quintana Roo, it is unknown which tree species are capable of growing these deep roots.

Figure 2.1 Cavers look up at tree roots extending from the ceiling of a cave in Quintana Roo, Mexico. Photograph: Sean Lewis.

2.3. Research objectives and methods

While conducting field work as part of a larger investigation into deep rooting by trees in Quintana Roo, we observed morphological and structural differences among the roots that could be organized into discrete groups. The immediate hypothesis is that these groups represent individual species, and so we sought to determine if these characteristics could be linked to specific species. We therefore described this variation in root characteristics and morphology and then used DNA barcoding to confirm if it was species-specific. This information provides insight into the diversity of species proliferating in the caves to support future studies concerning the physiological benefits of these deep roots and groundwater dependence in an understudied tropical forest. Furthermore, local landowners can benefit from the identification of deep rooting tree species on their properties with the potential to enhance their ecotourism operations as well as answer the question people who visit the caves in the Yucatán Peninsula often ask: *which trees do these roots belong to?*

We documented morphological and structural differences among roots at five caves along the Caribbean coast. In randomly established plots within the cave, all visible roots were documented with still photos and video accompanied by diameter and length measurements. Morphological differences of coarse roots were noted in the field, with particular focus on epidermis color and texture, cortex color, and presence or absence of latex in order to organize individual roots into potential species groups.

Species assignments for the groups were made following DNA barcoding of individual roots collected from the caves. This technique utilizes specific regions or markers within the genome that have species-to-species variation. DNA from root samples was extracted and amplified using a set of universal primers for the maturase K (*matK*) plastid region via polymerase chain reactions (PCR). Sequences obtained from root samples were compared to sequences from known species in GenBank using the basic local alignment search tool (BLAST). Accepted matches were those with percent identity values of 99% or above. Final species assignments were verified with a comprehensive list of plants native to Mexico along with comparisons to species that were expected to be present at these sites in Quintana Roo (Villaseñor, 2016). Root samples with the same species assignment were evaluated collectively to confirm unique morphological traits that contrasted with those of other species. Because the deep roots are prominent features in the caves, we created an identification key based on gross root morphology to aid others in identification for personal, educational, and scientific purposes. Voucher specimens of the roots were deposited at the S.M. Tracy Herbarium in College Station, Texas, USA (https://essm.tamu.edu/facilities/research/sm-tracy-herbarium/).

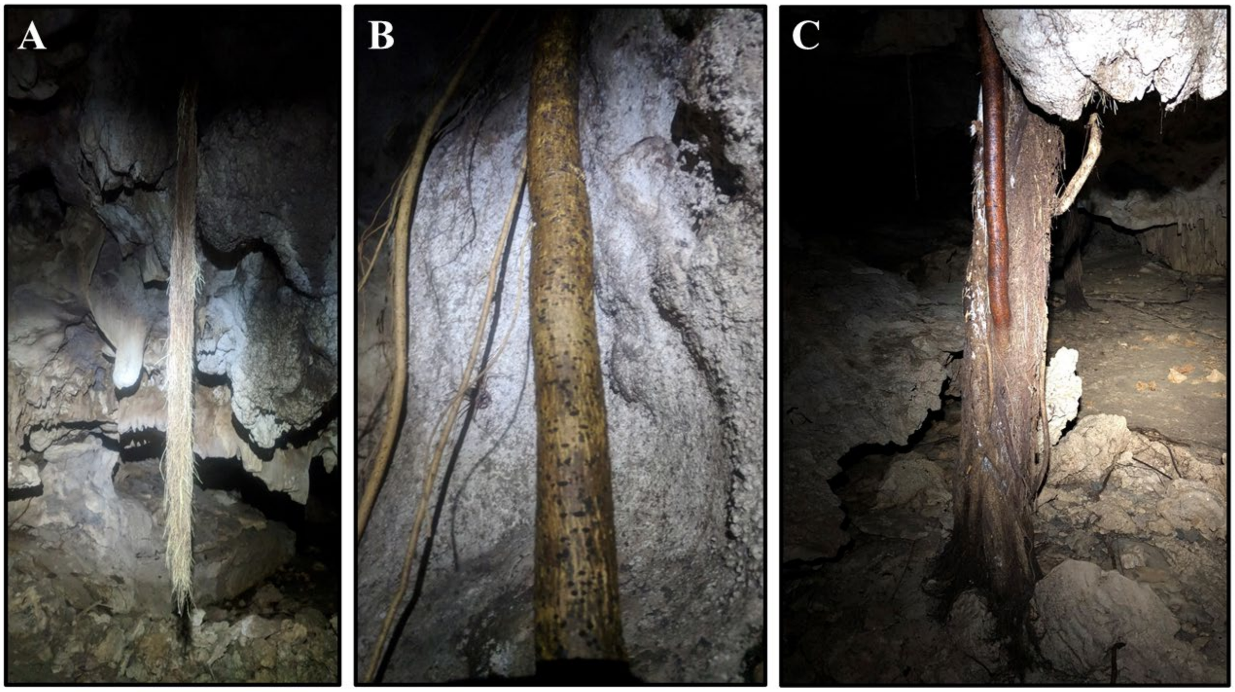

Figure 2.2 Fine roots (A); singular coarse roots (B); and large masses (C) are the three distinct root "structures" that appear at the study sites. For perspective, the fine roots are about 1 meter long, the singular coarse root is approximately five centimeters in diameter, and the large mass is twenty centimeters in diameter. Photograph: Jason B. West (A & B) and Rachel E. Adams (C).

2.4. Findings

2.4.1. Root “structures”

In Quintana Roo, roots exist in caves in a variety of different contexts and morphologies. We categorized these into three “structural” categories: *fine roots*, *coarse roots*, and *large masses* (Figure 2). *Fine roots* (<2 mm diameter) are common in water-filled passages, observed as dense bundles. In dry passages, these fine roots are often suspend from the cave ceiling. These may be the result of trees producing fast-growing roots to search for water. If the root reaches water, coarse roots are established to transport the water acquired by a larger network of fine roots, which are sometimes hidden under the cave floor. *Coarse roots* are individual roots (>2 mm) emerging from one conduit. They can either extend from the ceiling and grow straight through the cave floor or they can sprawl along the floor, sometimes for many meters. *Large masses* are groups of intertwined, coarse roots, often of multiple species that share ceiling conduits. Some of these masses can be up to thirty centimeters in diameter. In dry passages, large masses either grow through the cave floor or sprawl along the floor similar to the singular coarse roots. When large masses emerge over water, fine roots proliferate at the water surface, creating a trunk-like structure with a wide base. We observed fine roots emerging from these bases to often terminate within a few centimeters of entering the water. We also noted organic matter build up and formation of a soft substrate underneath the base. We frequently observed "moonmilk" around roots where they emerged from the bedrock. Moonmilk is a type of cave formation with a soft cottage cheese texture and appearance. While there is controversy surrounding the processes that govern the formation of moonmilk, this biokarst is thought to be the result of physiochemical interactions between microbes and carbonate, in which calcite is precipitated by filamentous bacteria and can result in significant deposits in the cave (Barton & Northup, 2007; Cañaveras et al., 2006). It is currently unknown how the roots influence moonmilk formation in these caves although the presence of root organic matter would be expected to be important to these microbial communities. Much more work needs to be done to understand potential "ecosystem engineering" in karst landscapes, in particular the likely interactions between plant roots and the microorganisms associated with them (Phillips, 2016).

2.4.2. Morphology and species identification

Coarse root morphologies were often strikingly unique. Select roots had white latex oozing from them when cut, a notable characteristic of Ficus trees (Figure 2.3A). Ficus, particularly Alamo (*Ficus cotinifolia* Kunth), commonly grow around cenotes, the openings to the aquifer, and their roots spill over the edges into the water. A notable and surprising observation were the roots of a palm (*Sabal yapa* C. Wright ex Becc.), a seemingly shallow-rooted species, emerging from stalactites up to five meters below the surface (Figure 2.3B). One of the most dominant species in the caves was *Lonchocarpus rugosus* Benth., with a yellow to tan, flaky epidermis, and dark stipules (Figure 2.3C). While the epidermis of two species may be similar, the cortex was distinct. For example, *Dalbergia glabra* (Mill.) Standl. and *Rourea glabra* Kunth, both lianas, have relatively smooth, dark brown exteriors, yet, the cortex of *Dalbergia glabra* is yellow-orange and *Rourea glabra* is reddish (Figure 2.3D). We were able to uniquely identify fourteen different tropical tree species capable of rooting deeply as well as one palm and four liana species present in the cave (Table 2.1; Figure A-1 a-s). Because of the distinct morphological differences among coarse roots and lianas, landowners and researchers may be able to utilize these descriptions as an initial assessment of deep rooting species at other locations on the peninsula.

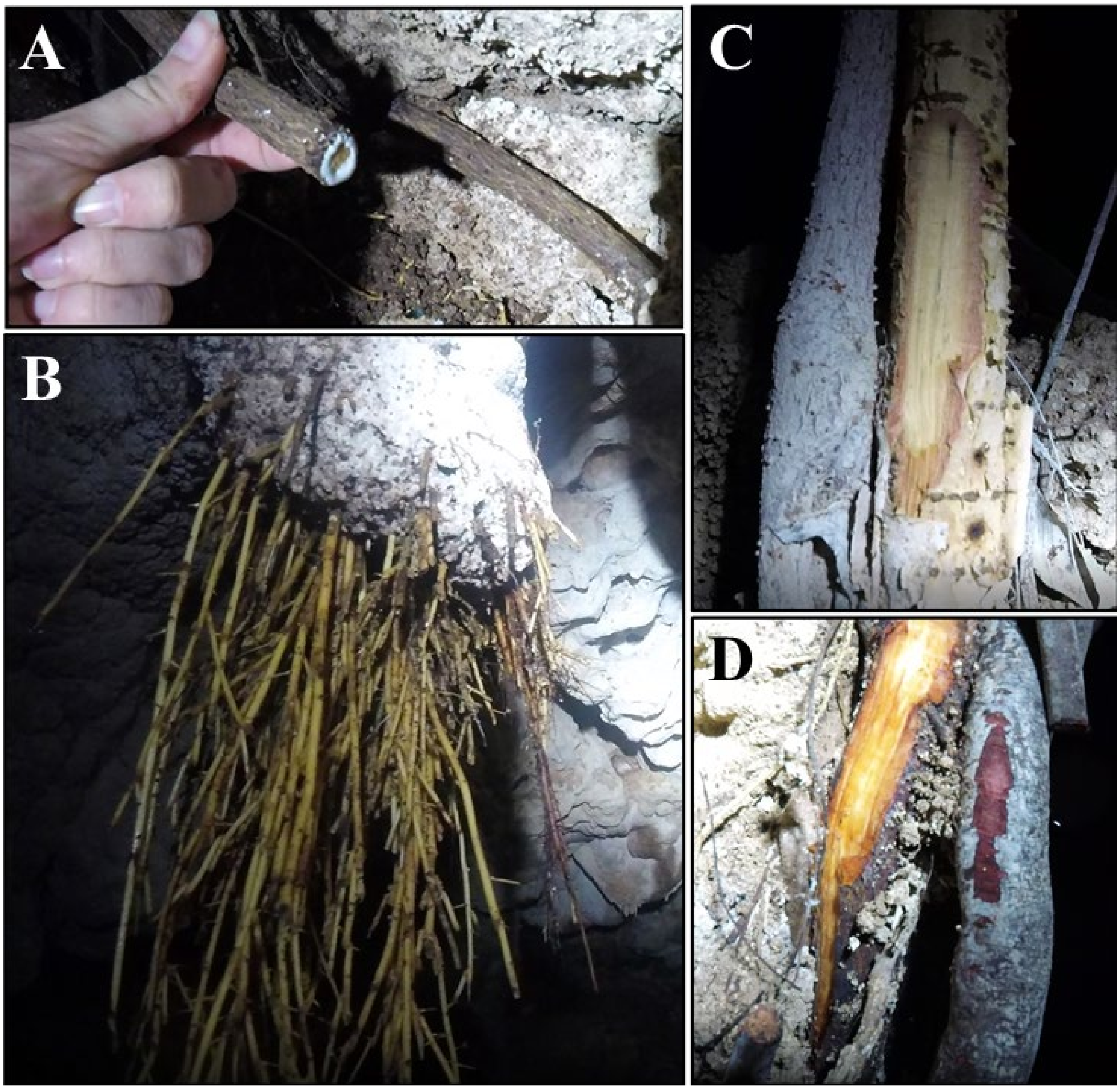

Figure 2.3 Unique morphology among roots in caves in Quintana Roo, Mexico. (A) *Ficus* spp.; (B) *Sabal yapa* C. Wright ex Becc; (C) *Lonchocarpus rugosus* Benth; (D) Lianas *Dalbergia glabra* (Mill.) Standl. (left) and *Rourea glabra* Kunth (right). Photograph: Rachel E. Adams.

Table 2.1 Gross morphology of coarse roots to use for identification of fourteen trees, four lianas, and one palm in Quintana Roo.

Species Name	**Epidermis Color**	**Cortex Color**	**Root Surface**
Blomia prisca (Standl.) Lundell	Light to dark grey	Tan	Grey, hard raised bumps
Brosimum alicastrum Sw.	Dark brown	Medium brown	Raised, longitudinal rings
Bursera simaruba (L.) Sarg.	Medium brown	Tan with red hue	Smooth to slightly flaky
Celtis iguanaea (Jacq.) Sarg.	Medium brown	Tan	Tan, slightly raised bumps
Coccoloba barbadensis Jacq.	Dark brown	Tan with red hue	Smooth
Cordia gerascanthus L.	Light to dark brown	Tan	Shallow to deep lateral furrows
Cupania glabra Sw.	Light grey to brown	Tan to white	Small lateral ridges
†*Dalbergia glabra* (Mill.) Standl.	Dark brown	Tan with yellow-orange hue	Lateral ridges, slightly scaly
Dendropanax arboreus (L.) Decne. & Planch.	Tan	Tan to white	Lateral ridges
Diospyros tetrasperma Sw.	Dark grey to black	Tan	Deep lateral furrows
Ficus spp.	Medium to dark brown	Light brown, white latex emerges when cut	Lateral ridges
Hyperbaena mexicana Miers	Light brown to grey	Tan to white	Furrows form rectangles
Lonchocarpus rugosus Benth.	Yellow to tan	Light pink and tan	Flaky with dark stipules
Mosannona depressa (Baill.) Chatrou	Dark grey	Tan to white	Small lateral ridges
Piscidia piscipula (L.) Sarg.	Reddish brown	Tan	Flaky with stipules
†*Rourea glabra* Kunth	Dark brown	Reddish brown	Furrows form rectangles
§*Sabal yapa* C. Wright ex Becc.	Orange to tan	Orange to tan	Smooth
†*Tanaecium tetragonolobum* (Jacq.) L.G. Lohmann	Light brown	Tan	Lateral ridges
†*Vitis tiliifolia* Humb. & Bonpl. ex Roem. & Schult.	Dark brown	Tan to white	Large lateral ridges

† **Liana**
§ **Palm**

It is important to note that root morphology can be altered by environmental factors such as water and nutrient availability and fungal associations (Rewald et al. 2012). Using only one characteristic, particularly color, to identify roots to species can be inaccurate. To avoid this, we provide identification criteria for multiple aspects of the root. In addition, since morphological changes are most pronounced for fine roots and the fine root to coarse root transition, we focus here on coarse roots. An additional variable for these karst systems is the effect of calcification on apparent external color. Recognition of this effect would be important in order to exclude calcified roots as candidates for morphological identification.

While we were able to identify approximately half of the species below ground that appear above ground at the sites with DNA barcoding, and we were able to document species-specific patterns in coarse root morphology for a multitude of species. We recognize that not every root can be assigned to a species morphologically; however, this work offers guidance to identify the distinct species present without time-consuming and costly DNA barcoding (Yanai et al. 2008). This is particularly useful for quick, widespread surveys as well as assessing presence or absence of key species at a single site. This can ensure that the roots of ecologically and aesthetically valuable species, like Alamo and other Ficus trees, are not disturbed in the caves. In addition, there are many aspects about these systems that have not been studied, particularly biotic-abiotic interactions between roots and bedrock as well as the potential dependence of the subterranean fauna on the roots. There may be species-specific relationships that influence these ecological processes, making better understanding the role of biodiversity in these scenarios an important avenue for future work.

2.4.3. Human connections

During the course of our field work in the Yucatán Peninsula, we found that people were rather curious about the roots that appear in the caves, including landowners, tourists, and tour guides. Some who visit commercial caves or cenotes may not see abundant tree roots below ground as it is common for landowners or tour operators to cut them in order to prevent people from climbing or swinging on them, and potentially causing injury (Figure 2.4). Trees in this context lose access to water in the caves and can subsequently die, while cave organisms lose a source of organic matter and shelter. Furthermore, interest and research about forest and caves are often separated. Forest ecologists focus on the aboveground component, cavers focus on the belowground. However, the two are difficult to separate ecologically considering the roots directly connect the surface and the subterranean. In our view, there is an opportunity to enhance what tourists get out of visiting these beautiful cave systems by better understanding how the aboveground forest is intimately linked with the cave environment and remembering that the roots are integral to symbolic Maya world tree.

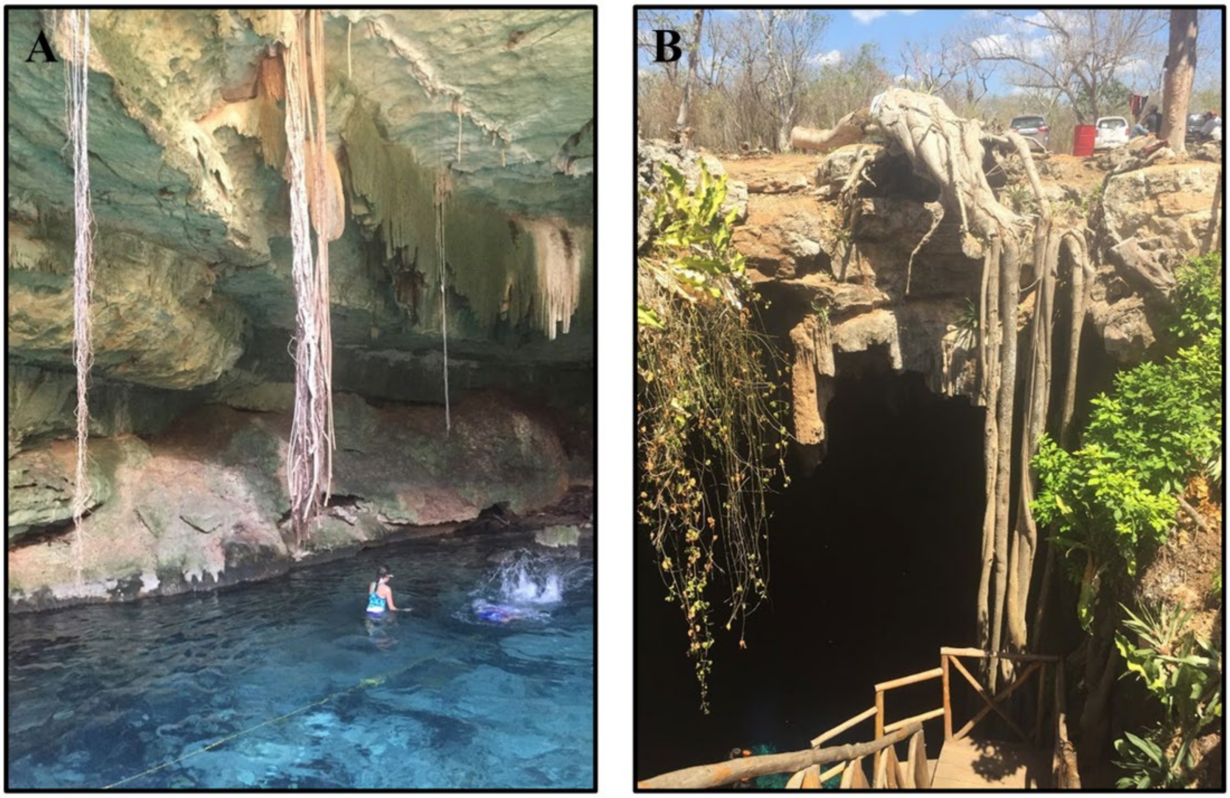

Figure 2.4 Tree roots at Cenote Kankirixché after being cut by the landowner (A) and resulting in the death of an Alamo tree at the entrance (B). Photograph: Rachel E. Adams.

2.5. Final thoughts

While tree roots have been studied in caves for decades (Jackson et al., 1999; Peñuelas & Filella, 2003), still relatively little is known about root characteristics in tropical systems, particularly for seasonally dry ecosystems where deep water access might be particularly important and where species-specific strategies are likely. This work documents observed rooting habits in caves as well as species-specific root morphologies for the first time. We were able to identify fourteen tropical tree species and one palm by root morphology along with four lianas. We hope to facilitate improved understanding of roots in caves and encourage more research on tree root exploration into rocks more broadly and the likely implications of this for above- and belowground processes. By discerning roots in situ, we also encourage landowners, tourist operations, and cavers to take note of the belowground biodiversity present to explicitly connect the forest overhead to the caves via these deep roots.

In addition, our work demonstrates that multiple species have the potential to access deep water in the caves and the karst aquifer. Understanding the holistic interactions between the surface and subterranean will better inform us about species-specific characteristics, biogeochemical processes occurring in the rhizosphere, and groundwater reliance in understudied tropical forests. This should contribute to protection and better management of the resources and ecosystem services that tropical forests and caves provide, especially in the face of expanding urbanization in Quintana Roo (Ellis et al., 2015). Describing and identifying these deep roots is just the beginning.

2.6. Acknowledgements

We would like to thank Peter Sprouse from Zara Environmental, LLC for providing information about the caves included in this study. This work was supported the National Geographic Society (CP-090ER-17), the MSC L.T. Jordan Institute for International Awareness at Texas A&M University, and the Department of Ecosystem Science and Management at Texas A&M University. The open access publishing fees for this article have been covered by the Texas A&M University Open Access to Knowledge Fund (OAKFund), supported by the University Libraries and the Office of the Vice President for Research.

2.7. References

Barton, H. A., and D. E. Northup. (2007). Geomicrobiology in cave environments: Past, current and future perspectives. *Journal of Cave and Karst Studies,* 69, 163–178.

Bleby, T. M., A. J. McElrone, and R. B. Jackson. (2010). Water uptake and hydraulic redistribution across large woody root systems to 20 m depth. *Plant, Cell and Environment,* 33, 2132–2148. https://doi.org/10.1111/j.1365-3040.2010.02212.x

Cañaveras J.C., Cuezva S., Sanchez-Moral S., Lario J., Laiz L., Gonzalez J.M., and C. Saiz-Jimenez. (2006). On the origin of fiber calcite crystals in moonmilk deposits. *Naturwissenschaften*, 93, 27-32. https://doi.org/10.1007/s00114-005-0052-3

Casper, B. B., H. J. Schenk, and R. B. Jackson. (2003). Defining a plant's belowground zone of influence. *Ecology,* 84, 2313–2321. https://doi.org/10.1890/02-0287

Durán-García, R., M. Méndez-Gonzalez, and A. Larqué-Saavedra. (2016). The biodiversity of the Yucatán Peninsula: a natural laboratory. *Progress in Botany*, 78, 237–258. https://doi.org/10.1007/124_2016_8

Ellis, E. A., K. A. Kainer, J. A. Sierra-Huelsz, P. Negreros-Castillo, D. Rodriguez-Ward, and M. DiGiano. (2015). Endurance and adaptation of community forest management in Quintana Roo, Mexico. *Forests,* 6, 4295–4327. https://doi.org/10.3390/f6114295

Estrada-Medina, H., R. C. Graham, M. F. Allen, J. J. Jiménez-Osornio, and S. Robles-Casolco. (2013). The importance of limestone bedrock and dissolution karst features on tree root distribution in northern Yucatán, México. *Plant and Soil,* 362, 37–50. https://doi.org/10.1007/s11104-012-1175-x

Howarth, F. G., S. A. James, W. McDowell, D. J. Preston, and C. T. Imada. (2007). Identification of roots in lava tube caves using molecular techniques: Implications for conservation of cave arthropod faunas. *Journal of Insect Conservation,* 11, 251–261. https://doi.org/10.1007/s10841-006-9040-y

Jackson, R. B., L. A. Moore, W. A. Hoffmann, W. T. Pockman, and C. R. Linder. (1999). Ecosystem rooting depth determined with caves and DNA. *Proceedings of the National Academy of Sciences of the United States of America,* 96, 11387–11392. https://doi.org/10.1073/pnas.96.20.11387

Jasinska, E. J., B. Knott, and A. J. McComb. (1996). Root mats in ground water: a fauna-rich cave habitat. *Journal of the North American Benthological Society,* 15, 508–519.

Maeght, J.-L., B. Rewald, and A. Pierret. (2013). How to study deep roots – and why it matters. *Frontiers in Plant Science,* 4, 1–14. https://dx.doi.org/10.3389%2Ffpls.2013.00299

McDonald, J.A. (2016). Deciphering the symbols and symbolic meaning of the Maya world tree. *Ancient Mesoamerica*, 27, 333–359. https://doi.org/10.1017/S0956536116000249

Peñuelas, J., and I. Filella. (2003). Deuterium labelling of roots provides evidence of deep water access and hydraulic lift by *Pinus nigra* in a Mediterranean forest of NE Spain. *Environmental and Experimental Botany,* 49, 201–208. https://doi.org/10.1016/S0098-8472(02)00070-9

Phillips, J.D. (2016) Biogeomorphology and contingent ecosystem engineering in karst landscapes. *Progress in Physical Geography,* 40, 503-526. https://doi.org/10.1177%2F0309133315624641

Poulter, B., D. Frank, P. Ciais, R. B. Myneni, N. Andela, J. Bi, G. Broquet, J. G. Canadell, F. Chevallier, Y. Y. Liu, S. W. Running, S. Sitch, and G. R. Van Der Werf. (2014). Contribution of semi-arid ecosystems to interannual variability of the global carbon cycle. *Nature,* 509, 600–603. https://doi.org/10.1038/nature13376

Rewald, B., C. Meinen, M. Trockenbrodt, J. E. Ephrath, and S. Rachmilevitch. (2012). Root taxa identification in plant mixtures – current techniques and future challenges. *Plant and Soil,* 359, 165–182. https://doi.org/10.1007/s11104-012-1164-0

Sánchez-Azofeifa, G.A., M. Quesada, J. P. Rodriguez, J. M. Nassar, K. E. Stoner, A. Castillo, T. Garvin, E. L. Zent, J. C. Calvo-Alvarado, M. E. R. Kalacska, L. Fajardo, J. A. Gamon, and P. Cuevas-Reyes. (2005). Research priorities for neotropical dry forests. *Biotropica,* 37, 477–485.

Schenk, H. J., and R. B. Jackson. (2005). Mapping the global distribution of deep roots in relation to climate and soil characteristics. *Geoderma,* 126, 129–140. https://doi.org/10.1016/j.geoderma.2004.11.018

Schwinning, S. 2010. The ecohydrology of roots in rocks. *Ecohydrology,* 3, 238–245. https://doi.org/10.1002/eco.134

Taboroši, D. (2006). Biologically influenced carbonate speleothems. *Perspectives on Karst Geomorphology, Hydrology, and Geochemistry - A Tribute Volume to Derek C. Ford and William B. White*. 307-317. https://doi.org/10.1130/2006.2404(26)

Villaseñor, J. L. (2016). Checklist of the native vascular plants of Mexico. *Revista Mexicana de Biodiversidad,* 87, 559–902. https://doi.org/10.1016/j.rmb.2016.06.017

Yanai, R.D., Fisk M.C., Fahey, T.J., Cleavitt, N.L., and B.B. Park. (2008). Identifying roots of northern hardwood species: patterns with diameter and depth. *Canadian Journal for Forest Research,* 38, 2862–2869. https://doi.org/10.1139/X08-125

3. BOUND AND MOBILE SOIL WATER ISOTOPE RATIOS ARE AFFECTED BY SOIL TEXTURE AND MINERALOGY, WHEREAS EXTRACTION METHOD INFLUENCES THEIR MEASUREMENT*

3.1. Abstract

Questions persist about interpreting isotope ratios of bound and mobile soil water pools, particularly relative to clay content and extraction conditions. Interactions between pools and resulting extracted water isotope composition are presumably related to soil texture, yet few studies have manipulated the bound pool to understand its influence on soil water processes. Using a series of drying and spiking experiments, we effectively labeled bound and mobile water pools in soils with varying clay content. Soils were first vacuum dried to remove residual water, which was then replaced with heavy isotope-enriched water prior to oven-drying and spiking with heavy isotope-depleted water. Water was extracted via centrifugation or cryogenic vacuum distillation (at four temperatures) and analyzed for oxygen and hydrogen isotope ratios via isotope ratio mass spectrometry. Water from centrifuged samples fell along a mixing line between the two added waters, but was more enriched in heavy isotopes than the depleted label, demonstrating that despite oven drying, a residual pool remains and mixes with the mobile water. Soils with higher clay + silt content appeared to have a larger bound pool. Water from vacuum distillation samples have a significant temperature effect, with high temperature extractions

---

* Reprinted with permission from "Bound and mobile soil water isotope ratios are affected by soil texture and mineralogy, whereas extraction method influences their measurement" by Adams, R.E., Hyodo, A., SantaMaria T., Wright, C.L., Boutton, T.W. and West J.B., 2020. *Hydrological Processes*, Vol. 34, pp 991-1003, Copyright 2020 John Wiley & Sons, Ltd.

yielding progressively more heavy-isotope enriched values, suggesting that Rayleigh fractionation occurred at low temperatures in the vacuum line. By distinctly labeling bound and mobile soil water pools, we detected interactions between the two that were dependent on soil texture. While neither extraction method appeared to completely extract the combined bound and mobile (total water) pool, centrifugation and high temperature cryogenic vacuum distillations were comparable for both δ^2H and δ^{18}O of soil water isotope ratios.

3.2. Introduction

Extraction of soil water for stable hydrogen and oxygen isotope (δ^2H and δ^{18}O) analyses has long been used to address ecological and hydrologic questions and has been approached using a variety of methodologies (Orlowski, Pratt, & McDonnell, 2016; Walker, Woods, & Allison, 1994). Recently, there has been increased interest in the impact that soil properties, namely clay minerals (Gaj et al., 2017a; Oerter et al., 2014), organic matter (Orlowski, Breuer, & McDonnell, 2016; Meißner, Köhler, Schwendenmann, Hölscher, & Dyckmans, 2014), and water content (Araguás-Araguás, Rozanski, Gonfiantini, & Louvat, 1995; Meißner et al., 2014; Newberry, Prechsl, Pace, & Kahmen, 2017) appear to have on measured soil water isotope ratios. In addition, lab studies under controlled conditions have revealed that sample preparation, extraction methods, and extraction conditions have the potential to alter the δ^2H and δ^{18}O of soil water (Araguás-Araguás et al., 1995; Gaj et al., 2017a; Orlowski et al., 2018b; Orlowski et al., 2016b). To determine the appropriate extraction method, interlaboratory comparisons across techniques and extraction conditions have been conducted using isotopically labeled water (Orlowski et al., 2018b; Walker et al., 1994). However, regardless of soil type, extraction method, or conditions, it is rare to reproduce the isotopic composition of water directly added to soils. This makes it difficult to identify the most reliable method for obtaining an accurate characterization of soil water isotope ratios.

In addition to the influence of soil properties and extraction conditions, the “two water worlds” hypothesis (Brooks, Barnard, Coulombe, & McDonnell, 2010; McDonnell, 2014) has entered the conversation. This concept is based on the idea that bound and mobile soil water are ecohydrologically separated within watersheds with important consequences for how we interpret water isotopes in these systems. The same concept might be applicable on a much smaller scale, in which bound water is described as hydration spheres associated with clay minerals and other particle surfaces and mobile water is the “free water” in soil pores (Araguás-Araguás et al., 1995; Kučerík, Tokarski, Demyan, Merbach, & Siewert, 2018; O’Neil & Truesdell, 1991; Savin & Hsieh, 1998). Some studies also include structurally bound water within clay minerals as a distinct bound pool, separate from water adsorbed on clay and organic matter surfaces (Savin & Hsieh, 1998). Recent studies that argue for the use of soil water vapor isotopes to quantify mobile and presumably plant-available pools (Oerter, Siebert, Bowling, & Bowen, 2019) or that find that mycorrhizal association affects the isotopic composition of plant-available water (Poca et al., 2019) highlight the need to improve our understanding of the isotopic composition of various soil water pools and how these relate to important hydrologic processes.

Attempts to resolve discrepancies between expected and observed soil water isotopic composition following extraction have included the use of mineral powders (Oerter et al. 2014), salt solutions (O’Neil & Truesdell, 1991), and silica gel (Asay & Kim, 2005; Lin, Horita, & Abe,

2018) to assess apparent isotopic fractionation associated with water-surface interactions (Chen, Auerswald, Schnyder, 2016). This is highlighted as causing predictable differences in $\delta^{18}O$ of mobile water from a reference water based on presence of particular clay minerals (Oerter et al., 2014). Gaj, Kaufhold, & McDonnell (2017) found that different clay minerals preferentially release adsorbed water at high temperatures and were more similar to the added reference water than extractions performed at lower temperatures. While these simplified systems offer important insight into potential mechanisms, they are less complex than real soils, in which multiple processes may be occurring simultaneously. Many studies oven dry soils at or above 105°C to remove residual water from the field before subjecting them to wetting treatments (Gaj et al., 2017a; Meißner et al., 2014; Newberry et al., 2017a & 2017b; Orlowski et al., 2018b; Orlowski et al., 2016a & 2016b; Orlowski et al., 2013; Thielemann, Gerjets, & Dyckmans, 2019; Walker et al., 1994). For high clay content soils, heating can potentially change soil structure and alter the way in which clays respond to rewetting (Jian, Berli, & Ghezzehei, 2018). On the other hand, if soils are not heated to remove residual water, this water may exchange with added water, making it difficult to assess potential extraction or handling effects. Some studies report that structural, interlayer water remains intact during drying at 105°C because this pool can only be removed at significantly higher temperature (>250°C) and under vacuum (Araguás-Araguás et al., 1995; Gaj et al., 2017b; Savin & Hsieh, 1998). Studies across extraction methods, though mainly via cryogenic vacuum distillation, have noted the influence of bound water on the isotopic composition of extracted soil water (Araguás-Araguás et al., 1995; Thielemann et al., 2019; Vargas, Schaffer, Yuhong, & Sternberg, 2017; Walker et al., 1994). Residual background water appears to leave a "memory effect" which causes deviation from reference water, particularly in high clay content soils (Newberry et al., 2017a). However, the magnitude of the effect that the bound pool has on the mobile pool is unknown. Few studies have effectively addressed this in full or manipulated the bound pool directly (Araguás-Araguás et al., 1995; Thielemann et al., 2019; Vargas, Schaffer, Yuhong, & Sternberg, 2017; Walker et al., 1994). Resolving these uncertainties is critical to our interpretations of soil water isotope ratios based on extracted soil moisture.

In this study, we separately labeled the bound and mobile pools in soils with varying clay content in order to detect mixing between the two. In addition, we compared the most common extraction techniques, cryogenic vacuum distillation and centrifugation, in an attempt to determine which method accurately captures the total soil water (bound and mobile pools). Vacuum extractions were further conducted under a range of temperatures to observe potential temperature effects on extraction efficiency. We hypothesized that: (i) soils with higher clay content would have stronger retention of labeled bound water compared to coarser-textured soils; (ii) cryogenic vacuum distillation would be more effective at removing total soil water (bound and mobile pools), whereas centrifugation would more readily extract the mobile fraction; and (iii) distillations performed at higher temperatures would release bound and mobile water and more accurately represent total soil water compared to lower temperature extractions and centrifugation.

3.3. Methods

Soils were collected from two locations in College Station, Texas, USA (soils TB and RA) and two locations at the Oklahoma State University Range Research Station near Stillwater, Oklahoma, USA (soils CD and CG). Sand (S; Pavestone Natural Play Sand, Atlanta, GA, USA) was also included in this experiment to represent a simple soil without the influence of clay minerals or organic matter (Kaiser & Guggenberger, 2003; Keil & Mayer, 2014). Soil texture was determined via hydrometer tests (Sheldrick & Wang, 1993). To assess clay mineralogy, X-ray diffraction (XRD) analysis was performed using a Bruker D8 diffractometer (Bruker AXS GmbH, Karlsruhe, Germany) at the Soil Mineralogy laboratory at Texas A&M University (Theisen & Bellis, 1964). The minerals contained in the samples were identified by matching against the mineral collection data from the International Centre for Diffraction Data (www.icdd.com) using the software, EVA from Bruker (Billerica, MA, USA).

Approximately 200 grams of each soil and S were air dried and sieved through a 2 mm screen sieve prior to water labeling and extraction. Soils and S were then vacuum dried (8.5 kPa, 105°C) for four days to constant weight to remove residual water. Samples were cooled inside the oven under vacuum in order to avoid rehydration with vapor or condensation. To label the bound pool, heavy isotope-enriched water (WaterE) of known isotopic composition (δ^2H: 165.4 ± 1.6 ‰, δ^{18}O: 19.91 ± 0.11 ‰; n = 9) was quickly added until samples were saturated. The samples were allowed to equilibrate for 72 hours in separate Whirlpak bags stored in a refrigerator (4°C) to minimize evaporation. Soils and S were then oven dried at 105°C to constant weight to remove the water, mimicking approaches used by other labs to presumably remove any mobile and bound water prior to labeling the soil water pool (Gaj et al., 2017a; Newberry et al., 2017a; Orlowski et al., 2016a; Orlowski et al., 2016b; Thielemann et al., 2019; Walker et al., 1994). Samples were again cooled inside the oven. Soils at this step could be exposed to vapor condensing from the laboratory environment while they cooled. The isotopic composition of this vapor would be on a mixing line between WaterE and the added heavy-isotope-depleted water (WaterD; see below), making its potential effect on total water difficult to distinguish from WaterE (results not presented). However, the rate of condensation is expected to be low relative to the exposure time, minimizing the influence of this water source. It is worth noting that similar studies either do not control for this or tend to ignore its presence (Newberry et al., 2017a; Orlowski et al., 2016a & 2016b; Thielemann et al., 2019). While it is expected to be minor, future work could address this potential complication directly through additional labeling experiments.

To label the mobile pool, the dried samples were then rewetted to saturation with heavy isotope-depleted water (WaterD) of a known composition (δ^2H: −93.7 ± 1.2 ‰, δ^{18}O: −15.29 ± 0.12 ‰; n = 12), followed again by a 72-hour equilibration period in separate Whirlpak bags in the refrigerator (4°C). After homogenization, glass scintillation vials (12 mL, Wheaton-DWK Life Sciences, Millville, NJ, USA) were promptly filled with wetted soil and sand, sealed, and placed in the freezer (0°C) until cryogenic vacuum distillation. Samples to be centrifuged were prepared at the same time. Pre-extraction soil weight was measured for all samples regardless of extraction method.

3.3.1. Centrifugation

A double-tube centrifuge setup was designed for this experiment (Figure B-1). Holes (1.5 mm) were drilled into the bottoms of 15 mL plastic centrifuge tubes (VWR International, LLC, Radnor, PA, USA). A piece of filter paper (Grade 1, 11 μm pore space, 70 mm diameter, Whatman, Inc., Piscataway, NJ, USA) was folded and placed inside each 15 mL tube to ensure that soil or sand remained in the tube but allowed water to escape. After being filled with wet sample (about 11 g for soil and 18 g for sand), the assemblage was placed in a 50 mL tube

(CentriStar™, Corning, Inc., Corning, NY, USA) and suspended with a washer in order to avoid contact between the sample and extracted water during centrifugation. Three replicates of each soil type were centrifuged using a Sorvall Legend RT+ (Thermo Fisher Scientific, Waltham, MA) at 5000 rpm (2700 *g*) for three 15-minute intervals at 20°C. Water collected in the large Falcon tube was removed after each round, weighed, and then mixed with the extracted water from subsequent rounds. Extracted water was transferred to vials (0.3 mL, Wheaton-DWK Life Sciences, Millville, NJ, USA) for stable isotope analysis. Samples were weighed after centrifuging to calculate water recovery rate. After centrifuging, soil or sand from each centrifuge tube was homogenized and transferred to individual scintillation vials for cryogenic vacuum distillation following the same protocol as described below. These distillation post-centrifuge (DPC) samples were extracted at 100°C.

3.3.2. Cryogenic vacuum distillation

Extractions were performed on a closed vacuum extraction line (West, Patrickson, & Ehleringer, 2006). Tubes on each port were outfitted with a metal sleeve, heating tape (Valin Thermal Solutions and Automation, Houston, TX, USA), and insulator to adjust and maintain temperature. Extractions were conducted at 80°C, 100°C, 150°C and 200°C in order to test the extraction efficiency at varying temperatures. Thermocouples connected to a CR1000 datalogger (Campbell Scientific, Logan, UT, USA) tracked the temperature of each port continuously. Extraction time varied with the amount of time that each initially frozen sample took to reach extraction temperature. Once extraction temperature was reached, the extraction continued for at least the length of time it took to reach that set temperature. This ensured that the sample spent a significant amount of time at the desired extraction temperature. The average extraction duration was 1.8 hours, with a minimum of 1.2 hours and a maximum of 3.2 hours. Extraction pressures began at 0.003 kPa. Extractions were considered complete when there was no longer vapor in the tubing and the tube on the cold finger was clear (no further visible condensation) in addition to remaining on the vacuum line for the allotted time at the desired extraction temperature. After extraction completion, both samples and recovered water were weighed to calculate water recovery rate. Soils and sand were weighed immediately post-extraction and weighed again after oven drying at 105°C for 48 hours.

3.3.3. Stable isotope analyses

Water recovered from centrifuged, cryogenic vacuum distillation, and DPC samples were transferred into vials for stable oxygen and hydrogen isotope analysis. Analyses were performed using a Delta V Advantage isotope ratio mass spectrometer linked to a High Temperature Conversion/Elemental Analyzer via a Conflo IV (Thermo Fisher Scientific, Waltham, MA, USA) at the Stable Isotope for Biosphere Science (SIBS) Laboratory (https://sibs.tamu.edu), at Texas A&M University. Calibration was performed using in-house water standards: SIBS-wA ($\delta^2H = -390.8 \pm 1.6$ ‰, $\delta^{18}O = -50.09 \pm 0.33$ ‰) and SIBS-wP ($\delta^2H = -34.1 \pm 1.9$ ‰, $\delta^{18}O = -4.60 \pm 0.24$ ‰). Quality control was performed using an in-house water standard, SIBS-wU ($\delta^2H = -120.2 \pm 1.5$ ‰, $\delta^{18}O = -15.95 \pm 0.27$ ‰). These in-house standards were calibrated using IAEA standards (VSMOW2, SLAP, and GISP). All isotope values are reported in VSMOW-SLAP scale.

3.3.4. Contribution of bound WaterE to water extracted via centrifugation

Following stable isotope analysis, we noted that the water extracted via centrifugation fell on a mixing line between WaterE and WaterD. We calculated the contribution of WaterE to $\delta^{18}O$ and δ^2H of the resulting water using a simple mixing model:

$$\text{Contribution of WaterE (\%)} = \frac{\delta_C - \delta_D}{\delta_E - \delta_D} \times 100 \qquad (1)$$

where δ_C, δ_D, and δ_E are the isotope ratios for the water extracted by centrifugation, WaterD, and WaterE, respectively. It is important to note that the measured isotope value for WaterE may not represent the actual bound water value after drying. During drying, isotopic fractionation is expected, resulting in bound water more enriched in heavy isotopes, making the difference between WaterE and WaterD greater. The magnitude of this enrichment in heavy isotopes could vary depending on soil characteristics, temperature, and potentially a minor effect of vapor isotopic composition. We did not attempt to estimate this effect given a lack of constraint on soil texture effects. Therefore, the measured value for WaterE is the lowest possible isotope value for the bound water in each soil. Since δ_E is the measured WaterE value, Equation 1 potentially overestimates the contribution of bound water to the measured composition of water extracted from soils and S via centrifuging.

3.3.5. Statistical evaluation

Data analysis was carried out with the statistical software R (R Core Team, 2019) run in RStudio (RStudio Team, 2016). Data was checked for normality using the Shapiro-Wilk normality test and checked for equal variance with the Brown-Forsythe test. If data was found to be normally distributed with equal variance, One-Way and Three-Way ANOVAs were conducted to compare the individual effects and combined interactions of variables (i.e. soil type, extraction method, extraction temperature, extraction duration) on resulting δ^2H and $\delta^{18}O$ values. Kruskal-Wallis tests were used if data had unequal variance. TukeyHSD mean comparisons provided insight into the differences between samples and extraction conditions. Linear regressions and one- or two-sample t-tests were also used to compare isotope results to soil properties and to other isotope results, respectively.

3.4. Results

3.4.1. Soil texture and mineralogy

Soils RA, TB, CD, and CG ranged in clay content from 9.9% to 27.2% (Table 3.1). The sand (S) was found to contain 2.5% clay-sized particles and 1.4% silt-sized particles. Soil organic carbon ranged from 1.32% to 1.92%. S did not contain organic carbon. The XRD analyses revealed that the major component of all soils and S was quartz, with an average relative abundance of 93.4% (Table 3.1). All four soils contained small amounts of orthoclase and albite while S contained orthoclase and calcite. CD and CG (Oklahoma soils) had low abundance of kaolinite and CD contained mica as well. While the Web Soil Survey suggested that both TB and RA (Texas soils) were smectitic soils (Soil Survey Staff, 2019), montmorillonite was only detected in TB.

Table 3.1 Characteristics of soils used in this study. Soil texture was assessed using the hydrometer method (Sheldrick & Wang, 1993). Soil organic carbon was measured by dry combustion using an Elemental Analyzer (Costech Analytical Tech, Inc, Valencia, CA, USA). Taxonomic class information was obtained from the USDA Natural Resources Conservation Service Web Soil Survey (Soil Survey Staff, 2019).

	CD	**CG**	**TB**	**RA**	**S**
Location	Stillwater, OK, USA	Stillwater, OK, USA	College Station, TX, USA	College Station, TX, USA	Not applicable
Latitude, Longitude	36.059600, -97.183233	36.055431, -97.190900	30.515792, -96.240623	30.574848, -96.363345	Not applicable
Taxonomic Class	Fine-loamy, siliceous, active, thermic Ultic Haplustalfs	Fine-loamy, siliceous, active, thermic Ultic Haplustalfs	Fine, smectitic, thermic Ultic Paleustalfs	Fine, smectitic, thermic Chromic Vertic Albaqualfs	Not applicable
Clay (%)	27.2	24.4	23.4	9.9	2.5
Silt (%)	3.4	42.9	34.2	25.5	1.4
Sand (%)	69.5	32.7	42.4	64.6	96.1
Soil Organic Carbon (%)	1.80	1.32	1.80	1.92	0
XRD analysis (relative %)					
Quartz	93	93	92	95	94
Albite	3	3	4	2	0
Orthoclase	3	3	3	3	2
Calcite	0	0	0	0	4
Montmorillonite	0	0	2	0	0
Mica	1	0	0	0	0
Kaolinite	1	2	0	0	0
Smectite	No	No	Yes	Yes	No

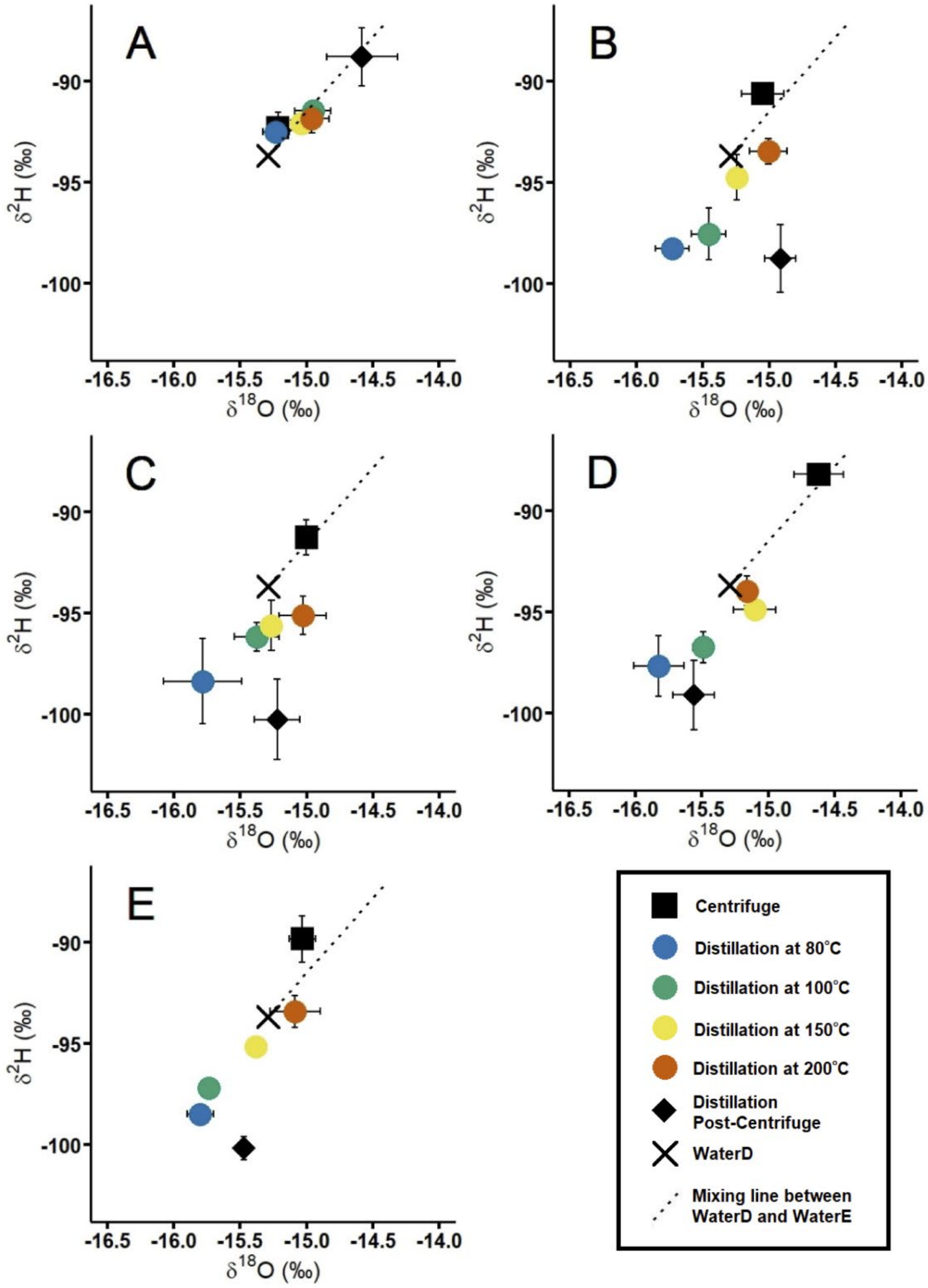

Figure 3.1 Isotope compositions of soil water extracted via centrifuging (square), vacuum distillation (circles), or distillation post-centrifuge (diamond) by soil type. Distillation extraction temperatures are denoted by color (80°C – blue, 100°C – green, 150°C – yellow, 200°C – orange). A mixing line (dashed line) between WaterD (×) and WaterE is δ2H = 7.359 δ18O + 18.89. Plots are organized by soils with increasing clay + silt content (A: sand, B: CD, C: RA, D: TB, E: CG). Error bars show the standard deviation of the three replicates for each sample.

3.4.2. Water extracted by centrifugation

Water extracted via centrifugation fell on a mixing line between the heavy isotope-enriched water (WaterE) and the heavy isotope-depleted water (WaterD; Figure 3.1). The $\delta^{18}O$ values of extracted water were significantly different from the $\delta^{18}O$ value of WaterD for all soil types ($p < 0.05$) except for CD ($t_2 = 2.62$, $p = 0.12$) (Figure 3.1B). The δ^2H of extracted water were significantly different from WaterD for all soil types ($p < 0.05$), except for S ($t_2 = 3.02$, $p = 0.09$) (Figure 3.1A). While the $\delta^{18}O$ values differed among soil types ($\chi^2(4, N = 15) = 11.08$, $p = 0.03$), only TB was significantly more ^{18}O-enriched than the other samples, which were all similar to each other (Figure 3.1D). The δ^2H values also differed among soil types ($\chi^2(4, N = 15) = 11.10$, $p = 0.03$), with generally more deuterium enriched water from soils with high clay + silt content. While the δ^2H values increased significantly with clay content ($R^2 = 0.47$, $p < 0.01$), the relationship was stronger when considering clay + silt content ($R^2 = 0.58$, $p < 0.01$).

Mean water recovery based on extracted water weight differed with soil type. More clayey soils had lower recovery (TB = 27.3%, CG = 36.2%) compared to sandy soils (RA = 45.8%, CD = 50.3%) and S (65.5%) with higher recovery ($F_{4, 10} = 5.70$, $p = 0.01$; Figure 3.2). Similar to the δ^2H values, water recovery decreased with clay content alone ($R^2 = 0.33$, $p = 0.03$), yet, the trend was stronger with clay and silt together ($R^2 = 0.61$, $p < 0.01$). There was more variability in recovery for S and sandy soils than clayey soils.

The contribution of WaterE to the centrifuged samples is an average of 1.26%, with a range of 0.21% to 2.24% for hydrogen and 0.15% to 2.50% for oxygen (Figure 3.3). The size of the bound pool remaining after oven-drying increased with clay content but, the relationship is only statistically significant for δ^2H ($R^2 = 0.47$, $p < 0.01$). When the relationship is assessed with clay and silt content combined, there is a significant increase in bound water contribution with increasing clay + silt content for δ^{18}O ($R^2 = 0.34$, $p = 0.02$) and δ^2H ($R^2 = 0.58$, $p < 0.01$).

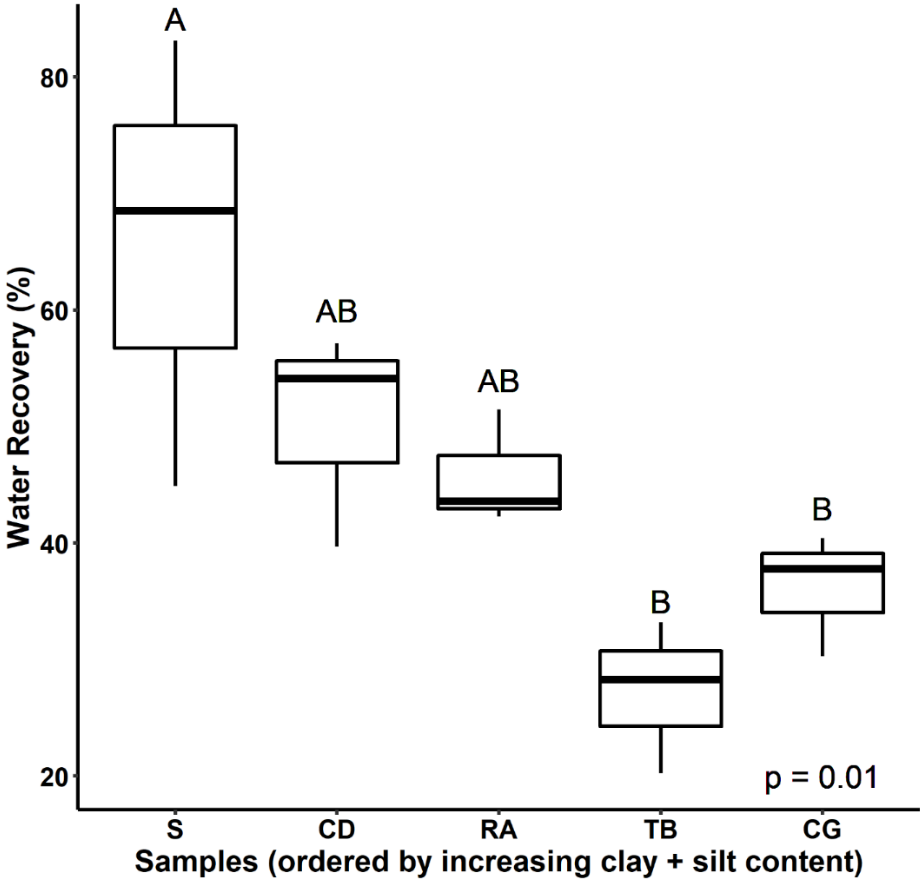

Figure 3.2 Water recovery by centrifuging. Water recovery was calculated by comparing the weight of water extracted to the calculated water in each sample. Three replicates per soil type were centrifuged. Samples on the x-axis are ordered by increasing clay + silt content.

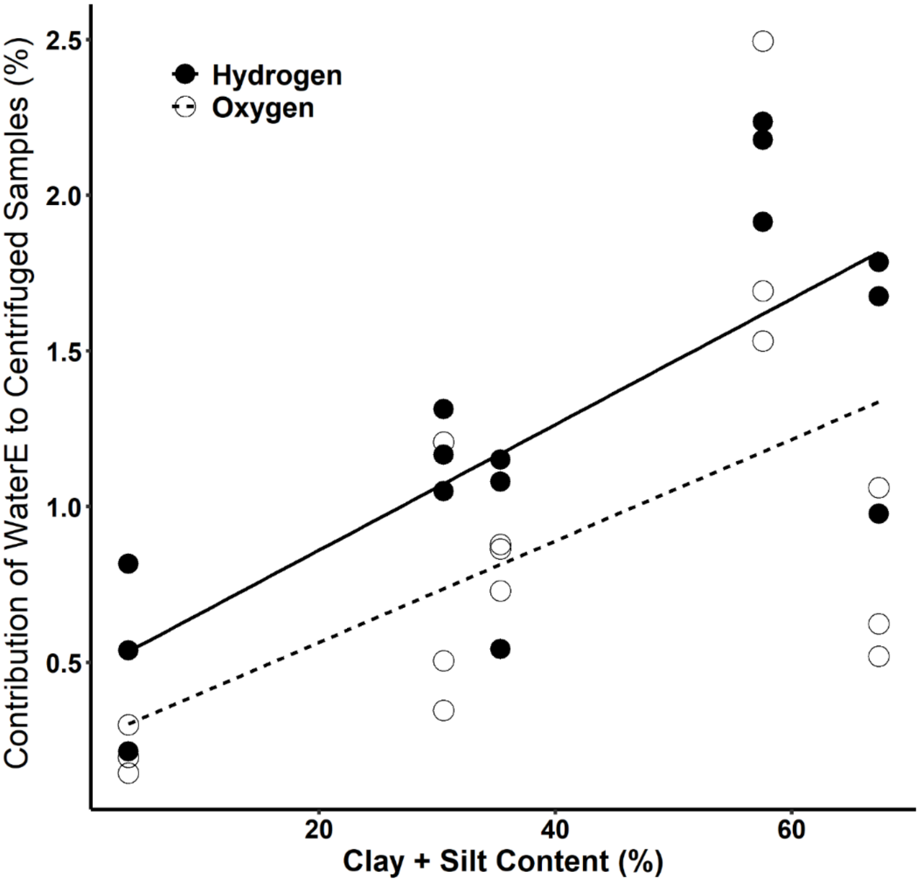

Figure 3.3 Contribution of WaterE to centrifuged samples based on δ^2H (closed circles; $R^2 = 0.58$, $p < 0.01$) and δ^{18}O (open circles; $R^2 = 0.34$, $p = 0.02$) as a function of clay and silt content. (See text for discussion on WaterE).

3.4.3. Water extracted by vacuum distillation

Compared to the water recovered from centrifuging, water extracted via cryogenic vacuum distillation did not fall on an isotope mixing line between WaterE and WaterD (Figure 3.1). Rather, the isotope values fell below the line and were overall heavy-isotope depleted. However, the δ^{18}O values of CD and S were the only ones statistically different from WaterD δ^{18}O values ($t_{10} = -2.32$, $p = 0.04$ and $t_{11} = 6.02$, $p < 0.01$, respectively). All soil types were different from WaterD based on δ^2H ($p < 0.01$ for all). Across soil types, there was a significant temperature effect on $\delta^{18}O$ ($\chi^2(3, N = 48) = 37.08$, $p < 0.01$) and δ^2H values ($\chi^2(3, N = 48) = 36.54$, $p < 0.01$), with higher extraction temperatures resulting in progressively more enriched water (Figure 3.4). Yet, extraction temperature did not impact water recovery rate based on water recovery weight ($F_{3,44} = 1.40$, $p = 0.26$; Table B-1) nor based on the difference between pre-and post-extraction soil weight ($F_{3,44} = 0.16$, $p = 0.92$; Table B-1).

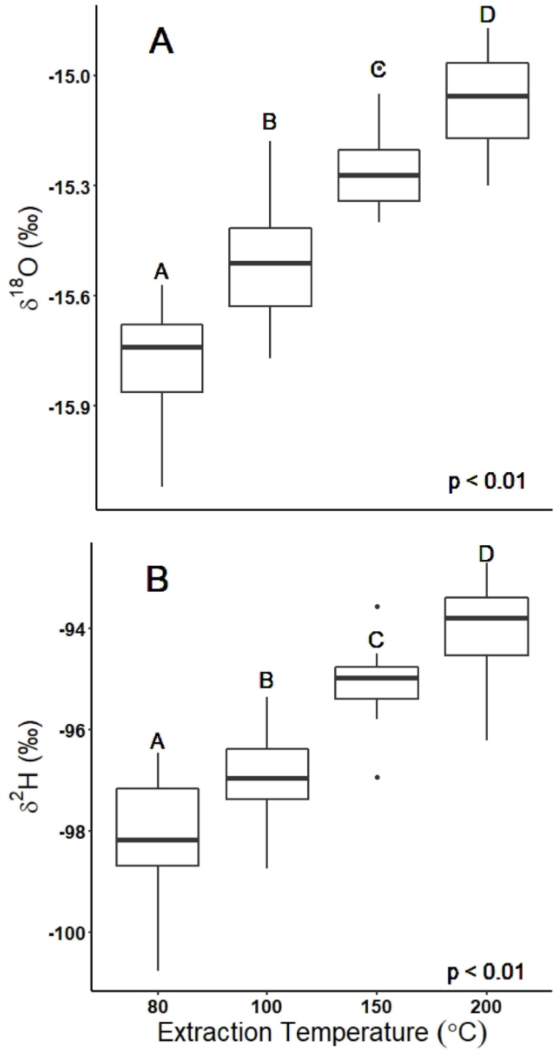

Figure 3.4 Temperature effect on $\delta^{18}O$ (A) and δ^2H (B) of water extracted from all soils via cryogenic vacuum distillation. S was not included in this comparison.

3.4.4. Distillation post-centrifuge (DPC)

The low water recovery (20.3 – 51.2% not including S; 83.1% with S) from centrifuging allowed us to extract the remaining water via vacuum distillation at 100°C. Water extracted from these samples differed in $\delta^{18}O$ across soil types, generally resulting in more heavy-isotope depleted values with decreasing sand content ($\chi^2(4, N = 14) = 12.12, p = 0.02$; Figure 3.5B). All soils with clay had similar δ^2H values and S had the highest δ^2H value ($\chi^2(4, N = 14) = 8.27, p = 0.08$; Figure 3.5F). Across soil types, recovery for DPC samples were not significantly different based on water weight ($F_{4,10} = 1.96, p = 0.18$) and sample weight ($F_{4,10} = 0.46, p = 0.77$).

DPC samples were more heavy-isotope depleted compared to the centrifuged and distillation samples. Overall, water extracted via distillation post-centrifuge had similar $\delta^{18}O$ ($F_{1,28} = 1.97, p = 0.17$) but differed in δ^2H ($\chi^2(1, N = 29) = 9.81, p < 0.01$) compared to their respective centrifuged samples. DPC samples differed from water extracted at 100°C via distillation (D100) for both $\delta^{18}O$ ($\chi^2(1, N = 28) = 4.03, p = 0.04$) and δ^2H ($\chi^2(1, N = 28) = 5.05, p = 0.03$).

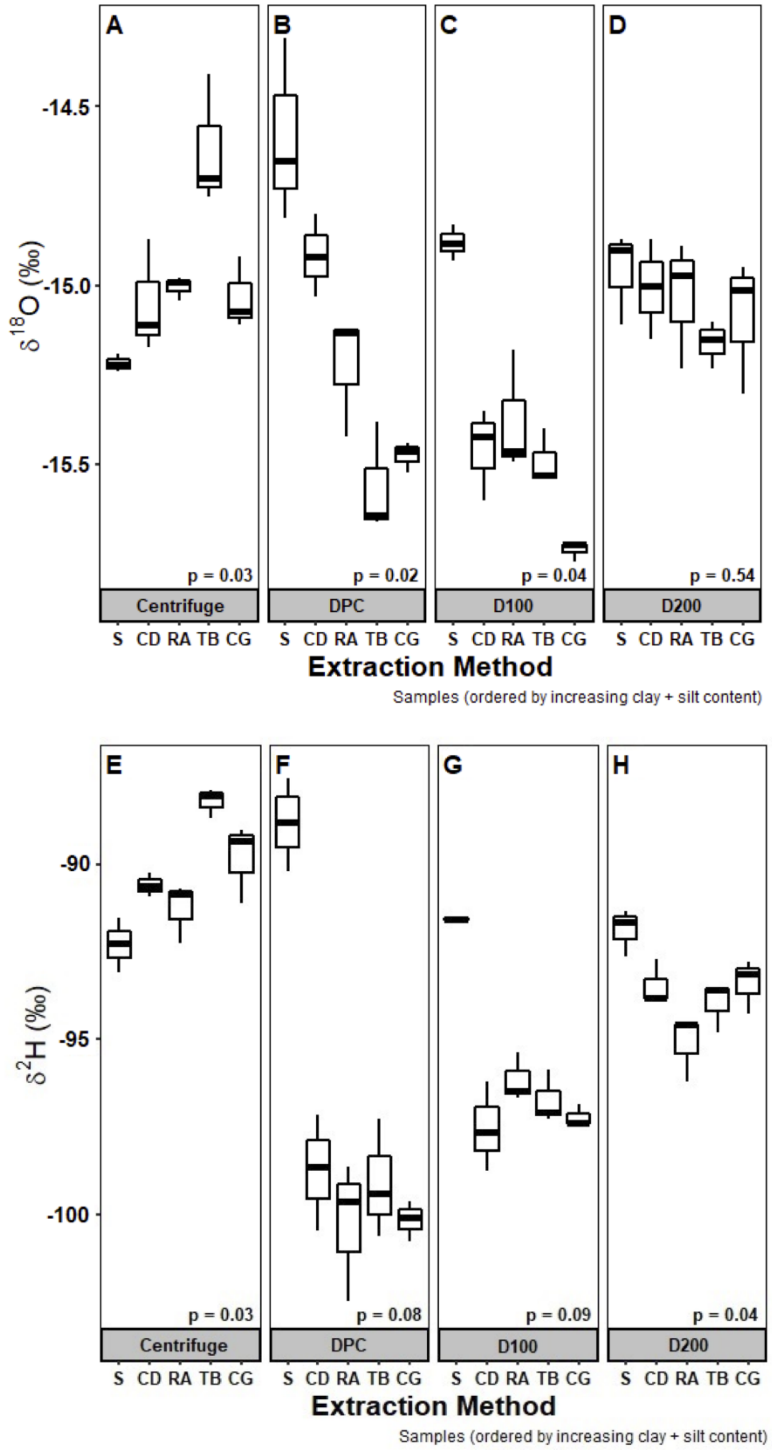

Figure 3.5 $\delta^{18}O$ and $\delta^{2}H$ of samples extracted by centrifuging, distillation post-centrifuge (DPC), vacuum distillation at 100°C (D100), and vacuum distillation at 200°C (D200). Samples are ordered by increasing clay + silt content.

3.4.5. Centrifugation versus cryogenic vacuum distillation

Water recovery based on extracted water weight between methods were significantly different ($\chi^2(4, N = 74) = 39.05$, $p < 0.01$). Centrifuging had an average water recovery rate of 45.0% (including S) and 39.9% (excluding S) and distillation had an average of 101.9% (including S) and 102.2% (excluding S).

Based on two-sample t-tests, the extractions conducted at 200°C (D200) were similar to their respective centrifuged samples in terms of $\delta^{18}O$ ($F_{1,28} = 0.85$, $p = 0.36$) but not δ^2H ($\chi^2(1, N = 29) = 18.08$, $p < 0.01$).

3.5. Discussion

3.5.1. Importance of sample preparation

We directly manipulated the bound pool in these soils by vacuum drying them prior to spiking with an isotopically distinct reference water, drying to mimic prior experimental pre-treatments and then labeling with a heavy isotope-depleted water to label both the apparent bound and mobile pools. This allowed us to remove a large fraction of residual water from the soils that we expected to otherwise have an influence on measured soil water isotope ratios and more directly test hypotheses about mismatches between "spike" water and measured water post extraction. The vacuum drying treatment was incorporated after a preliminary spiking experiment revealed the potential influence of residual water from the field (results not shown), consistent with reports from other studies (Araguás-Araguás et al., 1995; Newberry, Nelson, & Kahmen, 2017; Orlowski et al., 2016b).

Our results showed that the water extracted by centrifuging falls on a mixing line between WaterE and WaterD (Figure 3.1). We interpret this to mean that oven-drying at 105°C does not remove all bound water from soils and, while this bound water is not removed, it also readily mixes with the presumably mobile water added subsequently (Wang, Lu, Ren, & Li, 2011). The contribution of WaterE to the centrifuged samples ranged from 0.21% to 2.24% based on hydrogen and 0.15% to 2.50% based on oxygen. Retention increased with increasing clay + silt content (Figure 3.3). Again, the contribution of WaterE calculated using Equation 1 could overestimate the contribution of the bound water to the water extracted via centrifuging, as WaterE would have likely undergone evaporative enrichment during drying. However, the amounts calculated are in agreement with Thielemann et al., (2019), who found that soils with high clay content had bound pools accounting for 1.4% to 1.8% of the total soil water. Because the bound water and WaterD in our study are isotopically distinct from each other, only a small amount of heavy isotope-enriched bound water is needed to impact the isotopic composition of the extracted water. The calculated contribution amounts from Equation 1 exemplify this and are, therefore, useful, particularly when analyzing the impact of clay on soil water processes as described later in this discussion.

3.5.2. Impact of clay minerals on bound water

While we observed positive correlations between clay content and bound pool size, the type of clay minerals played an important role in these interactions. TB had only the third highest clay content and second highest clay + silt content among the soils in our study; however, it retained the most WaterE (Figure 3.3). This may be explained by the fact that TB contained montmorillonite, a 2:1 phyllosilicate smectite mineral (Table 3.1; Barnhisel & Bertsch, 1989; O’Neil & Kharaka, 1976). Smectite is noted to have double-layered hydration spheres adsorbed to clay particles, high cation exchange capacity, and therefore, increased matric potential (Oerter et al., 2014). While RA was reported to also contain smectite based on the USDA Web Soil Survey, the soil only contained 9.9% clay, decreasing the impact of the smectite clay minerals compared to TB (Soil Survey Staff, 2019). This is further supported by the fact that montmorillonite was not detected in the XRD analysis of RA (Table 3.1). According to the XRD analysis, CD and CG contained kaolinite, a common 1:1 layer mineral. Due to strong hydrogen bonding between layers, there is no interaction between soil water and these layers. Because of this, adsorption is limited to external surfaces, causing soils with 1:1 clay minerals to have low cation exchange capacity (Barton & Karathanasis, 2002). High temperature cryogenic vacuum distillation extractions on soils with kaolinite were found to produce isotope values similar to quartz, which is known to have negligible effects on soil water isotopes (Gaj et al., 2017a; Longstaff & Ayalon, 1990). Therefore, our results suggest that not only does clay content matter when evaluating relationships between bound and mobile soil water but clay mineral compositions, particularly the presence of smectite and other 2:1 layer clay minerals, may be crucial.

3.5.3. Isotopic patterns from centrifugation

Centrifuged samples showed that soils with higher clay + silt content appeared to have a larger bound pool as shown by the higher contribution of WaterE (Figure 3.3), which is consistent with prior reports (Araguás-Araguás et al., 1995; Gaj et al., 2017a; Orlowski et al., 2016a). In our experiment, finer-textured soils retained more water after oven drying, likely allowing for increased exchange with the mobile WaterD during the second 72-hour equilibration period.

However, texture alone cannot explain our results. The presence of montmorillonite in TB increased the retention of WaterE, even though it has only the second highest clay + silt content (Figure 3.3). Studies that assessed the exchange between water bound by clay mineral cations and mobile water suggested that cations like magnesium form inner and outer layers in the hydration spheres (Sposito et al., 1999). The inner layer forms strong hydrogen bonds preferentially with water molecules that have ^{18}O while the outer layer favors bonds with water molecules with ^{16}O (Oerter et al., 2014; O'Neil & Truesdell, 1991). If this mechanism is valid, one might expect that this exchange would result in lower δ^{18}O values of TB's mobile water pool relative to other soils. However, in our study, TB had the most ^{18}O enriched water extracted via centrifugation (Figure 3.1D). We suggest that the explanation of this apparent contradiction is that during the equilibration period after WaterE was added, inner and outer hydration spheres were formed on montmorillonite in TB as discussed in Oerter et al., (2014), causing TB's bound pool to have more ^{18}O from WaterE than the other soils after oven drying. When WaterD was added, there was still preferential bonding; however, WaterD had significantly less ^{18}O to contribute. Therefore, the large bound pool of ^{18}O from WaterE contributed to the majority of the mixing, resulting in a net enrichment of the mobile water extracted via centrifuging. It is important to note that there have been more studies on the isotopic effects of clay minerals on oxygen isotopes and few have commented on interactions with hydrogen (VanDeVelde & Bowen, 2013).

3.5.4. Centrifugation water does not represent the total water pool

It would be tempting to conclude that centrifuging is the "best" soil water extraction method because it captured this mixing and that water extracted with this method represents what is presumably a total water pool (bound plus mobile water). The distillation post-centrifuge (DPC) results provide additional insight to the underlying mechanisms. If there was complete mixing between the bound and mobile water pools (and no other extraction effects), the isotopic composition of the centrifuged water and the post-centrifuge water should be the same. By extracting the water remaining after centrifuging on the vacuum line, we showed that water extracted via centrifuging and DPC are different from each other, particularly in hydrogen (Figure 3.1). S shows most clearly this effect: the centrifugation values are most similar to WaterD and the DPC values fall along a mixing line between WaterD and WaterE (Figure 3.1A). The vacuum distillation values fall between these two extremes. These results suggest that centrifuged water represents a different portion of the total water pool, reflecting a mixture between the bound and mobile waters, but biased towards the mobile pool.

If the centrifuge water is biased towards the mobile pool, then the DPC water is biased towards the bound pool. This allows us to gain insight into the bound pool and the interactions between clay + silt content and clay mineralogy. In Figure 3.5B, it is shown that $\delta^{18}O$ declined with increasing clay + silt content, suggesting that vacuum distillation after centrifuging was able to extract the remainder of the mobile water plus an ^{18}O depleted bound pool. For TB, if we were able to capture all bound water (^{18}O-enriched inner and ^{18}O-depleted outer hydration spheres), it's respective DPC samples should be enriched in ^{18}O compared to the other samples (Oerter et al., 2014). However, this was not the case. We conclude that while vacuum distillation is able to extract bound water from clays, it is unable to access inner hydration spheres formed around particular cations at 100°C. We believe that this is related to the matric potential of the fine-grained soil particles (Trask, 1959). Interestingly, all soils have similar $\delta^{2}H$ values, except for S

(Figure 5F). It appears that the presence of fine-grained soil particles, interact with hydrogen in similar ways regardless of the amount.

To explore this further, we compared the DPC samples to the vacuum distillations performed at the same temperature (D100). For D100 samples, there were negative trends with $\delta^{18}O$ and increasing clay + silt content ($\chi^2(4, N = 14) = 9.79$, $p = 0.04$; Figure 3.5C) and significant deuterium enrichment in S relative to all the soils ($\chi^2(4, N = 14) = 8.04$, $p = 0.09$; Figure 3.5G). While these patterns in $\delta^{18}O$ and δ^2H were similar to the DPC samples, the $\delta^{18}O$ trend is not as strong for the D100 samples. This is most likely because the D100 and DPC samples do not reflect the same pools. There is significantly more mobile water in the D100 samples compared to the DPC samples, as the DPC samples represent the pool after a large portion of the mobile water was extracted via centrifuging. Despite this, we still find distinct differences in the effects of fine-grained soil particles on oxygen and hydrogen isotopes. When comparing $\delta^{18}O$ and δ^2H values for vacuum distillations conducted at 200°C (D200), there was no significant difference in $\delta^{18}O$ ($F_{4,10} = 0.83$, $p = 0.54$; Figure 3.5D) and δ^2H became more similar to S ($\chi^2(4, N = 15) = 10.17$, $p = 0.04$; Figure 3.5H), with the exception of RA and TB. At higher temperatures, the matric potential effects on oxygen and hydrogen both diminish as hydrogen bonds between fine-grained soil particles and bound water are more easily broken at high temperatures (Gaj et al., 2017b). This supports other studies which found that bound water is more readily released at higher temperatures (Araguás-Araguás et al., 1995; Gaj et al., 2017a; Walker et al., 1994; Wang et al., 2011).

3.5.5. Isotopic patterns from cryogenic vacuum distillation

There was a significant temperature effect for soils extracted on the vacuum line, with increasing extraction temperatures yielding more heavy-isotope enriched values and plotting along lines of apparent temperature-dependent fractionations, particularly for ^{18}O (Figure 3.1). The ^{18}O enrichment with temperature suggests a Rayleigh-type fractionation effect occurred in the vacuum line. Rayleigh fractionation is evident if evaporation is not complete and a portion of the original water is not captured (Majoube, 1971). This alters the isotopic composition of the collected water sample, as heavy-isotope depleted water evaporates more readily. In our study, higher extraction temperatures allowed for more water (both mobile and bound) to be released and resulted in a more complete extraction compared to those performed at lower temperatures. A similar temperature effect has been observed by other studies (Araguás-Araguás et al., 1995; Gaj et al., 2017a; Orlowski, Winkler, McDonnell, & Breuer, 2018).

Based on our calculations for water recovery for vacuum distillations, we found that the average recovery based on water weight was over 100% (Table B-1). The average recovery based on sample weight was 98.99% (Table B-1). These recovery assessments suggest that the extractions performed, regardless of temperature, were “complete”. But the isotope results show that some of the extractions were not complete, particularly those performed at lower temperatures (80°C and 100°C). This is consistent with observations by Gaj et al., (2017a). During distillation, soil particles transferred to the cold finger with the extracted water, even though quartz wool was placed above samples to prevent transfer (Thielemann et al., 2019). Particles in extracted water therefore will overestimate recovery based on water weight and will underestimate recovery based on sample weight. Common mass-based recovery estimates may be insufficient to describe completeness of extractions with respect to isotope ratios of the extracted water and perhaps in part explaining variability in results from seemingly complete extractions (Orlowski et al., 2018b).

3.5.6. Conceptual model for total soil water

Overall, our results are consistent with previous work showing that soil properties, in particular the presence and mineralogy of clays, have an influence on the isotopic composition of bound and mobile soil water pools, but that this influence remains poorly constrained, potentially limiting inferences that can be drawn from soil water isotopes in hydrological and ecological studies. Based on our results and prior published work, we developed a conceptual model of the oxygen isotope effects on observed in this experiment to better understand potential mechanisms here and suggest hypotheses to guide future work (Figure 3.6).

The following describes the patterns observed for the sand samples, non-smectitic soil samples, and smectitic soil samples and offers hypotheses for the underlying mechanisms. To begin, we assume that vacuum drying at 105°C removes residual mobile and bound water (including all or nearly all of the water in hydration spheres of soil cations), allowing the experiment to begin without initial isotopic influence. After vacuum oven drying, WaterE is added and all of the soils have total soil water pools that resemble WaterE. This water, however, is expected to partition into "perturbed" and free pools as a function of clay cation exchange capacity and the presence of adsorbed, hydrated cations (Oerter et al., 2014). When the soils are oven dried at 105°C (at ambient atmospheric pressure, mimicking common "spiking" experiment protocols), bound water in all soils and S will undergo some degree of evaporative enrichment, making the value for WaterE the lowest possible value for the bound water pool. At the same time, the non-smectitic soils (and sands to a lesser extent) preferentially retain ^{16}O in the bound, hydration spheres of adsorbed minerals associated with kaolinite clay minerals, expected to be dominated by monovalent cations like Na^+ and K^+. For the soils with smectite, the same depletion occurs for monovalent cations, as well as for the outer hydration spheres of divalent cations. However, a retention of ^{18}O in the inner hydration spheres of divalent cations is expected. This partitioning of ^{18}O to the inner hydration spheres is expected to have a relatively stronger heavy-isotope enrichment effect on retained water, resulting in a net enrichment of the total soil water pools in smectite soils compared to the other soils and WaterE following oven drying. When WaterD is subsequently added, it is a large fraction of the total water, causing overall heavy-isotope depletion of the total water pools. At this point, the amount of WaterE retained after oven drying matters to the isotopic composition of the total water pool based on mass balance. As shown in Figure 3.3, sand retained the least heavy-isotope enriched water while the soil with smectite (TB) retained the most. These differences in soil texture plus clay mineralogy result in enrichment of the total soil water compared to WaterD, with sand being the least enriched and smectite soils being the most (high clay content plus retention of ^{18}O-enriched water in hydration spheres). In addition, during this step, we believe mobile WaterD exchanges with the heavy isotope-enriched bound water, contributing heavy-isotope enriched water to the "free" water. During centrifugation, this mobile water is removed, with sand having the highest average water recovery (65.5%) and the smectite samples having the lowest (27.3%; Figure 3.2). Water extracted by the centrifuge should access the mobile pool only. For all soils, we expect some enrichment of the mobile pool as the fractionated, bound WaterE pool exchanges with WaterD in the prior step.

The degree of enrichment increases with a larger fine-grained fraction and the presence of smectitic clays. After centrifugation, the remaining water is biased towards WaterE as a function of soil matric potential (resisting water removal by centrifugation) and the isotope effects associated with cation hydration spheres and exchange with the added WaterD.

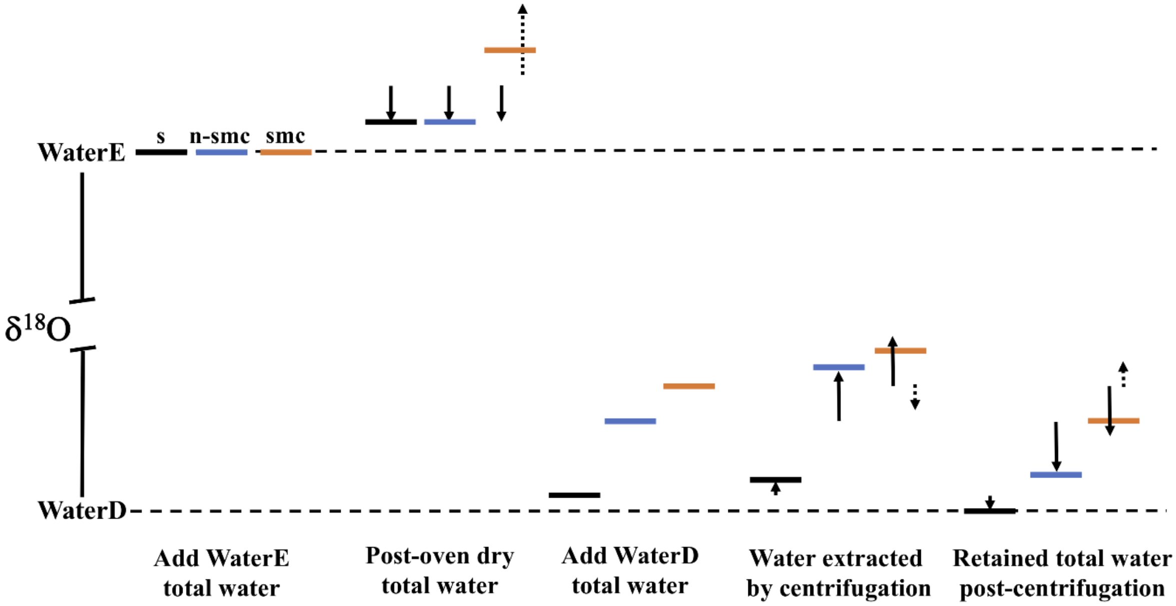

Figure 3.6 Conceptual model for observed oxygen isotope effects on the total soil water pool in sand (black bar), non-smectite soils (blue bar), and smectite soils (orange bar) at various steps in the experiment. Solid and dashed arrows indicate fractionation associated with monovalent and divalent cation hydration, respectively. The length denotes the relative degree of fractionation, incorporating the additional influence of fine-grained fraction driven water retention on the isotopic composition of the total soil water pool.

If this conceptual model is correct, one prediction is that the total water pool for all samples will not fall on a mixing line in δ^2H-δ^{18}O space between the two reference waters since we do not expect the isotope effects of ion hydration and exchange to be the same for δ^2H and δ^{18}O. It is important to note that while there is evidence for these underlying mechanisms for oxygen isotopes (Oerter et al., 2014), hydrogen isotope interactions in soils are less understood. This makes it difficult to accurately calculate the isotopic composition of the total water pool for both δ^2H and δ^{18}O, preventing us from making strong statements about the best extraction method. However, according to the model, the total soil water pool should be between WaterE and WaterD, though somewhat offset from a mixing line. In general, the water extracted via centrifuging, distillation at 150°C, and distillation at 200°C fall to the right of WaterD on the δ^2H-δ^{18}O plots (Figure 3.1). The differences between these three extraction methods are relatively small for all of the soils with limited or no montmorillonite, suggesting that centrifugation and high temperature distillations reasonably represent total soil water for non-smectitic clay soils. We suggest that future studies employ a similar sample preparation method to ours to control the isotopic composition of bound and mobile pools in order to directly study soil water extraction effects without the influence of residual water from the field. Further, studies should not only focus on clay content but also include soils with a wide range of clay types in order to directly assess the impacts of mineralogy and organic matter on soil water isotope composition. Extraction temperature is clearly important for cryogenic vacuum distillations in this and other studies, therefore future studies should avoid extractions at one temperature. Other common soil water extraction methods (for example, lysimeters) should also be considered to compare to distillation and centrifuging.

3.6. Conclusions

Consistent with prior reports, we demonstrated that oven-drying is inefficient in removing residual water from soils. By labeling this apparently bound water, we were further able to detect interactions between bound and mobile soil water pools. The isotope ratios of soil water obtained by centrifugation were consistent with bound and mobile water mixing but this mixing appeared to be incomplete, as shown by cryogenic vacuum extraction of water remaining after centrifugation. Cryogenic vacuum distillations had substantially higher water recovery, but the isotopic composition of extracted water was affected by temperature-dependent effects and was different from that obtained by centrifugation. High temperature (between 150°C and 200°C) distillations yielded water that was most similar to the WaterD value, however, water derived by centrifugation suggested the presence of a residual pool not clearly reflected in the distillation water. Based on these results, we suggest a conceptual model for water isotope fractionation in soils linked to both clay content and mineralogy but point out that important uncertainties remain. Future work evaluating extraction methods should include explicit characterization of clay mineralogy. In addition, our work implies caution in interpreting isotope ratios of extracted soil water and a need to better characterize processes that govern soil water fractionation.

3.7. Acknowledgements

Research was supported by USDA/NIFA Hatch Projects 1003961 and 1002535, the Sid Kyle Endowment and the Sid Kyle Graduate Merit Assistantship from the Department of Ecosystem Science and Management (ESSM) at Texas A&M University (TAMU), National Geographic Society Early Career Grant (CP-090ER-17), the National Science Foundation Graduate Research Fellowship Program, the TAMU ESSM Franklin F. Wasko Graduate Merit Fellowship, the TAMU Office of Graduate and Professional Studies Graduate Diversity Fellowship, and the TAMU AgriLife Strategic Initiative Assistantship. Xiangmin Sun provided the soils from Oklahoma as well as performed initial experiments, which provided a foundation for this study. We would like to thank Dr. Youjun Deng and Bidemi T. Fashina from the Soil Mineralogy laboratory in the Department of Soil and Crop Sciences at Texas A&M University for performing the XRD analysis and offering assistance to interpret the results.

3.8. References

Araguás-Araguás, L., Rozanski, K., Gonfiantini, R., & Louvat, D. (1995). Isotope effects accompanying vacuum extraction of soil water for stable isotope analyses. *Journal of Hydrology*, 168, 159–171.

Asay, D.B. & Kim S.H. (2005). Evolution of the Adsorbed Water Layer Structure on Silicon Oxide at Room Temperature. *The Journal of Physical Chemistry B*, 109, 16760–16763.

Barnhisel, R. I., & Bertsch, P. M. (1989). Chlorites and Hydroxy-Interlayered Vermiculite and Smectite. In S. B. Weed & J. B. Dixon (Eds.), *Minerals in Soil Environments* (2nd ed., pp. 729–788). Madison, WI, USA: Soil Science Society of America.

Barton, C. D., & Karathanasis, A. D. (2002). Clay Minerals. In R. Lal (Ed.), *Encyclopedia of Soil Science* (pp. 187–192). New York, New York, USA: Marcel Dekker, Inc.

Chen, G., Auerswald, K. & Schnyder, H. (2016). ^{2}H and ^{18}O depletion of water close to organic surfaces. *Biogeosciences,* 13, 3175–3186.

Gaj, M., Kaufhold, S., Koeniger, P., Beyer, M., Weiler, M., & Himmelsbach, T. (2017). Mineral mediated isotope fractionation of soil water. *Rapid Communications in Mass Spectrometry*, 31(3), 269–280.

Gaj, M., Kaufhold, S., & McDonnell, J. J. (2017). Potential limitation of cryogenic vacuum extractions and spiked experiments. *Rapid Communications in Mass Spectrometry*, 31, 821–823.

Jian, M., Berli, M., & Ghezzehei, T.A. (2018). Soil Structural Degradation During Low-Severity Burns. *Geophysical Research Letters,* 45, 5553–5561.

Kaiser, K., & Guggenberger, G. (2003). Mineral surfaces and soil organic matter. *European Journal of Soil Science*, 54, 219–236.

Keil, R. G., & Mayer, L. M. (2014). Mineral Matrices and Organic Matter. In H.D. Holland & K.K. Turekian (Eds.), *Treatise on Geochemistry* (2nd ed., pp. 337–359). Elsevier Ltd.

Kučerík, J., Tokarski, D., Demyan, M. S., Merbach, I., & Siewert, C. (2018). Linking soil organic matter thermal stability with contents of clay, bound water, organic carbon and nitrogen. *Geoderma*, 316, 38–46.

Lin, Y., Horita, J., & Abe, O. (2018). Adsorption isotope effects of water on mesoporous silica and alumina with implications for the land-vegetation-atmosphere system. *Geochimica et Cosmochimica Acta,* 223, 520–536.

Longstaffe, F. J., & Ayalon, A. (1990). Hydrogen-isotope geochemistry of diagenetic clay minerals from Cretaceous sandstones, Alberta, Canada: evidence for exchange. *Applied Geochemistry*, 5, 657–668.

Majoube, M. (1971). Fractionnement en oxygène 18 et en deutérium entre l'eau et sa vapeur. *Journal de Chimie Physique et de Physicochimie Biologique*, 68, 1423–1436.

McDonnell, J.J. (2014). The two water worlds hypothesis: ecohydrological separation of water between streams and trees? *WIREs Water*, 1, 323–329.

Meißner, M., Köhler, M., Schwendenmann, L., Hölscher, D., & Dyckmans, J. (2014). Soil water uptake by trees using water stable isotopes (δ^2H and δ^{18}O)–a method test regarding soil moisture, texture and carbonate. *Plant and Soil*, 376, 327–335.

Newberry, S.L., Prechsl, U. E., Pace, M., & Kahmen, A. (2017). Tightly bound soil water introduces isotopic memory effects on mobile and extractable soil water pools. *Isotopes in Environmental and Health Studies*, 53(4), 368–381.

Newberry, S.L., Nelson, D. B., & Kahmen, A. (2017). Cryogenic vacuum artifacts do not affect plant water-uptake studies using stable isotope analysis. *Ecohydrology*, 1–10.

Oerter, E.J., Siebert, G., Bowling, D.R., & Bowen, G. (2019). Soil water vapour isotopes identify missing water source for streamside trees. *Ecohydrology,* 12, 1-16.

Oerter, E.J., Finstad, K., Schaefer, J., Goldsmith, G. R., Dawson, T., & Amundson, R. (2014). Oxygen isotope fractionation effects in soil water via interaction with cations (Mg, Ca, K, Na) adsorbed to phyllosilicate clay minerals. *Journal of Hydrology*, 515, 1–9.

O'Neil, J. R., & Kharaka, Y. K. (1976). Hydrogen and oxygen isotope exchange reactions between clay minerals and water. *Geochimica et Cosmochimica Acta*, 40, 241–246.

O'Neil, J. R., & Truesdell, A. H. (1991). Oxygen isotope fractionation studies of solute-water interactions. In H. Taylor, J. R. O'Neil, & I. Kaplan (Eds.), *Stable Isotope Geochemistry: A Tribute to Samuel Epstein* (Vol. 3, pp. 17–25). Geochemical Society.

Orlowski, N., Winkler, A., McDonnell, J. J., & Breuer, L. (2018). A simple greenhouse experiment to explore the effect of cryogenic water extraction for tracing plant source water. *Ecohydrology*, 11, 1-12.

Orlowski, N., Breuer, L., Angeli, N., Boeckx, P., Brumbt, C., Cook, C. S., … McDonnell, J. J. (2018). Inter-laboratory comparison of cryogenic water extraction systems for stable isotope analysis of soil water. *Hydrology and Earth System Sciences*, 22, 3619–3637.

Orlowski, N., Breuer, L., & McDonnell, J. J. (2016). Critical issues with cryogenic extraction of soil water for stable isotope analysis. *Ecohydrology*, 9, 3–10.

Orlowski, N., Pratt, D. L., & McDonnell, J. J. (2016). Intercomparison of soil pore water extraction methods for stable isotope analysis. *Hydrological Processes*, 30, 3434–3449.

Poca, M., Coomans, O., Urcelay, C., Zeballos, S.R., Bodé, S., & Boeckx, P. (2019). Isotope fractionation during root water uptake by *Acacia caven* is enhanced by arbuscular mycorrhizas. *Plant and Soil*, 1-13.

Renée Brooks, J., Barnard, H. R., Coulombe, R., & McDonnell, J. J. (2010). Ecohydrologic separation of water between trees and streams in a Mediterranean climate. *Nature Geoscience*, 3, 100–104.

R Core Team (2019). R: A language and environment for statistical computing. R Foundation for Statistical Computing, Vienna, Austria. URL https://www.R-project.org/.

RStudio Team (2018). RStudio: Integrated Development for R. RStudio, Inc., Boston, MA URL http://www.rstudio.com/.

Savin, S. M., & Hsieh, J. C. C. (1998). The hydrogen and oxygen isotope geochemistry of pedogenic clay minerals: principles and theoretical background. *Geoderma*, 82, 227–253.

Sheldrick, B., & Wang, C. (1993). Particle Size Distribution. In M. R. Carter (Ed.), *Soil Sampling and Methods of Analysis* (pp. 499–511). Boca Raton, FL, USA: Lewis Publishers/CRC Press.

Sofer, Z., & Gat, J. R. (1972). Activities and concentrations of oxygen-18 in concentrated aqueous salt solutions: Analytical and geophysical implications. *Earth and Planetary Science Letters*, 15, 232–238.

Soil Survey Staff. (2019). Web Soil Survey. Retrieved from Natural Resources Conservation Service, United States Department of Agriculture https://websoilsurvey.sc.egov.usda.gov/.

Sposito, G., Skipper, N. T., Sutton, R., Park, S., Soper, A. K., & Greathouse, J. A. (1999). Surface geochemistry of the clay minerals. *Proceedings of the National Academy of Sciences*, *96,* 3358–3364.

Theisen, A. A., & Bellis, E. (1964). Quantitative analysis of clay mineral mixtures by X-ray diffraction. *Nature*, 204, 1228–1230.

Thielemann, L., Gerjets, R., & Dyckmans, J. (2019). Effects of soil-bound water exchange on the recovery of spike water by cryogenic water extraction. *Rapid Communications in Mass Spectrometry*, 33, 405–410.

Trask, P. D. (1959). Effect of grain size on strength of mixtures of clay, sand, and water. *Bulletin of the Geological Society of America*, 70, 569–580.

VanDeVelde, J. H., & Bowen, G. J. (2013). Effects of chemical pretreatments on the hydrogen isotope composition of 2:1 clay minerals: Clay mineral isotope treatment effects. *Rapid Communications in Mass Spectrometry*, 27, 1143–1148.

Vargas, A. I., Schaffer, B., Yuhong, L., & Sternberg, L. da S. L. (2017). Testing plant use of mobile vs immobile soil water sources using stable isotope experiments. *New Phytologist*, 215, 582–594.

Walker, G. R., Woods, P. H., & Allison, G. B. (1994). Interlaboratory comparison of methods to determine the stable isotope composition of soil water. *Chemical Geology: Isotope Geoscience*, 111, 297–306.

Wang, Y., Lu, S., Ren, T., & Li, B. (2011). Bound water content of air-dry soils measured by thermal analysis. *Soil Science Society of America Journal*, 75, 481.

West, A. G., Patrickson, S. J., & Ehleringer, J. R. (2006). Water extraction times for plant and soil materials used in stable isotope analysis. *Rapid Communications in Mass Spectrometry*, 20, 1317–1321.

4. INVESTIGATING DEEP ROOTING SPECIALIZATION IN A TROPICAL KARST REGION

4.1. Abstract

In seasonally dry and water-limited ecosystems, trees with deep roots can reach reliable water at depth, allowing them to maintain positive water status throughout dry periods. Yet, documenting rooting depth, root architecture, and below ground biodiversity is difficult. DNA barcoding of roots aids these assessments, providing insight into deep rooting specialization and connecting observations below ground to those easily made on the surface. While root diversity has been evaluated in a variety of locations globally, the semi-evergreen tropical forests of Quintana Roo, Mexico remain understudied. Here, deep roots in caves, some in contact with the shallow karst aquifer, provide the opportunity to directly survey root diversity and distribution. We evaluated relationships between above and below ground community structure to identify deep rooting species and potential controls on root prevalence. Paired above and below ground plots were established at five selected caves to assess relative abundance for each species in surface and cave plots with DNA barcoding. Patterns in above and below ground diversity were evaluated in relation to tree basal area, root basal area, and site characteristics. Results showed that 38 species had roots in the caves, including trees, lianas, and a palm; yet, below ground diversity was dominated by species from the genus *Ficus*. While some species with large individuals had roots in the caves, root abundance and deep rooting specialization was not easily predicted by tree size. Similar to other studies in karst systems, bedrock appears to limit root growth, as sites with larger conduits allowed for more roots to access the below ground environment. Across sites, tree, species, and root abundance decreased with increasing distance inland, implying depth to

groundwater influences community composition. These findings demonstrate that while there is specialization for deep rooting in this karst landscape, local and landscape geology and hydrology have apparent control on deep water access. Resulting competition for space and resources may have consequences for species-specific and community-level water use strategies to combat water stress in this seasonally dry tropical karst ecosystem.

4.2. Introduction

Deep rooting has been noted as an advantageous plant strategy, particularly in water-limited ecosystems, as it can allow access to reliable resources at depth (Meinzer et al. 1999, Mitchell et al. 2008, Johnson et al. 2014). Studies have shown that trees with deep roots often have more consistent sap flow, increased hydraulic conductance, more positive water potential, and overall lower water stress during dry seasons (McElrone et al. 2004, Doody and Benyon 2011, Johnson et al. 2014, Nardini et al. 2016). Understanding the structure and function of deep roots, and roots in general, is a critical aspect of plant physiology and ecosystem dynamics (Maeght et al. 2013, Pierret et al. 2016). Not only are deep roots avenues for water and nutrient uptake, they can play key roles in biogeochemical cycles and have implications for climate change survival strategies, especially when considering water access in drying conditions. The distribution of deep roots has been modeled in relation to potential evapotranspiration and soil texture (Schenk and Jackson 2005), predicting that they occur most commonly in dry to subhumid regions. However, much of the underlying empirical work is from temperate environments globally, despite this expected prevalence in arid or seasonally dry climates (Evaristo and McDonnell 2017). Therefore, documentation of deep roots and consequently the identification of deep rooting specialists in these regions remains inadequate.

Perhaps not surprisingly, maximum root depth is noted to be highest in trees compared to other plant forms (Canadell et al. 1996, Schenk and Jackson 2002), with a positive relationship between root and shoot biomass observations from forests and woodlands across the globe (Mokany et al. 2006). The repeated observation that species with significant above ground biomass support large root systems has led to hypotheses regarding deep rooting specialization and subsequent water access among individuals of different sizes and species capable of achieving significant amounts of above ground biomass (Dawson 1998, Meinzer et al. 1999). In addition, root architecture is important to consider as resources are distributed unevenly below ground and variation in access can influence plant performance (Lynch 1995, Bodner et al. 2013, Fry et al. 2018). Some species are characterized by dimorphic root systems, allowing them to shift water sources from shallower to deeper soil layers in the dry season to maintain plant performance and then shifting back to shallower sources in the wet season when soil is rewetted (Meinzer et al. 1999, Bleby et al. 2010, Nardini et al. 2016). This avoids expending unnecessary resources to bring water from depth when it is available for use closer to the surface. On the other hand, lateral root systems may be more common in areas with fine textured soils and hard pans (Casper et al. 2003), accompanied by physiological or morphological traits to withstand spatiotemporal water availability in shallow layers (Kukowski et al. 2013). Therefore, there are species differences, environmental influences, and mechanistic trade-offs, which make the phenomenon of deep rooting rather complex (Fan 2015, Silvertown et al. 2015, Weemstra et al. 2016).

A compelling region to study deep roots is the state of Quintana Roo, Mexico on the eastern edge of Yucatán Peninsula. Because of the seasonally dry climate (Durán-García et al. 2016), this is a location where deep rooting is predicted to occur. And in fact, numerous observations of roots emerging from the ceiling and walls of the shallow caves confirm this prediction (Adams et al. 2020). In addition, a relatively shallow karst aquifer underlies the entire peninsula (Bauer-Gottwein et al. 2011), seemingly accessible by vegetation and, potentially, a stable water source in the dry season. As water table depth has been shown to influence community composition (Goedhart and Pataki 2011, Zolfaghar et al. 2014) and rooting depth (Fan et al. 2017), notable variation in root abundance exposed in caves across the region suggest there may be underlying controls on root exploration and subsequent access to below ground resources. Despite the fact that roots in caves in Quintana Roo have been observed and photographed by tourists, cavers, and locals, to date, the wealth of potential insights to deep rooting afforded by the potential to access these roots directly has not been explored.

A few studies, often using indirect methods, have been conducted on the Yucatán Peninsula to investigate rooting depth, water access, and use by co-occurring tropical trees that grow atop limestone bedrock (Querejeta et al. 2007, Hasselquist et al. 2010, Estrada-Medina et al. 2013b, 2013a, Santiago et al. 2016). It has been found that roots were confined to the top layers of bedrock, limited by fractures and conduits. In the neighboring state of Yucatán, maximum rooting depths of 5 m were still several m away from the water table (Querejeta et al. 2006, Estrada-Medina et al. 2013a). This work showed that, surprisingly, the largest evergreen trees were not able to directly access groundwater but rely on water within the voids of the sascab, a softer layer in the bedrock at 2.5 – 5 m depth with high porosity. At the El Eden Ecological Reserve in northern Quintana Roo, evergreen trees were shown to be taking up water from deeper sources than deciduous species in early successional forests; however, the stable isotope composition of stem water from evergreens were, in general, heavy isotope-enriched compared to groundwater, suggesting the aquifer was still unreachable or not being readily utilized (Hasselquist et al. 2010). Yet, direct observations of roots in caves that are deeper than those in other locations on the peninsula imply deep rooting is more nuanced than previously discussed.

The caves in Quintana Roo therefore provide a window into the below ground environment, through which direct access to sample and study roots in situ is possible (Peñuelas et al. 2003, McElrone et al. 2007, Maeght et al. 2013, Nardini et al. 2016). This allows us to investigate below ground biodiversity and identify deep rooting specialists with molecular tools. Studies employing DNA barcoding, a technique that utilizes universal regions or markers within the genome that have species-to-species variation, have become more common to uncover below ground species abundance and rooting depth (Jackson et al. 1999, Howarth et al. 2007, Jones et al. 2011, Mommer et al. 2011, Ramalho et al. 2018). DNA barcoding has promising applications, allowing researchers to set the foundation for species abundance, richness, and diversity below ground across a variety of ecosystems (Pärtel et al. 2012, Träger et al. 2019). Patterns in rooting depth, root mass distribution, and presumed resource niches among different species provide insight into water and nutrient use strategies, competition, and specialization (Mommer et al. 2010, Jones et al. 2011, Kesanakurti et al. 2011). These studies have been crucial in expanding our perspective of vegetation composition, plant processes, and biological interactions beyond the above ground plant parts.

Therefore, this study sought to (1) identify potential deep rooting specialists in Quintana Roo, (2) determine if specialization and root abundance was predicted by above ground observations, and

(3) document the influence that depth to groundwater has on root prevalence in this region. Relative species abundance and root abundance was compared to respective measurements made above ground to uncover patterns in dominance above and below ground. We also evaluated the potential impact that site characteristics such as elevation, distance from the coast, and depth to groundwater had on tree, species, and root abundance. First, we hypothesized that (1) a fraction of tree species appear below ground, consistent with specialization among some species for deep rooting, resulting in a significant decrease in biodiversity from the above ground forest. We anticipated that (2) species with large individuals observed above ground would provide the majority of the roots in the caves and, consequently, sites with larger trees on the surface would have more roots exposed in the associated cave. We predicted that (3) sites closer to the coast with shallower depth to groundwater would have more roots.

4.3. Methods

4.3.1. Site descriptions

All sites were located in northern Quintana Roo, Mexico between the cities of Paamul and Akumual (Figure 4.1). The region is defined by a seasonally dry tropical climate with a distinct dry season between November and April during which only 20 to 30% of the annual 1400 mm of precipitation falls on average (Hernández-Terrones et al. 2015, Durán-García et al. 2016). A precipitation gradient, increasing from west to east, favors more evergreen species in Quintana Roo compared to the drier, western state of Yucatán (Sánchez-Sánchez and Islebe 2002). Historically, this region experienced disturbance in the form of agroforestry by the Maya, forest fires, and hurricanes (Sánchez-Sánchez et al. 2015), suggesting that the communities included in this study are all in some state of regeneration. Soils are thin and poorly developed, typically no more than 20 cm thick (Estrada-Medina et al. 2013a). Soil thickness is heterogeneous with areas of bare rock and others with deeper, soil-filled conduits in the bedrock. Weathering of the bedrock provides roots an avenue to grow deeply and potentially reach the subterranean environment below. Roots are seen in direct contact with the groundwater in many of the caves in the region (Adams et al. 2020).

Five caves that had existing below ground surveys and detailed cave maps were chosen to be included in this study (Trimmis 2018). To survey a cave, the location and elevation of a physical survey station at the cave entrance is recorded with a handheld GPS unit and verified with digital elevation models, if available. From this station, the distance, inclination, and direction to subsequent survey stations placed progressively deeper into the cave are measured. Simultaneously, an individual following the survey team sketches the features along the trajectory between survey stations to document passage size, speleothems, pools of water, and any other unique features. The survey data then yields two- and three-dimensional line plots and georeferenced shapefiles so the path, profile, and footprint of the system can be viewed (Texas Speleological Survey, Austin, TX, USA).

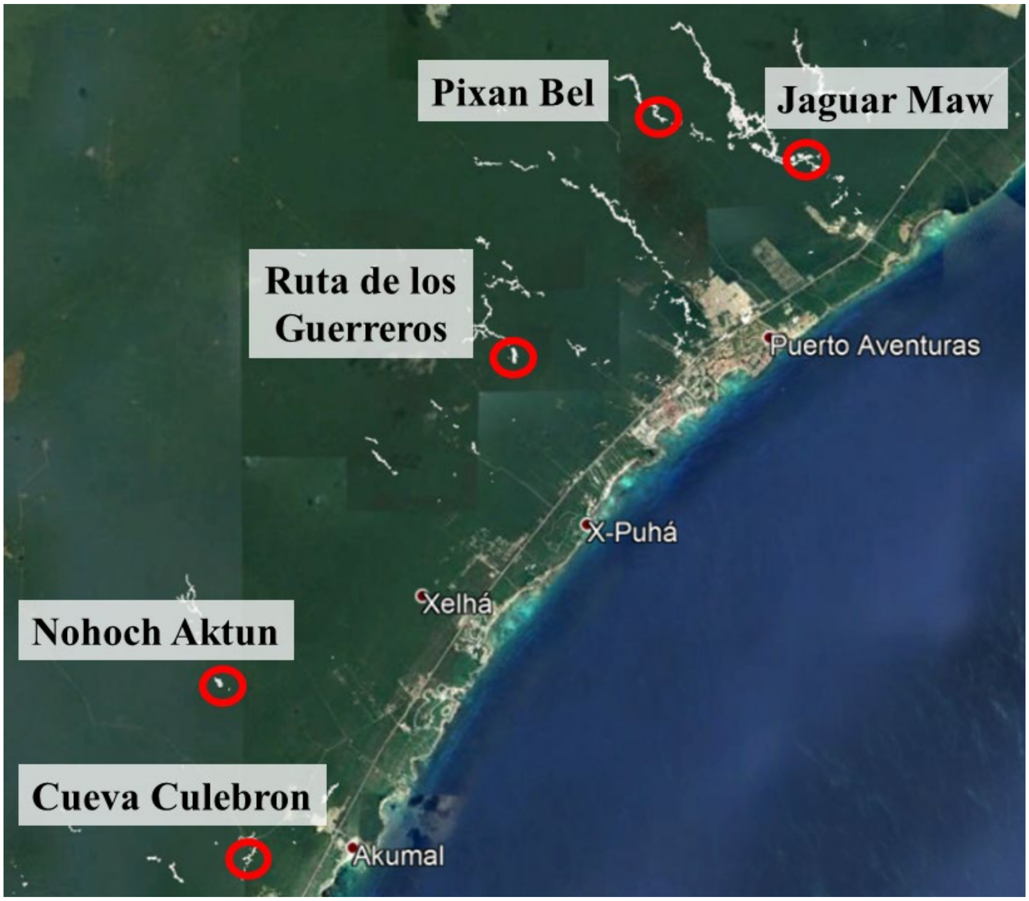

Figure 4.1 Site locations in Quintana Roo, Mexico.

4.3.2. Detailed site descriptions

Cueva Culebron: Cueva Culebron is commercial cave located near Akumal and 2 km from the coast. Depth to groundwater at the main entrance is 4.6 m with pools scattered throughout the meandering passages. Ceiling height is relatively even throughout the wide rooms, with an average of 2.4 m. Columns, associated formations, and Mayan stone walls guide cavers throughout system. The forest above ground is closed-canopy, reducing the abundance of understory trees, though palms are prevalent. Despite the cave being open for tours, the impact to the natural environment is minimal to none compared based on conversations with the landowners.

Jaguar Maw: Jaguar Maw is located near Paamul and 3.1 km from the coast. At the time of sampling, the cave was being developed as a show cave for an ecotourism operation. While clearing was not occurring on the headprint of the cave (the area above the cave), there were 1 to 2 m wide rock trails being built leading up to the entrances and flagging throughout the system to guide future visitors. The locations of the above and below ground plots used in this study were not included in this development, eliminating the human influence on our observations. Despite being relatively close to the coast, Jaguar Maw does not have exposed water, preventing us from making depth to groundwater measurements, though the maximum depth to the floor is 3.4 m. Passages are generally large and flat, with ceiling heights varying from 1.7 to 2.1 m. Though easy to walk through, many columns and a maze pattern can make it difficult to navigate.

Ruta de los Guerreros: This maze-like system is on the same property as a popular tourist cave and cenote, though this cave is not being utilized for tours. Located 3.7 km from coast and nearby Puerto Aventuras, the depth to groundwater was 9.3 m. Open rooms with tall ceilings (average 5.4 m tall) are contrasted by narrow passages with some places having prominent pools. Unlike the other sites, there are only two known entrances to this cave.

Nohoch Aktun: This commercial cave is close to the city of Akumal and 5.2 km from the coast. Defined by large collapses, it is difficult to travel far enough through the cave without seeing daylight. The depth to groundwater was recorded as 9.7 m below the surface at the collapse closest to the plots. Though this cave lacks prominent formations, the large, open passages and clear blue water is what attracts visitors. The landowners have been digging out the sediment mainly formed from sunken calcite rafts not only to make the pools deeper but to create an artificial path through the cave. Development is centered around the main entrance and parking lot, where trees have been cleared for buildings and trails. Therefore, initial plots that were within footprint of this development were excluded from the randomized selection, ensuring physical plots surveyed were further away from this portion of the system (see plot establishment description below).

Pixan Bel: The entrance to this extensive cave system, with nearly 12 kilometers of mapped passage, is located 6.4 km from the coast and the nearby town of Paamul, making this site the furthest inland and most remote of our study areas. There are many large trees and palms though some small trees and vines are still present. The main entrance was formed from a large collapse, which is common in this region. The depth-to-groundwater at the entrance was 11.4 m from the surface with the bedrock being around 3 m thick at the dripline. However, the ceiling rapidly slopes towards the main passage, increasing the bedrock thickness further into the cave. There is as much as an 8.7 m elevation change between below ground plots, according to the cave survey. Because the map available prior to arriving in the field only included the passages around the entrance, the sampling was focused here. Passage height in the areas surveyed ranged from 3.2 to 4.3 m.

4.3.3. Plot establishment

With the use of detailed cave maps and survey data, multiple paired above and below ground plots were randomly established at each site. To determine plot locations, hypothetical transects were established following the general direction and length of the cave passages. 100 m^2 plots were initially created on the transects with the number of plots corresponding to the length of the transect, requiring 10% of the transect to the included in the total plot area. For example, if the transect length is 100 meters, one 100 m^2 plot covered 10% of the transect. For those transects less than 100 meters, it was randomly determined if a plot was to be created on the transect or not. Then the plots physically established and surveyed in the field were randomly selected from those created prior to going to the field. Using the survey data, GPS locations on the surface mirroring the location of the survey stations below ground were gathered before arriving at the sites. While the above ground plots were 100 m^2 in size, the below ground plots averaged 500 m^2. The area of the plots inside the caves was increased to account for lateral root growth and to avoid the potential for root access to be restricted by speleothems, particularly large columns that are common in these systems. The area of the plot was calculated using the cave maps and the software, ImageJ (Java, 2019).

4.3.4. Above ground surveys

In the surface plots, surveys were conducted in order to assess forest composition. The diameter and height of all individuals with a diameter at breast height (DBH) $\geq$ 5 cm were measured and recorded. For multi-stemmed trees, the diameter of all stems associated with the individual were measured. Basal area for all trees was calculated by individual. For discussion purposes, individuals were noted as being small, medium, or large if the DBH was 5 to 14.9, 15 to 24.9, and $\geq$ 25 cm, respectively, based on anticipated tree sizes for this area (Whigham et al. 1991). Photographs of the leaves and bark of all individuals were captured to verify initial species assignments made in the field. Voucher specimens were collected for those individuals and species unable to be identified in the field. Leaf, seed, and bark characteristics were used to assign species as well as DNA barcoding (see protocol below). Species lists were created and relative species abundance within and across sites was calculated based on total counts and basal area. The voucher specimens were deposited at the S.M. Tracy Herbarium in College Station, Texas, USA (https://essm.tamu.edu/facilities/research/sm-tracy-herbarium/).

We addressed site-to-site variation by documenting differences in bedrock characteristics as these could potentially impact root abundance and access to groundwater. Therefore, depth to groundwater was evaluated at the entrance by measuring the distance from the edge of the entrance to the surface of the water. If the plumb line did not touch water, the distance and inclination to the nearest pool of water in the cave was recorded. Inside the cave, we recorded ceiling height within the below ground plots. Average depth underground and bedrock thickness was assessed by comparing the inclination of the survey stations within the below ground plots to the elevation of the entrance station and elevation of the land surface above the plot. Elevation and distance from the coast was evaluated using Google Earth.

4.3.5. Below ground surveys

Below ground, diameter was measured for all visible roots within the plot to complement the vegetation surveys made above ground. The structure of roots was noted as being fine (< 2 mm diameter), a singular coarse root (> 2 mm diameter), or a large mass of intertwined roots (Adams et al. 2020). When a large mass was encountered, the diameter of the entire mass was measured rather than measuring all the individual roots that comprised the mass. To relate to above ground basal area measurements, the cross-sectional area of all individual roots and root masses was calculated and compared to the area surveyed below ground. This allowed us to evaluate which sites had more roots, not only in terms of abundance based on total counts but size as well.

Samples of all visible roots were collected in each plot and blotted dry before being sealed in Whirl-Pak bags (Nasco, Fort Atkinson WI, USA) with silica gel (VWR International, LLC, Radnor, PA, USA), replaced as necessary to ensure complete drying. While a single root was gathered from the fine and singular coarse roots, multiple roots were sampled from the large masses. All roots with distinct morphological differences were collected from the large masses. All roots were transported to Texas A&M University (College Station, TX, USA) and kept in a dry environment until processing.

4.3.6. DNA barcoding protocol

DNA analysis was conducted at the Texas A&M AgriGenomics Laboratory. Samples were ground in a bead mill prior to DNA extraction with a NucleoSpin Plant II kit (Macherey-Nagel, Düren, Germany). Extractions were carried out according to the manufacturer's protocol. PCR amplification was conducted using the genetic markers, *matK* and *trnH-psbA* (Bolson et al. 2015, Rosario et al. 2019), and the KAPA 3G Plant PCR kit (Kapa Biosystems, Wilmington, MA, USA; (Schori et al. 2013). Cycling conditions were modified from Jones et al. 2011 for *matK* (95°C 3min; 95°C 20sec, 51°C 20sec, 72°C 1min x 40 cycles; 72°C 10min). The cycling protocol for *trnH-psbA* varied slightly (95°C 3min; 95°C 25sec, 51°C 25sec, 72°C 1min x 40 cycles; 72°C 5min). For leaves, we found that the internal transcribed spacer region, ITS2, along with *trnH-psbA* provided reliable species assignments (Chen et al. 2010, Tripathi et al. 2013, Bolson et al. 2015). Sequences, cycling conditions, amplification and sequencing success rates, and references for all primers used are provided in Table C-1.

Successfully amplified PCR products were purified with the QIAquick PCR Purification Kit (QIAGEN, Hilden, Germany) before being sequenced at the Laboratory for Genome Technology at the Institute for Plant Genomics and Biotechnology (Texas A&M University, College Station, TX, USA) via Sanger Sequencing. Species identification was performed using the basic local alignment search tool (BLAST) against the GenBank database. Trusted assignments were those with a query cover or percent identity of at least 99%. Final species assignments were verified with a comprehensive list of plants native to Mexico along with comparisons to species that were expected to be present at these sites in Quintana Roo (Villaseñor 2016). For low resolution assignments or species not available in the databases, samples were compared with sequences of leaves collected from above ground plots. Accession numbers used in this study are provided in Table C-4.

When amplification or sequencing failed, gross morphology of coarse roots aided in identification as there are several species with differences in epidermis color, cortex color, and features on the root surface (Adams et al. 2020). To compliment the biodiversity assessments on the surface, a list of species present below ground at each site was compiled and relative species abundance within and across sites was calculated based on total counts.

4.3.7. Rooting habit by species

We organized species into groups based on their prevalence below ground. There were three groups identified: above ground only, rare below ground, and common below ground. Those classified as common below ground had a relative abundance across sites of 5% or greater. We also noted that some species were found below ground only and were not captured on the surface. This categorization allowed us to understand the rooting habit of the species at the sites.

4.3.8. Above and below ground abundance index

We calculated the relative abundance above and below ground for each species and compared the two by:

$$\frac{(1 - \mathrm{R})}{(1 - \mathrm{S})} - 1, \tag{1}$$

where R is the fraction of roots and S is the fraction of stems identified for each species in relation to the total roots and stems observed across all sites. Therefore, for those species more abundant above ground than below ground, the value will be greater than 0 and if the species was more abundant below ground, the value will be less than 0. This allowed us to compare above and below ground abundance between species and assess patterns in dominance. Following DNA barcoding of the roots, we identified several species of lianas and one palm, which were not targeted in the above ground sampling. Because of this, calculations for below ground abundance excluded these roots for this index.

4.3.9. Statistical evaluation

All data analysis was conducted with the statistical software R (R Core Team, 2019) run in RStudio (RStudio Team, 2019). Relative species abundance of trees and roots identified was calculated across all sites in order to assess general patterns in above and below ground biodiversity in the region. Tree basal area (m^2/ha) by site as well as basal area by species was calculated. Root area (cm^2/m^2) by site was evaluated. For each site, the Simpson diversity index and rarefaction species richness was assessed for the above and below ground communities (excluding lianas and the palm) using the R package vegan. Changes in diversity between the surface and subterranean was evaluated Welch's t-test, as this data was found to have unequal variance. Linear and logistic regressions were used to evaluate relationships between tree and root abundance as well as root area and site characteristics (depth to groundwater, elevation, and distance from the coast) to uncover influences from physical differences among sites. Cave ceiling height, depth underground, and bedrock thickness was highly variable at each site and was not well constrained by our field assessments or use of the survey data. Therefore, these site characteristics were excluded from analyses.

4.4. Results

4.4.1. Site characteristics

Surveys of each site revealed variation in depth to groundwater, elevation, and distance from the coast within below ground plots (Table 4.1). Cueva Culebron was the site closest to the coast (2.0 km) with the lowest elevation (11.2 m above sea level). Consequently, Pixan Bel was the site furthest inland (6.4 km) with the highest elevation (18.7 m above sea level). Depth to groundwater measured at the cave entrance generally increased with distance inland.

Site	Elevation (masl)	Distance from the coast (km)	Depth to Groundwater (at entrance; m)	Average Ceiling Height (m)	Number of Paired Plots Surveyed
Cueva Culebron	11.2	2.0	4.6	2.4 ± 0.03	2
Jaguar Maw	11.3	3.1	> 3.4[†]	1.9 ± 0.29	2
Nohoch Aktun	14.8	5.2	9.7	4.6 ± 0.50	3
Pixan Bel	18.7	6.4	13.5	3.7 ± 0.80	4
Ruta de los Guerreros	14.2	3.7	9.3	5.4 ± 2.19	3

Site	Trees per Plot	Basal Area (m^2/ha)	Number of Species Above Ground	Simpson Diversity Above Ground	Root Masses per m^2	Root Area (cm^2/ m^2)	Number of Species Below Ground	Simpson Diversity Below Ground*
Cueva Culebron	21.5	21.3	25	0.93	0.052	4.17	12	0.67
Jaguar Maw	17.0	23.9	14	0.89	0.034	4.41	23	0.82
Nohoch Aktun	17.3	45.6	13	0.57	0.019	1.29	5	0.40
Pixan Bel	14.5	18.3	18	0.86	0.015	1.14	8	0.40
Ruta de los Guerreros	18.3	16.4	21	0.90	0.024	3.76	16	0.86

Table 4.1 Characteristics of sites included in this study. [†]Maximum depth to the cave floor in place of depth to groundwater measurement. *Simpson diversity below ground calculated without lianas and palm species.

4.4.2. Forest composition above ground

There were 14 paired plots established in total – 4 at Pixan Bel, 3 at Nohoch Aktun, 3 at Ruta de los Guerreros, 2 at Cueva Culebron, and 2 at Jaguar Maw. Cueva Culebron had the highest number of trees per plot (21.5) while Pixan Bel had the least (14.5; Table 4.1). Cross-sectional area of individual trees varied by site (χ^2 (4, N = 242) = 10.02, p = 0.04), with the largest trees being located at Nohoch Aktun. The largest individual was a *Ficus obtusifolia* Kunth tree with a DBH of 71.9 cm. Nohoch Aktun had the highest basal area of all the sites (45.6 m^2/ha), followed by Jaguar Maw (23.9 m^2/ha), Cueva Culebron (21.3 m^2/ha), Pixan Bel (18.3 m^2/ha), and Ruta de los Guerreros (16.4 m^2/ha; Table 4.1). The average tree size was 14.3 cm in diameter across sites.

Among the 233 trees identified in the 14 plots, 47 species were identified. In terms of number of stems, the most abundant species was *Oxandra lanceolata* (Sw.) Baill. (14.2%), although this species was observed only at Nohoch Aktun. *Bursera simaruba* (L.) Sarg., *Swartzia cubensis* (Britton & Wilson) Standl., and *Neea psychotrioides* Donn.Sm. had relative abundances of 8.6%, 6.4%, and 5.6%, respectfully, and were found at multiple sites. The rest of the species has relative abundances less than 5% (Figure 4.2A). The species with the highest basal area by species across sites were *F. obtusifolia* (3.94 m^2/ha), *Ficus cotinifolia* Kunth (2.46 m^2/ha), and *Leucaena leucocephala* (Lam.) de Wit (1.94 m^2/ha; Figure 4.2B). Species with individuals classified as large (≥ 25 cm DBH) included *F. cotinifolia*, *F. obtusifolia*, *Ficus trigonata* L., *Manilkara zapota* (L.) P. Royen, *Piscidia piscipula* (L.) Sarg., *Brosimum alicastrum* Sw., and *L. leucocephala*.

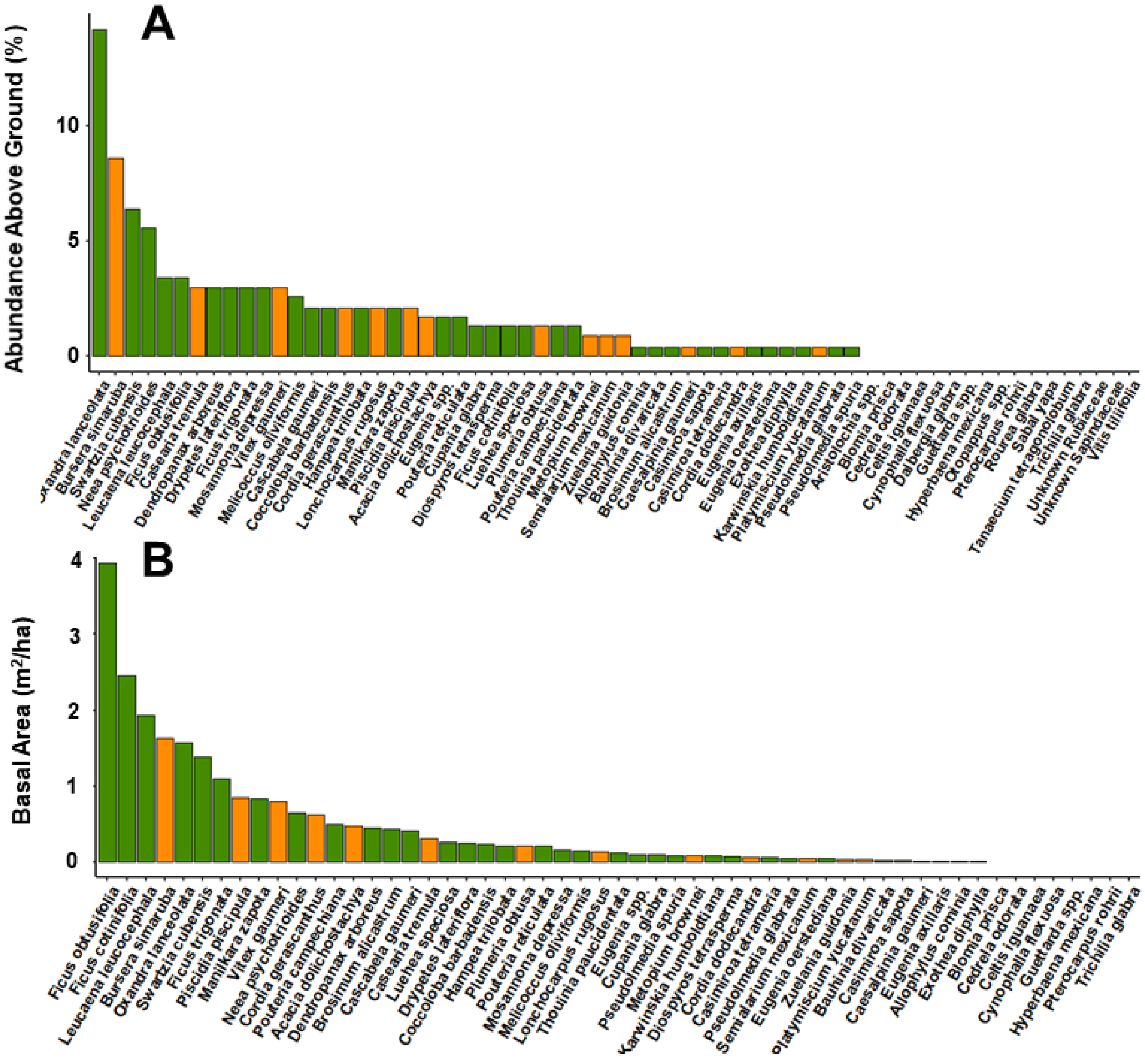

Figure 4.2 Species abundance above ground based on number of stems (out of 233 trees identified; A) and basal area (out of 0.14 total hectares surveyed; B). Shading corresponds to phenology, denoting evergreen (green) and deciduous (orange) species. Species without abundance information were found below ground only, including the 8 lianas and 1 palm.

4.4.3. Diversity among roots in the caves

Out of the 260 roots sampled across all sites, 219 were able to be identified using DNA barcoding or morphology. Those 219 roots represented 38 species identified as present in the caves. This includes 8 species of lianas and 1 palm, none of which were target plant forms in the above ground sampling. There were 8 tree species found below ground that were not identified in the plots above ground. Below ground, species from the genus *Ficus* were the most abundant, with a relative abundance of 35.8% (Figure 4.3). The genus *Pouteria* accounted for 8.7% of the identified roots. Unfortunately, for these two groups, we were unable to increase the resolution of assignment beyond genus. *L. leucocephala* had a relative abundance of 6.4% and was also easy to identify morphologically due to the matching bright red cortex of coarse roots and the trees' trunk. Interestingly, two liana species, *Rourea glabra* Kunth and *Dalbergia glabra* (Mill.) Standl. were commonly observed below ground with relative species abundances of 6.0% and 5.5%, respectively. All other species were classified as rare below ground, with relative abundances less than 5%.

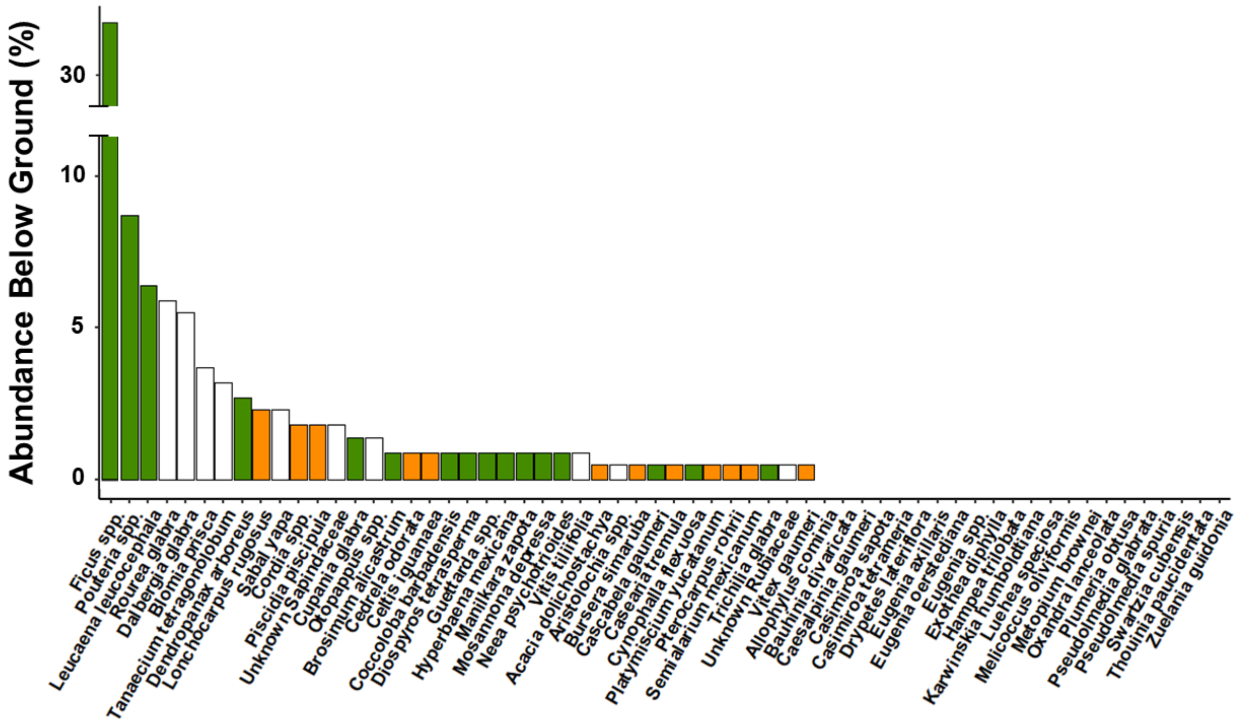

Figure 4.3 Relative abundance below ground by species based on total roots with successful species identifications (219 roots). Shading corresponds to phenology, denoting evergreen (green) and deciduous (orange) species. White shading represents the 8 lianas and 1 palm found below ground. Note that *B. prisca* is a tree identified below ground only, yet, information on leaf habit for this species was not available. Species without abundance information were found above ground only.

4.4.4. Above and below ground abundance index

Utilizing the above and below ground abundance index, we assessed patterns for each species. Not surprisingly, the three trees with roots common in the caves (*Ficus* spp., *L. leucocephala*, and *Pouteria* spp.) had the most negative values (Figure 4.4). *Blomia prisca* (Standl.) Lundell was a species observed below ground only, resulting in a similar value to *Pouteria* spp. On the opposite end of the spectrum, *O. lanceolata*, *B. simaruba*, *S. cubensis*, and *N. psychotrioides* had the most positive values as they were observed above ground only or rarely had roots exposed in the caves. Although these species were abundant and had high basal area, the representative individuals were generally small in diameter, suggesting that smaller individuals were less likely to root deeply compared to larger individuals, represented by *Ficus* spp. and *L. leucocephala*. Yet, a prominent exception to this generalization is the fact that the two *Pouteria* species, *Pouteria campechiana* (Kunth) Baehni and *Pouteria reticulata* (Engl.) Eyma, are small (9.2 ± 3.6 cm and 12.9 ± 3.6 cm DBH, respectively; Table C-2).

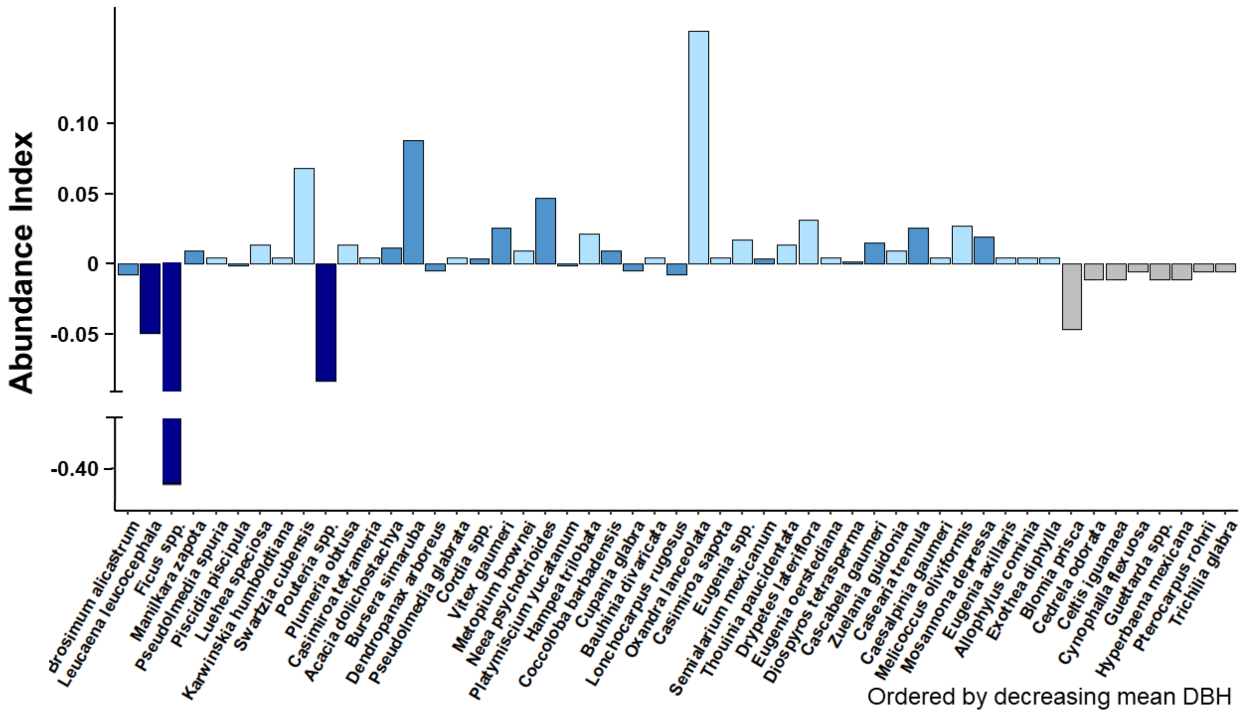

Figure 4.4 Relationship between above and below ground abundance by species. Higher abundance above ground represented by positive values and higher abundance below ground represented by negative values. Shading corresponds to rooting habit groups as follows: above ground only (light blue), rare below ground (medium blue), common below ground (dark blue) and below ground only (grey). Lianas and the palm were not included in this analysis. Species are ordered by decreasing mean DBH. Note that species found below ground only do not have data for tree size.

Furthermore, while two-thirds of the species had positive values, reflecting higher abundance above ground than below ground, there were several species, identified both in the surface and cave plots, with negative values. These included *Dendropanax arboreus* (L.) Decne. & Planch., *Cupania glabra* Sw., *Lonchocarpus rugosus* Benth., *Platymiscium yucatanum* Standl., and *P. piscipula.* Although these species did not have roots frequently observed in the caves compared to *Ficus* spp., *L. leucocephala*, or *Pouteria* spp., this group was more abundant below ground than above. With varying degrees of abundance based on number of stems and basal area (Figure 4.2), all individuals of these species are classified as small.

4.4.5. Above and below ground diversity by site

Above ground, the most diverse site was Cueva Culebron, with 25 species being represented in the 43 trees in the plots (Table 4.1) and a species richness of 20.8. The Simpson diversity index for this site was 0.93. Nohoch Aktun had the lowest diversity, with 13 species represented by the 52 trees in the plots and a species richness of 10.2. The Simpson diversity index at Nohoch Aktun was 0.57. The other three sites, Ruta de los Guerreros, Jaguar Maw, and Pixan Bel, had comparable diversity indices at 0.90, 0.89, and 0.86, respectively. The species richness at these sites were 17.2, 14.0, and 14.2, respectively.

Because lianas and palms were excluded from the above ground sampling, they were also excluded from the below ground Simpson diversity index calculations. Therefore, below ground, the most diverse sites were Ruta de los Guerreros and Jaguar Maw, with Simpson diversity indices of 0.86 and 0.82. Ruta de los Guerreros had a species richness of 9.0 while Jaguar Maw had a richness of 8.8. It is notable that Ruta de los Guerreros had the highest number of roots that could not be identified via DNA barcoding or morphology (14), suggesting an even higher diversity at that site than observed, while Jaguar Maw had the least (4). Cueva Culebron had an index of 0.67 while Pixan Bel and Nohoch Aktun both had an index of 0.40.

When comparing the diversity indices, each site decreased in diversity from above to below ground ($t_{4.2} = 2.65$, $p = 0.05$; Table 4.1). The index for above ground diversity at Nohoch Akun was removed from this comparison as it was an outlier. Interestingly, Ruta de los Guerreros and Jaguar Maw had fairly equal indices, as the ratio of above to below ground Simpson diversity was 1.09 and 1.05, respectively. Cueva Culebron had comparable above to below ground diversity ratios (1.39 and 1.43, respectively), while Pixan Bel was notably more diverse above ground than below (2.15). There was no relationship between the ratio of above to below ground Simpson diversity and various site characteristics (i.e. depth to groundwater, elevation, distance to the coast, trees per plot, number of species above ground, basal area, root masses per m^2, and number of species below ground; Figure C-1).

4.4.6. Tree and root abundance by site

Cueva Culebron had the highest number of roots exposed underground, with 61 fine roots, singular coarse roots, or large masses visible within the below ground plots (Figure 4.5). Pixan Bel had 22 roots, the lowest among the sites. The majority of roots observed at these two sites were singular coarse roots. Due to the prevalence of large root masses, Jaguar Maw had the highest root area among the sites (4.41 cm^2/m^2; Table 4.1). The largest of these masses was 50 cm in diameter, encompassing roots from seven different species.

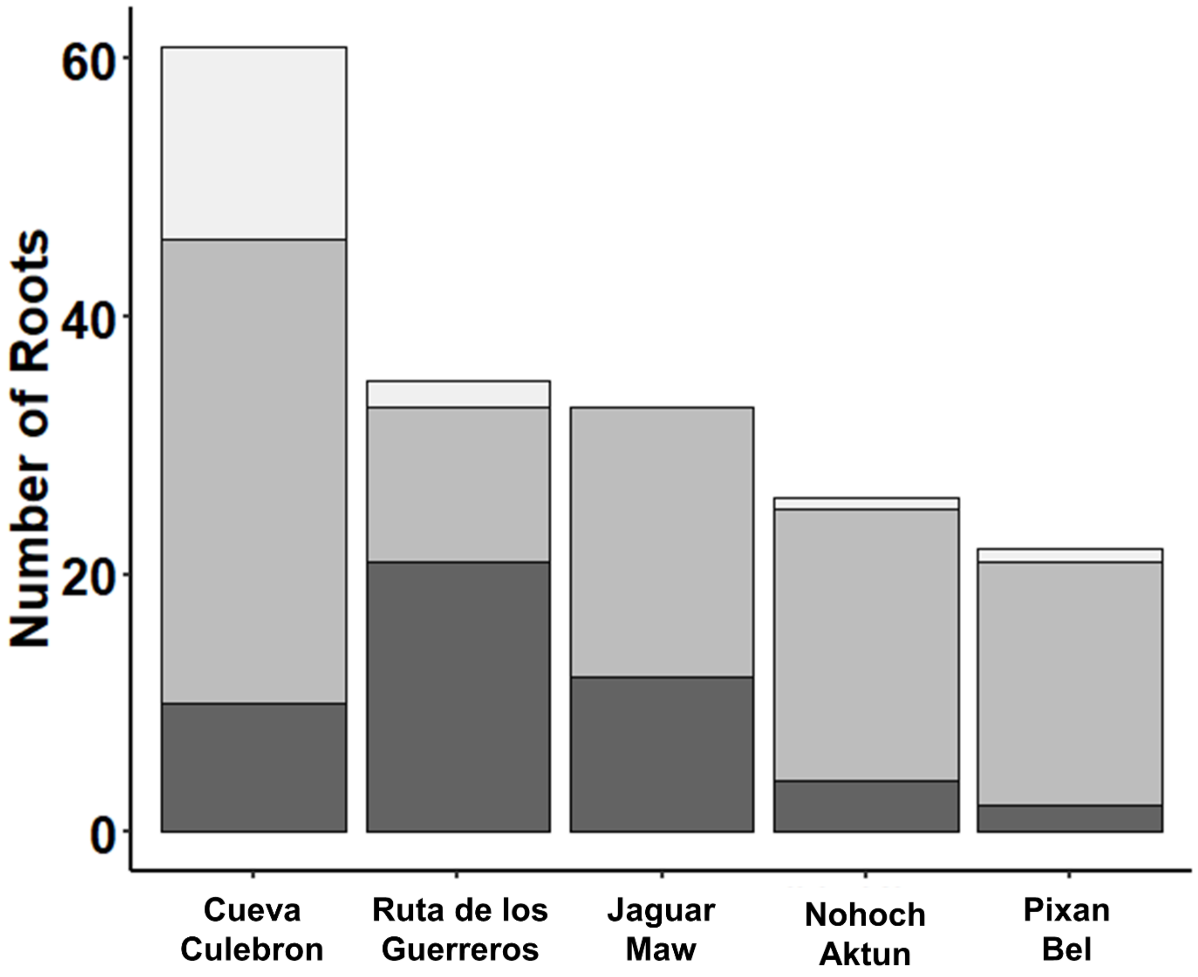

Figure 4.5 Root abundance by site, noting the distribution of root structures throughout the sites. The stacking order from top to bottom is fine roots, singular coarse roots, and large masses.

While there was a positive trend between the number of trees per plot and the number of roots observed per plot, the relationship was weakly statistically significant ($R^2 = 0.67$, $p = 0.06$; Figure C-2A). There was no relationship between the root area and the number of trees per plot across sites ($R^2 = 0.23$, $p = 0.24$). Furthermore, there is no correlation between observed the number of roots or root area below ground and basal area of the trees above ground ($R^2 = - 0.26$, $p = 0.71$ and $R^2 = - 0.05$, $p = 0.43$, respectively).

Interesting patterns emerged when tree, species, and root abundance was compared to several site characteristics. The number of trees per plot decreased with increasing depth to groundwater ($R^2 = 0.24$, $p = 0.23$), elevation ($R^2 = 0.46$, $p = 0.13$), and distance from the coast ($R^2 = 0.73$, $p = 0.04$; Figure 4.6A), with the latter being the only significant relationship. This was best fit with a non-linear regression. The number of tree species per plot decreased with increasing depth to groundwater ($R^2 = 0.29$, $p = 0.21$), elevation ($R^2 = 0.36$, $p = 0.17$), and distance from the coast ($R^2 = 0.86$, $p = 0.02$; Figure 4.6B). Again, distance from the coast was the only significant site characteristic and was best fit with a non-linear regression.

With regard to specific species, *Eugenia* spp., *Mosannona depressa* (Baill.) Chatrou, *Pouteria* spp., and *Vitex gaumeri* Greenm. were more common at sites closer to the coast while *Casearia tremula* (Griseb.) Griseb. ex C.Wright, *B. simaruba*, *L. leucocephala*, and *Melicoccus oliviformis* Kunth were more common at sites further from the coast. *Ficus* spp. and *N. psychotrioides* were observed at all sites. There was not a clear pattern in species composition at each site as evergreen and deciduous species, along with primary and secondary species, were observed at all sites. However, it is noteworthy that *Drypetes lateriflora* (Sw.) Krug & Urb. and *Ficus* spp., both evergreen species, dominated at Cueva Culebron, the site closest to the coast, while *B. simaruba*, a small deciduous species, dominated at Pixan Bel, the site furthest from the coast (Table C-3).

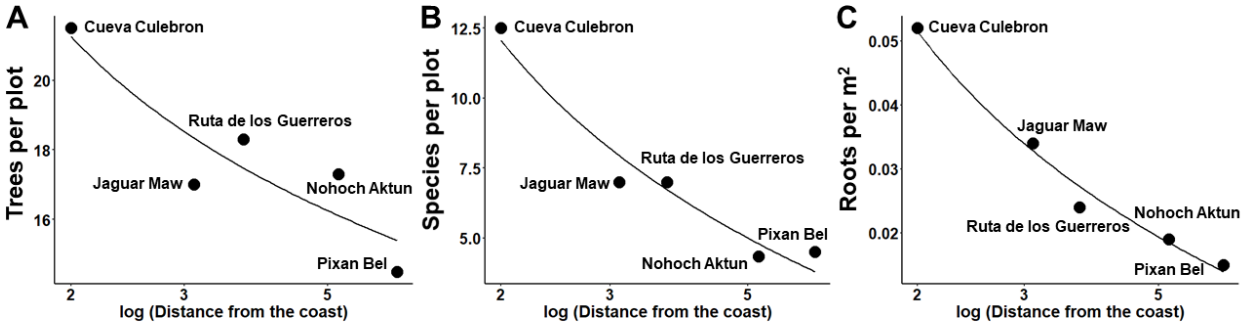

Figure 4.6 Trees per plot, species per plot, and root abundance in relation to depth to distance of the site from the coast, with the x-axis in log scale. A: $R^2 = 0.73$, $p = 0.04$, B: $R^2 = 0.86$, $p = 0.02$, C: $R^2 = 0.93$, $p < 0.01$.

The number of roots per m^2 decreased with increasing depth to groundwater ($R^2 = 0.58$, $p = 0.08$), elevation ($R^2 = 0.66$, $p = 0.06$), and distance from the coast, with the latter being the only significant relationship ($R^2 = 0.93$, $p < 0.01$; Figure 4.6C). This was best fit with a non-linear regression. Assessing site characteristics by root area showed similar trends. Root area decreased with increasing depth to groundwater ($R^2 = 0.65$, $p = 0.06$), elevation ($R^2 = 0.66$, $p = 0.06$), and distance from the coast ($R^2 = 0.82$, $p = 0.02$; Figure C-4E). Again, the only statistically significant analysis was between root area and distance from the coast.

Further, there was no significant relationship between roots per m^2 and the number of species observed in the above ground plots ($R^2 = 0.15$, $p = 0.29$). There is a positive trend between the number of species found below ground and root abundance, however, the relationship is not statistically significant ($R^2 = 0.61$, $p = 0.07$; Figure C-5B). Similarly, the number of species found below ground increased with root area, but the relationship was not statistically significant ($R^2 = 0.60$, $p = 0.08$).

4.5. Discussion

Our results from the DNA barcoding showed that 38 species had roots present in the caves. Of these, *Ficus* spp., *L. leucocephala,* and *Pouteria* spp. were the trees with roots commonly observed below ground. Interestingly, two liana species were also common below ground. The presence of lianas in the caves, alongside tree roots, and the prevalence of *R. glabra* and *D. glabra* compared to other tree species suggests that several lianas have deep rooting capabilities and may be competing with trees for resources (Andrade et al. 2005, van der Sande et al. 2013). Diversity across sites decreased from above and below ground, supporting our hypothesis that a fraction of the species observed above ground would have deep roots in the caves. This suggests that there are deep rooting specialists in Quintana Roo. While deep rooting capability was predicted by large tree size for some species (i.e. *Ficus* spp. and *L. leucocephala*), there were several exceptions to this assumption based on above ground observations. Therefore, tree size did not accurately reflect root abundance by species. Furthermore, Nohoch Aktun, despite having the largest trees, had the second lowest root abundance across sites. Rather than being related to tree abundance or basal area, root abundance significantly decreased with increasing distance from the coast. Along with this landscape-scale influence, fine-scale bedrock characteristics appear to control root exploration and prevalence in the caves. Together, these observations imply that deep water access in Quintana Roo is variable at a local and landscape-scale.

4.5.1. Diversity decreased from above to below ground

Via DNA barcoding, we were able to identify 38 species with roots in the caves. This diversity included 8 lianas, 1 palm, and 8 trees either not the focus of this study or not encompassed in the plots above ground. Therefore, 21 of the 47 tree species found above ground had roots exposed in the caves, resulting in a decrease in diversity from the surface to the subterranean across sites.

The decrease in diversity is in agreement with other studies with complimentary above and below ground diversity assessments (Frank et al. 2010, Jones et al. 2011, Kesanakurti et al. 2011). In addition, some studies identified species below ground that were not included in above ground plots (Frank et al. 2010, Kesanakurti et al. 2011, Hiiesalu et al. 2012). This could be from dead roots from historic species or lateral root growth (Mommer et al. 2011, Pärtel et al. 2012). There could also be undetected species resulting from failed PCR amplification and sequencing, potentially resulting in an underestimation of the below ground diversity at these sites.

It is important to note that the several related DNA barcoding studies have been conducted in grasslands, with the exception of Jones et al. (2011), which was located in Barro Colorado Island, Panama. Although also a highly diverse tropical system, they only identified 20% of the species found above ground among the roots (Jones et al. 2011). Different sampling methods may be causing this. Jones et al. (2011) included trees, shrubs, and palms with DBH ≥1 cm while we focused only on trees with DBH ≥ 5 cm, increasing the number of species observed in their study. Below ground, they performed DNA analysis on a limited number of roots from the soil cores, while we attempted DNA analysis on all roots observed and collected, potentially increasing the number of species identified below ground in our study. Moving forward, it is important to consider sampling protocols in similar studies to make them comparable yet accurate for the study system. Because of the limited knowledge about diversity, species richness, and distribution below ground, we advocate for more research in this area to provide insight into subsurface processes that may be driving resource acquisition, productivity, and competition in ecosystems globally.

4.5.2. Tree size did not predict deep rooting specialization

By calculating the ratio of above to below ground abundance, we created an index to evaluate deep rooting patterns across species. Results showed that several of the evergreen species with large individuals had high root abundance and species with small individuals either rarely or never had roots in the caves. However, there are several exceptions to this generalization. First, while *Pouteria* spp. was classified as common below ground, *P. campechiana* and *P. reticulata* trees on the surface were small. Second, two species with large individuals, *M. zapota* and *B. alicastrum*, rarely had roots exposed in the caves. Third, *D. arboreus*, *C. glabra*, *L. rugosus*, *P. yucatanum*, and *P. piscipula* were all more common below ground than above ground despite their small size.

These contradictions imply that tree size cannot be used as a reliable indicator for root abundance in Quintana Roo. While several studies found that tree size can provide insight into rooting depth and resource access, as evidenced by larger trees having deeper, more established root systems, complimented by deeper water use compared to smaller trees (Sayer and Newbery 2003, Hasselquist et al. 2010, Phillips et al. 2010), others have noted increased rooting depth in early successional species and forests (Paz et al. 2015, Waring and Powers 2017). Deep rooting by small, pioneer species in seasonally dry environments may assist in establishment and survival by securing access to reliable water at depth (Meinzer et al. 1999, Stratton et al. 2000, Hasselquist et al. 2010). On the other hand, large and presumably older trees, may allocate resources to conservative morphological traits, such as increased leaf and wood density, rather than root foraging (Wright et al. 2004, Méndez-Alonzo et al. 2012). After assessing the natural history of these species, we found that the small species with high root abundance were labeled as generalists, some with deciduous leaf habit (*L. rugosus* and *P. yucatanum;* García-Guzmán and Morales 2007, Derroire et al. 2018), fast growth rate (*P. piscipula;* Sánchez-Sánchez and Islebe 2002, Sanaphre-Villanueva et al. 2017), and shade intolerance (*D. arboreus;* Sorensen 2006). *M. zapota* and *B. alicastrum*, with less abundant, large individual, have been identified as characteristic species in medium statured, mature forests (Sánchez-Sánchez and Islebe 2002, García-Frapolli et al. 2007). By incorporating information regarding the life history of these species, we suggest that deep rooting specialization may be more related to life history and species-specific strategies rather than tree size alone.

4.5.3. Bedrock restricted root access

Related studies in the state of Yucatán found that roots were seemingly restricted to the soil and upper layer of bedrock, in some cases growing no more than 2 m below the surface (Querejeta et al. 2007, Hasselquist et al. 2010). Yet, we observed seemingly more roots, some larger and deeper than reported in these studies. We believe that the geologic setting in Quintana Roo, characterized by younger and more porous coastal limestone compared to Yucatán, allows for more deep rooting (Worthington et al. 2000). This is not to say that the bedrock did not have an impact on the vegetation in our study. The influence of the bedrock became apparent when evaluating patterns in root abundance and area across sites. While Cueva Culebron had the highest number of roots observed in the below ground plots, Jaguar Maw had the highest root area per m^2 surveyed. This discrepancy is the result of the root structures and respective sizes that were prevalent in each cave (Adams et al. 2020). We documented that the majority of the roots in Cueva Culebron were singular coarse roots with diameters ranging from 0.5 to 4.3 cm, emerging from solitary conduits in the bedrock. These coarse roots had smaller diameters compared to large masses of intertwined roots that were prevalent in Jaguar Maw. For comparison, the largest of the 12 masses in Jaguar Maw were 22.9, 24.7, and 50.0 cm in diameter, all densely packed with roots from multiple species. Naturally, the large masses originated from larger conduits in the ceiling compared to the singular coarse roots or fine roots. By evaluating the distribution of roots among the three structures at each site, we can make inferences about conduit sizes and, in turn, the space available for roots to grow.

We noted that Jaguar Maw, Ruta de los Guerreros, and Culebron had more large masses compared to Nohoch Aktun and Pixan Bel. This suggests that Jaguar Maw, Culebron, and Ruta de los Guerreros had more and larger conduits in the bedrock to accommodate more roots in the form of larger masses. High root abundance and root area exposed in the caves confirmed this. On the other hand, Nohoch Aktun and Pixan Bel had some masses but the exposed roots in these systems were predominantly fine or singular coarse roots. Consequently, these two sites had the lowest root abundance and root area. As observed in regions with weathered granite (Bornyasz et al. 2005), limestone (Estrada-Medina et al. 2013a), and shale (Hasenmueller et al. 2017), dense root mats filling fractures and conduits depict the control that bedrock has on root distribution and access. Unlike root elongation in soil, roots are unable to physically widen pores or conduits in bedrock, and therefore, exploit pre-existing cracks and conduits in bedrock to access water and nutrients at depth (Schwinning 2010, Gao et al. 2016). Overlapping root systems also imply there is competition for space as well as resources in this seasonally dry karst environment (Coomes and Grubb 2000, Casper et al. 2003). We established that root growth and access to the below ground environment was determined by the distribution and size of bedrock conduits, as sites with larger conduits had increased root abundance and area.

4.5.4. Site location influences tree and root abundance

We initially hypothesized that sites with larger trees would have more roots exposed in the cave associated with the site. Results showed that there was no relationship between root abundance or root area and tree basal area within the above ground plots. Nohoch Aktun had the largest trees but the second lowest root abundance and root area, followed by Pixan Bel. The lack of relationship is most likely related to the bedrock characteristics, described in the prior section. Though not statistically significant, there was a positive trend between root abundance and the number of trees per plot. While we recognize the relationship is not significant, it provided evidence that the above ground components of the vegetation are indeed related to the below ground components.

To further explore the variability in root abundance and area across sites, we compared these measurements to site characteristics associated with geology and water access at the landscape scale. While there were negative trends between trees per plot, species per plot, root abundance, and root area and site characteristics, such as depth to groundwater, elevation, and distance from the coast, the only feature with significant correlations to above and below ground vegetation measurements was distance from the coast. Interestingly, these relationships with distance inland were best fit with a logarithmic regression. It appears that the location of the caves within the study area has important implications for community structure. In Quintana Roo, the dissolution of the limestone and, in turn, cave development is linked to the depth of the mixing zone between the fresh and salt water lens of the aquifer (Smart et al. 2006). The depth to the halocline can be determined by the parabolic Dupuit-Ghyben-Herzberg relationship (Vacher 1988). During interglacial periods in the Pleistocene and the Holocene Thermal Maximum, rising sea levels subsequently raised the depth of the mixing zone relative to present day levels. Cave expansion occurred rapidly, resulting in large horizontal passages and channels at the halocline (van Hengstum et al. 2010). In theory, the depth of cave passages should increase with distance inland, corresponding to the non-linear Dupuit-Ghyben-Herzberg relationship. Within currently submerged cave systems, it has been established that depth of cave passages, in fact, increases with distance inland, but instead, in a linear fashion (Smart et al. 2006). The submerged systems, however, have likely been exposed to the dissolution potential of the halocline for longer, some still being influenced by its presence. Continued dissolution may influence the variability in passage depth within and among submerged caves (Smart et al. 2006). On the other hand, sites that are presently dry, as the ones in this study, had the influence of the mixing zone removed a after the Holocene Thermal Maximum when precipitation decreased and sea levels fell (Siddall et al. 2003, van Hengstum et al. 2010). Because of the shorter period of exposure to the halocline, the dry caves may maintain the expected parabolic relationship between passage depth and the depth to the halocline. The non-linear relationship between the biotic components and distance from the coast seem to display this. Tree and root abundance appear to be a function of the hydrogeological influences on cave development and passage depth in Quintana Roo. These landscape-scale patterns require further investigation to uncover potential differences between dry and submerged caves and subsequent influences on the overlying vegetation.

In addition, we noted that elevation increased with distance inland. Because the aquifer has a shallow hydraulic gradient, the surface of the water table is fairly level (Bauer-Gottwein et al. 2011). As elevation increases, the distance to the surface of the aquifer should increase as well. Therefore, caves further inland are deeper and rooting depth to groundwater is deeper, making access to the aquifer more difficult for vegetation. A meta-analysis reported that root biomass decreased with depth (Jackson et al. 1996) and this pattern was verified in regions with weathered bedrock, including the Yucatán (Bornyasz et al. 2005, Estrada-Medina et al. 2013a). Depth to groundwater has been shown to influence ecosystem rooting depth, encouraging deep rooting if the water table is relatively shallow or discouraging deep rooting if the water table is too deep (Fan et al. 2017). Our results showed that root abundance decreased with increasing depth to groundwater, elevation, and distance inland. We also provided evidence that root abundance had a positive relationship with trees per plot. Together, it can be implied that sites further inland with restricted access to groundwater have less trees above ground, resulting in less roots below ground. These speculations align with studies on plant responses to variable groundwater depths (Goedhart and Pataki 2011, Zolfaghar et al. 2014), which found that above ground biomass and net primary productivity was higher in locations with a shallower water table, highlighting links between groundwater resources and vegetation.

4.5.5. Implications for changes in community composition

Groundwater utilization has been shown to be critical in water-limited ecosystems globally (Eamus et al. 2015, Evaristo and McDonnell 2017). Although not formally evaluated, the semi-evergreen forests of Quintana Roo appear to be groundwater dependent, based on the framework established by Eamus et al. 2006. We support this classification through the observed impact of depth to groundwater, elevation, and distance from the coast on the vegetation. While more focused studies on changes in community composition in relation to groundwater depth are needed, we noted that the evergreen species, *D. lateriflora* and *Ficus* spp., were the most abundant species at Cueva Culebron while *B. simaruba*, a deciduous species, was the most abundant at Pixan Bel. Many of the evergreen species at Cueva Culebron were not present at

Pixan Bel. Observations from the closest and furthest sites from the coast hint that there may be shifts in dominant species corresponding to depth to groundwater. Locations with a shallower and more accessible water table may support more evergreen species with high water demands. In contrast, species with the ability to avoid or resist water stress (i.e. drought-deciduous, hardwoods) may be suited for locations with deeper groundwater.

Globally, groundwater dependent ecosystems are threatened by declining water table levels from groundwater pumping and lack of recharge during droughts (Eamus et al. 2006, Hartmann et al. 2014). While a falling water table level is not a concern in Quintana Roo, as the aquifer is equilibrium with the ocean, declining quality of the freshwater layer is the pressing issue. As urbanization and tourism increases, pumping of the freshwater layer is expected to increase (Escolero et al. 2002, Rodríguez-Huerta et al. 2019) and the displacement of freshwater is balanced by a rise in the saltwater layer (Doehring and Butler 1974). Coupled with expected sea level rise, the salinity of freshwater will most likely rise (Williams et al. 1999). Furthermore, a study in the Florida Keys noted that salinity of the freshwater lens of the karst aquifer increased with decreasing precipitation, accompanied by shifts in the community composition of the vegetation to more salt tolerant species and loss of native species (Ogurcak et al. 2019). Extended dry periods and droughts are predicted for future climate scenarios in the Caribbean (Singh 1997, De la Barreda et al. 2020), decreasing the recharge and replenishment of the freshwater lens that is currently buffering the impacts of salinity on vegetation in the Yucatan Peninsula (Barlow and Reichard 2010). Coastal forests, like those in Quintana Roo, are susceptible to significant shifts in community composition and structure in response to urbanization and climate change. Through this comparative study on above and below ground diversity in Quintana Roo, we provided insight into deep rooting capability and the role of local and landscape hydrogeologic characteristics play on plant access to resources at depth. Yet, in-depth research on groundwater utilization and resource use strategies is needed to properly predict and manage the impacts of future climatic regimes and anthropogenic pressures on the tropical forests in Quintana Roo.

4.6. Conclusions

We established foundational knowledge about the below ground diversity, deep rooting specialization, and root prevalence observed in shallow caves in Quintana Roo, Mexico. While nearly 50% of the species observed in the above ground plots had roots in the caves, below ground biodiversity was dominated by *Ficus* spp. Tree size was not an accurate predictor for root abundance and deep rooting specialization, as there were several exceptions to the generalization that large trees have deeper roots compared to smaller individuals. It appears that consideration for a species' natural history, particularly successional stage, better inform differences in rooting depth and root abundance compared to tree size. In addition, we noted that root abundance and area was highest in caves with larger conduits in the ceilings, which support large masses of intertwined roots. There is potential for these overlapping root systems to be competing for space and resources within this region. At the landscape scale, tree, species, and root abundance were negatively correlated with distance from the coast, elevation, and depth to groundwater. Shifts in community composition and structure appear to be related to past and present hydrogeologic conditions, displaying the influence that groundwater has on the vegetation in this system. In conclusion, while numerous species have access to resources at depth, species-specific strategies, bedrock characteristics, and water table depth limit and control deep rooting specialization, root exploration, and abundance, respectively, with apparent consequences on species abundance and productivity above ground. This research alludes to the complexity of water and nutrient access and use within seasonally dry karst regions. Further work is necessary to uncover species-specific and community-level water use to better understand dependence on groundwater resources and predict responses to shifting climate regimes.

4.7. Acknowledgments

Research was supported by the Sid Kyle Graduate Merit Assistantship from the Department of Ecosystem Science and Management (ESSM) at Texas A&M University (TAMU), National Geographic Society Early Career Grant (CP-090ER-17), and the MSC L.T. Jordan Institute for International Awareness at TAMU. We greatly appreciate Peter Sprouse of Zara Environmental, LLC for his guidance and hospitality as well as maps and survey data for all sites. We would like to thank the landowners for providing us access to their property to conduct this work. Dr. Nithya Subramanian provided training and assistance at the AgriGenomics Laboratory at TAMU. We would also like to thank Drs Claudio Casola and Daniel Spalink from the Ecology and Conservation Biology department for laboratory space and guidance. Dr. Eun Gyu No and Lyndsey Torrez at the Laboratory for Genome Technology at TAMU for performing the Sanger sequencing.

4.8. References

Adams, R. E., T. M. Iliffe, and J. B. West. 2020. Identifying tree roots in the caves of Quintana Roo, Mexico as a step toward ecological insights and improved conservation. *Plants, People, Planet* 2:133–139.

Andrade, J. L., F. C. Meinzer, G. Goldstein, and S. A. Schnitzer. 2005. Water uptake and transport in lianas and co-occurring trees of a seasonally dry tropical forest. *Trees* 19:282–289.

Barlow, P. M., and E. G. Reichard. 2010. Saltwater intrusion in coastal regions of North America. *Hydrogeology Journal* 18:247–260.

Bauer-Gottwein, P., B. R. N. N. Gondwe, G. Charvet, L. E. Marín, M. Rebolledo-Vieyra, and G. Merediz-Alonso. 2011. Review: The Yucatán Peninsula karst aquifer, Mexico. *Hydrogeology Journal* 19:507–524.

Beddows, P. A., P. L. Smart, F. F. Whitaker, and S. L. Smith. 2002. Density stratified groundwater circulation on the Caribbean Coast of the Yucatán Peninsula. *Karst Frontiers: Karst Water Institute Special Publication* 7:129–134.

Bleby, T. M., A. J. McElrone, and R. B. Jackson. 2010. Water uptake and hydraulic redistribution across large woody root systems to 20 m depth. *Plant, Cell & Environment* 33:2132–2148.

Bodner, G., D. Leitner, A. Nakhforoosh, M. Sobotik, K. Moder, and H.-P. Kaul. 2013. A statistical approach to root system classification. *Frontiers in Plant Science* 4:1–15.

Bolson, M., E. De Camargo Smidt, M. L. Brotto, and V. Silva-Pereira. 2015. ITS and *trnH-psbA* as Efficient DNA Barcodes to Identify Threatened Commercial Woody Angiosperms from Southern Brazilian Atlantic Rainforests. *PLoS ONE* 10:e0143049.

Bornyasz, M. A., R. C. Graham, and M. F. Allen. 2005. Ectomycorrhizae in a soil-weathered granitic bedrock regolith: linking matrix resources to plants. *Geoderma* 126:141–160.

Canadell, J., R. B. Jackson, J. R. Ehleringer, H. A. Mooney, O. E. Sala, and E. D. Schulze. 1996. Maximum Rooting Depth of Vegetation Types at the Global Scale. *Oecologia* 108:583–595.

Casper, B. B., H. J. Schenk, and R. B. Jackson. 2003. Defining a plant's belowground zone of influence. *Ecology* 84:2313–2321.

Chen, S., H. Yao, J. Han, C. Liu, J. Song, L. Shi, Y. Zhu, X. Ma, T. Gao, X. Pang, K. Luo, Y. Li, X. Li, X. Jia, Y. Lin, and C. Leon. 2010. Validation of the ITS2 region as a novel DNA barcode for identifying medicinal plant species. *PLoS ONE* 5:e8613.

Coomes, D. A., and P. J. Grubb. 2000. Impacts of Root Competition in Forests and Woodlands: A Theoretical Framework and Review of Experiments. *Ecological Monographs* 70:171–207.

Dawson, T. E. 1998. Fog in the California redwood forest: ecosystem inputs and use by plants. *Oecologia* 117:476–485.

De la Barreda, B., S. E. Metcalfe, and D. S. Boyd. 2020. Precipitation regionalization, anomalies and drought occurrence in the Yucatán Peninsula, Mexico. *International Journal of Climatology*.

Derroire, G., J. S. Powers, C. M. Hulshof, L. E. Cárdenas Varela, and J. R. Healey. 2018. Contrasting patterns of leaf trait variation among and within species during tropical dry forest succession in Costa Rica. *Scientific Reports* 8:1–11.

Doehring, D. O., and J. H. Butler. 1974. Hydrogeologic Constraints on Yucatán's Development. *Science* 186:591–595.

Doody, T. M., and R. G. Benyon. 2011. Direct measurement of groundwater uptake through tree roots in a cave. *Ecohydrology* 4:644–649.

Durán-García, R., M. Méndez-Gonzalez, and A. Larqué-Saavedra. 2016. The biodiversity of the Yucatán Peninsula: a natural laboratory. *Progress in Botany* 78:237–258.

Eamus, D., R. Froend, G. Hose, and B. Murray. 2006. A functional methodology for determining the groundwater regime needed to maintain the health of groundwater-dependent vegetation. *Australian Journal of Botany* 54:97–114.

Eamus, D., S. Zolfaghar, R. Villalobos-Vega, J. Cleverly, and A. Huete. 2015. Groundwater-dependent ecosystems: Recent insights from satellite and field-based studies. *Hydrology and Earth System Sciences* 19:4229–4256.

Escolero, O. A., L. E. Marin, B. Steinich, A. J. Pacheco, S. A. Cabrera, and J. Alcocer. 2002. Development of a Protection Strategy of Karst Limestone Aquifers: The Merida Yucatán, Mexico Case Study. *Water Resources Management* 16:351–367.

Estrada-Medina, H., R. C. Graham, M. F. Allen, J. J. Jiménez-Osornio, and S. Robles-Casolco. 2013a. The importance of limestone bedrock and dissolution karst features on tree root distribution in northern Yucatán, México. *Plant and Soil* 362:37–50.

Estrada-Medina, H., L. S. Santiago, R. C. Graham, M. F. Allen, and J. J. Jiménez-Osornio. 2013b. Source water, phenology and growth of two tropical dry forest tree species growing on shallow karst soils. *Trees* 27:1297–1307.

Evaristo, J., and J. J. McDonnell. 2017. Prevalence and magnitude of groundwater use by vegetation: a global stable isotope meta-analysis. *Scientific Reports* 7:1–12.

Fan, Y. 2015. Groundwater in the Earth’s critical zones: Relevance to large-scale patterns and processes. *Water Resources Research* 51:3052–3069.

Fan, Y., G. Miguez-Macho, E. G. Jobbágy, R. B. Jackson, and C. Otero-Casal. 2017. Hydrologic regulation of plant rooting depth. *Proceedings of the National Academy of Sciences* 114:10572–10577.

Frank, D. A., A. W. Pontes, E. M. Maine, J. Caruana, R. Raina, S. Raina, and J. D. Fridley. 2010. Grassland root communities: species distributions and how they are linked to aboveground abundance. *Ecology* 91:3201–3209.

Fry, E. L., A. L. Evans, C. J. Sturrock, J. M. Bullock, and R. D. Bardgett. 2018. Root architecture governs plasticity in response to drought. *Plant and Soil* 433:189–200.

Gao, W., L. Hodgkinson, K. Jin, C. W. Watts, R. W. Ashton, J. Shen, T. Ren, I. C. Dodd, A. Binley, A. L. Phillips, P. Hedden, M. J. Hawkesford, and W. R. Whalley. 2016. Deep roots and soil structure. *Plant, Cell & Environment* 39:1662–1668.

García-Frapolli, E., B. Ayala-Orozco, M. Bonilla-Moheno, C. Espadas-Manrique, and G. Ramos-Fernández. 2007. Biodiversity conservation, traditional agriculture and ecotourism: Land cover/land use change projections for a natural protected area in the northeastern Yucatán Peninsula, Mexico. *Landscape and Urban Planning* 83:137–153.

García-Guzmán, G., and E. Morales. 2007. Life-history strategies of plant pathogens: distribution patterns and phylogenetic analysis. *Ecology* 88:589–596.

Goedhart, C. M., and D. E. Pataki. 2011. Ecosystem effects of groundwater depth in Owens Valley, California. *Ecohydrology* 4:458–468.

Hartmann, A., N. Goldscheider, T. Wagener, J. Lange, and M. Weiler. 2014. Karst water resources in a changing world: Review of hydrological modeling approaches. *Reviews of Geophysics* 52:218–242.

Hasenmueller, E. A., X. Gu, J. N. Weitzman, T. S. Adams, G. E. Stinchcomb, D. M. Eissenstat, P. J. Drohan, S. L. Brantley, and J. P. Kaye. 2017. Weathering of rock to regolith: The activity of deep roots in bedrock fractures. *Geoderma* 300:11–31.

Hasselquist, N. J., M. F. Allen, and L. S. Santiago. 2010. Water relations of evergreen and drought-deciduous trees along a seasonally dry tropical forest chronosequence. *Oecologia* 164:881–890.

van Hengstum, P. J., E. G. Reinhardt, P. A. Beddows, and J. J. Gabriel. 2010. Linkages between Holocene paleoclimate and paleohydrogeology preserved in a Yucatán underwater cave. *Quaternary Science Reviews* 29:2788–2798.

Hernández-Terrones, L. M., K. A. Null, D. Ortega-Camacho, and A. Paytan. 2015. Water quality assessment in the Mexican Caribbean: Impacts on the coastal ecosystem. *Continental Shelf Research* 102:62–72.

Hiiesalu, I., M. Öpik, M. Metsis, L. Lilje, J. Davison, M. Vasar, M. Moora, M. Zobel, S. D. Wilson, and M. Pärtel. 2012. Plant species richness belowground: higher richness and new patterns revealed by next-generation sequencing. *Molecular Ecology* 21:2004–2016.

Howarth, F. G., S. A. James, W. McDowell, D. J. Preston, and C. T. Imada. 2007. Identification of roots in lava tube caves using molecular techniques: Implications for conservation of cave arthropod faunas. *Journal of Insect Conservation* 11:251–261.

Jackson, R. B., J. Canadell, J. R. Ehleringer, H. A. Mooney, O. E. Sala, and E. D. Schulze. 1996. A Global Analysis of Root Distributions for Terrestrial Biomes. *Oecologia* 108:389–411.

Jackson, R. B., L. A. Moore, W. A. Hoffmann, W. T. Pockman, and C. R. Linder. 1999. Ecosystem rooting depth determined with caves and DNA. *Proceedings of the National Academy of Sciences of the United States of America* 96:11387–92.

Johnson, D. M., M. E. Sherrard, J. C. Domec, and R. B. Jackson. 2014. Role of aquaporin activity in regulating deep and shallow root hydraulic conductance during extreme drought. *Trees* 28:1323–1331.

Jones, F. A., D. L. Erickson, M. A. Bernal, E. Bermingham, W. J. Kress, E. A. Herre, H. C. Muller-Landau, and B. L. Turner. 2011. The roots of diversity: Below ground species richness and rooting distributions in a tropical forest revealed by DNA barcodes and inverse modeling. *PLoS ONE* 6:e24506.

Kesanakurti, P. R., A. J. Fazekas, K. S. Burgess, D. M. Percy, S. G. Newmaster, S. W. Graham, S. C. H. Barrett, M. Hajibabaei, and B. C. Husband. 2011. Spatial patterns of plant diversity below-ground as revealed by DNA barcoding. *Molecular Ecology* 20:1289–1302.

Kukowski, K. R., S. Schwinning, and B. F. Schwartz. 2013. Hydraulic responses to extreme drought conditions in three co-dominant tree species in shallow soil over bedrock. *Oecologia* 171:819–830.

Lynch, J. 1995. Root Architecture and Plant Productivity. *Plant Physiology* 109:7–13.

Maeght, J.-L., B. Rewald, and A. Pierret. 2013. How to study deep roots-and why it matters. *Frontiers in Plant Science* 4:1–14.

McElrone, A. J., J. Bichler, W. T. Pockman, R. N. Addington, C. R. Linder, and R. B. Jackson. 2007. Aquaporin-mediated changes in hydraulic conductivity of deep tree roots accessed via caves. *Plant, Cell & Environment* 30:1411–1421.

McElrone, A. J., W. T. Pockman, J. Martínez-Vilalta, and R. B. Jackson. 2004. Variation in xylem structure and function in stems and roots of trees to 20 m depth. *New Phytologist* 163:507–517.

Meinzer, C. F., L. J. Andrade, G. Goldstein, M. N. Holbrook, J. Cavelier, and J. S. Wright. 1999. Partitioning of soil water among canopy trees in a seasonally dry tropical forest. *Oecologia* 121:293–301.

Méndez-Alonzo, R., H. Paz, R. C. Zuluaga, J. A. Rosell, and M. E. Olson. 2012. Coordinated evolution of leaf and stem economics in tropical dry forest trees. *Ecology* 93:2397–2406.

Mitchell, P. J., E. J. Veneklaas, H. Lambers, and S. S. O. Burgess. 2008. Leaf water relations during summer water deficit: Differential responses in turgor maintenance and variation in leaf structure among different plant communities in south-western Australia. *Plant, Cell & Environment* 31:1791–1802.

Mokany, K., R. J. Raison, and A. S. Prokushkin. 2006. Critical analysis of root : shoot ratios in terrestrial biomes. *Global Change Biology* 12:84–96.

Mommer, L., A. J. Dumbrell, C. A. M. Wagemaker, and N. J. Ouborg. 2011. Belowground DNA-based techniques: Untangling the network of plant root interactions. *Plant and Soil* 348:115–121.

Mommer, L., J. Van Ruijven, H. De Caluwe, A. E. Smit-Tiekstra, C. A. M. Wagemaker, N. Joop Ouborg, G. M. Bögemann, G. M. Van Der Weerden, F. Berendse, and H. De Kroon. 2010. Unveiling below-ground species abundance in a biodiversity experiment: a test of vertical niche differentiation among grassland species. *Journal of Ecology* 98:1117–1127.

Nardini, A., V. Casolo, A. Dal Borgo, T. Savi, B. Stenni, P. Bertoncin, L. Zini, and N. G. Mcdowell. 2016. Rooting depth, water relations and non-structural carbohydrate dynamics in three woody angiosperms differentially affected by an extreme summer drought. *Plant, Cell & Environment* 39:618–627.

Ogurcak, D. E., J. P. Sah, R. M. Price, and M. S. Ross. 2019. Shifting baselines in coastal forests: Rising seas transform plant communities from the 'ground' up. *Forest Ecology and Management* 453:117581.

Pärtel, M., I. Hiiesalu, M. Öpik, and S. D. Wilson. 2012. Below-ground plant species richness: New insights from DNA-based methods. *Functional Ecology* 26:775–782.

Paz, H., F. Pineda-García, and L. F. Pinzón-Pérez. 2015. Root depth and morphology in response to soil drought: comparing ecological groups along the secondary succession in a tropical dry forest. *Oecologia* 179:551–561.

Peñuelas, J., I. Filella, J. Peñuelas, and I. Filella. 2003. Deuterium labelling of roots provides evidence of deep water access and hydraulic lift by *Pinus nigra* in a Mediterranean forest of NE Spain. *Environmental and Experimental Botany* 49:201–208.

Phillips, O. L., G. van der Heijden, S. L. Lewis, G. López-González, L. E. O. C. Aragão, J. Lloyd, Y. Malhi, A. Monteagudo, S. Almeida, E. A. Dávila, I. Amaral, S. Andelman, A. Andrade, L. Arroyo, G. Aymard, T. R. Baker, L. Blanc, D. Bonal, Á. C. A. de Oliveira, K.-J. Chao, N. D. Cardozo, L. da Costa, T. R. Feldpausch, J. B. Fisher, N. M. Fyllas, M. A. Freitas, D. Galbraith, E. Gloor, N. Higuchi, E. Honorio, E. Jiménez, H. Keeling, T. J. Killeen, J. C. Lovett, P. Meir, C. Mendoza, A. Morel, P. N. Vargas, S. Patiño, K. S.-H. Peh, A. P. Cruz, A. Prieto, C. A. Quesada, F. Ramírez, H. Ramírez, A. Rudas, R. Salamão, M. Schwarz, J. Silva, M. Silveira, J. W. Ferry Slik, B. Sonké, A. S. Thomas, J. Stropp, J. R. D. Taplin, R. Vásquez, and E. Vilanova. 2010. Drought-mortality relationships for tropical forests. *New Phytologist* 187:631–646.

Pierret, A., J.-L. Maeght, C. Clément, J.-P. Montoroi, C. Hartmann, and S. Gonkhamdee. 2016. Understanding deep roots and their functions in ecosystems: an advocacy for more unconventional research. *Annals of Botany* 118:621-635.

Querejeta, J. I., H. Estrada-Medina, M. F. Allen, and J. J. Jiménez-Osornio. 2007. Water source partitioning among trees growing on shallow karst soils in a seasonally dry tropical climate. *Oecologia* 152:26–36.

Querejeta, J. I., H. Estrada-Medina, M. F. Allen, J. J. Jiménez-Osornio, and R. Ruenes. 2006. Utilization of bedrock water by *Brosimum alicastrum* trees growing on shallow soil atop limestone in a dry tropical climate. *Plant and Soil* 287:187–197.

R Core Team. (2019). R: A language and environment for statistical computing. Vienna, Austria: R Foundation for Statistical Computing. https://www.R-project.org/

R Studio Team (2019). RStudio: Integrated Development for R. RStudio, Inc., Boston, MA http://www.rstudio.com/.

Ramalho, A. J., D. C. Zappi, G. L. Nunes, M. T. C. Watanabe, S. Vasconcelos, M. C. Dias, R. Jaffé, X. Prous, T. C. Giannini, G. Oliveira, and A. M. Giulietti. 2018. Blind Testing: DNA Barcoding Sheds Light Upon the Identity of Plant Fragments as a Subsidy for Cave Conservation. *Frontiers in Plant Science* 9:1–10.

Rodríguez-Huerta, E., M. Rosas-Casals, and L. M. Hernández-Terrones. 2019. Water societal metabolism in the Yucatán Peninsula. The impact of climate change on the recharge of groundwater by 2030. *Journal of Cleaner Production* 235:272–287.

Rosario, L. H., J. O. Rodríguez Padilla, D. R. Martínez, A. M. Grajales, J. A. Mercado Reyes, G. J. Veintidós Feliu, B. Van Ee, and D. Siritunga. 2019. DNA Barcoding of the Solanaceae Family in Puerto Rico Including Endangered and Endemic Species. *Journal of the American Society for Horticultural Science* 144:363–374.

Sanaphre-Villanueva, L., J. M. Dupuy, J. L. Andrade, C. Reyes-García, P. C. Jackson, and H. Paz. 2017. Patterns of plant functional variation and specialization along secondary succession and topography in a tropical dry forest. *Environmental Research Letters* 12:1–9.

Sánchez-Sánchez, O., and G. A. Islebe. 2002. Tropical forest communities in Southeastern Mexico. *Plant Ecology* 158:183–200.

Sánchez-Sánchez, O., G. A. Islebe, P. J. Ramírez-Barajas, and N. Torrescano-Valle. 2015. Natural and Human Induced Disturbance in Vegetation. Pages 153–167 *in* G. A. Islebe, S. Calmé, J. L. León-Cortés, and B. Schmook, editors. *Biodiversity and Conservation of the Yucatán Peninsula*. Switzerland: Springer International Publishing.

van der Sande, M. T., L. Poorter, S. A. Schnitzer, and L. Markesteijn. 2013. Are lianas more drought-tolerant than trees? A test for the role of hydraulic architecture and other stem and leaf traits. *Oecologia* 172:961–972.

Santiago, S. L., D. Bonal, M. E. De Guzman, and E. Ávila-Lovera. 2016. Drought Survival Strategies of Tropical Trees. *Tropical Tree Physiology* 6:243–258.

Sayer, E. J., and D. M. Newbery. 2003. The role of tree size in the leafing phenology of a seasonally dry tropical forest in Belize, Central America. *Journal of Tropical Ecology* 19:539–548.

Schenk, H. J., and R. B. Jackson. 2002. Rooting depths, lateral root spreads and belowground aboveground allometries of plants in water limited ecosystems. *Journal of Ecology* 90:480–494.

Schori, M., M. Appel, A. Kitko, and A. M. Showalter. 2013. Engineered DNA Polymerase Improves PCR Results for Plastid DNA. *Applications in Plant Sciences* 1:1–7.

Schwinning, S. 2010. The ecohydrology of roots in rocks. *Ecohydrology* 3:238–245.

Siddall, M., E. J. Rohling, A. Almogi-Labin, Ch. Hemleben, D. Meischner, I. Schmelzer, and D. A. Smeed. 2003. Sea-level fluctuations during the last glacial cycle. *Nature* 423:853–858.

Silvertown, J., Y. Araya, and D. Gowing. 2015. Hydrological niches in terrestrial plant communities: A review. *Journal of Ecology* 103:93–108.

Singh, B. 1997. Climate-related global changes in the southern Caribbean: Trinidad and Tobago. *Global and Planetary Change* 15:93–111.

Smart, P. L., P. A. Beddows, J. Coke, S. Doerr, S. Smith, and F. F. Whitaker. 2006. Cave Development on the Caribbean coast of the Yucatán Peninsula, Quintana Roo, Mexico. *Geological Society of America* 2404:105–128.

Sorensen, N. 2006. Regeneration and Growth of Several Canopy Tree Species in the Maya Forest of Quintana Roo, Mexico: The Role of Competition and Microhabitat Conditions. Oregon State University.

Stratton, L. C., G. Goldstein, and F. C. Meinzer. 2000. Temporal and spatial partitioning of water resources among eight woody species in a Hawaiian dry forest. Oecologia 124:309–317.

Träger, S., M. Öpik, M. Vasar, and S. D. Wilson. 2019. Belowground plant parts are crucial for comprehensively estimating total plant richness in herbaceous and woody habitats. *Ecology* 100:1–12.

Trimmis, K. P. 2018. Paperless mapping and cave archaeology: A review on the application of DistoX survey method in archaeological cave sites. *Journal of Archaeological Science: Reports* 18:399–407.

Tripathi, A. M., A. Tyagi, A. Kumar, A. Singh, S. Singh, L. B. Chaudhary, and S. Roy. 2013. The Internal Transcribed Spacer (ITS) Region and *trnH-psbA* Are Suitable Candidate Loci for DNA Barcoding of Tropical Tree Species of India. *PLoS ONE* 8:e57934.

Vacher, H. L. 1988. Dupuit-Ghyben-Herzberg analysis of strip-island lenses. *Geological Society of America Bulletin* 100:580–591.

Villaseñor, J. L. 2016. Checklist of the native vascular plants of Mexico. *Revista Mexicana de Biodiversidad* 87:559–902.

Waring, B. G., and J. S. Powers. 2017. Overlooking what is underground: Root:shoot ratios and coarse root allometric equations for tropical forests. *Forest Ecology and Management* 385:10–15.

Weemstra, M., L. Mommer, E. J. W. Visser, J. van Ruijven, T. W. Kuyper, G. M. J. Mohren, and F. J. Sterck. 2016. Towards a multidimensional root trait framework: a tree root review. *New Phytologist* 211:1159–1169.

Whigham, D. F., I. Olmsted, E. C. Cano, and M. E. Harmon. 1991. The Impact of Hurricane Gilbert on Trees, Litterfall, and Woody Debris in a Dry Tropical Forest in the Northeastern Yucatán Peninsula. *Biotropica* 23:434–441.

Williams, K., K. C. Ewel, R. P. Stumpf, F. E. Putz, W. Thomas, and T. W. Workman. 1999. Sea-level rise and coastal forest retreat on the west coast of Florida, USA. *Ecology* 80:2045–2063.

Worthington, S. R. H., D. C. Ford, and P. A. Beddows. 2000. Porosity and permeability enhancement in unconfined carbonate aquifers as a result of solution. Pages 463–471 *in* A. Klimchouk, D. Ford, A. Palmer, and W. Dreybrodt, editors. *Speleogenesis: Evolution of Karst Aquifers*. Huntsville, AL, USA: The National Speleological Society.

Wright, I. J., P. B. Reich, M. Westoby, D. D. Ackerly, Z. Baruch, F. Bongers, J. Cavender-Bares, T. Chapin, J. H. C. Cornellssen, M. Diemer, J. Flexas, E. Garnier, P. K. Groom, J. Gulias, K. Hikosaka, B. B. Lamont, T. Lee, W. Lee, C. Lusk, J. J. Midgley, M. L. Navas, Ü. Niinemets, J. Oleksyn, H. Osada, H. Poorter, P. Pool, L. Prior, V. I. Pyankov, C. Roumet,

S. C. Thomas, M. G. Tjoelker, E. J. Veneklaas, and R. Villar. 2004. The worldwide leaf economics spectrum. *Nature* 428:821–827.

Zolfaghar, S., R. Villalobos-Vega, J. Cleverly, M. Zeppel, R. Rumman, and D. Eamus. 2014. The influence of depth-to-groundwater on structure and productivity of *Eucalyptus* woodlands. *Australian Journal of Botany* 62:428–437.

5. FUNCTIONAL GROUPS MASK INTER- AND INTRASPECIFIC VARIATION IN WATER USE STRATEGIES IN A TROPICAL SEMI-EVERGREEN FOREST

5.1. Abstract

Across the karst landscape of Quintana Roo, Mexico, plant access to water and nutrients is limited by shallow soil. This soil is underlain by heterogeneous pockets in limestone bedrock and deeper but stable groundwater. If species differentially access these, substantial differences in resource uptake would be expected. The biodiverse forests in this seasonally dry tropical region are classified as semi-evergreen, suggesting that there are several strategies that maintain plant performance among co-occurring trees. This diversity has been previously organized into functional groups based on leaf and wood traits that are expected to also relate to resource use strategies, though this is rarely directly tested. Although surprisingly understudied, this system provides an opportunity to directly assess soil resource use strategies by direct root observation in the numerous, shallow caves found there and test functional group theory. We made three specific predictions: (1) that evergreen species would be more reliant on groundwater and more dominant in caves than deciduous species, (2) that trees with lower wood density would have lower water use efficiency than high wood density species and more reliant on deep water than high wood density species, and (3) species with larger individuals aboveground would also be dominant in the caves with consistent deep-water access. We assessed deep water access, utilization, and water use efficiency of trees at four sites along the Caribbean coast of Quintana Roo during the dry season to uncover relationships between rooting habit, tree size, and functional groups. In randomly established plots, species and diameter at breast height (DBH) were recorded for all trees with a DBH ≥ 5 cm above ground and in paired belowground plots roots were identified to species using DNA barcodes and abundances and size were recorded. Species were organized into rooting habit groups based on below ground root abundance and into functional groups based on phenology and wood density. Stem and leaf samples were collected from each individual and later analyzed for $\delta^{18}O$ and $\delta^{2}H$ as well as $\delta^{13}C$ and $\delta^{15}N$, respectively. Results showed that deciduous and evergreen species have overlapping rooting systems with the potential to access groundwater. Relative abundance of roots in the caves did not correspond with stable isotope ratio measurements. However, a decline in $\delta^{18}O$ among the largest trees in the plots provides evidence for deep water use by select species and individuals based on tree size. Interestingly, as trees became larger, $\delta^{13}C$ increased until a distinct size threshold in which $\delta^{13}C$ then declined. Deeper water use by larger trees corresponding to a decrease in water use efficiency suggests increased vulnerability to water limitation, a tendency reported in other seasonally dry tropical forests. However, our results point to the possibility that this reverses for the largest trees when groundwater is relatively readily accessible. Phenology and wood density did not predict stable isotope ratios indicating they were poor predictors of resource use in this system. Rather, significant, and relevant, intraspecific variation driven by tree size, site, and natural history appears to be lost in broad functional groups. Our work demonstrates that co-occurring tropical trees in Quintana Roo employ numerous resource acquisition strategies, which are not accurately predicted by functional groups, implying that inter- and intraspecific variation could impact community composition and ecosystem functioning in this seasonally dry region.

5.2. Introduction

All terrestrial plants must regulate carbon uptake and water loss. The balance is particularly strained during times of water limitation, presenting significant trade-offs (McDowell et al.

2008). Among species, many plant traits have been identified that increase water uptake, reduce water loss, or increase tolerance of water stress. These include high stomatal sensitivity (Henry et al. 2019), high leaf mass per area (Givnish 2002, Wright et al. 2004), high cavitation resistance (Steudle 2001, Sperry 2003, Chave et al. 2009, Trueba et al. 2017), deciduousness (Álvarez-Yépiz et al. 2017), and deep roots to access reliable water at depth (Bleby et al. 2010, Doody and Benyon 2011, Nardini et al. 2016, Pierret et al. 2016). Evaluating plant adaptations, physiological responses to environmental pressures, and resource niches reveals variation in water acquisition and use strategies within and across ecosystems (Osmond et al. 1987, Lavorel and Garnier 2002, Maire et al. 2015, Díaz et al. 2016, Funk et al. 2017). It has been observed that leaf and wood traits generally align with each other, meaning that a species with low wood density (and higher hydraulic efficiency) tend to have thin, light leaves with short lifespans (Wright et al. 2004, Méndez-Alonzo et al. 2012). On the other hand, species with high wood density tend to have dense, tough leaves with longer lifespans. These endmembers can be classified as resource acquisitive and resource conservative, respectively and are often linked to deciduous and evergreen growth forms (Markesteijn et al. 2011, Álvarez-Yépiz et al. 2017). Typically, acquisitive species have traits related to a “boom and bust” style, fast-growing and capitalizing on resources when they are available (Reich 2014, Weemstra et al. 2016). Naturally, conservative species generally have the opposite traits, allowing them to persist through dry periods (Aerts 1995). These conservative traits allow evergreens to maintain plant performance, not only in low nutrient environments but often in regions with variable precipitation regimes (Mitchell et al. 2008, Hasselquist et al. 2010, Ellsworth and Sternberg 2015). By categorizing co-occurring species into functional groups defined by the fundamental tradeoffs that plants face, we gain insight into the range of strategies in an ecosystem and their potential causes and consequences.

It is crucial to note that frameworks organizing water use strategies within and across plant communities are derived primarily from above ground observations and seemingly leave out the parts of the plant that are responsible for water uptake - the roots. While hydrologic niche separation below ground has been identified as a driver of community composition and structure (Silvertown et al. 1999, Swaffer et al. 2014, Ellsworth and Sternberg 2015, Brum et al. 2019), the majority of our insight into rooting depth is implied from functional groups or assessed through above ground measurements, such as the natural abundance of oxygen and hydrogen stable isotopes of stem water (Ehleringer and Dawson 1992). Roots being underground, of course, are difficult to study without excavation and manipulation, which precludes direct physiological measurements (Maeght et al. 2013, Pierret et al. 2016). Researchers have attempted to link leaf traits with root traits to establish a whole plant economic spectrum (Freschet et al. 2015, McCormack et al. 2015, Roumet et al. 2016). Yet, several studies have demonstrated a disconnect between the above and below ground (Roumet et al. 2016), begging the question about whether or not below ground observations, particularly rooting depth, aligns with presumed divisions between deciduous and evergreen species.

Tropical forests, in particular, seasonally dry tropical forests, are compelling ecosystems to investigate resource use strategies due to obvious challenges associated with water availability (Santiago et al. 2004). Having notable high phylogenetic and functional diversity (Eamus 1999, Cavender-Bares et al. 2016, DRYFLOR 2016), seasonally dry tropical forests are crucial landscapes for carbon sequestration and storage, holding as much as 8.7 Pg of carbon globally (Becknell et al. 2012). Unfortunately, they are among the most threatened of the global tropical forests, often impacted by deforestation for agriculture and urbanization (Arturo Sánchez-Azofeifa et al. 2005). Because of the plant diversity and water limitation as well as the need for research and conservation efforts, studies have focused on understanding plant traits and functional groups in seasonally dry tropical forests (Powers and Tiffin 2010, Santiago et al. 2017), with research expanding in the Yucatán Peninsula in southeast Mexico, a relatively understudied seasonally dry region. A precipitation gradient across the peninsula, from the drier northwest to wetter southeast, influences the distribution of vegetation types (Durán-García et al. 2016). Deciduous forests dominate in the state of Yucatán to the west, while semi-evergreen tropical forests dominate in the eastern state of Quintana Roo (Ibarra-Manríquez et al. 2002). There is a distinct dry season from November to May, in which only 20% of the annual precipitation is deposited, contributing to seasonal water limitation for the vegetation.

In addition, the Yucatán Peninsula is a vast karst landscape, which further exacerbates water limitation (Geekiyanage et al. 2019). Characterized by thin soils (less than 20 cm deep) atop limestone bedrock, water content and storage varies with the heterogeneous distribution of cavities in the rock (Querejeta et al. 2007, Hasselquist et al. 2010, Estrada-Medina et al. 2013a). The cavities are subjected to seasonal filling and draining (Estrada-Medina et al. 2013a) and both the water content in the soil and bedrock rapidly changes. This dynamism is contrasted by the karst aquifer, a reliable water source, that underlies the entire peninsula (Bauer-Gottwein et al. 2011). It is rather stable, with a hydraulic gradient of 5 to 10 mm change per kilometer (Marín et al. 2001). The distance to the surface of the freshwater lens varies across the peninsula, from 4 to

5 meters deep in northern Quintana Roo between 9 and 20 meters deep near Mérida in the northwest (Hasselquist et al. 2010, Estrada-Medina et al. 2013a, Durán-García et al. 2016). The presence of evergreen species among deciduous species and the increase in abundance along the precipitation but also depth to groundwater gradient begs questions about species-specific patterns in water use, with evergreens potentially accessing the reliable groundwater at depth as observed in other locations (Nepstad et al. 1994, Bleby et al. 2010, Swaffer et al. 2014, Ellsworth and Sternberg 2015, Nardini et al. 2016).

Although understudied compared to other seasonally dry topical forests, several studies have been carried out to understand water use strategies in the Yucatán Peninsula, particularly comparing the ecophysiology of co-occurring trees in order to identify hydraulic strategies in the diverse seasonally dry forests (Andrade et al. 2005, Querejeta et al. 2007, Hasselquist et al. 2010, Valdez-Hernández et al. 2010, Reyes-García et al. 2012, Estrada-Medina et al. 2013b). Based on leaf phenology and functional groups, researchers hypothesized that deciduous species utilize shallow water while evergreen species utilize groundwater. Many studies have found that root density was highest, and seemingly, limited to the upper layers of the bedrock, suggesting that the limestone itself prevents deep water access, even to the evergreens (Querejeta et al. 2007, Estrada-Medina et al. 2013a). Investigations into water use by co-occurring trees, via stable isotope analysis, revealed that trees were not utilizing groundwater (Querejeta et al. 2006, Estrada-Medina et al. 2013a, 2013b). While there was vertical partitioning with water sources, there was no clear division between evergreen and deciduous species (Querejeta et al. 2007). In a related study in northern Quintana Roo, researchers found separation in water use between evergreen and deciduous species but only in early successional forests (Hasselquist et al. 2010).

It appears there is hydrologic niche separation among co-occurring species, however, it does not follow expected patterns about water utilization between functional groups, contradicting assumptions about water use between evergreen and deciduous species (Eamus 1999). Advancing understanding of the roots in this system may help to explain these observations.

It is important to note that the majority of these studies have been isolated to a specific area of the peninsula, not surprisingly around the city of Mérida where there are several research institutions. In addition, investigations of water use strategies have been limited to a very small fraction of the estimated 500 tree species native to the peninsula (Valdez-Hernández et al. 2015). We know very little about how the species in this region are managing seasonal water limitation and how this system will respond to shifting temperature and precipitation regimes associated with climate change (De la Barreda et al. 2020). Loss of biodiversity and biomass is a prominent threat in tropical regions (Nepstad et al. 2007, Phillips et al. 2010, Rowland et al. 2015, Trueba et al. 2017). Not only are these important questions in functional ecology but answering them could help make predictions about how the vegetation in these seasonally dry tropical systems will respond to future climate scenarios.

For this research, we focused on the eastern state of Quintana Roo. This portion of the peninsula receives between 1200 to 1500 mm of precipitation annually, with a distinct dry period (Bauer-Gottwein et al. 2011, Durán-García et al. 2016). Forests are classified as semi-evergreen, meaning that 25% of the trees lose their leaves in the dry season (Sánchez-Sánchez and Islebe 2002). Below ground, extensive cave systems have formed by dissolution of the limestone bedrock (Smart et al. 2006, van Hengstum et al. 2010). In these caves, it is common to see tree roots emerging from conduits in the ceiling, walls, and speleothems (Adams et al. 2020a). While some hang from the ceiling or grow through the cave floor, some are in direct contact with pools of water. Anecdotal observations of the roots provide evidence that some trees are indeed accessing and utilizing deep water. This suggests that water use strategies may change as a function of depth to groundwater, with important consequences for forest species composition and responses to seasonal or longer water limitation.

We therefore wanted to know if this dominance and potential access to resources below ground corresponded to patterns in plant performance and resource acquisition strategies observed above ground. We made three specific predictions: (1) that evergreen species would be more reliant on groundwater and more dominant in caves than deciduous species, (2) that trees with lower wood density would have lower water use efficiency than high wood density species and more reliant on deep water than high wood density species, and (3) species with larger individuals aboveground would also be dominant in the caves with consistent deep-water access.

5.3. Methods

5.3.1. Site description and plot establishment

This work was conducted at four sites along the Caribbean coast of Quintana Roo, Mexico. The sites, Cueva Culebron, Jaguar Maw, Nohoch Aktun, and Ruta de los Guerreros, were located between the cities of Paamul and Akumal. Each site was associated with a cave network, allowing direct access to roots, as well as an assessment of the bedrock, depth to groundwater, and the groundwater itself. Because of the aim to directly connect the surface to the subterranean, detailed cave surveys and maps were required for each site in order to be selected. Using cave survey data, surface plots were randomly established at each site directly above cave passages and paired with below ground plots used to assess root biodiversity and abundance (Adams 2020). To determine plot locations, hypothetical transects were established following the general direction and length of cave passages. 100 m^2 plots were initially created on the transects with the number of plots corresponding to the length of the transect, requiring 10% of the transect be included in the total plot area. For example, if the transect length is 100 meters, one 100 m^2 plot covered 10% of the transect. For those transects less than 100 meters, it was randomly determined if a plot was to be created on the transect or not. Then plots physically established and surveyed in the field were randomly selected from those created prior to going to the field. Using survey data, GPS locations on the surface mirroring the location of the survey stations below ground were gathered before arriving at the sites. Two plots were selected per site.

5.3.2. Detailed site descriptions

Cueva Culebron: Cueva Culebron is commercial cave located near Akumal and 2 km from the coast. Depth to groundwater at the main entrance is 4.6 m with pools scattered throughout the meandering passages. Ceiling height is relatively even throughout the wide rooms, with an average of 2.4 m. Columns, associated formations, and Mayan stone walls guide cavers throughout system. The forest above ground is closed-canopy, reducing the abundance of understory trees, though palms are prevalent. Despite the cave being open for tours, the impact to the natural environment is minimal to none compared based on conversations with the landowners.

Jaguar Maw: Jaguar Maw is located near Paamul and 3.1 km from the coast. At the time of sampling, the cave was being developed as a show cave for an ecotourism operation. While clearing was not occurring on the headprint of the cave (the area above the cave), there were 1 to 2 m wide rock trails being built leading up to the entrances and flagging throughout the system to guide future visitors. The locations of the above and below ground plots used in this study were not included in this development, eliminating the human influence on our observations. Despite being relatively close to the coast, Jaguar Maw does not have exposed water, preventing us from making depth to groundwater measurements, though the maximum depth to the floor is 3.4 m. Passages are generally large and flat, with ceiling heights varying from 1.7 to 2.1 m. Though easy to walk through, many columns and a maze pattern can make it difficult to navigate.

Ruta de los Guerreros: This maze-like system is on the same property as a popular tourist cave and cenote, though this cave is not being utilized for tours. Located 3.7 km from coast and nearby Puerto Aventuras, the depth to groundwater was 9.3 m. Open rooms with tall ceilings (average 5.4 m tall) are contrasted by narrow passages with some places having prominent pools. Unlike the other sites, there are only two known entrances to this cave.

Nohoch Aktun: This commercial cave is close to the city of Akumal and 5.2 km from the coast. Defined by large collapses, it is difficult to travel far enough through the cave without seeing daylight. The depth to groundwater was recorded as 9.7 m below the surface at the collapse closest to the plots. Though this cave lacks prominent formations, the large, open passages and clear blue water is what attracts visitors. The landowners have been digging out the sediment mainly formed from sunken calcite rafts not only to make the pools deeper but to create an artificial path through the cave. Development is centered around the main entrance and parking lot, where trees have been cleared for buildings and trails. Therefore, initial plots that were within footprint of this development were excluded from the randomized selection, ensuring physical plots surveyed were further away from this portion of the system (see plot establishment description below).

5.3.3. Vegetation surveys

Field work was conducted between December 28, 2017 and January 8, 2018. Sampling was conducted in the dry season because we were interested in capturing differences in resource acquisition strategies during a time of limited water availability. To assess the above ground community composition, all individuals were identified to species either in the field, using pressed leaves, or via DNA barcoding (Adams 2020). Larger branches, seeds, and fruit when available were collected and included with voucher specimens for each species. All trees with a diameter at breast height (DBH) ≥ 5 cm had DBH recorded. Basal area was calculated for each tree and evaluated by species and site. For discussion purposes, individuals were noted as being small, medium, or large if the DBH was 5 to 14.9, 15 to 24.9, and ≥ 25 cm, respectively, based on anticipated tree sizes for this area (Whigham et al. 1991). Stems and leaves of all individuals measured were collected for later stem water (δ^{2}H and δ^{18}O) and leaf C (δ^{13}C) and N (δ^{15}N) stable isotope analysis. Stems were stripped of bark in the field, placed in glass scintillation vials with lined screw caps (12 mL, Wheaton-DWK Life Sciences, Millville, NJ, USA), and then wrapped with Parafilm. Vials were stored on ice in the field and then frozen until transport to the United States. Leaves were placed in Whirlpak bags (Nasco, Fort Aktinson, WI, USA) filled with silica gel (VWR International, LLC, Radnor, PA, USA) in order to rapidly dry the leaves in the field.

Soil samples were collected in the middle of the north half of each plot. These samples were later used to characterize the isotopic composition of the soil water. Soil was collected at 5 and 10 cm from the surface after removing the litter layer. Scintillation vials were filled three quarters full, sealed as above for stems, and stored and transported the same way. When the samples arrived at Texas A&M University, stem and soil samples were stored in a freezer (0°C) for later processing. Leaves were stored in the lab with added silica gel to ensure samples remained dry until processing.

5.3.4. Surveys below ground

As each plot on the surface was associated with a cave, we were able to characterize the below ground environment. Diversity of the roots exposed in the caves was assessed with DNA barcoding (Adams 2020). Species observed in above ground plots were organized into groups based on relative species abundance below ground (Table D-1). There were three groups; above ground only, rare below ground (< 5% relative abundance), and common below ground (> 5% relative abundance). These groups based on rooting habit were used to assess patterns in water use and water use efficiency.

Water was sampled from pools in the caves for a synoptic assessment of groundwater isotope ratios. No cave water samples were collected at Jaguar Maw as there was no exposed water in this system. The sites Ruta de los Guerreros and Nohoch Aktun were visited in the wet season (August 2017) as well and cave water was sampled during this time. For collection, glass vials (20 mL, VWR International, LLC, Radnor, PA, USA) were filled completely to minimize headspace and capped and sealed as above. Once at Texas A&M University, water samples were stored in a refrigerator (4°C) until stable isotope analysis.

5.3.5. Categorizing functional groups

Tree species were organized into functional groups based on phenology and wood density. Associated information was gathered from existing literature from the Yucatán Peninsula and other tropical forests (Table D-1). Distinction between lightwoods, softwoods, and hardwoods followed Borchert 1994, with wood density values of < 0.05 g/cm^3, 0.5 to 0.8 g/cm^3, and > 0.8 g/cm^3, respectively.

5.3.6. Sample processing

Water was extracted from stem and soil samples via cryogenic vacuum distillation. Extractions were performed at 100°C on a closed vacuum extraction line (West et al. 2006). We recognize that extraction temperature and soil texture potentially interact to affect the isotopic composition of extracted water (Adams et al. 2020b). We chose to perform extractions at this temperature to be consistent with other published work and with our objective of comparing among individuals with access to soils with similar clay content (Orlowski et al. 2016). Glass wool was placed above soil samples to inhibit soil particles from transferring to the cold finger. Extraction pressures began at 0.003 kPa. Extractions were considered complete when no further visible condensation was observed in the cold finger. For two stem water samples, an extended period was spent attempting to restore baseline pressure after frozen samples were placed on the line. Once analyzed, it was clear that these samples were outliers with evaporative losses from the extraction process and so were removed from subsequent analyses.

Water recovered from extractions as well as water collected from caves were transferred into vials (0.3 mL, Wheaton-DWK Life Sciences, Millville, NJ, USA) for stable O and H isotope analysis. Analyses were performed using a Delta V Advantage isotope ratio mass spectrometer linked to a High Temperature Conversion/Elemental Analyzer via a Conflo IV (Thermo Fisher Scientific, Waltham, MA, USA). Calibration was performed using in-house water standards: SIBS-wA (δ^2H = - 390.8 ± 0.8 ‰, δ^{18}O = - 50.10 ± 0.22 ‰; n = 9) and SIBS-wP (δ^2H = - 34.1 ± 1.0 ‰, δ^{18}O = - 4.61 ± 0.20 ‰; n = 9). Quality control was performed using an additional in-house water standard, SIBS-wU (δ^2H = - 120.2 ± 1.1 ‰, δ^{18}O = - 15.97 ± 0.22 ‰; n = 9). These in-house standards were previously calibrated using IAEA standards (VSMOW2, SLAP, and GISP). All isotope values are reported in VSMOW-SLAP scale.

Leaves were ground to powder using a Ball Mill (MM 400; Retsch GmbH, Haan, Germany). Ground samples were placed in tin capsules (Costech, Valencia, CA, USA) and weighed prior to C and N concentration and isotope analysis. Samples were loaded and subsequently combusted with a Costech ECS 4010 elemental combustion system (Costech Analytical Technologies Inc., Valencia, CA, USA) prior to isotope analysis with the Delta V Advantage isotope ratio mass spectrometer via the ConFlo IV. Calibration curves were derived using the following standards: USGS Glutamic Acid 40 δ^{13}C = - 26.39 ‰, δ^{15}N = - 4.52 ‰; n = 5) and USGS Glutamic Acid 41 δ^{13}C = 36.55 ‰, δ^{15}N = 47.55 ‰; n = 3). Internal plant standards were analyzed to determine the accuracy and precision of isotopic analysis. The isotope ratios were reported relative to Vienna Pee Dee Belemnite (VPDB) for C (Coplen 1995) and air for N (Hoefs 1997), and are expressed in per mil (‰) using standard delta notation (δ).

All sample processing and stable isotope analysis was performed at the Stable Isotope for Biosphere Science (SIBS) Laboratory (https://sibs.tamu.edu) at Texas A&M University.

5.3.7. Stable isotope analysis

Isotopic composition of stem water from individual trees was compared to soil water and cave water collected from each site. This allowed for evaluation of an individual tree's water source given the assumption that stem water is a weighted average of the water acquired by the tree and there is no fractionation during water uptake (Ehleringer and Dawson 1992). Trees were identified as utilizing shallow water if it resembled the heavy isotope-enriched soil water value or deep water if it resembled the heavy isotope-depleted cave water value. We did not attempt to quantify the fraction of groundwater use as we were interested in relative differences among individuals to deeper, heavy isotope-depleted water. As no precipitation was collected, a local meteoric water line was constructed based on precipitation collection from Playa del Carmen (Medina-Elizalde et al. 2016).

5.3.8. Statistical evaluation

Data analysis was carried out with the statistical software R (R Core Team, 2019) run in RStudio (RStudio Team, 2019). Data was checked for normality using the Shapiro-Wilk normality test and checked for equal variance with the Brown-Forsythe test. If data was found to be normally distributed with equal variance, effect of site, species, rooting habit, basal area, and functional group on $\delta^{18}O$, $\delta^{2}H$, $\delta^{13}C$, and $\delta^{15}N$ values were evaluated using one-way ANOVAs. Kruskal-Wallis tests were used if data had unequal variance. TukeyHSD mean comparisons provided insight into the differences between species groups and tree size. If data had unequal variance, Dunn-Bonferroni post hoc tests were performed. Linear and quadratic regressions were used to compare general patterns between $\delta^{18}O$, $\delta^{15}N$, and $\delta^{13}C$ along with $\delta^{18}O$, $\delta^{13}C$, and cross-sectional area of individual trees. Independent two sample t-tests were employed to determine if there were differences in soil water isotopes from different depths and cave water collected from different seasons.

5.4. Results

5.4.1. Above ground community composition

Of the 45 species identified across sites, the most abundant species was *Oxandra lanceolata* (Sw.) Baill. (18.9%), despite the species being present only at Nohoch Aktun (Table D-1). *Swartzia cubensis* (Britton & Wilson) Standl. had a relative abundance of 16.0% but was mainly observed at Ruta de los Guerreros. *Dendropanax arboreus* (L.) Decne. & Planch., *Drypetes lateriflora* (Sw.) Krug & Urb., *Ficus obtusifolia* Kunth, *Neea psychotrioides* Donn.Sm., and *Vitex gaumeri* Greenm. all had a relative abundance of 10.2%. These sites contain characteristic species of secondary seasonally dry semi-evergreen tropical forests expected in Quintana Roo (Sánchez-Sánchez and Islebe 2002, Adams 2020).

Among the 45 species observed, there were 30 evergreens and 15 deciduous species. Based on wood density, there were 7 lightwoods, 28 softwoods, 8 hardwoods, and 2 species without available wood density data. Overall, evergreen softwood was the most common functional group among trees in above ground plots.

5.4.2. Inferring rooting habit from below ground biodiversity

Based on identification of roots via DNA barcoding and morphological differences (Adams 2020), species observed above ground were grouped based on relative abundance below ground. 29 of the 38 of species identified from the roots were trees, with the rest being lianas and a palm. *Ficus* spp. dominated the below ground species composition along with *Pouteria* spp. and *Leucaena leucocephala* (Lam.) de Wit, classifying them as being common below ground, as their relative abundance below ground was 5% or greater. The remaining species observed below ground were categorized as rare below ground, with relative species abundances less than 5%. Species not observed below ground were classified as above ground only, assuming the majority of the roots are occupying the bedrock above the cave or are not exposed. See Table D-1 and Adams (2020) for more details.

Of the 29 tree species with roots exposed in the caves, there were 16 evergreens, 12 deciduous species, and 1 (*Blomia prisca* (Standl.) Lundell) that was unable to be categorized as information on phenology was not available. The common below ground group consisted of only evergreen species. The rare below ground group was fairly equally represented by evergreens (47%) and deciduous (53%) species while the above ground only group had 15 evergreens and 5 deciduous species. Overall, 47% of the evergreen species above ground had roots in the caves, while 63% of the deciduous species had roots in the caves.

5.4.3. Water stable isotopes

Cave water was collected during the dry season from Cueva Culebron and Ruta de los Guerreros and during the wet season at Ruta de los Guerreros and Nohoch Aktun. Water was not collected from Nohoch Aktun during the dry season as we anticipated sampling cave water when we returned to sample the second above ground plot. However, we were unable to visit the site after the first day. Yet, independent two sample t-tests showed that water collected in the dry season did not differ from water collected during the wet season for both δ^{18}O and δ^{2}H ($t_{14} = 1.89$, $p = 0.08$ and $t_{14} = -0.15$, $p = 0.88$, respectively). Therefore, the average isotopic composition of cave water was δ^{2}H: - 27.1 ± 1.6 ‰, δ^{18}O: - 4.48 ± 0.25 ‰; n = 11. Soil water from 5 and 10 cm in the dry season was δ^{2}H: - 14.1 ± 4.2 ‰, δ^{18}O: - 1.4 ± 0.69 ‰; n = 12. There was not a significant difference between the $\delta^{18}O$ and $\delta^{2}H$ values of the water extracted from the soils collected from 5 centimeters compared to 10 centimeters for ($t_{10} = - 1.24$, $p = 0.24$ and $t_{10} = - 1.05$, $p = 0.32$, respectively), though soil water from the 10 cm samples were generally more heavy isotope-depleted. There were no differences between soil water $\delta^{18}O$ and $\delta^{2}H$ values and site ($F_{3,8} = 1.52$, $p = 0.28$ and $F_{3,8} = 2.56$, $p = 0.13$, respectively).

Stem water $\delta^{18}O$ values ranged from - 4.93 to - 1.57 ‰ with an average of - 3.21 ± 0.79 ‰. $\delta^{2}H$ values ranged from - 37.7 to - 11.5 ‰ with an average of - 22.8 ± 6.1 ‰. $\delta^{18}O$ varied significantly across sites (χ^2 (3, N = 142) = 12.09, $p < 0.01$). We note that this data was found to have unequal variance according to Brown-Forshythe test, therefore, statistical differences between groups was assessed with Kruskal-Wallis tests. Trees from Cueva Culebron had stem water that was more heavy isotope-depleted compared to Jaguar Maw ($p < 0.01$; Figure 5.1A). $\delta^{2}H$ values from stem water also significantly varied by site (χ^2 (3, N = 142) = 21.83, $p < 0.01$), with Cueva Culebron, Ruta de los Guerreros, and Jaguar Maw all being different from each other while Nohoch Aktun overlapped with Cueva Culebron and Ruta de los Guerreros (Figure 5.1B). Jaguar Maw was had the highest mean $\delta^{2}H$, matching the pattern observed for $\delta^{18}O$.

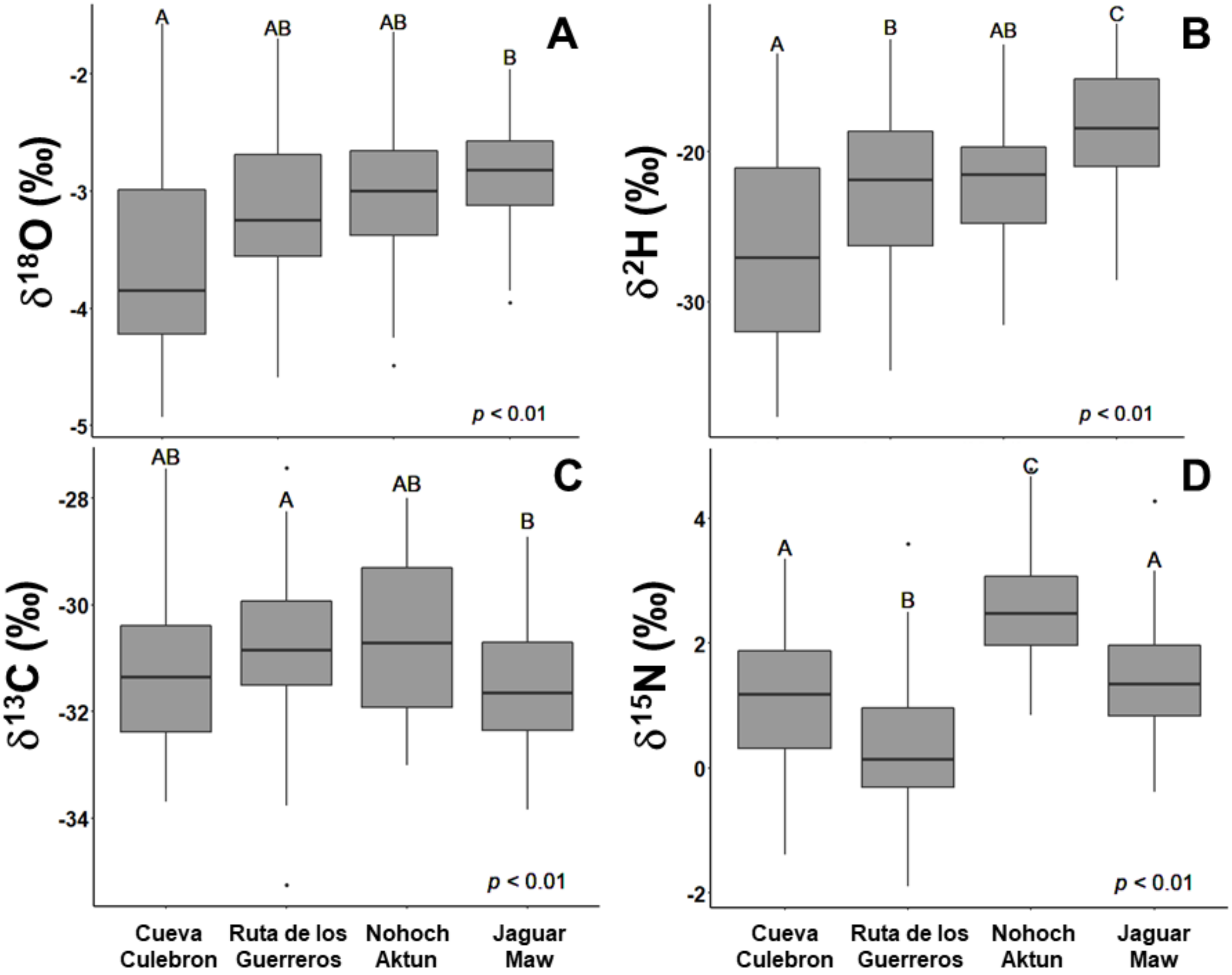

Figure 5.1 $\delta^{18}O$ (A), $\delta^{2}H$ (B), $\delta^{13}C$ (C), and $\delta^{15}N$ (D) by study site. Legumes are included in the $\delta^{15}N$ analysis. $\delta^{18}O$ and $\delta^{2}H$ values were obtained from stem water while $\delta^{13}C$ and $\delta^{15}N$ values were obtained from leaves.

5.4.4. Leaf stable isotopes

Across sites, leaf $\delta^{13}C$ ranged from - 35.3 to - 27.4 ‰, with an average of - 31.1 ± 1.5 ‰. There was a significant difference in $\delta^{13}C$ values among sites (χ^2 (3, N = 143) = 11.61, $p < 0.01$), yet only Ruta de los Guerreros and Jaguar Maw differed from each other ($p = 0.05$; Figure 5.1C).

Leaf $\delta^{15}N$ varied from - 1.9 to 4.8 ‰, with an average of 1.2 ± 1.2 ‰. As expected, legumes had $\delta^{15}N$ values that were closer to 0‰, compared to non-nitrogen fixing species ($F_{1,142} = 17.1$, $p < 0.01$). $\delta^{15}N$ increased with increasing $\delta^{18}O$ values among individual trees ($R^2 = 0.11$, $p < 0.01$), with legumes and non-legumes both having significantly positive relationships ($R^2 = 0.26$, $p = 0.01$ and $R^2 = 0.07$, $p < 0.01$, respectively; Figure 5.2A). There was a significant difference in $\delta^{15}N$ values by site (χ^2 (3, N = 144) = 12.61, $p < 0.01$), with all sites being different from each other ($p < 0.01$) except for Cueva Culebron and Jaguar Maw. Nohoch Aktun had the highest $\delta^{15}N$ values, due to the dominance of *O. lanceolata*, a shallow rooted species, and Ruta de los Guerreros having the lowest $\delta^{15}N$ values, as *S. cubensis*, a legume, was the most common tree at this site (Figure 5.1D).

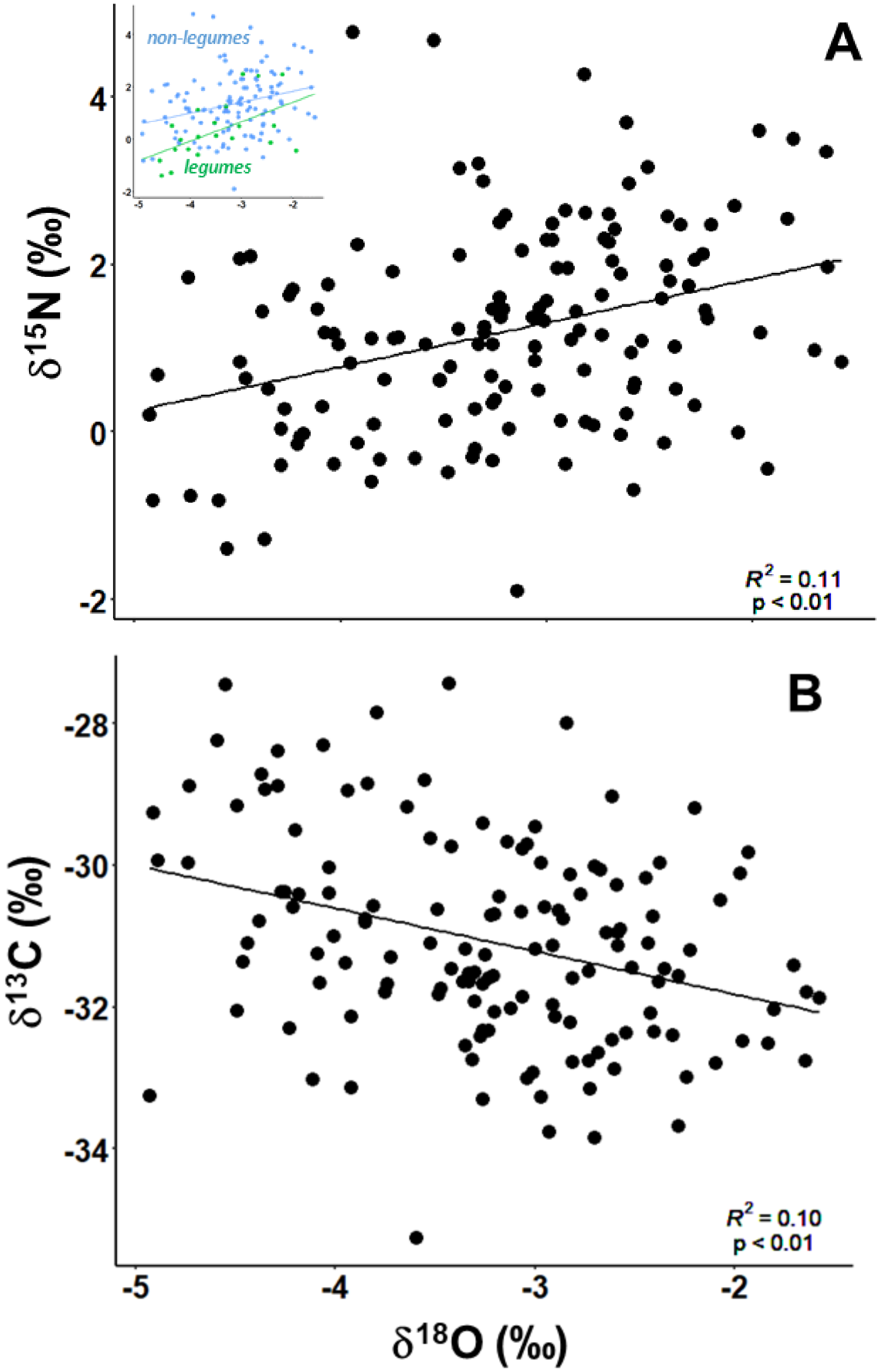

Figure 5.2 Relationships between $\delta^{18}O$ from stem water and $\delta^{15}N$ (A) and $\delta^{13}C$ (B) from leaves among individual trees. The inset in (A) depicts the linear regressions for non-legumes (R^2 = 0.07, $p < 0.01$) and legumes ($R^2 = 0.26$, $p = 0.01$).

5.4.5. Water and carbon isotopes based on rooting habit

$\delta^{18}O$ and $\delta^{2}H$ from extracted stem water did not vary between rooting habit groups ($F_{2,139} = 0.19$, $p = 0.83$ and $\chi^2 (2, N = 142) = 2.91$, $p = 0.23$, respectively; Figure 5.3A and Figure D-3A). Likewise, leaf $\delta^{13}C$ and $\delta^{15}N$ did not vary between rooting habit groups ($F_{2,140} = 0.75$, $p = 0.47$ and $F_{2,143} = 0.75$, $p = 0.48$, respectively; Figure 5.3B and Figure D-3B). The relationship with $\delta^{15}N$ did not change when legumes were excluded from the analysis ($F_{2,118} = 1.89$, $p = 0.16$; Figure D-3C), although the mean $\delta^{15}N$ value of the common below ground group was slightly heavy-isotope depleted compared to the above ground only and rare below ground groups.

When evaluating water stress by water use, there is a negative correlation across all individuals between $\delta^{13}C$ and $\delta^{18}O$ ($R^2 = 0.10$, $p < 0.01$) among individual trees (Figure 5.2B). We separated individuals into their respective rooting habit groups based on root abundance (Figure D-2). Individuals in the rare below ground and common below ground groups have significant relationships between $\delta^{13}C$ and $\delta^{18}O$ values ($R^2 = 0.09$, $p < 0.01$ and $R^2 = 0.55$, $p < 0.01$, respectively) while individuals in the above group only group do not ($R^2 = 0.02$, $p = 0.13$).

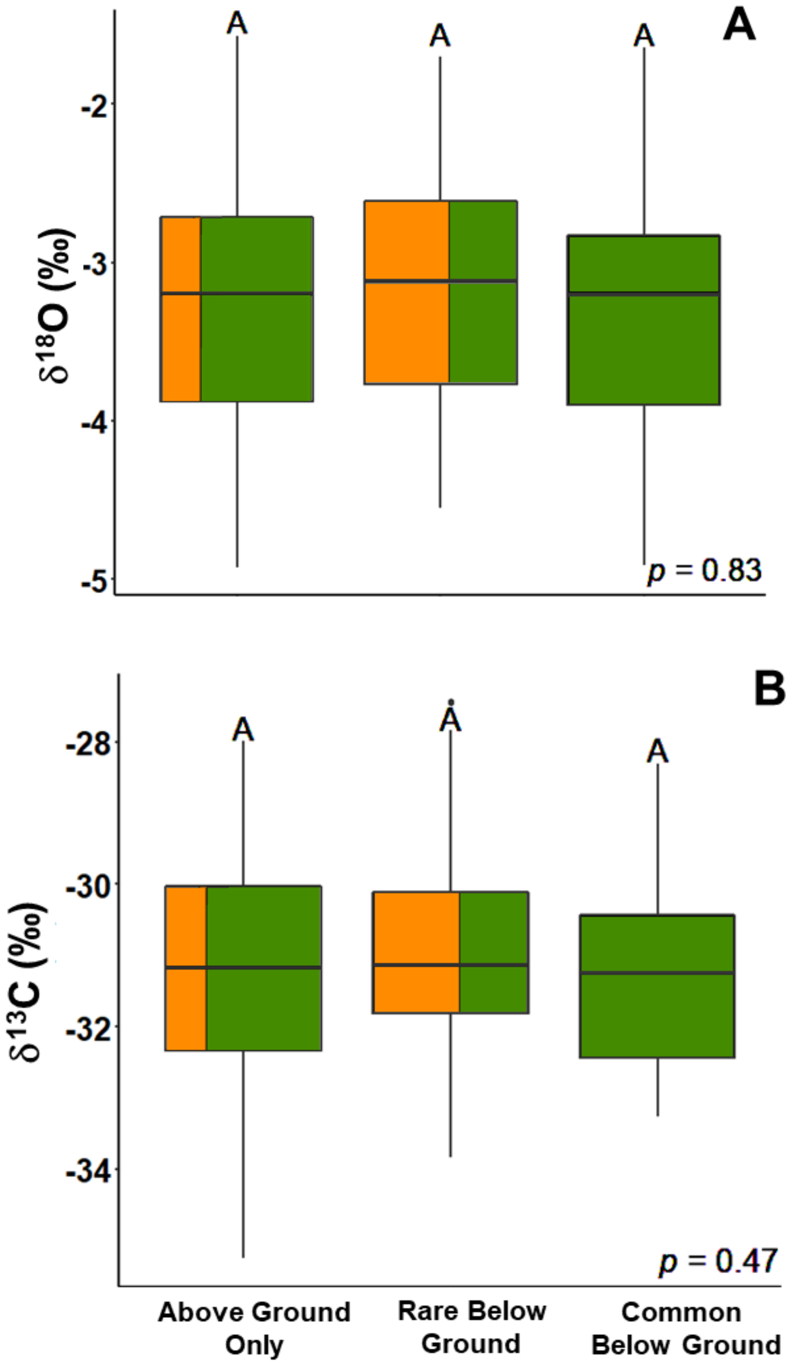

Figure 5.3 Stem water $\delta^{18}O$ (A) and leaf $\delta^{13}C$ (B) by rooting habit groups. Species classified as common below ground had relative root abundance of 5% or greater. Shading shows the fraction of deciduous (orange) and evergreen (green) species in each group.

5.4.6. Water and carbon isotopes based on tree size

Individuals were organized into size classes based on their cross-sectional area, each class corresponding to their respective diameter measurements in 5-cm increments. $\delta^{18}O$ values from extracted stem water were significantly different among size classes ($F_{5,136} = 3.35$, $p < 0.01$); Figure 5.4A). Results showed that $\delta^{18}O$ values varied among individuals classified as small, medium, and large ($F_{2,139} = 5.16$, $p < 0.01$). While large trees (≥ 25 cm DBH) had relatively having more heavy isotope-depleted values, the wide range of $\delta^{18}O$ among the small (5 to 14.9 cm DBH) and medium (15 to 24.5 cm DBH) overlapped with the narrow range observed in the large trees. However, $\delta^{2}H$ was not vary with cross-sectional area (χ^2 (5, N = 142) = 4.65, p = 0.46) but did significantly vary with tree size ($F_{2,139} = 3.74$, $p = 0.03$), following the same trend as $\delta^{18}O$ (Figure D-4).

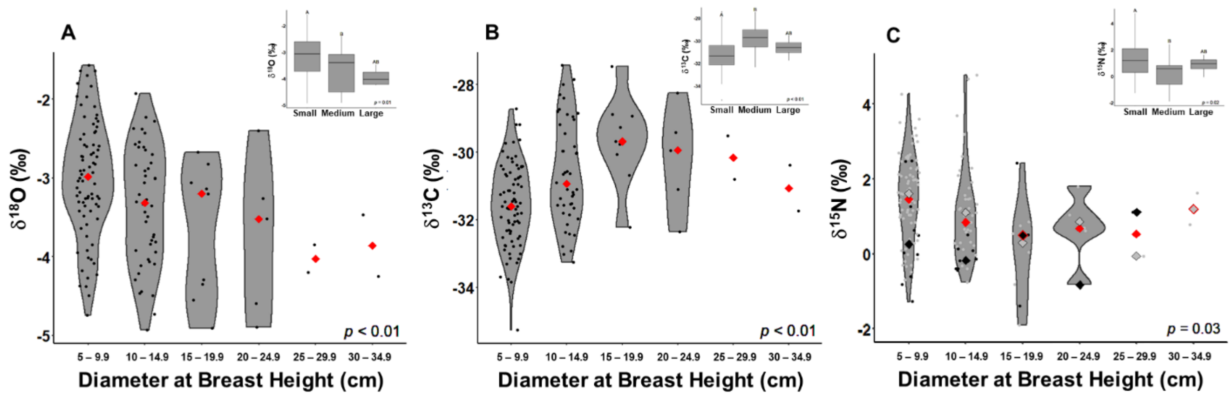

Figure 5.4 $\delta^{18}O$ from stem water (A), leaf $\delta^{13}C$ (B), and leaf $\delta^{15}N$ (C) by cross-sectional area, ranging from 5 to 35 cm, in 5-cm increments. The insets show $\delta^{18}O$, $\delta^{13}C$, and $\delta^{15}N$ by small (5 – 14.9 cm), medium (15 – 24.9 cm), and large trees (≥ 25 cm). The overall mean (red diamond) is shown for each size class. Legumes are included in the $\delta^{15}N$ analysis. Legumes and the associated mean for each size class are denoted as black diamonds while non-legumes and the associated mean are denoted as grey diamonds.

With regards to leaf $\delta^{13}C$, as cross-sectional area increased, $\delta^{13}C$ values became increasingly heavy isotope-enriched yet became heavy isotope-depleted after trees reached a certain size, seemingly around 20 cm in diameter ($F_{5,137} = 5.70, p < 0.01$; Figure 5.4B). A quadratic curve fit this relationship better, as represented by a lower AIC value than a line, though both regressions were significant ($R^2 = 0.15, p = < 0.01$ and $R^2 = 0.06, p < 0.01$, respectively). Further, results showed that $\delta^{13}C$ values were statistically different between individuals classified as small, medium, and large ($F_{2,140} = 6.05, p < 0.01$), showing the same non-linear pattern, though only the small and medium groups were different ($p < 0.01$). Leaf $\delta^{15}N$, evaluated with and without legumes, varied with cross-sectional area ($F_{5,138} = 2.61, p = 0.03$ and $F_{5,115} = 2.90, p = 0.02$, respectively) and tree size ($F_{2,141} = 4.20, p = 0.02$ and $F_{2,118} = 4.54, p = 0.01$, respectively; Figure 5.4C). $\delta^{15}N$ had the same non-linear pattern as $\delta^{13}C$, with small and medium trees being significantly different from each other ($p = 0.01$), despite the variation in these two groups.

5.4.7. Water use strategies among functional groups

There was no statistical difference in $\delta^{18}O$, $\delta^{2}H$, and $\delta^{13}C$ values among species grouped by phenology ($F_{1,142} = 1.05, p = 0.31$, χ^2 (1, N = 142) = 0.04, $p = 0.85$, and $F_{1,143} = 2.4, p = 0.12$, respectively), although the mean $\delta^{13}C$ value of the evergreens was slightly more heavy-isotope depleted compared to the deciduous species. Leaf $\delta^{15}N$ among evergreens was significantly more heavy-isotope enriched compared to deciduous species when evaluated with and without legumes ($F_{1,143} = 8.87, p < 0.01$ and $F_{2,119} = 6.89, p < 0.01$, respectively). $\delta^{18}O$, $\delta^{2}H$, and $\delta^{13}C$ values did not differ among species grouped by wood density ($F_{2,132} = 1.32, p = 0.27$, χ^2 (2, N = 134) = 4.96, $p = 0.08$, and $F_{2,133} = 0.37, p = 0.69$, respectively). Leaf $\delta^{15}N$ did not differ by wood density when analyzed with legumes ($F_{2,134} = 0.45, p = 0.64$) but when legumes were excluded, there was variation among wood density groups ($F_{2,111} = 3.94$, $p = 0.02$). In this case, hardwoods were significantly heavy-isotope enriched compared to softwoods ($p = 0.02$). Further separating species into functional groups based on phenology and wood density together did not result in significant differences in δ^{18}O, δ^{2}H, or δ^{13}C values ($F_{5,129} = 0.917$, $p = 0.47$, χ^2 (5, N = 135) = 5.14, $p = 0.40$, and $F_{5,130} = 1.33$, $p = 0.26$, respectively; Figure 5.5A, 5.5B, and 5.5C). While leaf δ^{15}N did not differ by functional groups ($F_{5,131} = 1.63$, $p = 0.16$; Figure 5.5D), conducting the analysis without legumes showed significant variation among functional groups ($F_{4,109} = 2.65$, $p = 0.04$), with evergreen hardwoods being heavy-isotope enriched compared to deciduous softwoods ($p = 0.03$). Variation in each group appears to be related to sample size, as the groups with the smaller ranges had the fewest observations and represented fewer species (deciduous lightwood and deciduous hardwood groups both had 5 samples from 2 species).

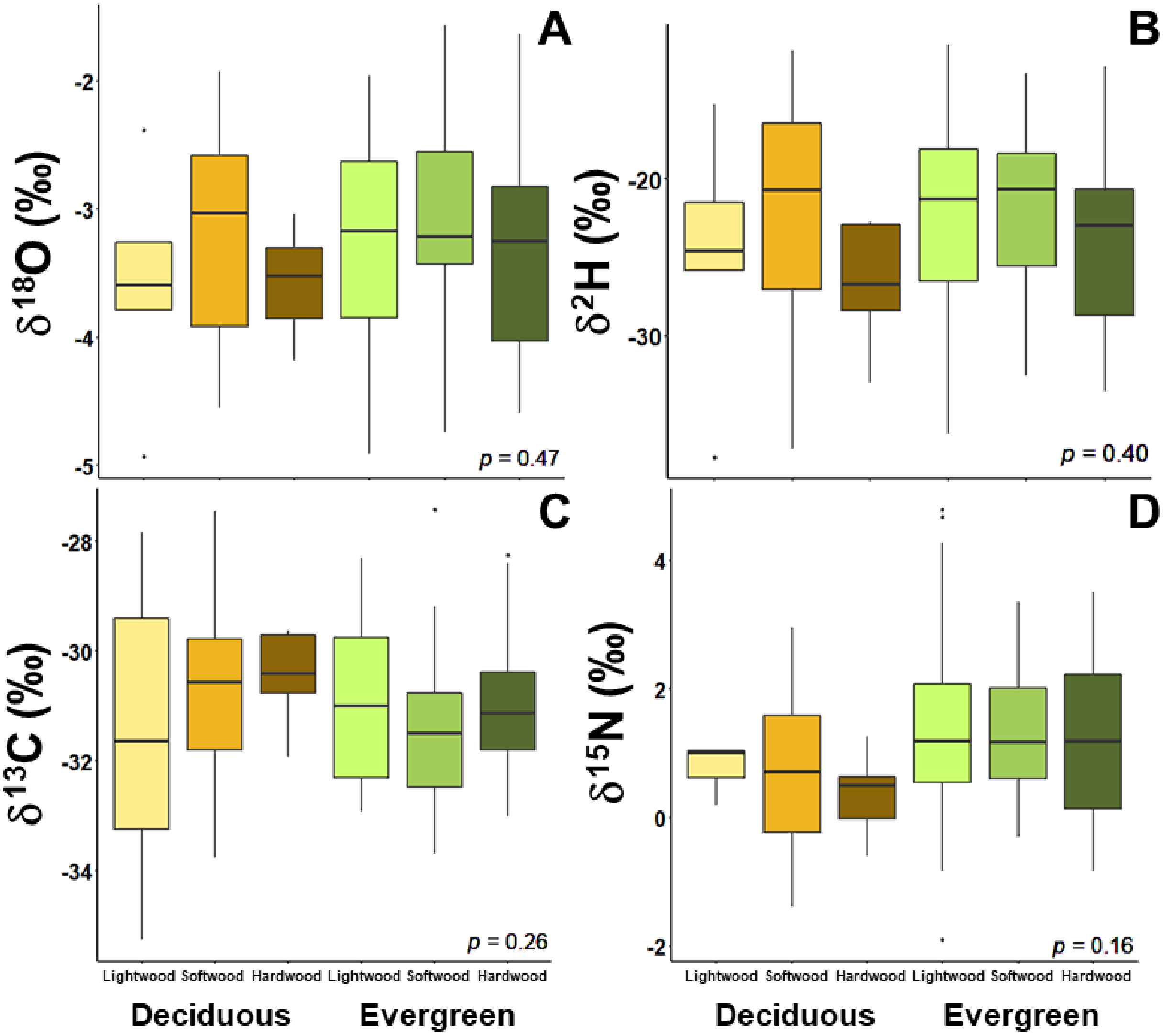

Figure 5.5 δ^{18}O (A), δ^{2}H (B), δ^{13}C (C), and δ^{15}N (D) by functional group. Legumes are included in the δ^{15}N analysis. δ^{18}O and δ^{2}H values were obtained from stem water while δ^{13}C and δ^{15}N values were obtained from leaves.

5.4.8. Evaluation of abundant species

To conduct a robust assessment of species differences in water use and water use efficiency, we limited the following analyses to species commonly found above ground across sites. These include 14 species with 4 or more individuals. *Bursera simaruba* (L.) Sarg. was included to represent the functional group, deciduous lightwood, even though there were only 3 individuals of this species in the above ground plots. Further, *Mosannona depressa* (Baill.) Chatrou was excluded, despite the fact that it was an abundant species, because there was no information available for wood density. Again, $\delta^{18}O$ and $\delta^{13}C$ was similar across functional groups (χ^2 (5, N = 90) = 9.96, $p = 0.08$ and (χ^2 (5, N = 91) = 6.42, $p = 0.27$, respectively). However, $\delta^{2}H$ differed among functional groups (χ^2 (5, N = 90) = 12.0, $p = 0.04$), yet only evergreen softwoods and evergreen hardwoods were different ($p = 0.03$). $\delta^{15}N$ differed among functional groups when evaluated with legumes (χ^2 (5, N = 92) = 13.46, $p = 0.02$) and without legumes (χ^2 (4, N = 77) = 12.02, $p = 0.02$). Among the non-legumes, evergreen hardwoods were significant heavy-isotope enriched compared to the deciduous lightwoods ($p = 0.05$) and deciduous softwoods ($p = 0.04$). There were significant differences in $\delta^{18}O$, $\delta^{2}H$, and $\delta^{13}C$ among species (χ^2 (8, N = 90) = 20.4, $p < 0.01$, χ^2 (8, N = 90) = 25.3, $p < 0.01$, and $F_{14,76} = 5.25$, $p < 0.01$, respectively; Figure 5.6A and 5.6B, Figure D-5). $\delta^{15}N$ also differed by species (χ^2 (8, N = 92) = 17.80, $p = 0.02$) and generally decreased with increasing deep water use, although there were some species that deviated from the trend, in particular *N. psychotrioides*, *O. lanceolata*, and *M. zapota* (Figure 5.6C).

Pouteria reticulata (Engl.) Eyma had the highest mean $\delta^{18}O$ and the lowest mean $\delta^{13}C$ while *Manilkara zapota* (L.) P. Royen had the lowest mean $\delta^{18}O$ and midrange mean $\delta^{13}C$. Following the overall patterns observed between water use and water use efficiency, the 4 species with the lowest mean $\delta^{18}O$ had the among lowest mean $\delta^{13}C$ (*P. reticulata*, *Cordia gerascanthus* L., *D. lateriflora*, and *D. arboreus*). The remainder of the species do not have a striking pattern in water use and water use efficiency. Variation within species appeared to be attributed to size and site differences. For example, *F. obtusifolia* showed the widest range of $\delta^{18}O$ and $\delta^{13}C$ among the abundant species, as individuals ranged in DBH from 8.8 to 19.2 cm. *N. psychotrioides*, on the other hand, were all small individuals, but individuals were present across all four sites. While some species express the expected patterns in water use and water use based on phenology, wood density, rooting habit, tree size, and life history (for example, *M. zapota* had large individuals with roots present in the caves, with low $\delta^{18}O$ stem water and relatively low $\delta^{13}C$), many do not follow expected patterns (for example, although *S. cubensis* is a secondary successional evergreen species observed above ground only, individuals had a low mean $\delta^{18}O$ and relatively high $\delta^{13}C$).

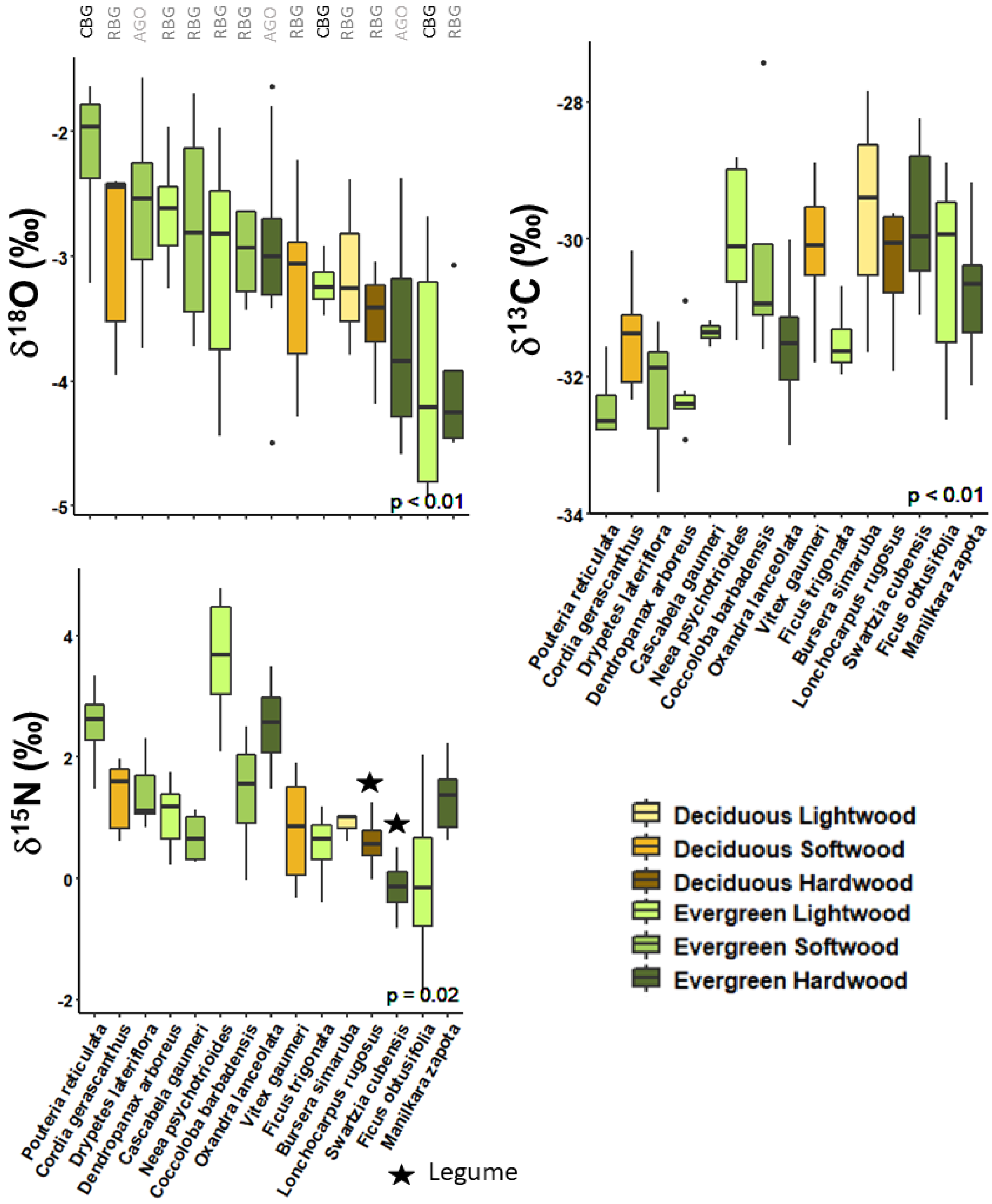

Figure 5.6 Patterns in $\delta^{18}O$ from stem water (A), leaf $\delta^{13}C$ (B), and leaf $\delta^{15}N$ (C) among abundant species (those with 4 or more individuals across sites). Rooting habit group is denoted above panel A (AGO = above ground only, RBG = rare below ground, CBG = common below ground).

5.5. Discussion

The results of our study depict striking variation in water access and water use strategies among species in the seasonally dry semi-evergreen tropical forests in Quintana Roo. We showed that water utilization and water use efficiency among co-occurring species was generally not predicted by rooting habit or functional groups, implying that generalizations about rooting depth and resource use strategies based on functional groups do not hold in this system. Tree size appeared to be more important across species than functional group, with large trees in general utilizing deep water sources compared to smaller trees. However, this deep water use did not correlate with lower water use efficiency. Interestingly, smaller trees and those with shallow water access generally expressed the lowest water use efficiency in spite of our expectation that these trees would face the greatest water limitation. Our assessment of multiple species allowed us to capture the inter- and intra-specific variation in water access in this karst landscape.

5.5.1. Evergreen and deciduous species have overlapping root zones

Through direct access to the roots in the caves, we were able to test assumptions about rooting depth and deep water access based on phenology. We identified 29 tree species in the caves, indicating that a multitude of species potentially have access to groundwater via deep roots (Adams 2020). Yet three species: *Ficus* spp., *Pouteria* spp., and *L. leucocephala* were most common below ground, accounting for the majority of root observations. While these three species frequently observed in the caves are evergreen species, consistent with our general prediction that evergreens would be most common below ground, only 16 of the 29 tree species with roots in the caves were evergreen, with 12 deciduous species identified below ground. Based on their abundance in above ground plots, deciduous species were more likely to root into the caves than the evergreen species. Therefore, our observations do not support deep rooting specialization by evergreens in general. Rather, evergreen and deciduous species have overlapping root zones with perhaps select evergreen species strongly specializing in deep rooting. This finding supports observations from other parts of the peninsula that showed no significant division between water sources among deciduous and evergreen species (Querejeta et al. 2007, Hasselquist et al. 2010). A related study on root density in Yucatán found that *B. simaruba*, a deciduous species, had 25% of its roots in the lowest layers of the bedrock (Estrada-Medina et al. 2013a). To explain this, observations from a study on tree seedlings from savannas found that deciduous species allocate more biomass to roots than leaves compared to evergreen species (Tomlinson et al. 2012). This group had rapid root extension to search for water. Related studies on tropical tree seedlings from Bolivia found that the majority of deciduous species had taproots compared to evergreen species (Poorter and Markesteijn 2008). Further, an investigation of root growth into bedrock under irrigation treatments found that the deciduous species responded to drought by increasing root growth into the rock fractures (Nie et al. 2017). While these observations were on seedlings in greenhouses, they suggest that deciduous species may have aggressive root foraging strategies, which appear to persist as trees age. These findings combined with our observations suggest that deciduous species are capable of rooting deeply, alongside evergreen species in Quintana Roo.

Our findings oppose those from other tropical forests in Venezuela and Panama, which found that evergreens had evidence of deeper water use from water potential measurements and stable isotope assessments (Sobrado 1986, Jackson et al. 1995, Meinzer et al. 1999). Research on root biomass in Bolivia found that drought-delaying species with conservative traits had deeper root systems compared to resource acquisitive species (Markesteijn and Poorter 2009). A potential explanation for this discrepancy may be related to the deeper soils in these forests, providing more opportunities for root exploration and vertical partitioning compared to our karst system, which limits root exploration to pre-existing conduits (Schwinning 2010, Gao et al. 2016). Therefore, our observations challenge assumptions about rooting depth made from above ground observations and expectations based on phenology alone (Eamus 1999). Overall, these findings show that multiple species, across phenology groups, have the potential to access deep water sources in Quintana Roo. Further work on traits that may favor deep rooting specialization in these two groups is warranted.

5.5.2. Importance of combining root observations with stable isotopes

The DNA barcoding and direct root observation was a necessary step allowing us to identify the species capable of rooting deeply into the caves. However, we recognize that there are caveats with basing deep water access conclusions with this approach alone. First, we only sampled the roots that we could access; however, there could roots we missed because they were encased the bedrock or speleothems (Klappa 1980, Taborosi 2006). Avoiding exposure in the cave environment can prevent desiccation of the roots, which some species may be more tolerant of, and therefore more likely to be observed, than others. Second, it is commonly assumed that individuals associated with the roots are utilizing the resources they are in contact with or have access to. An absence of strong connections between root biomass and resource uptake has been documented by tracking uptake of added labelled tracers (Kulmatiski et al. 2017). Resource uptake appears to relate more to the location of the resource, root system architecture, and functional differences between fine and coarse roots rather than presence and abundance of roots (Bleby et al. 2010, da Silva et al. 2011, Kiba and Krapp 2016). Therefore, we coped with these limitations by incorporating stable isotope analysis to assess water source and water use efficiency among co-occurring trees.

Focusing first on root observations, we noted that roots from *Pouteria* spp. were primarily solitary bundles of fine roots suspended from the ceiling. *L. leucocephala* roots, on the other hand, were more commonly coarse roots embedded in large masses, in the presence of other roots and organic matter. *Ficus* spp. roots were found as fine and coarse roots, both solitary and in large masses. These observations suggest that even though all three species are commonly found in the caves, *Pouteria* spp. roots can withstand dry conditions, potentially dominating underutilized locations in the bedrock or cave while *L. leucocephala* roots remain in dense groups and follow rooting patterns of other species. *Ficus* spp. roots seems to be versatile, rooting alongside other species and tolerating dry locations, which may make it possible to successfully deploy roots in a variety of conditions and leading to dominance below ground. Species-specific patterns in root exploration and growth influence which species were observed in the caves and explain variation in water use. It is notable that the water isotope patterns follow the root observation patterns among these species. *Pouteria* species (*P. reticulata* and *P. campechiana*) had the least negative $\delta^{18}O$ and $\delta^{2}H$ values, suggesting strong dependence on shallow water sources, as *Pouteria* roots were visibly not contacting water in the caves. On the other hand, *Ficus* species had among the most negative $\delta^{18}O$ and $\delta^{2}H$ values, suggesting deep water dependence and aligning with the striking dominance below ground, even compared to *Pouteria* spp. and *L. leucocephala*. The intermediate water isotope values observed among *L. leucocephala* potentially reflect a combination of shallow and deep water use as a result of fine and tap roots, as they compete other species for resources and space below ground (Normaniza et al. 2008, Saifuddin et al. 2013). For these species commonly observed below ground, the water isotopes provide complimentary insights to root deployment strategies and water resource use.

Interestingly, rather than clustering around relatively high δ^{18}O values as would be expected for species dependent on shallow water sources, the group of species we observed above ground only exhibited the full range of observed δ^{18}O values. This provides evidence that some species may be utilizing pathways to groundwater that rarely result in exposed roots in caves. For example, *Hampea trilobata* Standl., a species without roots identified in the caves had among the lowest mean δ^{18}O values and mean δ^{13}C values in the entire dataset (Figure D-1A and D-1D). It is further notable that this species had consistently lower δ^{13}C values compared to species with roots in the caves with similar δ^{18}O values. In addition, *Thouinia paucidentata* Radlk. was observed above ground only, supporting the low abundance of root tips observed by Estrada-Medina et al (2013) in the bedrock at a quarry and suspected shallow water use. In our study, a surprisingly wide range of δ^{18}O values was found among individuals, potentially as the result of site differences. Interestingly, variation in δ^{18}O did not lead to variation in δ^{13}C. Rather, the fact that this species is an endemic, generalist with high specific leaf area, suggesting high water use efficiency, seemingly regardless of water access (Bhaskar et al. 2014, Sanaphre-Villanueva et al. 2017). In this and other cases, morphological and physiological traits are informative. For example, *Melicoccus oliviformis* Kunth reportedly utilized bedrock water predominately during the dry season, suggesting shallow rooting (Querejeta et al. 2007). Researchers also found this species to have among the lowest δ^{13}C values, as this evergreen species flushes new leaves at the beginning of the wet season. In our study, *M. oliviformis* was observed above ground only, with relatively high δ^{18}O values and low δ^{13}C values, supporting the reported reliance on bedrock water. Comparable δ^{18}O and δ^{13}C values among *D. lateriflora* imply similar strategies to *M. oliviformis*, despite the fact that these two species have differing life history trends (*D. lateriflora* is late successional while *M. oliviformis* is rare and uncommon in mature forests; Schultz et al. 2005). *D. lateriflora* has been identified as a diffuse-porous species with thick vessel walls, suggesting increased hydraulic resistance, which may explain the ability to successfully utilize shallow water sources and potentially maintain low water stress (Ramírez-Martínez et al. 2017). Therefore, by incorporating the stable isotope data, we avoided making assumptions about water access based on root observations alone, and instead highlighted the apparent variation in water use strategies in karst landscapes.

5.5.3. Tree size influences water access and use

Our results showed that tree size influenced water use and water use efficiency. A negative correlation between δ^{18}O values of extracted stem water and tree size, confirmed, as expected, that large individuals utilized deep water more than smaller individuals. These larger individuals were represented by *M. zapota, F. trigonata, B. alicastrum,* and *L. leucocephala*, which all had roots present in the caves with *Ficus* spp. and *L. leucocephala* being common below ground. While both are evergreen, *Ficus cotinifolia* Kunth was found to have shallow water use in a previous study (Querejeta et al. 2007) and *L. leucocephala* has been noted as having a more isohydric water use strategy, which might suggest a conservative water use strategy and shallower rooting (Liang and Zhang 1999). *M. zapota* and *B. alicastrum* are notable species in mature, old forests (García-Frapolli et al. 2007) and important species for Maya agroforestry (Querejeta et al. 2006, Sánchez-Sánchez et al. 2015); however, limited studies have been conducted on water use strategies of these key species (Benjamin et al. 2001, Querejeta et al.

2006). Yet, the factors that connect these species are large size and root presence in the caves, making them comparable in terms of water use. These findings agree with studies that show, in general, below ground biomass positively correlates with above ground biomass (Schenk and Jackson 2002, Casper et al. 2003), leading to deeper water use compared to smaller trees with shallower root penetration (Sayer and Newbery 2003, Hasselquist et al. 2010, Phillips et al. 2010).

We noted related patterns between $\delta^{18}O$, $\delta^{15}N$, and cross-sectional area of individual trees, with depletion in these stem water and leaf stable isotopes with increased size when species are binned by DBH. As there was a significant positive trend between $\delta^{15}N$ and $\delta^{18}O$, it appears that the leaf N isotopes provide insight into rooting depth and compliment the tree water source information in the water isotope results. The relationship is to be expected in seasonally dry systems, with increased denitrification in surface layers and increased leaching with high mean annual precipitation in tropical systems (Pataki et al. 2008, Roa-Fuentes et al. 2015, Craine et al. 2015, Campo 2016). In addition, in karst soils, nitrogen binds to soil organic matter in the presence of Ca from the calcium carbonate bedrock (Clarholm et al. 2015, Pan et al. 2016). This decreases plant available nitrogen, which may be exacerbated with increasing depth and decreasing amounts of soil within bedrock conduits from the surface. Therefore, the smallest trees appear to be accessing shallow sources, as evidenced by the relatively heavy-isotope enriched $\delta^{15}N$ and $\delta^{18}O$ values. The observed depletion of $\delta^{15}N$ from the smallest to the medium-sized individuals may be the result of reduced nitrogen availability from leaching and stabilization in soil organic matter at depth. It is crucial to note that the legumes are not driving the depletion among the medium-sized trees, as evidenced by a comparable mean $\delta^{15}N$ among legumes and non-legumes in the 15 – 19.9 cm DBH class. Overall, leaf $\delta^{15}N$ appears to be indicative of rooting depth, providing further support for water access and utilization among individuals of different sizes in our study.

Interestingly, this relationship with tree size and water use does not correspond to other studies conducted in the Yucatán Peninsula. Similar investigations utilizing water and stable isotopes report no relationship between water source depth and tree size (Querejeta et al. 2006, 2007, Hasselquist et al. 2010, Estrada-Medina et al. 2013b). Rather, it has been previously noted that deep water use by small individuals, particularly among deciduous species, may be a critical water use strategy during early life stages (Meinzer et al. 1999, Stratton et al. 2000, Hasselquist et al. 2010). Establishing deep roots with reliable water access early on has been suggested to increase survival in seasonally dry environments (Paz et al. 2015). Considering the small individuals in our study expressed the full range of $\delta^{18}O$ values observed, it is possible that some of the variation is attributed to young, acquisitive species, whereas some species clearly utilize a different strategy. It does appear that with increasing tree size, variation decreases with the largest trees on the landscape relying more heavily on deeper water during the dry season.

5.5.4. Deep water use does not equate to lower water use efficiency

Comparing $\delta^{13}C$ to cross-sectional area of individual trees showed an increase in $\delta^{13}C$ values with tree size until a threshold, after which $\delta^{13}C$ then declined. This suggests that water use efficiency increases with tree size until trees reach a certain size, seemingly around 20 cm in diameter, after which efficiency declines. Previously we interpreted the water isotope results as indicating deeper water use by larger trees. We would expect that deeper water access would result in a more stable water source and that would yield lower water use efficiency with increasing tree size. We observed the opposite pattern. This suggests that while deep water use increases with tree size, complimentary decrease in water use efficiency is not observed until the tree reaches a certain size suggesting that water limitation in fact increases for all but the very largest trees on the landscape. We noted that the corollary to this is that small trees, without deep water use, had comparable $\delta^{13}C$ values to the large trees. This seems surprising as previous work showed that thin top soil and heterogenous conduits in the bedrock affect the spatial distribution of water in these karstic systems (Estrada-Medina et al. 2013a). Studies from the Edwards Plateau in Texas, USA have shown that evapotranspiration and soil moisture tended to be dynamic near the surface, suggesting short-term and readily depleted soil water storage (McCole and Stern 2007, Heilman et al. 2014). Yet, small trees in our system utilizing shallow water appear to withstand these fluctuations in water availability, potentially because the lower water demands by small trees are being met by the soil-filled voids in the limestone (Schwartz et al. 2013, Ding et al. 2018). On the other hand, the medium sized trees display high water use efficiency and potential water stress, as their relatively higher water demands are apparently not being satisfied by the often low and variable water in the cavities and pores. These trees do not appear to be large enough to support extensive deep roots with deep water access. The observed patterns in water use and water use efficiency highlights the range of strategies, even among individuals, and suggests that tree size is important to consider when evaluating water use and water use strategies among co-occurring species. Furthermore, there may be implications for how size distribution among species and with communities may impact responses to disturbance and climate change.

5.5.5. Functional groups mask relevant species-specific water use strategies

We predicted that functional groups would inform water use strategies among species in these semi-evergreen tropical forests. Yet, the functions we observed inferred from stable isotopes and direct root observations were not well-predicted by existing functional groups for these dry tropical forest species. While the functional group framework has been highly productive and useful for predicting vegetation responses to environmental change (Lavorel and Garnier 2002, Sterck et al. 2006, Poorter and Bongers 2006, Maire et al. 2015), some studies in seasonal tropical systems have found that organizing species based on a few leaf or wood traits does not explain variation in responses to water limitation. For example, a study from a tropical dry forest in Costa Rica showed that canopy position and leaf toughness explained variation in leaf $\delta^{13}C$ while phenology did not (Leffler and Enquist 2002). In our study, significant variation within groups resulted in a lack of variation between groups, similarly observed by Powers and Tiffin (2010).

Focusing on the more abundant species revealed the breadth of water use strategies at play. Again, there were not differences among root habit or functional groups but there were significant differences in $\delta^{18}O$ and $\delta^{13}C$ among species. Focusing on a limited number of species also allowed us to reveal the intraspecific variation, seemingly driven by tree size, site, and in some cases, root distribution, as discussed previously. Trait variation within species has been noted to be important for community composition and ecosystem processes (Bolnick et al. 2011, Enquist et al. 2015, Siefert et al. 2015), as interactions by individuals with the environment influence survivorship of the species over time. Specifically in seasonally dry systems, climate, soils, and stand age have been found to influence leaf traits, wood traits, water sources, and community composition (Becknell and Powers 2014, Plourde et al. 2015, Voltas et al. 2015, Souza et al. 2018). Souza et al (2018) noted that species with high plasticity may be able to successfully persist in future climate scenarios due to their ability to withstand a range of environmental conditions. However, evaluating water use strategies by functional groups masks relevant species variation that could impact community composition and ecosystem functioning, particularly in diverse tropical regions.

5.6. Conclusions

Investigating water use strategies in seasonally dry tropical systems is crucial to understand how these biodiverse regions will respond to future precipitation regimes. The karst topography of the Quintana Roo provided the unique opportunity to evaluate water access, utilization, and water use efficiency through above and below ground observations. Through direct root observation in caves, we showed that rooting depth does not match predictions based solely on functional groups. Evergreen and deciduous species were observed rooting together with overlapping root zones and in fact a higher fraction of deciduous species appeared to access groundwater than evergreen, although all of the species dominant in the caves were evergreens. This finding implies that there is competition for resources and potentially space in the limestone in Quintana Roo and possibly karst landscapes in general. Rooting depth and root abundance did not predict water use efficiency, suggesting that some species can manage resources effectively, even without deep water access. Differences in water use and water use efficiency was better explained by tree size. Progressively larger trees were utilizing deep water, but small trees had overlapping $\delta^{13}C$ values with the large trees, suggesting the water demands of the small individuals were being met by water in shallow soils and bedrock while large trees were successfully accessing groundwater to increase plant performance. This relates to differences among successional stages, with implications for how size distribution among species and with communities may impact responses to disturbance and climate change. Finally, functional groups did not accurately depict water use strategies among co-occurring species. This framework appears to mask relevant species variation, as observed among the abundant species, that could impact community composition and ecosystem functioning in this seasonally dry region. Therefore, consideration and research on species-specific resource acquisition strategies and ecophysiological responses to water availability needs to be on the forefront to properly assess the trajectories of these and other seasonally dry tropical forests in future climate scenarios.

5.7. Acknowledgements

Research was supported by the Sid Kyle Graduate Merit Assistantship from the Department of Ecosystem Science and Management (ESSM) at Texas A&M University (TAMU), National Geographic Society Early Career Grant (CP-090ER-17), and the MSC L.T. Jordan Institute for International Awareness at TAMU. We greatly appreciate Peter Sprouse of Zara Environmental, LLC for his guidance and hospitality as well as maps and survey data for all sites. We would like to thank the landowners for providing us access to their property to conduct this work.

5.8. References

Adams, R. E. 2020. Landscape controls on and physiological benefits of deep rooting by trees in Quintana Roo, Mexico. Texas A&M University.

Adams, R. E., T. M. Iliffe, and J. B. West. 2020a. Identifying tree roots in the caves of Quintana Roo, Mexico as a step toward ecological insights and improved conservation. *Plants, People, Planet* 2:133–139.

Adams, R. E., A. Hyodo, T. SantaMaria, C. L. Wright, T. W. Boutton, and J. B. West. 2020b. Bound and mobile soil water isotope ratios are affected by soil texture and mineralogy, whereas extraction method influences their measurement. *Hydrological Processes* 34:991–1003.

Aerts, R. 1995. The advantages of being evergreen. *Trends in Ecology & Evolution* 10:402–407.

Álvarez-Yépiz, J. C., A. Búrquez, A. Martínez-Yrízar, M. Teece, E. A. Yépez, and M. Dovciak. 2017. Resource partitioning by evergreen and deciduous species in a tropical dry forest. *Oecologia* 183:607–618.

Andrade, J. L., F. C. Meinzer, G. Goldstein, and S. A. Schnitzer. 2005. Water uptake and transport in lianas and co-occurring trees of a seasonally dry tropical forest. *Trees* 19:282–289.

Arturo Sánchez-Azofeifa, G., M. Quesada, J. P. Rodriguez, J. M. Nassar, K. E. Stoner, A. Castillo, T. Garvin, E. L. Zent, J. C. Calvo-Alvarado, M. E. R. Kalacska, L. Fajardo, J. A. Gamon, and P. Cuevas-Reyes. 2005. Research Priorities for Neotropical Dry Forests. *Biotropica* 37:477–485.

Bauer-Gottwein, P., B. R. N. N. Gondwe, G. Charvet, L. E. Marín, M. Rebolledo-Vieyra, and G. Merediz-Alonso. 2011. Review: The Yucatán Peninsula karst aquifer, Mexico. *Hydrogeology Journal* 19:507–524.

Becknell, J. M., L. Kissing Kucek, and J. S. Powers. 2012. Aboveground biomass in mature and secondary seasonally dry tropical forests: A literature review and global synthesis. *Forest Ecology and Management* 276:88–95.

Becknell, J. M., and J. S. Powers. 2014. Stand age and soils as drivers of plant functional traits and aboveground biomass in secondary tropical dry forest. *Canadian Journal of Forest Research* 44:604–613.

Benjamin, T. J., P. I. Montanez, J. J. M. Jimenez, and A. R. Gillespie. 2001. Carbon, water and nutrient flux in Maya homegardens in the Yucatán Peninsula of Mexico. *Agroforestry Systems* 53:103–111.

Bhaskar, R., T. E. Dawson, and P. Balvanera. 2014. Community assembly and functional diversity along succession post-management. *Functional Ecology* 28:1256–1265.

Bleby, T. M., A. J. McElrone, and R. B. Jackson. 2010. Water uptake and hydraulic redistribution across large woody root systems to 20 m depth. *Plant, Cell & Environment* 33:2132–2148.

Bolnick, D. I., P. Amarasekare, M. S. Araújo, R. Bürger, J. M. Levine, M. Novak, V. H. W. Rudolf, S. J. Schreiber, M. C. Urban, and D. A. Vasseur. 2011. Why intraspecific trait variation matters in community ecology. *Trends in Ecology & Evolution* 26:183–192.

Brum, M., M. A. Vadeboncoeur, V. Ivanov, H. Asbjornsen, S. Saleska, L. F. Alves, D. Penha, J. D. Dias, L. E. O. C. Aragão, F. Barros, P. Bittencourt, L. Pereira, and R. S. Oliveira. 2019. Hydrological niche segregation defines forest structure and drought tolerance strategies in a seasonal Amazon forest. *Journal of Ecology* 107:318–333.

Campo, J. 2016. Shift from ecosystem P to N limitation at precipitation gradient in tropical dry forests at Yucatán, Mexico. Environmental Research Letters 11.

Casper, B. B., H. J. Schenk, and R. B. Jackson. 2003. Defining a plant's belowground zone of influence. *Ecology* 84:2313–2321.

Cavender-Bares, J., D. D. Ackerly, S. E. Hobbie, and P. A. Townsend. 2016. Evolutionary Legacy Effects on Ecosystems: Biogeographic Origins, Plant Traits, and Implications for Management in the Era of Global Change. *Annual Review of Ecology, Evolution, and Systematics* 47:433–462.

Chave, J., D. Coomes, S. Jansen, S. L. Lewis, N. G. Swenson, and A. E. Zanne. 2009. Towards a worldwide wood economics spectrum. *Ecology Letters* 12:351–366.

Clarholm, M., U. Skyllberg, and A. Rosling. 2015. Organic acid induced release of nutrients from metal-stabilized soil organic matter – The unbutton model. *Soil Biology and Biochemistry* 84:168–176.

Coplen, T. B. 1995. New IUPAC guidelines for the reporting of stable hydrogen, carbon, and oxygen isotope-ratio data. *Journal of Research of the National Institute of Standards and Technology* 100:285.

Craine, J. M., E. N. J. Brookshire, M. D. Cramer, N. J. Hasselquist, K. Koba, E. Marin-Spiotta, and L. Wang. 2015. Ecological interpretations of nitrogen isotope ratios of terrestrial plants and soils. *Plant and Soil* 396:1–26.

De la Barreda, B., S. E. Metcalfe, and D. S. Boyd. 2020. Precipitation regionalization, anomalies and drought occurrence in the Yucatán Peninsula, Mexico. *International Journal of Climatology*.

Díaz, S., J. Kattge, J. H. C. Cornelissen, I. J. Wright, S. Lavorel, S. Dray, B. Reu, M. Kleyer, C. Wirth, I. Colin Prentice, E. Garnier, G. Bönisch, M. Westoby, H. Poorter, P. B. Reich, A. T. Moles, J. Dickie, A. N. Gillison, A. E. Zanne, J. Chave, S. Joseph Wright, S. N. Sheremet Ev, H. Jactel, C. Baraloto, B. Cerabolini, S. Pierce, B. Shipley, D. Kirkup, F. Casanoves, J. S. Joswig, A. Günther, V. Falczuk, N. Rüger, M. D. Mahecha, and L. D. Gorné. 2016. The global spectrum of plant form and function. *Nature* 529:167–171.

Ding, Y., Y. Nie, S. Schwinning, H. Chen, J. Yang, W. Zhang, and K. Wang. 2018. A novel approach for estimating groundwater use by plants in rock-dominated habitats. *Journal of Hydrology* 565:760–769.

Doody, T. M., and R. G. Benyon. 2011. Direct measurement of groundwater uptake through tree roots in a cave. *Ecohydrology* 4:644–649.

DRYFLOR. 2016. Plant diversity patterns in neotropical dry forests and their conservation implications. *Science* 353:1383–1387.

Durán-García, R., M. Méndez-Gonzalez, and A. Larqué-Saavedra. 2016. The biodiversity of the Yucatán Peninsula: a natural laboratory. *Progress in Botany* 78:237–258.

Eamus, D. 1999. Ecophysiological traits of deciduous and evergreen woody species in the seasonally dry tropics. *Trends in Ecology & Evolution* 14:11–16.

Ehleringer, J. R., and T. E. Dawson. 1992. Water uptake by plants: perspectives from stable isotope composition. *Plant, Cell & Environment* 15:1073–1082.

Ellsworth, P. Z., and L. S. L. Sternberg. 2015. Seasonal water use by deciduous and evergreen woody species in a scrub community is based on water availability and root distribution. *Ecohydrology* 8:538–551.

Enquist, B. J., J. Norberg, S. P. Bonser, C. Violle, C. T. Webb, A. Henderson, L. L. Sloat, and V. M. Savage. 2015. Scaling from Traits to Ecosystems: Developing a General Trait Driver Theory via Integrating Trait-Based and Metabolic Scaling Theories. Pages 249–318 *Advances in Ecological Research*. Amsterdam, Netherlands: Elsevier.

Estrada-Medina, H., R. C. Graham, M. F. Allen, J. J. Jiménez-Osornio, and S. Robles-Casolco. 2013a. The importance of limestone bedrock and dissolution karst features on tree root distribution in northern Yucatán, México. *Plant and Soil* 362:37–50.

Estrada-Medina, H., L. S. Santiago, R. C. Graham, M. F. Allen, and J. J. Jiménez-Osornio. 2013b. Source water, phenology and growth of two tropical dry forest tree species growing on shallow karst soils. *Trees* 27:1297–1307.

Freschet, G. T., E. M. Swart, and J. H. C. Cornelissen. 2015. Integrated plant phenotypic responses to contrasting above- and below-ground resources: Key roles of specific leaf area and root mass fraction. *New Phytologist* 206:1247–1260.

Funk, J. L., J. E. Larson, G. M. Ames, B. J. Butterfield, J. Cavender-Bares, J. Firn, D. C. Laughlin, A. E. Sutton-Grier, L. Williams, and J. Wright. 2017. Revisiting the Holy Grail: using plant functional traits to understand ecological processes. *Biological Reviews* 92:1156–1173.

Gao, W., L. Hodgkinson, K. Jin, C. W. Watts, R. W. Ashton, J. Shen, T. Ren, I. C. Dodd, A. Binley, A. L. Phillips, P. Hedden, M. J. Hawkesford, and W. R. Whalley. 2016. Deep roots and soil structure. *Plant, Cell & Environment* 39:1662–1668.

García-Frapolli, E., B. Ayala-Orozco, M. Bonilla-Moheno, C. Espadas-Manrique, and G. Ramos-Fernández. 2007. Biodiversity conservation, traditional agriculture and ecotourism: Land cover/land use change projections for a natural protected area in the northeastern Yucatán Peninsula, Mexico. *Landscape and Urban Planning* 83:137–153.

Geekiyanage, N., U. M. Goodale, K. Cao, and K. Kitajima. 2019. Plant ecology of tropical and subtropical karst ecosystems. *Biotropica* 51:626–640.

Givnish, T. 2002. Adaptive significance of evergreen vs. deciduous leaves: solving the triple paradox. *Silva Fennica* 36.

Hasselquist, N. J., M. F. Allen, and L. S. Santiago. 2010. Water relations of evergreen and drought-deciduous trees along a seasonally dry tropical forest chronosequence. *Oecologia* 164:881–890.

Heilman, J. L., M. E. Litvak, K. J. Mcinnes, J. F. Kjelgaard, R. H. Kamps, and S. Schwinning. 2014. Water-storage capacity controls energy partitioning and water use in karst ecosystems on the Edwards Plateau, Texas. *Ecohydrology* 7:127–138.

van Hengstum, P. J., E. G. Reinhardt, P. A. Beddows, and J. J. Gabriel. 2010. Linkages between Holocene paleoclimate and paleohydrogeology preserved in a Yucatán underwater cave. *Quaternary Science Reviews* 29:2788–2798.

Henry, C., G. P. John, R. Pan, M. K. Bartlett, L. R. Fletcher, C. Scoffoni, and L. Sack. 2019. A stomatal safety-efficiency trade-off constrains responses to leaf dehydration. *Nature Communications* 10:3398.

Hoefs, J. 1997. *Stable Isotope Geochemistry*. Berlin, Germany: Springer.

Ibarra-Manríquez, G., J. L. Villaseñor, R. Durán, and J. Meave. 2002. Biogeographical analysis of the tree flora of the Yucatán Peninsula. *Journal of Biogeography* 29:17–29.

Jackson, P. C., J. Cavelier, G. Goldstein, F. C. Meinzer, and N. M. Holbrook. 1995. Partitioning of water resources among plants of a lowland tropical forest. *Oecologia* 101:197–203.

Kiba, T., and A. Krapp. 2016. Plant Nitrogen Acquisition Under Low Availability: Regulation of Uptake and Root Architecture. *Plant and Cell Physiology* 57:707–714.

Klappa, C. F. 1980. Rhizoliths in terrestrial carbonates: classification, recognition, genesis and significance. *Sedimentology* 27:613–629.

Kulmatiski, A., P. B. Adler, J. M. Stark, and A. T. Tredennick. 2017. Water and nitrogen uptake are better associated with resource availability than root biomass. *Ecosphere* 8:e01738.

Lavorel, S., and E. Garnier. 2002. Predicting changes in community composition and ecosystem functioning from plant traits: revisiting the Holy Grail. *Functional Ecology* 16:545–556.

Leffler, A. J., and B. J. Enquist. 2002. Carbon isotope composition of tree leaves from Guanacaste, Costa Rica: comparison across tropical forests and tree life history. *Journal of Tropical Ecology* 18:151–159.

Liang, J., and J. Zhang. 1999. The relations of stomatal closure and reopening to xylem ABA concentration and leaf water potential during soil drying and rewatering. *Plant Growth Regulation* 29:77–86.

Maeght, J.-L., B. Rewald, and A. Pierret. 2013. How to study deep roots-and why it matters. *Frontiers in Plant Science* 4:1–14.

Maire, V., I. J. Wright, I. C. Prentice, N. H. Batjes, R. Bhaskar, P. M. van Bodegom, W. K. Cornwell, D. Ellsworth, Ü. Niinemets, A. Ordonez, P. B. Reich, and L. S. Santiago. 2015. Global effects of soil and climate on leaf photosynthetic traits and rates: Effects of soil and climate on photosynthetic traits. *Global Ecology and Biogeography* 24:706–717.

Marín, L. E., E. C. Perry, H. I. Essaid, and B. Steinich. 2001. Hydrogeological Investigations and Numerical Simulation of Groundwater Flow in the Karstic Aquifer of Northwestern Yucatán, Mexico, presented at First International Conference on Saltwater Intrusion and Coastal Aquifers - Monitoring, Modeling, and Management. Essaouira, Morocco, 2001.

Markesteijn, L., and L. Poorter. 2009. Seedling root morphology and biomass allocation of 62 tropical tree species in relation to drought- and shade-tolerance. Journal of Ecology 97:311–325.

Markesteijn, L., L. Poorter, F. Bongers, H. Paz, and L. Sack. 2011. Hydraulics and life history of tropical dry forest tree species: coordination of species’ drought and shade tolerance. *New Phytologist* 191:480–495.

McCole, A. A., and L. A. Stern. 2007. Seasonal water use patterns of *Juniperus ashei* on the Edwards Plateau, Texas, based on stable isotopes in water. *Journal of Hydrology* 342:238–248.

McCormack, M. L., I. A. Dickie, D. M. Eissenstat, T. J. Fahey, C. W. Fernandez, D. Guo, H. S. H. S. Helmisaari, E. A. Hobbie, C. M. Iversen, R. B. Jackson, J. Leppälammi-Kujansuu, R. J. Norby, R. P. Phillips, K. S. Pregitzer, S. G. Pritchard, B. Rewald, M. Zadworny, J. Lepp??lammi-Kujansuu, R. J. Norby, R. P. Phillips, K. S. Pregitzer, S. G. Pritchard, B. Rewald, and M. Zadworny. 2015. Redefining fine roots improves understanding of below-ground contributions to terrestrial biosphere processes. *New Phytologist* 207:505–518.

McDowell, N., W. T. Pockman, C. D. Allen, D. D. Breshears, N. Cobb, T. Kolb, J. Plaut, J. Sperry, A. West, D. G. Williams, and E. A. Yepez. 2008. Mechanisms of plant survival and mortality during drought: why do some plants survive while others succumb to drought? *New Phytologist* 178:719–739.

Medina-Elizalde, M., S. J. Burns, J. M. Polanco-Martínez, T. Beach, F. Lases-Hernández, C.-C. Shen, and H.-C. Wang. 2016. High-resolution speleothem record of precipitation from the Yucatán Peninsula spanning the Maya Preclassic Period. *Global and Planetary Change* 138:93–102.

Meinzer, C. F., L. J. Andrade, G. Goldstein, M. N. Holbrook, J. Cavelier, and J. S. Wright. 1999. Partitioning of soil water among canopy trees in a seasonally dry tropical forest. *Oecologia* 121:293–301.

Méndez-Alonzo, R., H. Paz, R. C. Zuluaga, J. A. Rosell, and M. E. Olson. 2012. Coordinated evolution of leaf and stem economics in tropical dry forest trees. *Ecology* 93:2397–2406.

Mitchell, P. J., E. J. Veneklaas, H. Lambers, and S. S. O. Burgess. 2008. Leaf water relations during summer water deficit: Differential responses in turgor maintenance and variation in leaf structure among different plant communities in south-western Australia. *Plant, Cell & Environment* 31:1791–1802.

Nardini, A., V. Casolo, A. Dal Borgo, T. Savi, B. Stenni, P. Bertoncin, L. Zini, and N. G. Mcdowell. 2016. Rooting depth, water relations and non-structural carbohydrate dynamics in three woody angiosperms differentially affected by an extreme summer drought. *Plant, Cell & Environment* 39:618–627.

Nepstad, D. C., C. R. de Carvalho, E. A. Davidson, P. H. Jipp, P. A. Lefebvre, G. H. Negroiros, E. D. da Silva, T. A. Stone, S. E. Trumbore, and S. Vierira. 1994. The role of deep roots in the hydrological cycles of Amazonian forest and pastures. *Nature* 372:666–669.

Nepstad, D. C., I. M. Tohver, D. Ray, P. Moutinho, and G. Cardinot. 2007. Mortality of large trees and lianas following experimental drought in an Amazon forest. *Ecology* 88:2259–2269.

Nie, Y., H. Chen, Y. Ding, J. Yang, and K. Wang. 2017. Comparison of Rooting Strategies to Explore Rock Fractures for Shallow Soil-Adapted Tree Species with Contrasting Aboveground Growth Rates: A Greenhouse Microcosm Experiment. *Frontiers in Plant Science* 8:1651.

Normaniza, O., H. A. Faisal, and S. S. Barakbah. 2008. Engineering properties of *Leucaena leucocephala* for prevention of slope failure. *Ecological Engineering* 32:215–221.

Orlowski, N., L. Breuer, and J. J. McDonnell. 2016. Critical issues with cryogenic extraction of soil water for stable isotope analysis: Issues with Cryogenic Soil Water Extraction. *Ecohydrology* 9:1–5.

Osmond, C. B., M. P. Austin, J. A. Berry, W. D. Billings, J. S. Boyer, J. W. H. Dacey, P. S. Nobel, S. D. Smith, and W. E. Winner. 1987. Stress Physiology and the Distribution of Plants. *BioScience* 37:38–48.

Pan, F., Y. Liang, W. Zhang, J. Zhao, and K. Wang. 2016. Enhanced Nitrogen Availability in Karst Ecosystems by Oxalic Acid Release in the Rhizosphere. *Frontiers in Plant Science* 7:1–9.

Pataki, D. E., S. A. Billings, E. Naumburg, and C. M. Goedhart. 2008. Water sources and nitrogen relations of grasses and shrubs in phreatophytic communities of the Great Basin Desert. *Journal of Arid Environments* 72:1581–1593.

Paz, H., F. Pineda-García, and L. F. Pinzón-Pérez. 2015. Root depth and morphology in response to soil drought: comparing ecological groups along the secondary succession in a tropical dry forest. *Oecologia* 179:551–561.

Phillips, O. L., G. van der Heijden, S. L. Lewis, G. López-González, L. E. O. C. Aragão, J. Lloyd, Y. Malhi, A. Monteagudo, S. Almeida, E. A. Dávila, I. Amaral, S. Andelman, A. Andrade, L. Arroyo, G. Aymard, T. R. Baker, L. Blanc, D. Bonal, Á. C. A. de Oliveira, K.-J. Chao, N. D. Cardozo, L. da Costa, T. R. Feldpausch, J. B. Fisher, N. M. Fyllas, M. A. Freitas, D. Galbraith, E. Gloor, N. Higuchi, E. Honorio, E. Jiménez, H. Keeling, T. J. Killeen, J. C. Lovett, P. Meir, C. Mendoza, A. Morel, P. N. Vargas, S. Patiño, K. S.-H. Peh, A. P. Cruz, A. Prieto, C. A. Quesada, F. Ramírez, H. Ramírez, A. Rudas, R. Salamão, M. Schwarz, J. Silva, M. Silveira, J. W. Ferry Slik, B. Sonké, A. S. Thomas, J. Stropp, J. R. D. Taplin, R. Vásquez, and E. Vilanova. 2010. Drought-mortality relationships for tropical forests. *New Phytologist* 187:631–646.

Pierret, A., J.-L. Maeght, C. Clément, J.-P. Montoroi, C. Hartmann, and S. Gonkhamdee. 2016. Understanding deep roots and their functions in ecosystems: an advocacy for more unconventional research. *Annals of Botany* 118:621–635.

Plourde, B. T., V. K. Boukili, and R. L. Chazdon. 2015. Radial changes in wood specific gravity of tropical trees: inter- and intraspecific variation during secondary succession. *Functional Ecology* 29:111–120.

Poorter, L., and F. Bongers. 2006. Leaf traits are good predictors of plant performance across 53 rain forest species. *Ecology* 87:1733–1743.

Poorter, L., and L. Markesteijn. 2008. Seedling Traits Determine Drought Tolerance of Tropical Tree Species. *Biotropica* 40:321–331.

Powers, J. S., and P. Tiffin. 2010. Plant functional type classifications in tropical dry forests in Costa Rica: leaf habit versus taxonomic approaches: Leaf habit and functional traits of dry forest trees. *Functional Ecology* 24:927–936.

Querejeta, J. I., H. Estrada-Medina, M. F. Allen, and J. J. Jiménez-Osornio. 2007. Water source partitioning among trees growing on shallow karst soils in a seasonally dry tropical climate. *Oecologia* 152:26–36.

Querejeta, J. I., H. Estrada-Medina, M. F. Allen, J. J. Jiménez-Osornio, and R. Ruenes. 2006. Utilization of bedrock water by *Brosimum alicastrum* trees growing on shallow soil atop limestone in a dry tropical climate. *Plant and Soil* 287:187–197.

R Core Team. (2019). R: A language and environment for statistical computing. Vienna, Austria: R Foundation for Statistical Computing. https://www.R-project.org/

R Studio Team (2019). RStudio: Integrated Development for R. RStudio, Inc., Boston, MA http://www.rstudio.com/.

Ramírez-Martínez, M., T. Terrazas, S. Aguilar-Rodríguez, and J. G. Martínez-Ávalos. 2017. Anatomía de la madera de especies de la selva baja caducifolia de Tamaulipas, México. *Madera y Bosques* 23:21–41.

Reich, P. B. 2014. The world-wide 'fast-slow' plant economics spectrum: a traits manifesto. *Journal of Ecology* 102:275–301.

Reyes-García, C., J. L. Andrade, J. L. Simá, R. Us-Santamaría, and P. C. Jackson. 2012. Sapwood to heartwood ratio affects whole-tree water use in dry forest legume and non-legume trees. *Trees* 26:1317–1330.

Roa-Fuentes, L. L., P. H. Templer, and J. Campo. 2015. Effects of precipitation regime and soil nitrogen on leaf traits in seasonally dry tropical forests of the Yucatán Peninsula, Mexico. *Oecologia* 179:585–597.

Roumet, C., M. Birouste, C. Picon-Cochard, M. Ghestem, N. Osman, S. Vrignon-Brenas, K. fang Cao, and A. Stokes. 2016. Root structure-function relationships in 74 species: Evidence of a root economics spectrum related to carbon economy. *New Phytologist* 210:815–826.

Rowland, L., A. C. L. da Costa, D. R. Galbraith, R. S. Oliveira, O. J. Binks, A. A. R. Oliveira, A. M. Pullen, C. E. Doughty, D. B. Metcalfe, S. S. Vasconcelos, L. V. Ferreira, Y. Malhi, J. Grace, M. Mencuccini, and P. Meir. 2015. Death from drought in tropical forests is triggered by hydraulics not carbon starvation. *Nature* 528:119–122.

Saifuddin, M., D. M. Chandy, N. Osman, and N. Khalid. 2013. Induction of fine roots in *Leucaena leucocephala* using *Agrobacterium rhizogenes*. *Australian Journal of Crop Science* 7:573–579.

Sanaphre-Villanueva, L., J. M. Dupuy, J. L. Andrade, C. Reyes-García, P. C. Jackson, and H. Paz. 2017. Patterns of plant functional variation and specialization along secondary succession and topography in a tropical dry forest. *Environmental Research Letters* 12:1–9.

Sánchez-Sánchez, O., and G. A. Islebe. 2002. Tropical forest communities in Southeastern Mexico. *Plant Ecology* 158:183–200.

Sánchez-Sánchez, O., G. A. Islebe, P. J. Ramírez-Barajas, and N. Torrescano-Valle. 2015. Natural and Human Induced Disturbance in Vegetation. Pages 153–167 *in* G. A. Islebe, S. Calmé, J. L. León-Cortés, and B. Schmook, editors. *Biodiversity and Conservation of the Yucatán Peninsula*. Switzerland: Springer International Publishing.

Santiago, L. S., K. Kitajima, S. J. Wright, and S. S. Mulkey. 2004. Coordinated changes in photosynthesis, water relations and leaf nutritional traits of canopy trees along a precipitation gradient in lowland tropical forest. *Oecologia* 139:495–502.

Santiago, L. S., K. Silvera, J. L. Andrade, and T. E. Dawson. 2017. Functional strategies of tropical dry forest plants in relation to growth form and isotopic composition. *Environmental Research Letters* 12:115006.

Sayer, E. J., and D. M. Newbery. 2003. The role of tree size in the leafing phenology of a seasonally dry tropical forest in Belize, Central America. *Journal of Tropical Ecology* 19:539–548.

Schenk, H. J., and R. B. Jackson. 2002. Rooting depths, lateral root spreads and belowground aboveground allometries of plants in water limited ecosystems. *Journal of Ecology* 90:480–494.

Schultz, G. P. 2005. Vascular flora of the El Edén Ecological Reserve, Quintana Roo, Mexico. *Journal of the Torrey Botanical Society* 132:311–322.

Schwartz, B. F., S. Schwinning, B. Gerard, K. R. Kukowski, C. L. Stinson, H. C. Dammeyer, H. C. Dam, C. L. Stinson, and H. C. Dammeyer. 2013. Using hydrogeochemical and ecohydrologic responses to understand epikarst process in semi-arid systems, Edwards Plateau, Texas, USA. *Acta Carsologica* 42:315–325.

Schwinning, S. 2010. The ecohydrology of roots in rocks. *Ecohydrology* 3:238–245.

Siefert, A., C. Violle, L. Chalmandrier, C. H. Albert, A. Taudiere, A. Fajardo, L. W. Aarssen, C. Baraloto, M. B. Carlucci, M. V. Cianciaruso, V. de L. Dantas, F. de Bello, L. D. S. Duarte, C. R. Fonseca, G. T. Freschet, S. Gaucherand, N. Gross, K. Hikosaka, B. Jackson, V. Jung, C. Kamiyama, M. Katabuchi, S. W. Kembel, E. Kichenin, N. J. B. Kraft, A. Lagerström, Y. L. Bagousse-Pinguet, Y. Li, N. Mason, J. Messier, T. Nakashizuka, J. M. Overton, D. A. Peltzer, I. M. Pérez-Ramos, V. D. Pillar, H. C. Prentice, S. Richardson, T. Sasaki, B. S. Schamp, C. Schöb, B. Shipley, M. Sundqvist, M. T. Sykes, M. Vandewalle, and D. A. Wardle. 2015. A global meta-analysis of the relative extent of intraspecific trait variation in plant communities. *Ecology Letters* 18:1406–1419.

da Silva, E. V., J.-P. Bouillet, J. L. de Moraes Gonçalves, C. H. A. Junior, P. C. O. Trivelin, P. Hinsinger, C. Jourdan, Y. Nouvellon, J. L. Stape, and J.-P. Laclau. 2011. Functional specialization of *Eucalyptus* fine roots: contrasting potential uptake rates for nitrogen, potassium and calcium tracers at varying soil depths. *Functional Ecology* 25:996–1006.

Silvertown, J., M. E. Dodd, D. J. G. Gowing, and J. O. Mountford. 1999. Hydrologically defined niches reveal a basis for species richness in plant communities. *Nature* 400:61–63.

Smart, P. L., P. A. Beddows, J. Coke, S. Doerr, S. Smith, and F. F. Whitaker. 2006. Cave Development on the Caribbean coast of the Yucatán Peninsula, Quintana Roo, Mexico. *Geological Society of America* 2404:105–128.

Sobrado, M. A. 1986. Aspects of tissue water relations and seasonal changes of leaf water potential components of evergreen and deciduous species coexisting in tropical dry forests. *Oecologia* 68:413–416.

Souza, M. L., A. A. Duarte, M. B. Lovato, M. Fagundes, F. Valladares, and J. P. Lemos-Filho. 2018. Climatic factors shaping intraspecific leaf trait variation of a neotropical tree along a rainfall gradient. *PLoS ONE* 13:e0208512.

Sperry, J. S. 2003. The Evolution of Water Transport and Xylem Structure. *International Journal of Plant Sciences* 164:S115–S127.

Sterck, F. J., L. Poorter, and F. Schieving. 2006. Leaf Traits Determine the Growth-Survival Trade-Off across Rain Forest Tree Species. *The American Naturalist* 167:758–765.

Steudle, E. 2001. The Cohesion-Tension Mechanism and the Acquisition of Water By Plant Roots. *Annual Review of Plant Biology* 58:847–875.

Stratton, L. C., G. Goldstein, and F. C. Meinzer. 2000. Temporal and spatial partitioning of water resources among eight woody species in a Hawaiian dry forest. *Oecologia* 124:309–317.

Swaffer, B. A., K. L. Holland, T. M. Doody, C. Li, and J. Hutson. 2014. Water use strategies of two co-occurring tree species in a semi-arid karst environment. *Hydrological Processes* 28:2003–2017.

Taboroši, D. 2006. Biologically influenced carbonate speleothems. Pages 307–317 *in* R.S. Harmon and C.M. Wicks, editors. *Perspectives on Karst Geomorphology, Hydrology,* *and Geochemistry - A Tribute Volume to Derek C. Ford and William B. White*. Boulder, Colorado, USA: Geological Society of America.

Tomlinson, K. W., F. J. Sterck, F. Bongers, D. A. da Silva, E. R. M. Barbosa, D. Ward, F. T. Bakker, M. van Kaauwen, H. H. T. Prins, S. de Bie, and F. van Langevelde. 2012. Biomass partitioning and root morphology of savanna trees across a water gradient. *Journal of Ecology* 100:1113–1121.

Trueba, S., R. Pouteau, F. Lens, T. S. Feild, S. Isnard, M. E. Olson, and S. Delzon. 2017. Vulnerability to xylem embolism as a major correlate of the environmental distribution of rain forest species on a tropical island. *Plant, Cell & Environment* 40:277–289.

Valdez-Hernández, M., J. L. Andrade, P. C. Jackson, and M. Rebolledo-Vieyra. 2010. Phenology of five tree species of a tropical dry forest in Yucatán, Mexico: Effects of environmental and physiological factors. *Plant and Soil* 329:155–171.

Valdez-Hernández, M., C. González-Salvatierra, C. Reyes-García, P. C. Jackson, and J. L. Andrade. 2015. Physiological Ecology of Vascular Plants. Pages 97–129 *in* G. A. Islebe, S. Calmé, J. L. León-Cortés, and B. Schmook, editors. *Biodiversity and Conservation of the Yucatán Peninsula*. Switzerland: Springer International Publishing.

Voltas, J., D. Lucabaugh, M. R. Chambel, and J. P. Ferrio. 2015. Intraspecific variation in the use of water sources by the circum-Mediterranean conifer *Pinus halepensis*. *New Phytologist* 208:1031–1041.

Weemstra, M., L. Mommer, E. J. W. Visser, J. van Ruijven, T. W. Kuyper, G. M. J. Mohren, and F. J. Sterck. 2016. Towards a multidimensional root trait framework: a tree root review. *New Phytologist* 211:1159–1169.

West, A. G., S. J. Patrickson, and J. R. Ehleringer. 2006. Water extraction times for plant and soil materials used in stable isotope analysis. *Rapid Communications in Mass Spectrometry* 20:1317–1321.

Whigham, D. F., I. Olmsted, E. C. Cano, and M. E. Harmon. 1991. The Impact of Hurricane Gilbert on Trees, Litterfall, and Woody Debris in a Dry Tropical Forest in the Northeastern Yucatán Peninsula. *Biotropica* 23:434–441.

Wright, I. J., P. B. Reich, M. Westoby, D. D. Ackerly, Z. Baruch, F. Bongers, J. Cavender-Bares, T. Chapin, J. H. C. Cornellssen, M. Diemer, J. Flexas, E. Garnier, P. K. Groom, J. Gulias, K. Hikosaka, B. B. Lamont, T. Lee, W. Lee, C. Lusk, J. J. Midgley, M. L. Navas, Ü. Niinemets, J. Oleksyn, H. Osada, H. Poorter, P. Pool, L. Prior, V. I. Pyankov, C. Roumet, S. C. Thomas, M. G. Tjoelker, E. J. Veneklaas, and R. Villar. 2004. The worldwide leaf economics spectrum. *Nature* 428:821–827.

6. CONCLUSIONS

The research outlined in this document has greatly expanded our knowledge about the interactions between the above and below ground realms in Quintana Roo, Mexico. Despite findings of shallow rooting in the state of Yucatán, the deep roots frequently observed in Quintana Roo hinted at specialization in water use, with potential impacts on plant performance, productivity, and forest composition in the coastal region. Through broad surveys, molecular techniques, and stable isotope applications, the prevalence and benefits of deep rooting in this seasonally dry tropical forest became apparent.

We identified, for the first time, species with roots present in the caves. 38 species were identified below ground, including 8 lianas and 1 palm. While DNA barcoding, particularly utilizing the primers *matK* and *trnH-psbA*, was highly successful and critical to assign roots to species, we observed variation in coarse root morphology, corresponding to species-species characteristics and features. An identification key was developed to aid in future work, relieving the need for costly and time-consuming genetic analyses. Further, we noted that three different root structures were observed in the caves. The distribution of roots among these structures became an important piece when determining the controls on root abundance between sites.

Though not directly related to the work conducted in Quintana Roo, time spent evaluating soil water extraction techniques revealed the influences soil properties and extraction method have on the measured isotopic composition of soil water. By labeling bound and mobile pools, we determined that mixing occurs, though the degree of mixing is dependent on soil texture. Clay mineralogy played a role in this interaction, as smectitic clay minerals retained the heavy isotope-enriched bound water more readily than non-smectitic clays. A significant temperature effect was observed in soil water extracted with cryogenic vacuum distillation, suggesting that lower temperature may not accurately reflect the total soil water pool compared to extractions carried out at higher temperatures. This work contributes to the growing literature regarding soil water extractions and how these methods influence our interpretations of plant water use.

Furthermore, patterns in plant water use have been shown to rooting depth, exhibiting that plants with large above ground structures have deep rooting capabilities. Through our complimentary observations of the surface and subsurface, we established that several species represented by large individuals on the surface dominated the root diversity. Yet, there were prominent exceptions to this generalization. While there appears to be specialization for deep rooting by select species, rooting depth and abundance was better informed by a species' natural history rather than tree size. Similar to other studies in karst regions, we noted the influence that site-level bedrock characteristics had on root exploration. We found that sites with large conduits in the bedrock provided more space for more roots. The prevalence of large masses of intertwined roots at our sites depicts this control on root access to deep resources. On the landscape-scale, results showed negative correlations between root abundance and characteristics such as site elevation and distance from the coast. This implies that the hydrologic processes governing cave development and depth to groundwater influences the prevalence of deep roots and, in turn, access to reliable water. Changes in forest composition appear to track changes in deep water access, suggesting that vegetation in Quintana Roo is indeed groundwater dependent.

Through the use of stable isotopes, we tested the application of the functional group framework and investigated patterns in water use and water use efficiency among co-occurring species in Quintana Roo. While the species commonly observed in the caves were all evergreens, we showed that evergreen and deciduous species have overlapping root zones, implying space and resource access is highly competed for in this karst landscape. Root depth and root abundance did not inform differences in water use or water use efficiency. Rather, patterns in stem water and leaf stable isotopes were apparent when tree size was considered. Deep water use increased with tree size, coupled with a decrease in water use efficiency. Interestingly, leaf $\delta^{13}C$ among the large individuals overlapped with leaf $\delta^{13}C$ among small individuals, suggesting that shallow water sources satisfied water demands of small individuals while large individuals required deep water. We found significant differences in water use and water use efficiency among species, yet, inter- and intraspecific variation was masked when species were organized into functional groups based on phenology and wood density. The apparent species-specific water use strategies may be more crucial to consider when evaluating community composition patterns and ecosystem processes. These findings correlate with other studies conducted in seasonally dry tropical forests, which found that high species diversity and water limitation encouraged a multitude of water use strategies, allowing co-occurring species to thrive in a seasonally dry environment. We stress the need to expand ecophysiological studies in Quintana Roo and other tropical forests to better understand how these ecosystems respond to water limitation.

Together, these research endeavors dramatically expand existing research on deep rooting to an important and understudied region, potentially transforming our understanding of the relationships between seasonally dry tropical forests and groundwater resources. Documenting how groundwater influences the performance of key species, particularly in relation to seasonal variation is crucial, as there is potential to expand these efforts to infer vegetation responses to drought and climate change. We have high confidence that temperatures will rise and total rainfall may decrease and become more variable in dryland systems globally, raising questions about future ecological trajectories. Water limitation is a critical issue as population growth coincides with ongoing climate changes, this is likely to be exacerbated in the future. Particularly in the Yucatán Peninsula, expanding urbanization and tourism increases quantity of wastewater contamination as well as increasing the amount of freshwater being pumped from the aquifer. This increases the pressure on water resources for humans and natural ecosystems. Therefore, these results provided valuable insights into vegetation dependence on groundwater, variation among species, and the role these characteristics might play as these important ecosystems respond to ongoing global changes.

Despite their incredible biodiversity and the large human populations dependent on them, seasonally dry tropical forests are among the most threatened of the global tropical forests. Deforestation for agriculture and urbanization is occurring in the Yucatán Peninsula at an alarming rate. Caves is Mexico are being exploited and destroyed as there is no formal agency that encourages their protection and conservation. Caves here are the one of the final frontiers, with much left to discover. Yet, major landscape alterations simultaneously occurring above and below ground deny the opportunity to truly understand the ecological processes that are at work here. Understanding the interactions between the surface and the subterranean realm will encourage protection and better management of the resources and ecosystem services that seasonally dry tropical forests and caves provide.

APPENDIX A

SUPPORTING INFORMATION FOR CHAPTER 2

Figure A-1 a-s Images of roots from fourteen tree species and one palm as well as four lianas observed in caves in Quintana Roo, Mexico.

a. ***Blomia prisca*** **(Standl.) Lundell**

© 2019 Rachel E. Adams

Figure A-1 Continued

b. ***Brosimum alicastrum*** **Sw.**

Figure A-1 Continued

c. ***Bursera simaruba*** **(L.) Sarg.**

Figure A-1 Continued

d. ***Celtis iguanaea*** **(Jacq.) Sarg.**

Figure A-1 Continued

e. ***Coccoloba barbadensis* Jacq.**

© 2019 Rachel E. Adams

Figure A-1 Continued

f. ***Cordia gerascanthus*** **L.**

© 2019 Rachel E. Adams

Figure A-1 Continued

g. *Cupania glabra* Sw.

Figure A-1 Continued

h. ***Dalbergia glabra*** **(Mill.) Standl., a liana.**

© 2019 Rachel E. Adams

Figure A-1 Continued

i. ***Dendropanax arboreus*** **(L.) Decne. & Planch.**

© 2019 Rachel E. Adams

Figure A-1 Continued

j. ***Diospyros tetrasperma*** **Sw.**

Figure A-1 Continued

k. ***Ficus* spp.**

Figure A-1 Continued

l. *Hyperbaena mexicana* Miers. The root on the far right shows early stages of calcification.

© 2019 Rachel E. Adams

Figure A-1 Continued

m. ***Lonchocarpus rugosus*** **Benth.**

Figure A-1 Continued

n. ***Mosannona depressa*** **(Baill.) Chatrou**

Figure A-1 Continued

o. ***Piscidia piscipula*** **(L.) Sarg.**

Figure A-1 Continued

p. ***Rourea glabra*** **Kunth, a liana.**

Figure A-1 Continued

q. ***Sabal yapa*** **C. Wright ex Becc., a palm.**

Figure A-1 Continued

r. ***Tanaecium tetragonolobum*** **(Jacq.) L.G. Lohmann, a liana.**

Figure A-1 Continued

s. ***Vitis tiliifolia*** **Humb. & Bonpl. ex Roem. & Schult., a liana.**

APPENDIX B

SUPPORTING INFORMATION FOR CHAPTER 3

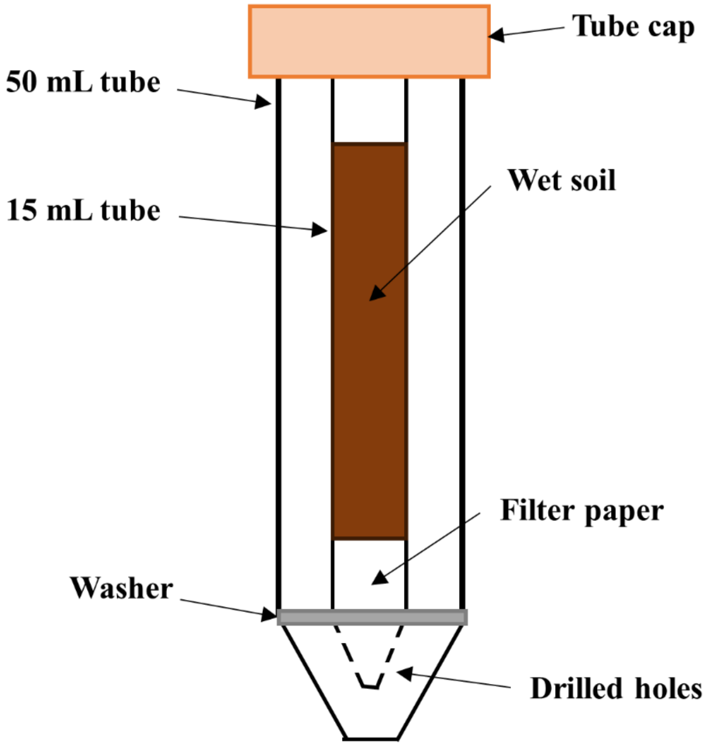

Figure B-1 Schematic of the double-tube centrifuge set up.

Table B-1 δ^{18}O and δ^{2}H results for all soils and sand extracted via vacuum distillation at 80°C, 100°C, 150°C, and 200°C, centrifugation, and distillation post-centrifuge. Water recovery based on water weight and sample weight are provided as well as extraction duration.

Extraction Method	Soil	Extraction Temperature (°C)	δ^{2}H	δ^{18}O	Water recovery based on water weight (%)	Water recovery based on sample weight (%)	Extraction Duration (hr)
Distillation	RA	80	-97.1 ± 1.1	-15.57 ± 0.24	99.02	97.52	2.32
			-100.8 ± 0.3	-16.12 ± 0.04	97.54	99.22	3.10
			-97.2 ± 1.0	-15.67 ± 0.07	108.07	76.40	3.12
		100	-95.4 ± 0.2	-15.18 ± 0.02	98.32	95.68	3.15
			-96.5 ± 1.3	-15.49 ± 0.10	101.42	98.86	3.18
			-96.7 ± 0.6	-15.46 ± 0.14	103.06	97.96	2.27
		150	-96.9 ± 1.3	-15.35 ± 0.02	100.90	97.93	1.98
			-94.5 ± 1.0	-15.21 ± 0.16	100.94	98.64	2.02
			-95.4 ± 0.9	-15.24 ± 0.06	101.64	98.69	2.03
		200	-94.6 ± 0.7	-15.23 ± 0.14	99.93	97.53	1.67
			-94.5 ± 1.1	-14.97 ± 0.1	101.07	98.22	2.02
			-96.2 ± 0.6	-14.89 ± 0.43	99.42	97.18	1.57
	TB	80	-97.2 ± 1.7	-15.76 ± 0.22	102.03	100.05	1.38
			-96.5 ± 0.6	-15.68 ± 0.06	104.16	100.02	1.43
			-99.3 ± 1.5	-16.04 ± 0.17	100.65	98.89	1.60
		100	-95.9 ± 0.8	-15.54 ± 0.10	101.70	99.14	1.65
			-97.1 ± 0.9	-15.53 ± 0.15	100.56	98.71	1.73
			-97.3 ± 0.2	-15.40 ± 0.06	100.65	98.66	1.65
		150	-94.9 ± 0.8	-15.05 ± 0.13	102.94	99.25	1.28
			-94.5 ± 0.5	-14.98 ± 0.12	102.51	100.20	1.43
			-95.3 ± 0.5	-15.28 ± 0.13	102.38	100.25	1.57
		200	-94.8 ± 1.3	-15.23 ± 0.04	104.55	101.53	1.32

Table B-1 Continued

Extraction Method	Soil	Extraction Temperature (°C)	δ^2H	$\delta^{18}O$	Water recovery based on water weight (%)	Water recovery based on sample weight (%)	Extraction Duration (hr)
			-93.5 ± 0.5	-15.10 ± 0.07	102.06	99.42	1.20
			-93.6 ± 0.3	-15.15 ± 0.18	102.18	100.15	1.50
	CD	80	-98.1 ± 0.3	-15.86 ± 0.08	106.54	102.02	2.03
			-98.0 ± 0.8	-15.61 ± 0.22	106.14	118.97	1.98
			-98.7 ± 0.2	-15.72 ± 0.11	105.90	84.58	1.67
		100	-96.2 ± 1.3	-15.35 ± 0.31	104.09	99.50	1.90
			-98.8 ± 1.0	-15.60 ± 0.02	103.54	102.35	1.57
			-97.6 ± 0.2	-15.42 ± 0.12	104.57	100.08	1.63
		150	-95.8 ± 0.7	-15.18 ± 0.08	101.92	101.29	1.17
			-93.6 ± 1.0	-15.30 ± 0.18	103.11	100.07	1.28
			-94.9 ± 1.0	-15.26 ± 0.04	100.20	99.01	1.68
		200	-93.8 ± 1.2	-14.87 ± 0.28	101.99	99.64	1.18
			-93.8 ± 0.9	-15.15 ± 0.12	99.23	98.07	1.83
			-92.7 ± 0.1	-15.00 ± 0.07	100.40	98.66	1.47
	CG	80	-98.4 ± 0.6	-15.84 ± 0.06	102.95	100.15	1.92
			-98.3 ± 0.4	-15.87 ± 0.04	103.34	100.55	1.73
			-98.8 ± 0.8	-15.69 ± 0.11	100.94	99.16	1.75
		100	-97.4 ± 0.6	-15.77 ± 0.06	102.36	99.60	1.55
			-97.4 ± 0.8	-15.72 ± 0.07	103.27	100.32	1.58
			-96.8 ± 0.3	-15.72 ± 0.12	103.27	99.91	1.78
		150	-95.1 ± 1.1	-15.40 ± 0.04	102.58	100.39	1.53
			-94.9 ± 0.4	-15.40 ± 0.12	101.51	99.88	1.18
			-95.5 ± 0.7	-15.34 ± 0.15	100.44	98.19	1.55
		200	-92.8 ± 0.7	-14.95 ± 0.15	102.27	99.66	2.32

Table B-1 Continued

Extraction Method	Soil	Extraction Temperature (°C)	δ^2H	$\delta^{18}O$	Water recovery based on water weight (%)	Water recovery based on sample weight (%)	Extraction Duration (hr)
			-93.1 ± 0.8	-15.01 ± 0.14	102.67	99.74	2.32
			-94.3 ± 1.3	-15.30 ± 0.14	102.43	99.47	1.67
	S	80	-92.6 ± 0.7	-15.30 ± 0.14	100.20	100.32	1.23
			-92.4 ± 0.5	-15.16 ± 0.07	105.60	112.68	2.02
			-91.3 ± 1.0	-15.10 ± 0.12	104.93	103.23	1.90
		100	-91.5 ± 0.7	-14.93 ± 0.02	99.34	102.55	1.93
			-91.6 ± 0.5	-14.83 ± 0.10	101.05	101.48	1.97
			-92.2 ± 0.4	-14.97 ± 0.23	102.07	102.10	1.33
		150	-92.1 ± 0.7	-15.12 ± 0.14	103.03	108.22	1.27
			-91.9 ± 0.4	-15.04 ± 0.17	101.31	105.00	1.67
			-91.3 ± 0.8	-14.87 ± 0.23	94.79	98.16	1.28
		200	-92.6 ± 0.6	-14.9 ± 0.11	101.58	98.36	1.53
			-91.6 ± 0.4	-15.11 ± 0.19	96.51	100.30	1.80
Centrifuge	RA	20	-90.7 ± 1.3	-15.04 ± 0.24	51.47	–	0.75
			-92.2 ± 0.3	-14.98 ± 0.18	42.29	–	0.75
			-90.9 ± 0.4	-14.99 ± 0.11	43.59	–	0.75
	TB	20	-88.7 ± 0.6	-14.70 ± 0.12	33.20	–	0.75
			-87.9 ± 0.8	-14.41 ± 0.29	28.29	–	0.75
			-88.0 ± 0.4	-14.75 ± 0.19	20.26	–	0.75
	CD	20	-90.9 ± 1.1	-15.17 ± 0.01	39.68	–	0.75
			-90.3 ± 0.4	-15.11 ± 0.17	57.18	–	0.75
			-90.6 ± 0.8	-14.87 ± 0.55	54.13	–	0.75
	CG	20	-89.3 ± 1.2	-15.07 ± 0.23	40.42	–	0.75
			-89.0 ± 0.5	-14.92 ± 0.15	37.78	–	0.75

Table B-1 Continued

Extraction Method	Soil	Extraction Temperature (°C)	δ^2H	$\delta^{18}O$	Water recovery based on water weight (%)	Water recovery based on sample weight (%)	Extraction Duration (hr)
	S	20	-91.1 ± 1.0	-15.11 ± 0.18	30.29	–	0.75
			-91.5 ± 0.8	-15.24 ± 0.05	44.89	–	0.75
			-93.1 ± 0.4	-15.22 ± 0.22	83.10	–	0.75
			-92.3 ± 0.8	-15.19 ± 0.33	68.57	–	0.75
Distillation Post-Centrifuge	RA	100	-99.6 ± 0.8	-15.12 ± 0.36	70.86	71.59	1.27
			-98.6 ± 0.5	-15.13 ± 0.16	66.99	64.58	1.22
			-102.5 ± 1.1	-15.42 ± 0.14	71.71	68.48	0.85
	TB	100	-100.6 ± 1.4	-15.66 ± 0.33	90.24	87.93	1.17
			-99.4 ± 0.6	-15.64 ± 0.19	90.47	87.65	1.27
			-97.3 ± 0.7	-15.38 ± 0.21	87.04	84.71	1.12
	CD	100	-97.1 ± 0.9	-14.80 ± 0.08	68.02	67.55	1.32
			-98.6 ± 1.1	-14.92 ± 0.02	87.78	85.02	1.63
			-100.5 ± 0.5	-15.03 ± 0.08	81.04	83.40	1.15
	CG	100	-100.8 ± 0.7	-15.46 ± 0.29	92.67	90.60	1.75
			-100.1 ± 0.7	-15.44 ± 0.23	100.22	98.49	1.60
			-99.6 ± 0.7	-15.52 ± 0.11	85.71	83.07	1.68
	S	100	-90.2 ± 1.3	-14.81 ± 0.13	49.35	52.49	0.80
			-88.8 ± 0.6	-14.65 ± 0.06	99.95	132.08	1.13
			-87.3 ± 0.9	-14.29 ± 0.06	37.94	35.53	0.72

APPENDIX C

SUPPORTING INFORMATION FOR CHAPTER 4

Table C-1 Sequences, cycling conditions, success rates, and references for all primers used.

Primer	**Sequence (5’ – 3’)**	**Cycling Conditions**	**Amplification and Sequencing Success Rates**		**References**
			Roots	**Leaves**	
ITS2	S2F: ATGCGATACTTGGTGTGAAT S3R: GACGCTTCTCCAGACTACAAT	95°C 3min; 95°C 25sec, 51°C 25sec, 72°C 1min x 40 cycles; 72°C 5min	18/88 (20.5%)	49/58 (84.5%)	Chen et al. (2010) Cycling conditions modified from Olivar et al. (2014) and Li et al. (2012)
			5/14 (35.7%)	26/45 (57.8%)	
matK	1R_KIM: ACCCAGTCCATCTGGAAATCTTGGTTC 3F_KIM: CGTACAGTACTTTTGTGTTTACGAG	95°C 3min; 95°C 20sec, 51°C 20sec, 72°C 1min x 40 cycles; 72°C 10min	183/260 (70.4%)	10/40 (25.0%)	Kim, unpublished Cycling conditions modified from Jones et al. (2011)
			169/183 (92.3%)	8/10 (80.0%)	
trnH-psbA	trnH: CGCGCATGGTGGATTCACAATCC psbA: GTTATGCATGAACGTAATGCTC	95°C 3 min; 95°C 25sec, 51°C 25sec, 72°C 1min x 40 cycles; 72°C 5min	144/181 (79.6%)	21/33 (63.6%)	Fazekas et al. (2008) Cycling conditions modified from Olivar et al. (2014) and Li et al. (2012)
			44/144 (53.5%)	9/19 (47.4%)	

Table C-2 Species found above ground at the five study sites and associated information regarding relative abundance (out of 233 trees identified), basal area (out of 0.14 total hectares surveyed), mean DBH, and rooting habit (based on relative abundance below ground). *Rooting habit was classified at the genus level.

Species	**Relative Abundance (%)**	**Basal Area (m^2/ha)**	**Mean DBH (cm)**	**Rooting Habit**
***Oxandra lanceolata* (Sw.) Baill.**	14.2	1.57	6.8 ± 2.8	Above Ground Only
***Bursera simaruba* (L.) Sarg.**	8.6	1.63	10.0 ± 4.6	Rare Below Ground
***Swartzia cubensis* (Britton & Wilson) Standl.**	6.4	1.38	12.0 ± 4.7	Above Ground Only
***Neea psychotrioides* Donn.Sm.**	5.6	0.66	8.7 ± 2.8	Rare Below Ground
***Ficus obtusifolia* Kunth**	3.4	3.94	19.6 ± 18.9	*Common Below Ground
***Leucaena leucocephala* (Lam.) de Wit**	3.4	1.94	10.9 ± 6.3	Common Below Ground
***Casearia tremula* (Griseb.) Griseb. ex C.Wright**	3.0	0.32	6.0 ± 2.8	Rare Below Ground
***Dendropanax arboreus* (L.) Decne. & Planch.**	3.0	0.45	10.0 ± 4	Rare Below Ground
***Drypetes lateriflora* (Sw.) Krug & Urb.**	3.0	0.25	6.5 ± 1.8	Above Ground Only
***Ficus trigonata* L.**	3.0	1.09	13.1 ± 5.2	*Common Below Ground
***Mosannona depressa* (Baill.) Chatrou**	3.0	0.16	5.4 ± 1.7	Rare Below Ground
***Vitex gaumeri* Greenm.**	3.0	0.80	9.3 ± 3.9	Rare Below Ground
***Melicoccus oliviformis* Kunth**	2.6	0.15	5.9 ± 1.8	Above Ground Only
***Cascabela gaumeri* (Hemsl.) Lippold**	2.2	0.42	6.2 ± 4.5	Rare Below Ground
***Coccoloba barbadensis* Jacq.**	2.2	0.23	8.0 ± 2.6	Rare Below Ground
***Cordia gerascanthus* L.**	2.2	0.62	9.2 ± 5.4	Rare Below Ground
***Hampea trilobata* Standl.**	2.2	0.22	8.3 ± 3.5	Above Ground Only
***Lonchocarpus rugosus* Benth.**	2.2	0.14	7.0 ± 1.1	Rare Below Ground
***Manilkara zapota* (L.) P. Royen**	2.2	0.84	15.4 ± 8.7	Rare Below Ground

Table C-2 Continued

Species	Relative Abundance (%)	Basal Area (m^2/ha)	Mean DBH (cm)	Rooting Habit
***Piscidia piscipula* (L.) Sarg.**	2.2	0.85	12.9 ± 7.6	Rare Below Ground
***Acacia dolichostachya* S.F. Blake**	1.7	0.48	10.1 ± 2.4	Rare Below Ground
***Eugenia* spp.**	1.7	0.10	6.7 ± 1.6	Above Ground Only
***Pouteria reticulata* (Engl.) Eyma**	1.7	0.21	9.2 ± 3.6	*Common Below Ground
***Cupania glabra* Sw.**	1.3	0.10	7.7 ± 1.1	Rare Below Ground
***Diospyros tetrasperma* Sw.**	1.3	0.07	6.4 ± 1.5	Rare Below Ground
***Ficus cotinifolia* Kunth**	1.3	2.46	21.1 ± 23.3	*Common Below Ground
***Luehea speciosa* Willd.**	1.3	0.27	12.5 ± 2.7	Above Ground Only
***Plumeria obtusa* L.**	1.3	0.22	11.0 ± 3.4	Rare Below Ground
***Pouteria campechiana* (Kunth) Baehni**	1.3	0.49	12.9 ± 3.6	*Common Below Ground
***Thouinia paucidentata* Radlk.**	1.3	0.12	6.5 ± 1.1	Above Ground Only
***Metopium brownei* (Jacq.) Urb.**	0.9	0.09	9.0 ± 2.1	Above Ground Only
***Semialarium mexicanum* (Miers) Mennega**	0.9	0.05	6.6 ± 0.6	Rare Below Ground
***Zuelania guidonia* (Sw.) Britton & Millsp.**	0.9	0.04	6.2 ± 1.6	Above Ground Only
***Allophylus cominia* (L.) Sw.**	0.4	0.02	5.2	Above Ground Only
***Bauhinia divaricata* L.**	0.4	0.03	7.0	Above Ground Only
***Brosimum alicastrum* Sw.**	0.4	0.44	27.9	Rare Below Ground
***Caesalpinia gaumeri* Greenm.**	0.4	0.02	6.0	Above Ground Only
***Casimiroa sapota* Oerst.**	0.4	0.03	6.7	Above Ground Only
***Casimiroa tetrameria* Millsp.**	0.4	0.06	10.3	Above Ground Only
***Cordia dodecandra* A.DC.**	0.4	0.07	10.8	Rare Below Ground
***Eugenia axillaris* (Sw.) Willd.**	0.4	0.02	5.4	Above Ground Only
***Eugenia oerstediana* O.Berg**	0.4	0.05	6.5 ± 0.7	Above Ground Only

Table C-2 Continued

Species	**Relative Abundance (%)**	**Basal Area (m^2/ha)**	**Mean DBH (cm)**	**Rooting Habit**
Exothea diphylla **(Standl.) Lundell**	0.4	0.02	5.2	Above Ground Only
Rhamnus humboldtiana **Willd. ex Schult.**	0.4	0.09	12.4	Above Ground Only
Platymiscium yucatanum **Standl.**	0.4	0.04	8.6	Rare Below Ground
Pseudolmedia glabrata **(Liebm.) C.C.Berg**	0.4	0.05	9.9	Above Ground Only
Pseudolmedia spuria **(Sw.) Griseb.**	0.4	0.09	13	Above Ground Only

Table C-3 Site-level community composition.

Species	Relative Abundance (%) based on total trees at each site				
	Cueva Culebron	Jaguar Maw	Nohoch Aktun	Pixan Bel	Ruta de los Guerreros
***Acacia dolichostachya* S.F. Blake**	0.0	2.9	3.9	1.9	0.0
***Allophylus cominia* (L.) Sw.**	2.3	0.0	0.0	0.0	0.0
***Bauhinia divaricata* L.**	0.0	0.0	2.0	0.0	0.0
***Brosimum alicastrum* Sw.**	2.3	0.0	0.0	0.0	0.0
***Bursera simaruba* (L.) Sarg.**	2.3	2.9	3.9	30.8	0.0
***Caesalpinia gaumeri* Greenm.**	0.0	0.0	0.0	0.0	1.9
***Cascabela gaumeri* (Hemsl.) Lippold**	0.0	0.0	0.0	1.9	7.5
***Casearia tremula* (Griseb.) Griseb. ex C.Wright**	2.3	2.9	0.0	9.6	0.0
***Casimiroa sapota* Oerst.**	0.0	0.0	0.0	1.9	0.0
***Casimiroa tetrameria* Millsp.**	0.0	0.0	0.0	0.0	1.9
***Coccoloba barbadensis* Jacq.**	2.3	0.0	0.0	1.9	5.7
***Cordia dodecandra* A.DC.**	0.0	0.0	0.0	0.0	1.9

Table C-3 Continued

Species	**Relative Abundance (%) based on total trees at each site**				
	Cueva Culebron	**Jaguar Maw**	**Nohoch Aktun**	**Pixan Bel**	**Ruta de los Guerreros**
***Cordia gerascanthus* L.**	0.0	11.8	0.0	0.0	1.9
***Cupania glabra* Sw.**	0.0	2.9	0.0	0.0	3.8
***Dendropanax arboreus* (L.) Decne. & Planch.**	0.0	20.6	0.0	0.0	0.0
***Diospyros tetrasperma* Sw.**	2.3	0.0	0.0	0.0	3.8
***Drypetes lateriflora* (Sw.) Krug & Urb.**	16.3	0.0	0.0	0.0	0.0
***Eugenia axillaris* (Sw.) Willd.**	0.0	0.0	0.0	0.0	1.9
***Eugenia oerstediana* O.Berg**	2.3	0.0	0.0	0.0	0.0
***Eugenia* spp.**	7.0	0.0	2.0	0.0	0.0
***Exothea diphylla* (Standl.) Lundell**	2.3	0.0	0.0	0.0	0.0
***Ficus cotinifolia* Kunth**	2.3	0.0	3.9	0.0	0.0
***Ficus obtusifolia* Kunth**	14.0	0.0	2.0	0.0	1.9
***Ficus trigonata* L.**	0.0	11.8	0.0	5.8	0.0
***Hampea trilobata* Standl.**	2.3	0.0	0.0	1.9	5.7

Table C-3 Continued

Species	Relative Abundance (%) based on total trees at each site				
	Cueva Culebron	**Jaguar Maw**	**Nohoch Aktun**	**Pixan Bel**	**Ruta de los Guerreros**
***Leucaena leucocephala* (Lam.) de Wit**	0.0	5.9	0.0	11.5	0.0
***Lonchocarpus rugosus* Benth.**	2.3	0.0	0.0	1.9	5.7
***Luehea speciosa* Willd.**	0.0	0.0	0.0	1.9	3.8
***Manilkara zapota* (L.) P. Royen**	7.0	0.0	3.9	0.0	0.0
***Melicoccus oliviformis* Kunth**	2.3	2.9	2.0	5.8	0.0
***Metopium brownei* (Jacq.) Urb.**	0.0	0.0	0.0	3.8	0.0
***Mosannona depressa* (Baill.) Chatrou**	2.3	11.8	0.0	0.0	3.8
***Neea psychotrioides* Donn.Sm.**	2.3	2.9	5.9	9.6	5.7
***Oxandra lanceolata* (Sw.) Baill.**	0.0	0.0	64.7	0.0	0.0
***Piscidia piscipula* (L.) Sarg.**	2.3	0.0	2.0	3.8	1.9
***Platymiscium yucatanum* Standl.**	2.3	0.0	0.0	0.0	0.0
***Plumeria obtusa* L.**	2.3	0.0	2.0	1.9	0.0

Table C-3 Continued

Species	**Relative Abundance (%) based on total trees at each site**				
	Cueva Culebron	**Jaguar Maw**	**Nohoch Aktun**	**Pixan Bel**	**Ruta de los Guerreros**
***Pouteria campechiana* (Kunth) Baehni**	0.0	5.9	0.0	1.9	0.0
***Pouteria reticulata* (Engl.) Eyma**	9.3	0.0	0.0	0.0	0.0
***Pseudolmedia glabrata* (Liebm.) C.C.Berg**	2.3	0.0	0.0	0.0	0.0
***Pseudolmedia spuria* (Sw.) Griseb.**	0.0	0.0	2.0	0.0	0.0
***Rhamnus humboldtiana* Willd. ex Schult.**	2.3	0.0	0.0	0.0	0.0
***Semialarium mexicanum* (Miers) Mennega**	0.0	0.0	0.0	0.0	3.8
***Swartzia cubensis* (Britton & Wilson) Standl.**	0.0	2.9	0.0	0.0	26.4
***Thouinia paucidentata* Radlk.**	2.3	0.0	0.0	1.9	1.9
***Vitex gaumeri* Greenm.**	0.0	11.8	0.0	0.0	5.7
***Zuelania guidonia* (Sw.) Britton & Millsp.**	0.0	0.0	0.0	0.0	3.8
TOTAL TREES	**43**	**34**	**51**	**52**	**53**

Table C-4 A list of species identified above and below ground with relative abundance below ground based on number of roots (219 roots) and GenBank accession numbers. Markers without reported accession numbers were either not used or unavailable for specific species.

Species	**Relative Abundance Below Ground (%)**	**GenBank Accession Numbers**		
		matK	***trnH-psbA***	**ITS**
***Acacia dolichostachya* S.F. Blake**	0.46	DQ371896	AF525009	-
***Allophylus cominia* (L.) Sw.**	0	-	-	KX584893
†*Aristolochia* spp.	0.46	-	KM213929	-
***Bauhinia divaricata* L.**	0	KX783640	-	HG963683
***Blomia prisca* (Standl.) Lundell**	3.67	EU720611	-	EU720444
***Brosimum alicastrum* Sw.**	0.92	GQ981947	HG963667	MN077181
***Bursera simaruba* (L.) Sarg.**	0.46	JQ587166	KJ426630	GQ378108
***Caesalpinia gaumeri* Greenm.**	0	-	-	KP003692
***Cascabela gaumeri* (Hemsl.) Lippold**	0.46	JQ586579	HG963819	-
***Casearia tremula* (Griseb.) Griseb. ex C.Wright**	0.46	JQ587936	-	-
***Casimiroa sapota* Oerst.**	0	-	-	-
***Casimiroa tetrameria* Millsp.**	0	-	-	-
***Cedrela odorata* L.**	0.92	JQ588335	KM408364	KF840436
***Celtis iguanaea* (Jacq.) Sarg.**	0.92	JQ589362	HG963813	AY488719
***Coccoloba barbadensis* Jacq.**	0.92	-	-	-
***Cordia dodecandra* A.DC.**	1.83	-	-	-
***Cordia gerascanthus* L.**		KM219828	JF427961	JF332100
***Cupania glabra* Sw.**	1.38	JQ589135	-	-
***Cynophalla flexuosa* (L.)**	0.46	EU371760	-	-
†*Dalbergia glabra* (Mill.) Standl.	5.50	JQ587581	-	-
***Dendropanax arboreus* (L.) Decne. & Planch.**	2.75	JQ586664	GQ982206	-
***Diospyros tetrasperma* Sw.**	0.92	DQ924059	FJ238237	-
***Drypetes lateriflora* (Sw.) Krug & Urb.**	0	KJ012574	KJ426710	
***Eugenia axillaris* (Sw.) Willd.**	0	MH621619	KJ426719	KJ187607
***Eugenia oerstediana* O.Berg**	0	JQ588485	-	-
***Eugenia* spp.**	0	-	-	-
***Exothea diphylla* (Standl.) Lundell**	0	-	-	-

Table C-4 Continued

Species	**Relative Abundance Below Ground (%)**	**GenBank Accession Numbers**		
		matK	***trnH-psbA***	**ITS**
***Ficus cotinifolia* Kunth**	35.78	-	HG963603	-
***Ficus obtusifolia* Kunth**		GQ981996	HG963743	AY730084
***Ficus trigonata* L.**		-	-	EU091607
***Guettarda* spp.**	0.92	-	-	-
***Hampea trilobata* Standl.**	0	KT966969		KT966931
***Hyperbaena mexicana* Miers**	0.92	KX384071	-	-
***Leucaena leucocephala* (Lam.) de Wit**	6.42	KX518643	GU135371.2	KY700392
***Lonchocarpus rugosus* Benth.**	2.29	JQ587741	-	KJ411695
***Luehea speciosa* Willd.**	0	JQ589346	-	-
***Manilkara zapota* (L.) P. Royen**	0.92	MN295595	GU135342.2	KF686242
***Melicoccus oliviformis* Kunth**	0	-	-	-
***Metopium brownei* (Jacq.) Urb.**	0	-	-	-
***Mosannona depressa* (Baill.) Chatrou**	0.92	MG680705	MG680714	-
***Neea psychotrioides* Donn.Sm.**	0.92	KY952467	-	EF079505
†*Otopappus* spp.	1.38	-	-	-
***Oxandra lanceolata* (Sw.) Baill.**	0	KJ012702	KJ426857	-
***Piscidia piscipula* (L.) Sarg.**	1.83	AF142710	-	AF467490
***Platymiscium yucatanum* Standl.**	0.46	EU735988	-	EU735931
***Plumeria obtusa* L.**	0	MH621523	MH622032	-
***Pouteria campechiana* (Kunth) Baehni**	8.72	KX426215	DQ344130	DQ246688
***Pouteria reticulata* (Engl.) Eyma**		JQ589189	GQ982327	KJ399434
***Pseudolmedia glabrata* (Liebm.) C.C.Berg**	0	-	-	-
***Pseudolmedia spuria* (Sw.) Griseb.**	0	JQ588430	HM446988	-
***Pterocarpus rohrii* Vahl**	0.46	MG718756	GQ982349	EF451061
***Rhamnus humboldtiana* Willd. ex Schult.**	0	-	-	JN900297
†*Rourea glabra* Kunth	5.96	JQ587280	-	-
†Rubiaceae	0.46	-	-	-
§*Sabal yapa* C. Wright ex Becc.	2.29	KY020661	EF688512	EF688500
†Sapindaceae	1.83	-	-	-

Table C-4 Continued

Species	**Relative Abundance Below Ground (%)**	**GenBank Accession Numbers**		
		matK	***trnH-psbA***	**ITS**
Semialarium mexicanum **(Miers) Mennega**	0.46	JQ588033	-	HM230151
Swartzia cubensis **(Britton & Wilson) Standl.**	0	JQ587869	-	EF560840
†*Tanaecium tetragonolobum* **(Jacq.) L.G. Lohmann**	3.21	KJ593801	KR534325	-
Thouinia paucidentata **Radlk.**	0	KM219806	-	KX584973
Trichilia glabra **L.**	0.46	JQ588355	-	-
Vitex gaumeri **Greenm.**	0.46	-	-	FM200131
†*Vitis tiliifolia* **Humb. & Bonpl. ex Roem. & Schult.**	0.92	NC_039681	HQ656479	KT344660
Zuelania guidonia **(Sw.) Britton & Millsp.**	0	-	GQ982412	-

†Liana
§Palm

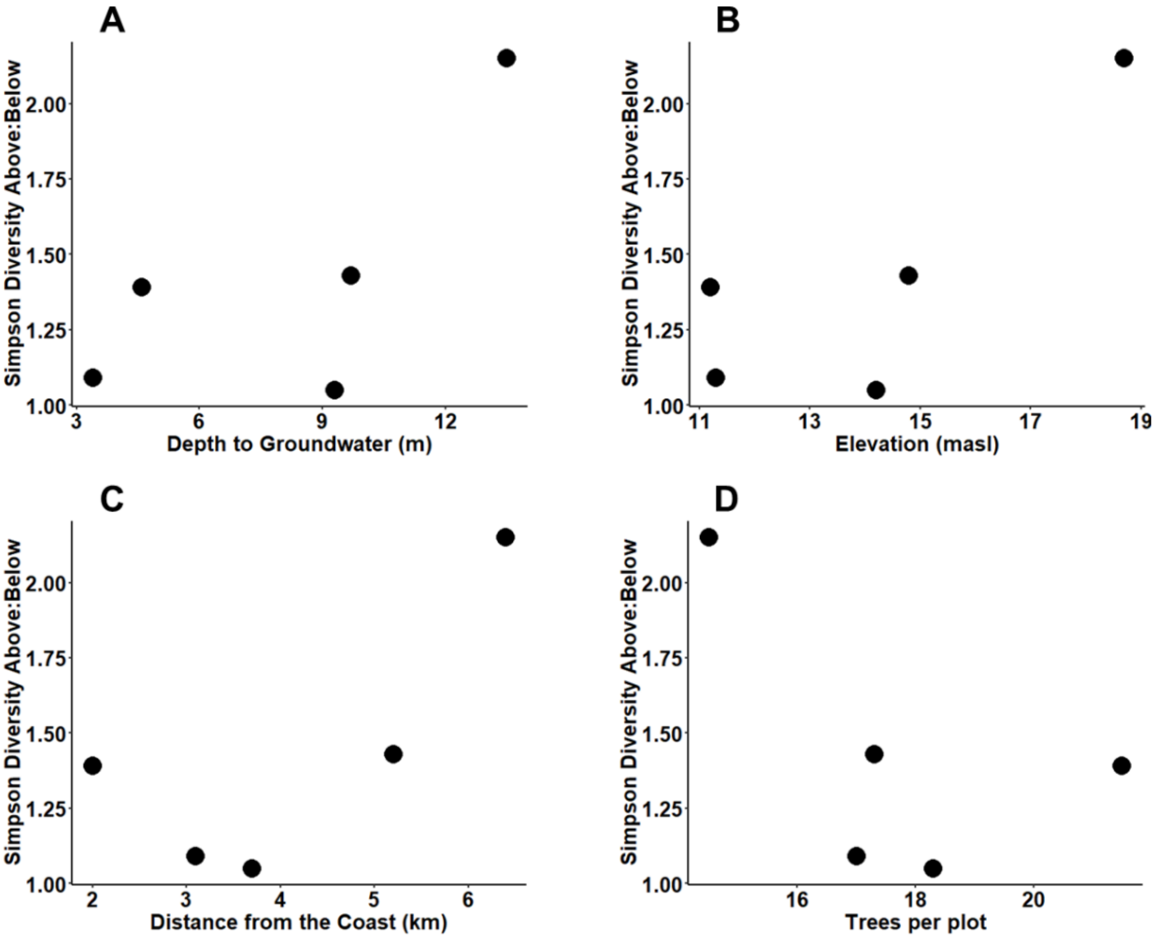

Figure C-1 Simpson diversity above ground to below ground compared with site characteristics, including (A) depth to groundwater, (B) elevation, (C) distance to the coast, (D) trees per plot, (E) basal area, (F) number of species above ground, (G) root masses per m^2, and (H) number of species below ground. A: $R^2 = 0.34$, $p = 0.18$, B: $R^2 = 0.52$, $p = 0.11$, C: $R^2 = 0.37$, $p = 0.16$, D: $R^2 = 0.07$, $p = 0.34$, E: $R^2 = - 0.33$, $p = 0.94$, F: $R^2 = - 0.33$, $p = 0.99$, G: $R^2 = - 0.11$, $p = 0.49$, H: $R^2 = 0.23$, $p = 0.24$.

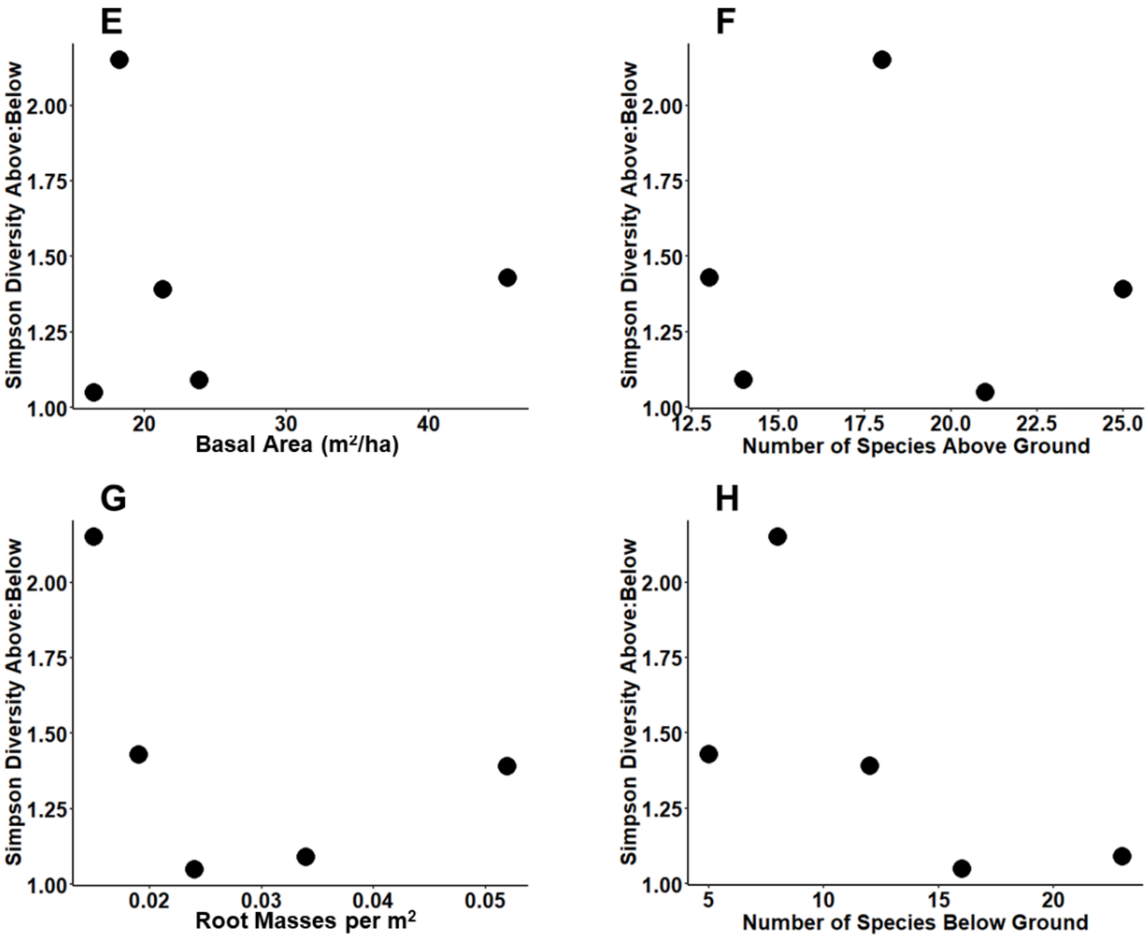

Figure C-1 Continued.

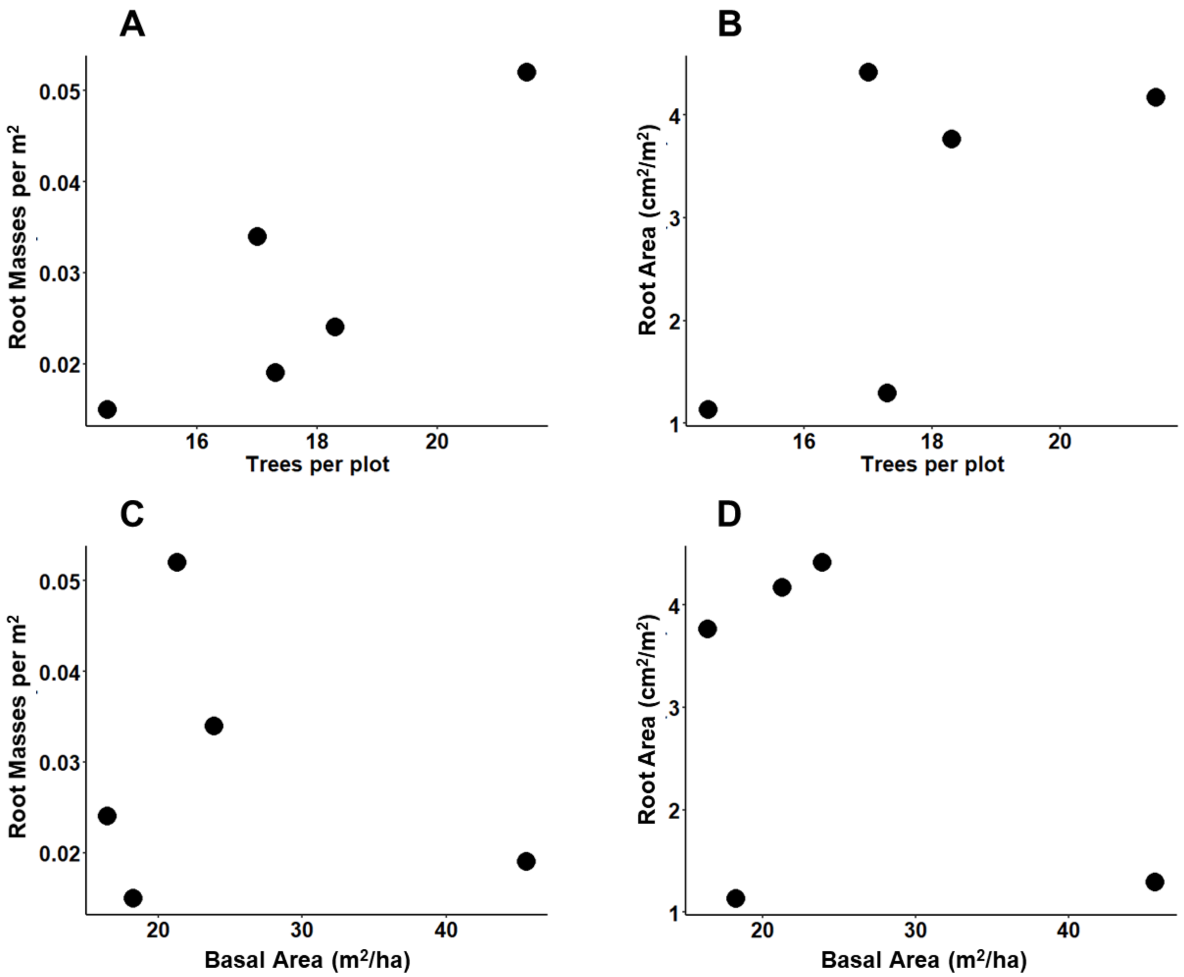

Figure C-2 Relationships between root masses and root area with trees per plot (A and B) and basal area (C and D). A: $R^2 = 0.67$, $p = 0.06$, B: $R^2 = 0.23$, $p = 0.24$, C: $R^2 = - 0.26$, $p = 0.71$, D: $R^2 = - 0.05$, $p = 0.43$.

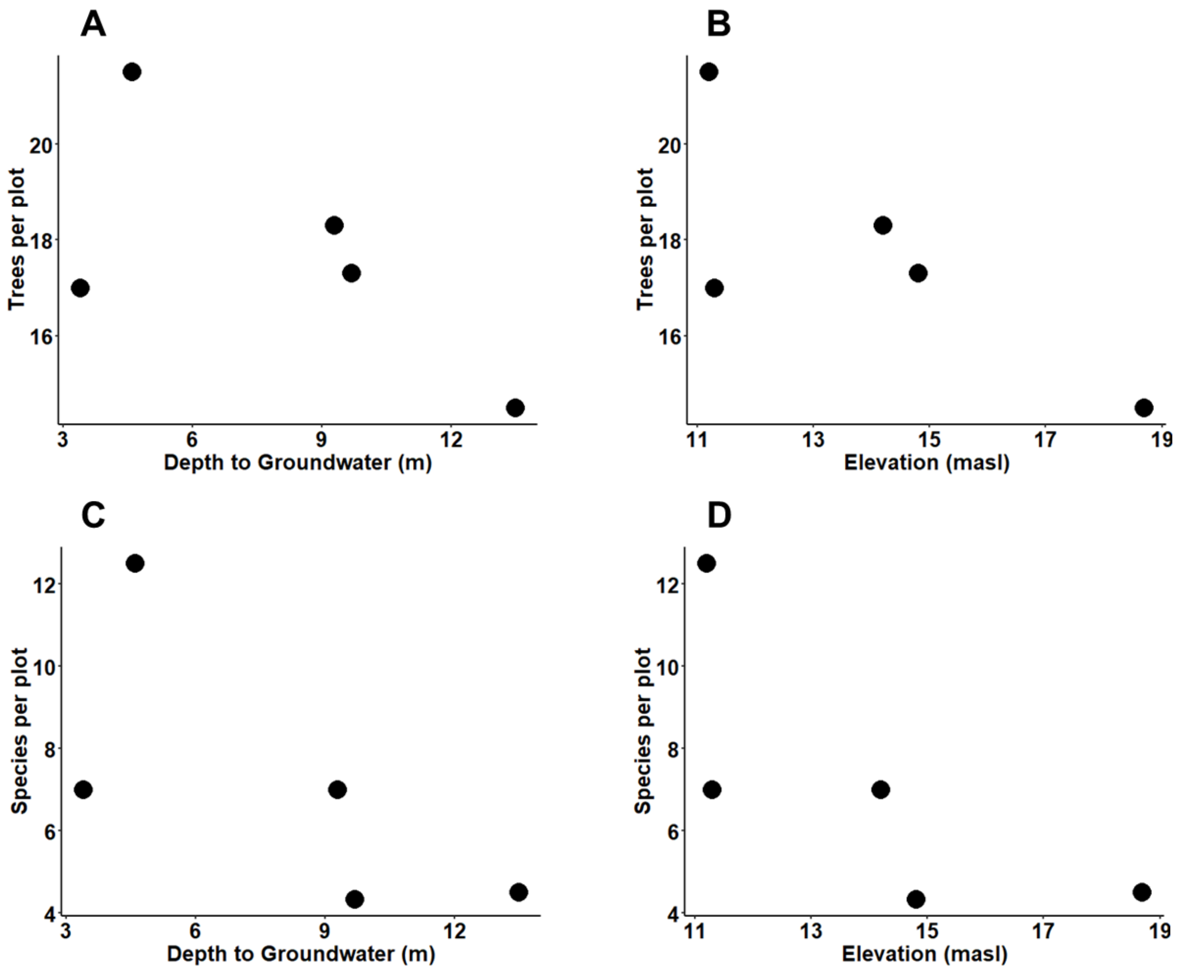

Figure C-3 Relationships between trees per plot and species per plot with depth to groundwater at the cave entrance (A and C) and site elevation (B and D). A: $R^2 = 0.24$, $p = 0.23$, B: $R^2 = 0.46$, $p = 0.13$, C: $R^2 = 0.29$, $p = 0.21$, D: $R^2 = 0.36$, $p = 0.17$.

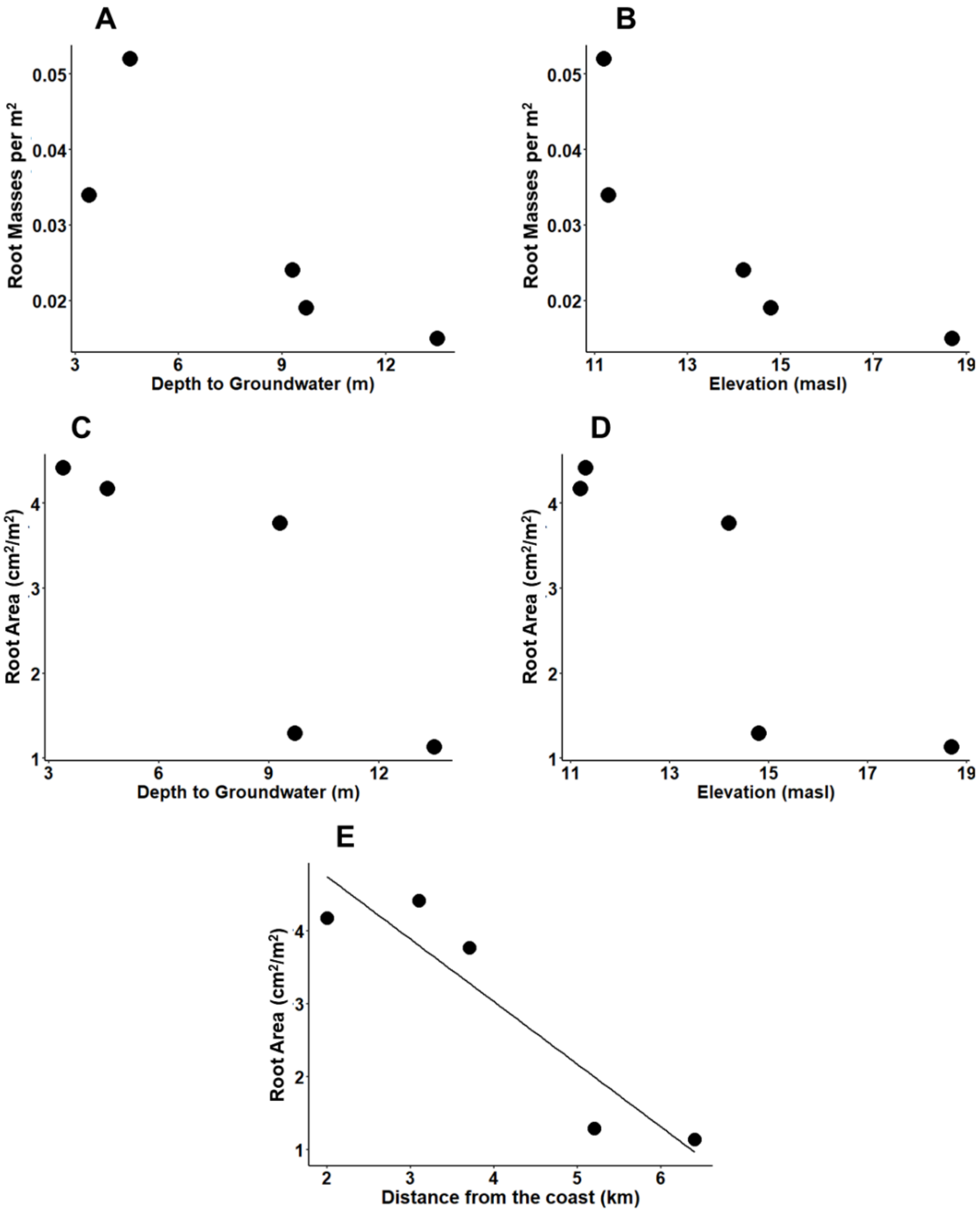

Figure C-4 Root abundance and root area compared to various site characteristics, including depth to groundwater (A and C), elevation (B and D), and distance from the coast (E). A: $R^2 = 0.58$, $p = 0.08$, B: $R^2 = 0.66$, $p = 0.06$, C: $R^2 = 0.65$, $p = 0.06$, D: $R^2 = 0.66$, $p = 0.06$, E: $R^2 = 0.82$, $p = 0.02$.

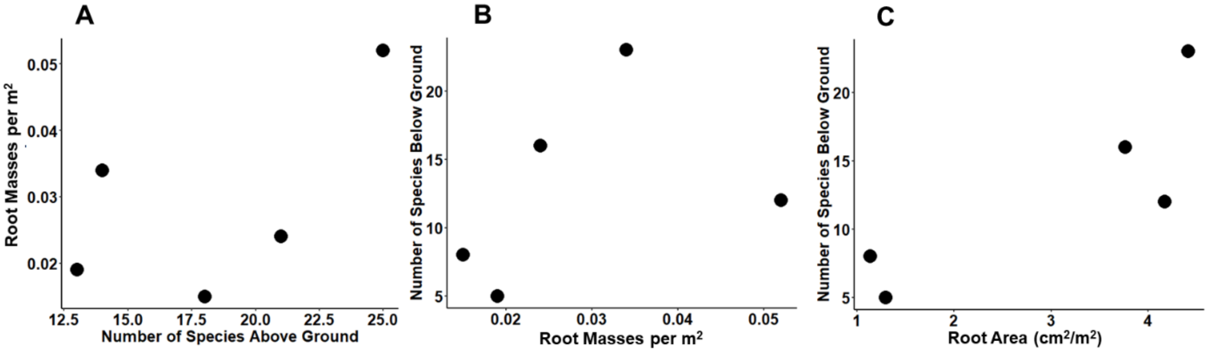

Figure C-5 Relationships between number of species above or below ground with root abundance (A and B) and root area (C). A: $R^2 = 0.15$, $p = 0.29$, B: $R^2 = 0.61$, $p = 0.07$, C: $R^2 = 0.60$, $p = 0.08$.

APPENDIX D

SUPPORTING INFORMATION FOR CHAPTER 5

Table D-1 Information on species found above ground across site, including abundance, root habit group, phenology, wood density, and associated references. * denotes when information was applied from another species in the same genus.

Species	Relative Abundance (%)	Rooting Habit	Phenology	Phenology References	Wood Density (g/cm^3)	Wood Density References
***Acacia dolichostachya* S.F. Blake**	1.5	Rare Below Ground	Deciduous	Encyclopedia of Life	0.53	Bhaskar et al 2014
***Allophylus cominia* (L.) Sw.**	1.5	Above Ground Only	Evergreen	Wright et al 2013	0.77*	Barajas-Morales 1987
***Bauhinia divaricata* L.**	1.5	Above Ground Only	Evergreen	Wright et al 2013, Maire et al 2015, Zanne et al 2013	0.54 ± 0.18	Reyes et al 1992, Bhaskar et al 2014
***Brosimum alicastrum* Sw.**	1.5	Rare Below Ground	Evergreen	Wright et al 2013, García-Guzmán et al 2007	0.59 ± 0.13	Barajas-Morales 1987, Reyes et al 1992, Gripenberg et al 2017
***Bursera simaruba* (L.) Sarg.**	4.4	Rare Below Ground	Deciduous	Wright et al 2013, Gutiérrez-Granados et al 2011, Borchert 1994, Maire et al 2015	0.38 ± 0.08	Werden et al 2018, Borchert 1994, Reyes et al 1992
***Caesalpinia gaumeri* Greenm.**	1.5	Above Ground Only	Deciduous	Hasselquist et al 2010, Gutiérrez-Granados et al 2011, Borchert 1994	0.74	Borchert 1994

Table D-1 Continued

Species	Relative Abundance (%)	Rooting Habit	Phenology	Phenology References	Wood Density (g/cm^3)	Wood Density References
***Cascabela gaumeri* (Hemsl.) Lippold**	5.8	Rare Below Ground	Evergreen	http://www.pitchandikulam-herbarium.org/contents/phenology.php?id=172	0.54*	Pérez-Harguindeguy et al 2013
***Casearia tremula* (Griseb.) Griseb. ex C.Wright**	2.9	Rare Below Ground	Deciduous	García-Guzmán et al 2007	0.68 ± 0.08	Chave et al 2009, Reyes et al 1992
***Casimiroa tetrameria* Millsp.**	1.5	Above Ground Only	Evergreen	TRY	NA	NA
***Coccoloba barbadensis* Jacq.**	5.8	Rare Below Ground	Evergreen	Wright et al 2013	0.71 ± 0.01	Barajas-Morales 1987
***Cordia dodecandra* A.DC.**	1.5	Rare Below Ground	Deciduous	Querejeta et al 2007, Borchert 1994, Rosado-Sánchez et al 2017, García-Guzmán et al 2007	0.62 ± 0.12	Borchert 1994, Reyes et al 1992
***Cordia gerascanthus* L.**	7.3	Rare Below Ground	Deciduous	Wright et al 2013, Borchert 1994, García-Guzmán et al 2007	0.63 ± 0.15	Borchert 1994, Reyes et al 1992, Bhaskar et al 2014
***Cupania glabra* Sw.**	4.4	Rare Below Ground	Evergreen	Wright et al 2013, García-Guzmán et al 2007	0.61 ± 0.07	Gripenberg et al 2017, Barajas-Morales 1987

Table D-1 Continued

Species	**Relative Abundance (%)**	**Rooting Habit**	**Phenology**	**Phenology References**	**Wood Density (g/cm^3)**	**Wood Density References**
***Dendropanax arboreus* (L.) Decne. & Planch.**	10.2	Rare Below Ground	Evergreen	Wright et al 2013, Maire et al 2015, García-Guzmán et al 2007	0.41	Gripenberg et al 2017
***Diospyros tetrasperma* Sw.**	4.4	Rare Below Ground	Evergreen	Wright et al 2013	0.81	Chave et al 2009
***Drypetes lateriflora* (Sw.) Krug & Urb.**	10.2	Above Ground Only	Evergreen	Wright et al 2013	0.62 ± 0.01	http://www.fao.org/3/w4095e/w4095e0c.htm), Gripenberg et al 2017
***Eugenia axillaris* (Sw.) Willd.**	1.5	Above Ground Only	Evergreen	Wright et al 2013	0.65	Reyes et al 1992
***Eugenia oerstediana* O.Berg**	1.5	Above Ground Only	Evergreen	Wright et al 2013	0.65 ± 0.0	Reyes et al 1992, Paine et al 2015
***Eugenia* sp.**	4.4	Above Ground Only	Evergreen	Wright et al 2013	0.65	Reyes et al 1992
***Exothea diphylla* (Standl.) Lundell**	1.5	Above Ground Only	Evergreen*	Wright et al 2013	0.71	Bhaskar et al 2014
***Ficus cotinifolia* Kunth**	1.5	Common Below Ground	Evergreen	Querejeta et al 2007	0.40	Barajas-Morales 1987
***Ficus obtusifolia* Kunth**	10.2		Evergreen	Maire et al 2015	0.37 ± 0.06	Reyes et al 1992, Gripenberg et al 2017
***Ficus trigonata* L.**	5.8		Evergreen	Wright et al 2013	0.47	Barajas-Morales 1987

Table D-1 Continued

Species	Relative Abundance (%)	Rooting Habit	Phenology	Phenology References	Wood Density (g/cm^3)	Wood Density References
Hampea trilobata **Standl.**	2.9	Above Ground Only	Evergreen*	Wright et al 2013	0.39*	Barajas-Morales 1987
Leucaena leucocephala **(Lam.) de Wit**	2.9	Common Below Ground	Evergreen	Wright et al 2013, Maire et al 2015	0.74 ± 0.14	Barajas-Morales 1987, Reyes et al 1992
Lonchocarpus rugosus **Benth.**	5.8	Rare Below Ground	Deciduous	Derroire et al 2018, Borchert 1994, García-Guzmán et al 2007	0.91	Borchet et al 1994
Luehea speciosa **Willd.**	2.9	Above Ground Only	Evergreen	Wright et al 2013	0.91	Borchet et al 1994
Manilkara zapota **(L.) P. Royen**	7.3	Rare Below Ground	Evergreen	Wright et al 2013	0.85 ± 0.06	Chave et al 2009, Reyes et al 1992
Melicoccus oliviformis **Kunth**	4.4	Above Ground Only	Evergreen	Querejeta et al 2007, Gutiérrez-Granados et al 2011	0.84	Huerta and Martinez 1982
Mosannona depressa **(Baill.) Chatrou**	8.7	Rare Below Ground	Evergreen	Wright et al 2013	NA	NA
Neea psychotrioides **Donn.Sm.**	10.2	Rare Below Ground	Evergreen	Wright et al 2013, Garcia-Guzman et al 2007	0.26	Barajas-Morales 1987

Table D-1 Continued

Species	**Relative Abundance (%)**	**Rooting Habit**	**Phenology**	**Phenology References**	**Wood Density (g/cm^3)**	**Wood Density References**
Oxandra lanceolata **(Sw.) Baill.**	18.9	Above Ground Only	Evergreen	Wright et al 2013	0.82	Chave et al 2009
Piscidia piscipula **(L.) Sarg.**	2.9	Rare Below Ground	Deciduous	Estrada-Medina et al 2013, Rosado-Sánchez et al 2017, Islebe et al 2015	0.59	Reyes-Garcia et al 2012
Platymiscium yucatanum **Standl.**	1.5	Rare Below Ground	Deciduous	http://tropical.theferns.info/viewtropical.php?id=Platymiscium+pinnatum	0.81 ± 0.04	Chave et al 2009, Reyes et al 1992
Plumeria obtusa **L.**	2.9	Rare Below Ground	Deciduous	Wright et al 2013, Islebe et al 2015	0.53*	Pérez-Harguindeguy et al 2013
Pouteria campechiana **(Kunth) Baehni**	2.9	Common Below Ground	Evergreen	Wright et al 2013	0.79	Barajas-Morales 1987
Pouteria reticulata **(Engl.) Eyma**	5.8		Evergreen	Wright et al 2013	0.69 ± 0.08	Baraloto et al 2010, Paine et al 2015
Pseudolmedia glabrata **(Liebm.) C.C.Berg**	1.5	Above Ground Only	Evergreen	Wright et al 2013, García-Guzmán et al 2007	0.68	Barajas-Morales 1987
Pseudolmedia spuria **(Sw.) Griseb.**	1.5	Above Ground Only	Evergreen*	Wright et al 2013	0.75	Chave et al 2009

Table D-1 Continued

Species	**Relative Abundance (%)**	**Rooting Habit**	**Phenology**	**Phenology References**	**Wood Density (g/cm^3)**	**Wood Density References**
***Rhamnus humboldtiana* Willd. ex Schult.**	1.5	Above Ground Only	Evergreen	https://aggie-horticulture.tamu.edu/ornamentals/nativeshrubs/karwinskiahumbold.htm	0.70	Reyes-Garcia et al 2012
***Semialarium mexicanum* (Miers) Mennega**	1.5	Rare Below Ground	Deciduous	Powers and Tiffin 2012, Enquist and Sullivan 2001	0.51	Werden et al 2018
***Swartzia cubensis* (Britton & Wilson) Standl.**	16.0	Above Ground Only	Evergreen	Wright et al 2013	0.93 ± 0.03	Chave et al 2009, Reyes et al 1992
***Thouinia paucidentata* Radlk.**	2.9	Above Ground Only	Evergreen	Wright et al 2013, Zanne et al 2013, García-Guzmán et al 2007	0.74 ± 0.18	Barajas-Morales 1987, Bhaskar et al 2014, Reyes-Garcia et al 2012
***Vitex gaumeri* Greenm.**	10.2	Rare Below Ground	Deciduous	Gutiérrez-Granados et al 2011	0.56	Chave et al 2009, Reyes et al 1992
***Zuelania guidonia* (Sw.) Britton & Millsp.**	2.9	Above Ground Only	Deciduous	Wright et al 2013, Powers and Tiffin 2012	0.59 ± 0.04	Chave et al 2009, Gripenberg et al 2017

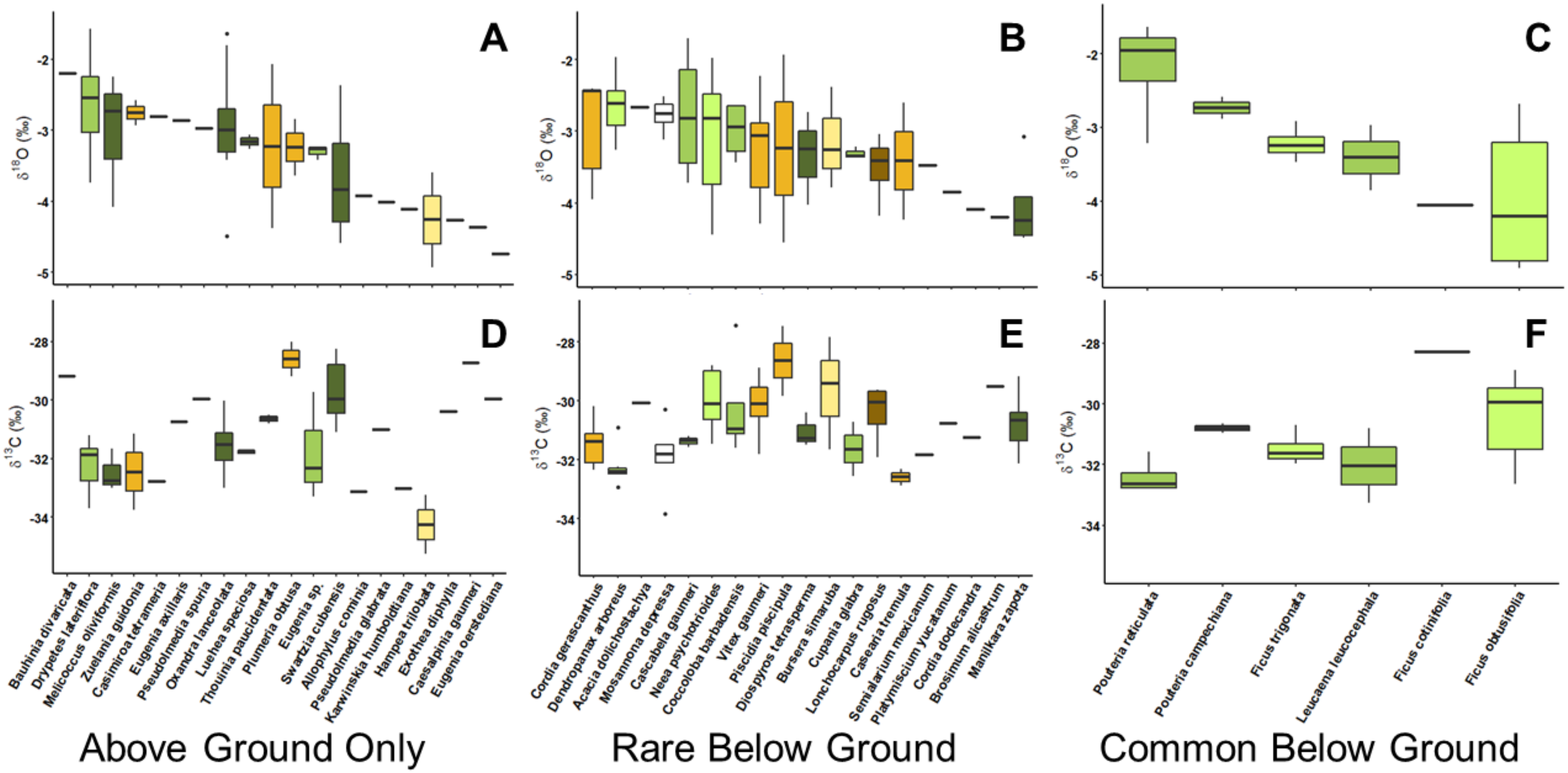

Figure D-1 Patterns in by stem water $\delta^{18}O$ and leaf $\delta^{13}C$ among species in the above ground only (A and D), rare below ground (B and E), and common below ground (C and F) groups.

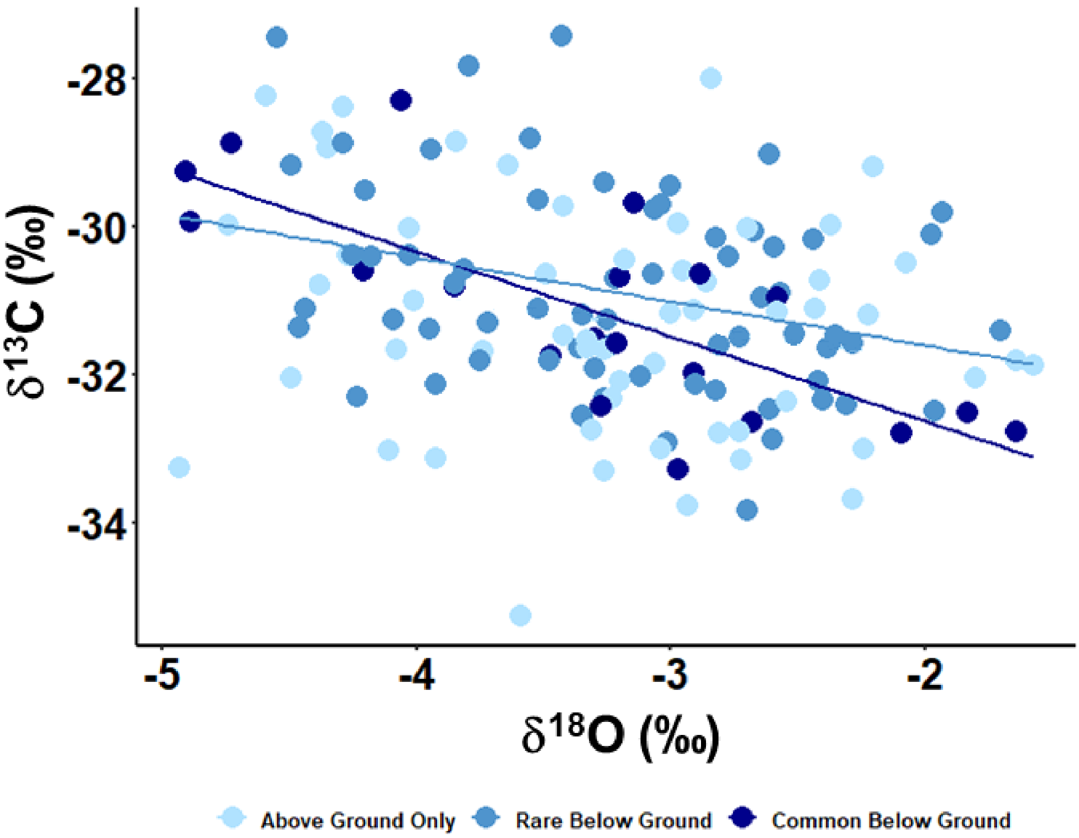

Figure D-2 Leaf $\delta^{13}C$ by stem water $\delta^{18}O$ and the relationships among rooting habit groups. The linear regression for the above ground only group (light blue) was not significant ($R^2 = 0.02$, $p = 0.13$), while the regressions for the rare below ground (medium blue) and common below ground (dark blue) groups were significant ($R^2 = 0.09$, $p < 0.01$ and $R^2 = 0.55$, $p < 0.01$, respectively).

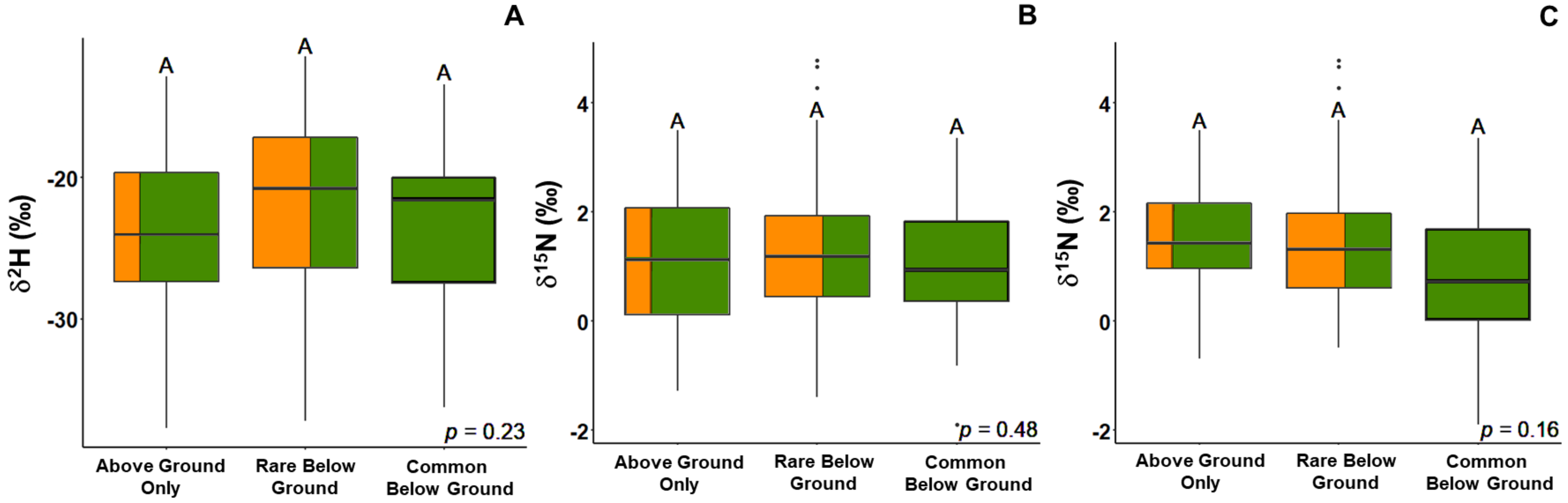

Figure D-3 Stem water δ^2H (A) and leaf δ^{15}N with (B) and without (C) legumes by rooting habit groups. Species classified as common below ground had relative root abundance of 5% or greater. Shading shows the fraction of deciduous (orange) and evergreen (green) species in each group.

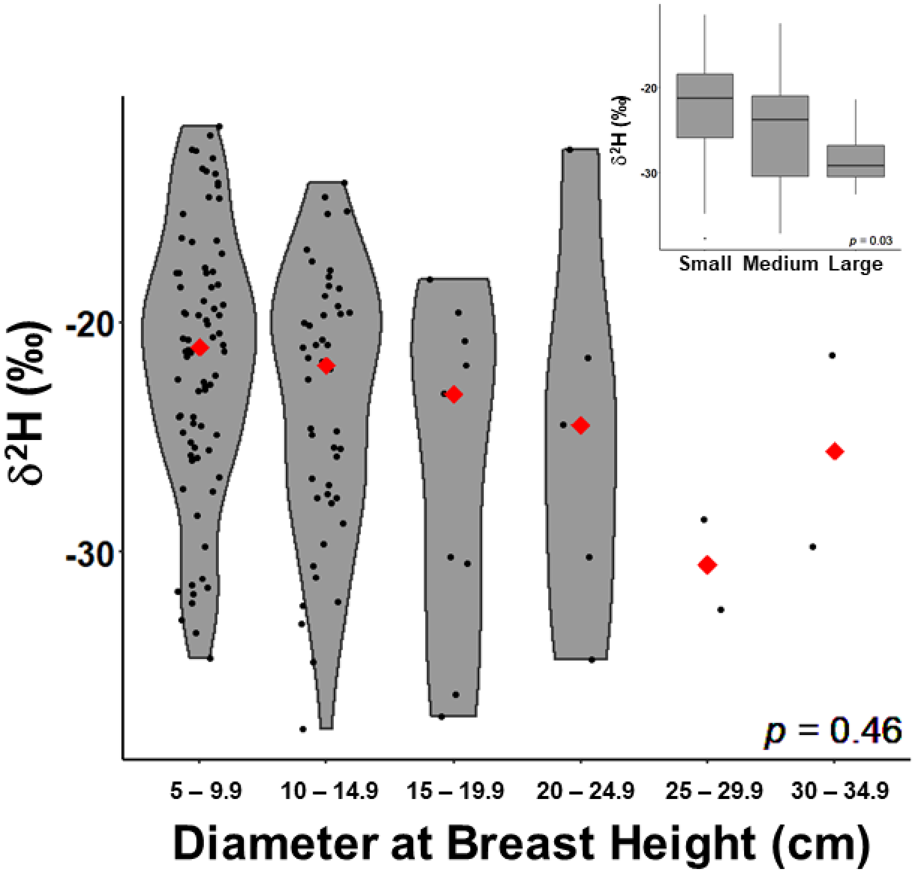

Figure D-4 δ^{2}H from stem water by cross-sectional area, ranging from 5 to 35 cm, in 5-cm increments. The inset shows δ^{2}H by small (5 – 14.9 cm), medium (15 – 24.9 cm), and large trees (≥ 25 cm). The overall mean (red diamond) is shown for each size class.

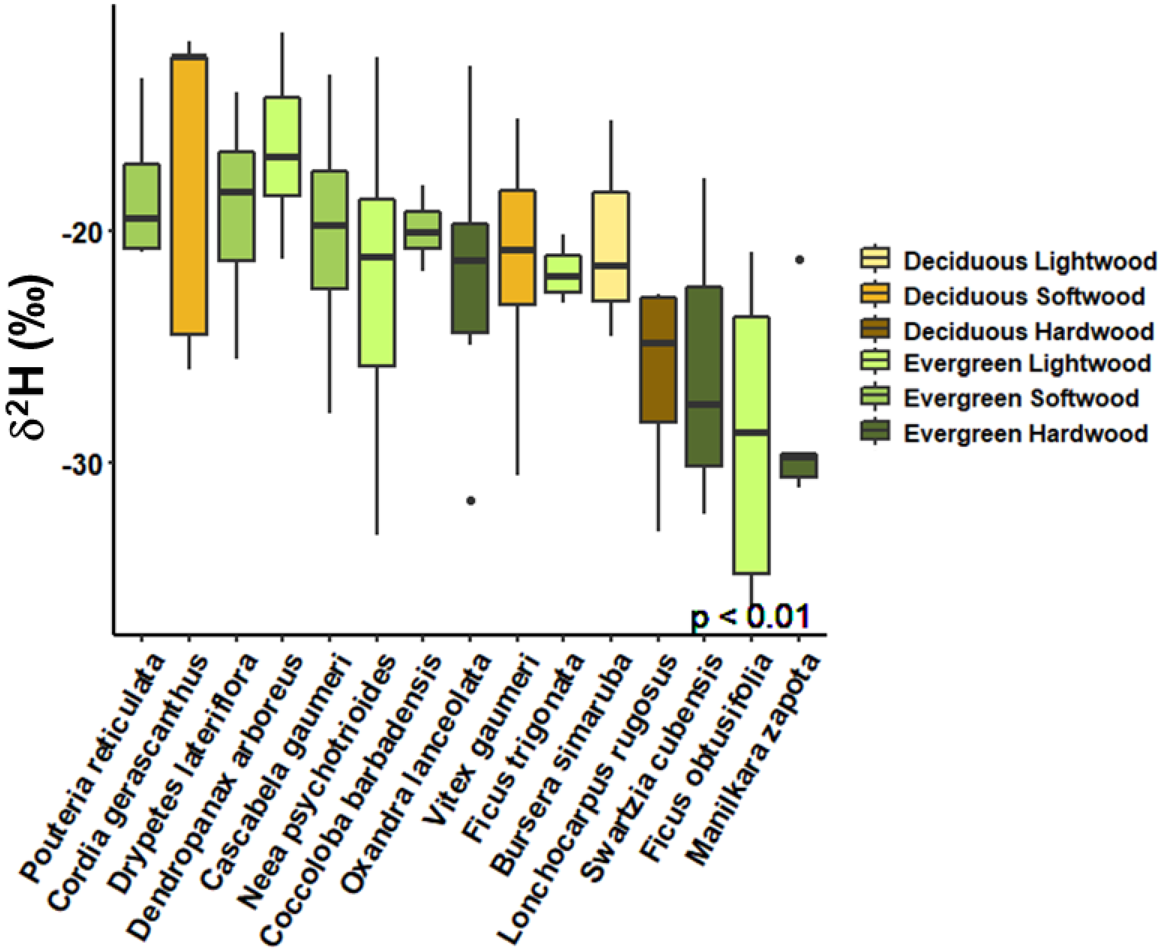

Figure D-5 Patterns in δ^2H from stem water among abundant species (those with 4 or more individuals across sites). Species are ordered by decreasing δ^{18}O (see Figure 5.6A).